THE UNIVERSITY *of* EDINBURGH

An Investigation into Phosphorus Removal by Iron Ochre for the Potential Treatment of Aquatic Phosphorus Pollution

Stephen Carr

Doctor of Philosophy

The University of Edinburgh

~ 2012 ~

Declaration

Name: Stephen Carr

Name of Degree: Doctor of Philosophy

Title of work: An Investigation into Phosphorous Removal by Iron Ochre for the Potential Treatment of Aquatic Phosphate Pollution

Declaration:

• The thesis has been composed by the candidate named above.

• All work included is either the named candidate's own, or, if the candidate has been a member of a research group, that the candidate has made a substantial contribution to the work, such contribution being clearly indicated.

• The work has not been submitted for any other degree or professional qualification except as specified above.

Signature ……

Date ……..

Abstract

Phosphorus (P) pollution of waterbodies is a global issue with detrimental environmental, social and economic impacts. Low-cost and sustainable P removal technologies are therefore required to tackle P pollution, whilst also offering a technique for reclaiming P. Ochre, a waste product from minewater treatment plants (MWTPs), has been proposed as a suitable material for the removal of P from enriched waters due to a high content of Fe, Al, Ca and Mg, which have high affinities for P removal.

Whilst a range of studies have been conducted investigating ochre as a P adsorbent, most of these are large-scale field experiments and lack understanding of the underlying processes of P removal by ochre. There have also been very few detailed comparisons of different ochre types. The primary focus of this thesis is thus to provide a process-based understanding of P removal by various ochres, in order to investigate the optimal conditions for the use of ochres in the treatment of aquatic P pollution. Seven ochres from six MWTPs in the UK and Ireland were investigated, one of which was in a pelleted form. The ochres were largely comprised of Al, Ca, Fe and Mg (42-68 % by dry weight), had a high B.E.T. surface area, 56-243 m^2 g^{-1}, and contained mineral surfaces with a high affinity for P adsorption, such as goethite and calcite.

A novel batch experiment methodology was utilised to calculate the adsorption characteristics of ochre at discrete pH conditions. The variation of these characteristics with pH indicates the importance and requirement for such a method to study adsorption by materials at the expected pH conditions of application. At the pH conditions of wastewater streams (~pH 7), the P adsorption capacities of the ochres, determined from fitting adsorption isotherms, was 11.8–43.1 mg P g^{-1}.

Results of P adsorption batch experiments were modelled in ORCHESTRA, wherein P removal by the ochres was described well by adsorption onto hydrous ferric oxides. Three of the ochres contain relatively high calcite contents and due to a poor

fit of the model to the observed datasets at high pH conditions, with equilibrium P concentrations lower in the batch experiments than the modelled result, adsorption onto calcite is suggested as a P removal mechanism for these ochres at pH > 7.

Environmental application of ochre filters will require P removal under flow-through transport conditions. Column experiments were therefore conducted using two ochres, coarse-grained Polkemmet ochre and Acomb pellets (column volume 1055 cm^3, pore space 490-661 cm^3, typical pore volumes of experiments: 220-400). P removal efficiency increased with contact time, and the presence of competing ions had only marginal effects on P removal. Resting the column substrate for 48 hours between P applications greatly increased the P removal efficiency of a packed column of Polkemmet ochre, resulting in 81 % of influent P removed over 1000 pore volumes of operation (7.68 mg P g^{-1}). Acomb pellets had a lower P removal efficiency than Polkemmet ochre. It is suggested that the high calcium content of the pellets, as a result of the pelletisation process, has created a substrate where the dominant P removal mechanism at neutral pH conditions is adsorption to calcite, which has slower reaction kinetics than adsorption onto goethite. Therefore, this pelleted ochre requires a higher contact time for adsorption reactions to occur.

It is suggested that ochre filters are most suitable for application in situations where flow rate is constant or can be controlled e.g. septic tank effluent. Ochres which dry to a coarse particle size are preferred for use as a substrate as pelletisation requires capital, expertise and can produce substrates with slower P sorption kinetics. Resting the filter substrate between P application regenerates surface sites for adsorption, and filters should be run in parallel to maximise P removal efficiency. Acomb pellets, which are a mix of iron hydroxides and alkaline materials, may have potential application as a permeable reactive barrier substrate to treat P enriched ground waters. Further research utilising fine-grained ochres as an additive to P rich fertilisers or for use in continuously stirred tank reactors is recommended.

Key words: ochre, phosphorus, batch experiment, column experiment, adsorption isotherms, ORCHESTRA.

Acknowledgments

I would firstly like to acknowledge the contribution of Dr. Kate Heal, without whose expertise, knowledge and commitment, this doctoral thesis would not have been possible; her supervisory assistance and feedback has encouraged and challenged me throughout my PhD and made my work all the better for it. I acknowledge the contribution to my thesis from working with Dr. David Lumsdon and Dr. Andy Vinten at the James Hutton Institute, whose expertise and assistance has helped to shape and guide this thesis to its final form.

I would like to thank all those who have at one time or another inhabited the 'Crew Attic'. The friendships and camaraderie developed within those four walls, and under the skylights, have helped me through the hard times and magnified the good. I would also like to thank Amy Prior, who has helped and encouraged me through the past couple of years and without whose presence this thesis would have less meaning. Special thanks also to Denny Roberts, never afraid to lend a helping hand whilst taking me out for a beer or a coffee when I didn't realise quite how much I needed one.

Methodological and analytical assistance has been provided from a variety of people over the past four years, for their help I would like to thank Andy Gray and Jon Morman from the University of Edinburgh and Yvonne Cook, Fiona Sturgeon, Susan McIntyre, Carol Curran and Helen Watson from the James Hutton Institute.

Funding this project is made possible by the UK Natural Environment Research Council (NERC) and the James Hutton Institute (formerly the Macaulay Institute) to whom I am extremely grateful.

Finally I would like to thank my family, without whose love and support I would not be in the position I am in today.

Contents

List of Figures

List of Tables

List of Abbreviations

Abbreviation	Definition
Ag	Silver
AIC	Akaike's Information Criterion
Al	Aluminium
ALD	Anoxic Limestone Drain
As	Arsenic
B	Boron
Be	Beryllium
BFA	Bottom Fly Ash
BOD	Biological Oxygen Demand
Ca	Calcium
CaO	Calcium Oxide
Cd	Cadmium
CF	Correction Factor
Cl^-	Chloride
Co	Cobalt
C_{out}/ C_{in}	Effluent Concentration divided by Influent Concentration
Cr	Chromium
CRM	Certified Reference Material
CSTR	Continuously Stirred Tank Reactor
Cu	Copper
D	Dispersion Coefficient
DDLM	Diffuse Double Layer Model
DEFRA	Department for Environment, Food and Rural Affairs
DO	Dissolved Oxygen
D_{wt}	By Dry Weight

E	Model Efficiency
EA	Environmental Agency
EC	European Commission
EEC	European Economic Community
EU	European Union
EUWFD	European Union Water Framework Directive
Fe	Iron
Fe (II)	Iron Oxidation State II
Fe (III)	Iron Oxidation State III
Fe^{2+}	Ferrous Iron
Fe_2O_3	Iron Oxide
Fe^{3+}	Ferric Iron
FeS	Pyrite
GFO	Granular Ferric Oxide
GUI	General User Interface
H_2O_2	Hydrogen Peroxide
Ha	Hectare
HFO	Hydrous Ferric Oxide
HFO-SA	Hydrous Ferric Oxide Surface Area
Hg	Mercury
ICP-AES	Inductively Coupled Plasma Atomic Emission Spectroscopy
ICP-OES	Inductively Coupled Plasma Optical Emission Spectrometry
K	Potassium
K_d	Partition coefficient
K_f	Freundlich adsorption capacity
KH_2PO_4	Potassium Dihydrogen Phosphate
Km	Kilometre

L	Litre
MAFF	Ministry of Agriculture, Fisheries and Food
Mg	Magnesium
Mn	Manganese
mS	Milli Siemens
MSc	Master of Science
MWTPs	Mine Water Treatment Plants
Na	Sodium
$NaNO_3$	Sodium Nitrate
Ni	Nickel
OCP	Octacalcium Phosphate
ORCHESTRA	Object Representation of Chemical Speciation and Transport M*o*dels
P	Phosphorus
Pb	Lead
Pe	Péclet Number
PRB	Permeable Reactive Barrier
PTEs	Potentially Toxic Elements
Pv	Pore Volume
PVC	Polyvinyl Chloride
pzc	Point of zero charge
R^2	Coefficient of Determination
Rpm	Revolutions per minute
S	Sulphur
s.d.	Standard Deviation
s.e.	Standard Error
SA_{BET}	B.E.T Surface Area
SCM	Surface Complexation Models

SEPA	Scottish Environmental Protection Agency
Si	Silicon
SiO_2	Silicon Dioxide
S_{max}	Langmuir adsorption capacity
Sn	Tin
SRP	Soluble Reactive Phosphorus
SS	Suspended Sediment
SSE	Sum of the Standard Errors
STANmod	Studio of Analytical Models
Sv	Strontium
SynS	Synthetic Sewage
TP	Total Phosphorus
USEPA	US Environmental Protection Agency
V	Vanadium
v	Pore Water Velocity
WFD	Water Framework Directive
WHO	World Health Organisation
WV Ochre	West Virginia Ochre
WWTPS	Waste Water Treatment Plants
XRD	X-Ray Powder Diffraction
Yr	Year
Zn	Zinc
ΣSSE	Sum of the Sum of the Squared Error

Chapter 1
Phosphorus pollution and the formation of ochre

This thesis focuses upon ochre, an Iron (Fe) rich material generated at minewater treatment plants (MWTPs), and its potential development as a low-cost and sustainable treatment system to remove phosphorus (P) from nutrient enriched inland surface waters. Although groundwaters can become P enriched, this thesis focuses upon the much greater problem of surface water eutrophication.

This Chapter elucidates the environmental, historical and economic contexts for this use of ochre. P is introduced as an essential nutrient for biological activity, but also as a potential cause of eutrophication; and the consequent requirement for the development of environmentally- and financially- responsible treatment systems to treat P-enriched waters is discussed. In order to assess appropriate conditions for the application of ochre for P removal, there is a need to understand the sources and processes causing P pollution. Sources of P pollution, such as septic tanks, wastewater treatment plants (WWTPs) and diffuse pollution are therefore examined to gain an understanding of the conditions in which treatment systems would be required to operate.

The formation of ochre, a by-product of the treatment of minewater, is then presented, and its potential as a filter substrate for the removal of P from wastewater streams is discussed. The suitability of ochre filters for treating sources of aquatic P pollution, in light of filter design considerations, is then examined before the appropriate situations for the use of ochre are determined.

In the final sections, the research questions and objectives of this thesis are formulated and the study outline presented.

1.1 Phosphorus pollution

Phosphorus is an essential nutrient for cellular growth and is cycled through the natural environment. Enrichment of surface waters with P can, however, lead to eutrophication and related environmental, economic and social issues. A driving force behind remediation of surface waters is the EU Water Framework Directive (WFD). This key piece of legislation aims to improve the quality of all surface waters and groundwaters in the EU to a "good status" and will thus require the tackling of P-enriched waters.

P pollution of surface waters is a symptom of the single-use, and ultimately unsustainable, utilisation of the nutrient. Current agricultural practices depend upon the mining of phosphate rock which is refined into fertilisers. P is a finite resource, and there is thus a need to develop sustainable techniques to reuse P rather than merely depending upon diminishing supplies of phosphate rock.

1.1.1 Sources and cycling of phosphorus

P is a fundamental nutrient for cellular processes in organisms. Under natural conditions, P is found in low concentrations in comparison to other nutrients and therefore often limits biological activity (Moss, 1988). In terrestrial systems with little human influence, P is recycled between plants and soil with minimal losses from the system. Anthropogenic processes lead to losses from the system via point and diffuse sources producing pollution of surface waters (D'Arcy et al., 2000). The agricultural P cycle is therefore dependent upon a continued influx of P to accommodate losses from the system (Figure 1.1).

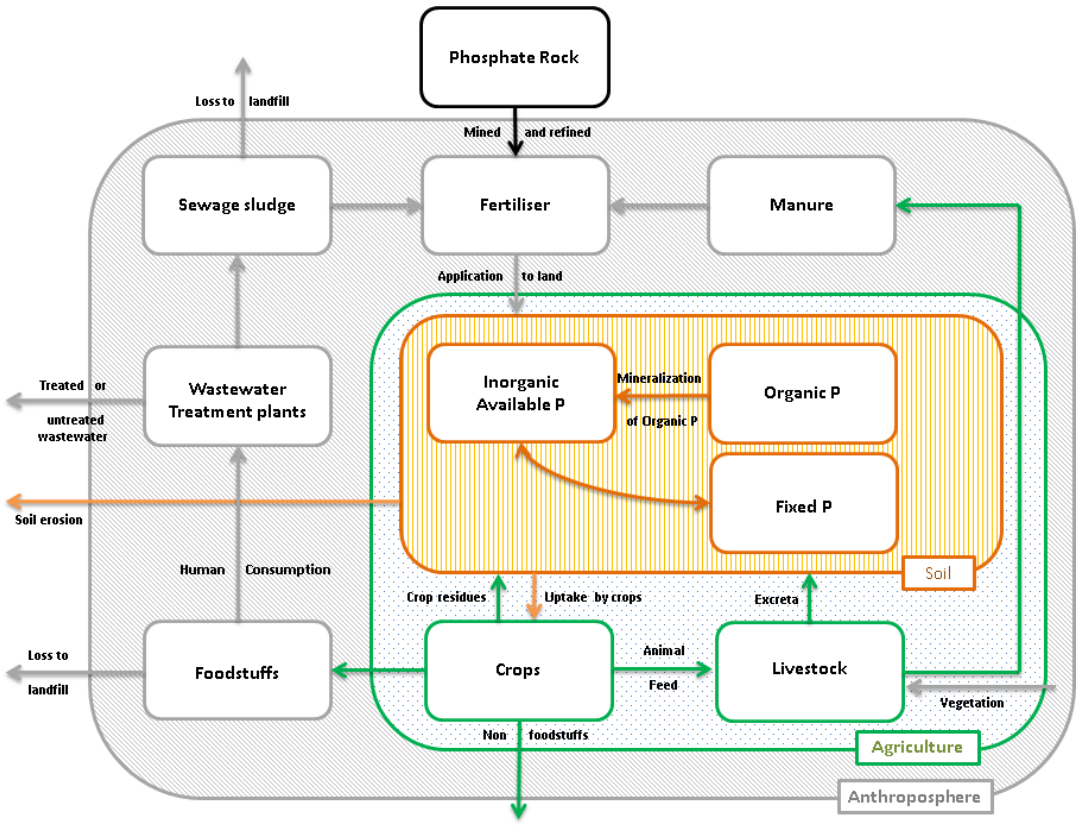

Figure 1.1: The anthropological P cycle: Flows of P indicated by arrows, with stores displayed as boxes. Losses from the system require addition of phosphate rock to ensure agricultural yields are maintained.

Soil erosion, and treated or untreated wastewater, are losses from the system (Figure 1.1) that result in P-enrichment of surface waters. The effect of increasing P concentrations in aquatic systems is to stimulate biological activity where P is commonly the limiting factor. Photosynthesis and respiration are terms that describe the production and decay of living matter, Eq. 1.1, with the balance between these governing the oxygen concentration in the surrounding environment (Emsley and Hall, 1976).

$$106CO_2 + 16NO_3^- + H_2PO_4^- + 122H_2O + 17H^+ \underset{\text{Respiration}}{\overset{\text{Photosynthesis}}{\Longleftrightarrow}} C_{106}H_{263}O_{110}N_{16}P + 138O_2$$

Equation 1.1: A simplified equation based on the creation and decay of algal protoplasm ($C_{106}H_{263}O_{110}P$) by photosynthesis and respiration. The stoichiometric 106:16:1 ratio of C:N:P is the Redfield ratio, first described by Redfield (1934).

The nitrogen to P ratio in Eq. 1.1 is 16:1, equivalent to that in the oceans, suggesting that either algae determine this ratio, or they have adapted to it (Emsley and Hall, 1976). At equilibrium, photosynthesis is equal to respiration, maintaining the chemostasis of the water and a constant population of organisms, i.e. homeostasis. If photosynthesis and respiration are not equal, the result is pollution. If the rate of photosynthesis is greater than respiration, due to an influx of nutrients, then algae proliferate. Conversely, if the rate of respiration is greater than photosynthesis, secondary pollution is caused by the depletion of available oxygen (Emsley and Hall, 1976).

The aquatic P cycle, is regulated by biological activity (Figure 1.2). Producer organisms utilise inorganic P, with consumer organisms feeding upon them and decomposer organisms breaking down higher organisms. The consumers include insects and their larvae, fish, and crustaceans, collectively termed zooplankton. These predate upon the primary producers, algae, with bacteria and fungi forming the decomposer group. Inorganic P may be present in soluble and insoluble forms, with the majority of P in solution in the form HPO_4^{2-}, in equilibrium with $H_2PO_4^-$, PO_4^{3-} and H_3PO_4 (Emsley and Hall, 1976). Inorganic insoluble P is found in the form of metal phosphates, with P precipitating with Al, Ca and Fe in most instances.

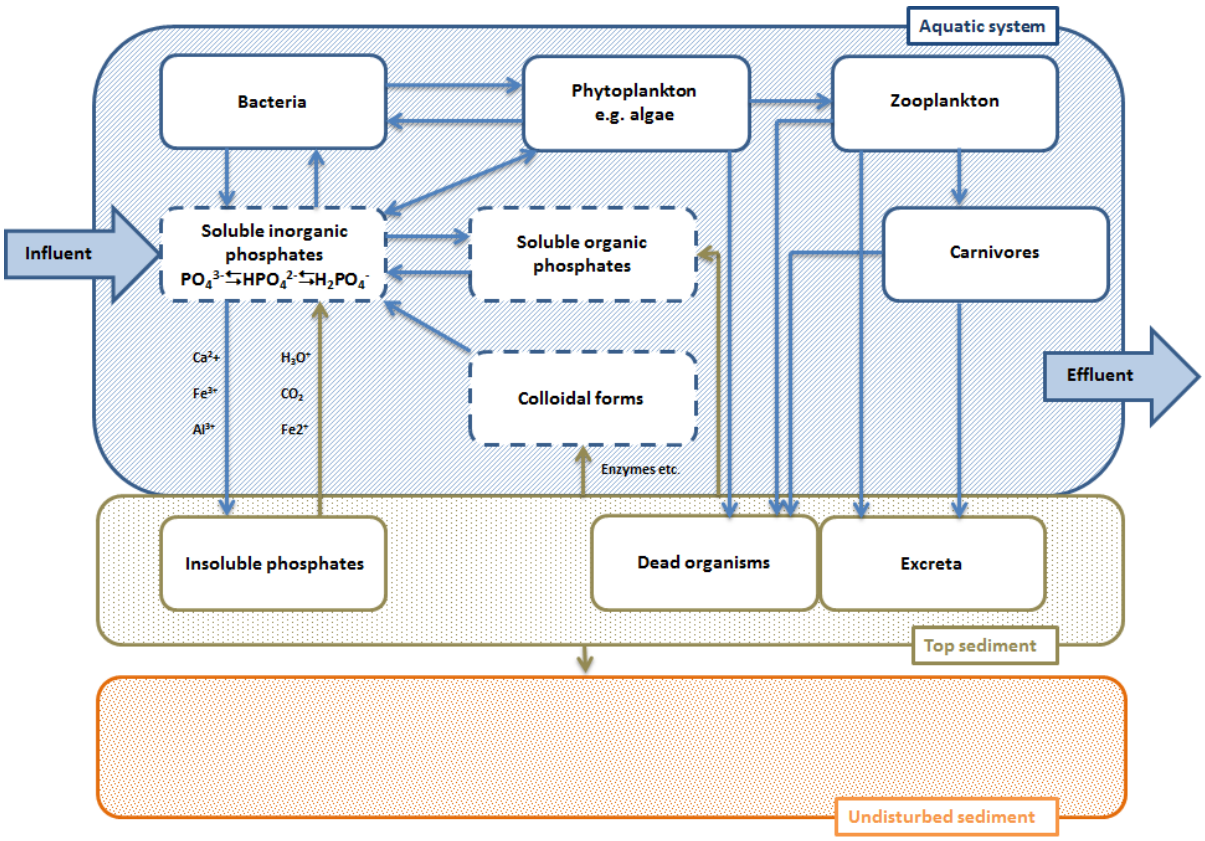

Figure 1.2: The aquatic P cycle, adapted from Emsley and Hall (1976). Flows of P represented by arrows between the various pools. Dashed lines indicate pools of soluble P.

P can be present in the environment in a variety of forms. An analytical distinction is often made between dissolved or particulate forms of P. P that does not pass through a 0.45 μm membrane filter is in a particulate form, and the P passing through the filter is in a dissolved form. Another important distinction is whether P is molybdate reactive (Murphy and Riley, 1962). Generally, molybdate reactive P tends to be inorganic and readily available for uptake for biological activity. P which is not molybdate reactive is often considered inorganic and unreactive. The major pool of P affecting the eutrophication status of a waterbody in Figure 1.2 is therefore soluble inorganic phosphates, also known as soluble reactive phosphates (SRP). This pool of P is readily available for uptake by organisms leading to the symptoms associated with eutrophication.

1.1.2 Eutrophication

Historically surface waters have been seen as a means to dilute and remove pollution away from society, leading to the widespread degradation of rivers and lakes across the world. Pollutants enter surface waters from either point or diffuse sources. Point sources are clearly identifiable, localised sources of pollution, such as a sewage outfall. Diffuse sources are less identifiable, and arise from a non-localised source, such as soil erosion. The input of diffuse pollution is variable over time and is dependent on weather conditions.

The major environmental consequence of P pollution in waterbodies is eutrophication. In aquatic systems, P tends to be the limiting factor in biological activity, therefore when P is imported biological activity may increase dramatically. Under certain conditions 0.45 kg P applied to an aquatic system can lead to the growth of over 159 kg of green algae (EA, 2007).

Eutrophication has four major impacts: increased plant growth, oxygen depletion, pH variability and effects on plant species (Sharpley et al., 1994). Upon eutrophication, rapid growth of algae and phytoplankton species occurs, creating blooms which can inhibit sunlight penetration of the water column and stress submerged vegetation.

Following a phytoplankton or algal bloom, the bloom is decomposed by bacteria. This process has a high biological oxygen demand (BOD), leading to a decline in the dissolved oxygen (DO) present in the aquatic system (Sharpley et al., 1994). Low DO concentrations lead to suffocation of respiratory fauna, resulting in death. In 2002 there were 30 major fish kills in England and Wales, which were the result of poorly oxygenated water caused by algae decomposition (EA, 2007). The incidence of blue-green algae blooms during a ten year period in England and Wales highlights the frequency of eutrophic conditions (Table 1.1).

Table 1.1: Incidence of reported blue-green algae blooms in England and Wales for a ten year period (1990-1999), adapted from Pretty et al. (2003).

Region	No. Incidents	No. Waterbodies	Blooms waterbody^{-1} year^{-1}
Anglian	624	440	1.42
Midlands	928	635	1.46
North East	365	241	1.52
North West	486	305	1.59
Southern	95	85	1.12
South West	649	452	1.44
Thames	551	368	1.50
Welsh	295	184	1.60
Total	3993	2710	1.47

In terms of impact to human society, P pollution can also lead to numerous problems associated with water quality. Blooms can clog filters at water treatment plants reducing the efficiency of treatment systems (Sharpley, 1994). Certain species of blue-green algae produce toxins which can be hazardous to human and animal health (Kotak et al., 1993). Algal blooms can contribute to the formation trihalomethane during chlorination at water treatment plants, which is carcinogenic (Palmstrom et al., 1988) and can also lead to discolouration or decreased palatability of the water (Sharpley et al., 1994).

The effects of eutrophication have an associated financial cost. The total cost of eutrophication in England and Wales was calculated in 2002 as between £129.8 M and £169.1 M yr^{-1}, of which £75 - 114.3 M yr^{-1} was as a result of social and ecological damage, and £54.8 M yr^{-1}, the expense of policy response (Pretty et al., 2003). Although the damage costs originate from a variety of sources, seven main contributing factors were identified (Table 1.2).

Table 1.2: The cost of eutrophication in terms of social and ecological damage, adapted from Pretty et al. (2003).

Social and Ecological Damage	Cost (£M yr^{-1})
Reduced value of water front dwellings	9.78
Drinking water treatment	19.98
Reduced recreational and amenity value of water bodies	9.61-33.39
Drinking water treatment costs for removal of algal toxins and decomposition products	18.91
Reduced value of non-polluted atmosphere	5.10-7.96
Negative ecological effects on biota	7.31-10.07
Net economic losses from the tourist industry	2.93-10.07

The treatment of P-related pollution will therefore provide a range of social, economic and environmental advantages. The economic benefits can be used to offset the costs involved with the legislative procedure and the implementation of treatment schemes.

In an attempt to achieve "good ecological status" in all inland water bodies in the EU, the WFD was agreed in 2000 (EC, 2000). This is a legal agreement between EU member states to appoint bodies to oversee, and achieve, 'near natural' water quality and quantity standards of surface waters by 2015. The responsible bodies have been appointed as the Environment Agency (EA) for England and Wales and the Scottish Environmental Protection Agency (SEPA) for Scotland.

For surface waters, the objective of the WFD is to achieve "good" ecological and chemical quality status. "Good" ecological status is achieved if there is only a slight departure from the biological community that would be expected under conditions of minimal anthropogenic impact (Kallis and Butler, 2001). For rivers in the UK, the target maximum P concentrations for SRP are 0.05-0.12 mg L^{-1} to achieve "good

ecological status", and 0.02-0.05 mg L^{-1} to achieve "high ecological status" (UKTAG, 2007).

1.1.3 Phosphorus as a finite resource

Across most of the world, P is being used in an open, one-use system, whereby P is mined, refined into fertilisers and applied to agricultural land to boost crop yield. This system is unsustainable and is only possible with a constant supply of low-cost fertiliser.

Global supplies of P rock that is economically viable to mine are estimated at 18,000 million tonnes (Jasinski, 2008) which would last for the next 50-100 years, based on the demand for P rock over the past decade. Using a similar technique to that implemented by Hubbert (1949) to investigate peak oil, peak maximum P-production could occur by 2033 (Cordell et al., 2009).

The majority of remaining P rock reserves which are economical to mine are controlled by a few countries, notably Morocco, China and the USA. Morocco has a near-monopoly over the reserves located in the Western Sahara, whilst China has drastically reduced export of P to secure domestic supply. It is estimated that the USA has less than 30 years supply, whilst Western Europe is entirely reliant upon imports (Cordell et al., 2009).

Cordell et al. (2009) note that whilst P production will follow a peak production curve in a similar manner to non-renewable resources such as oil, peak P production will differ in two important ways. Firstly, oil can be replaced with alternative sources of energy once resources are depleted, but there is no alternative for P in the food chain. Secondly, oil can only be combusted once, whilst P has the potential to be recovered from the food chain and recycled where technically and economically feasible. The recovery of P from domestic, industrial or environmental sources, will decrease reliance on an increasingly scarce supply of P rock.

1.2 Sources of P pollution

P pollution originates from a variety of sources and the enrichment of surface waters will most likely be a combination of several of these. Different sources of P pollution have different characteristics, and therefore require different treatment approaches. These sources are discussed below.

1.2.1 Septic tanks

Septic tanks (Figure 1.3) are used to treat a household's wastewater when connection to mains sewerage is not possible or economically viable. The tank is sized so that flow is regulated through the system at a constant rate allowing solids to settle within the tank. Effluent from the tank should therefore be free from any particulate matter, but will still have high concentrations of contaminants which are in solution, such as P and nitrogen.

Most commonly, effluent from a septic tank passes through a subsurface area called a leachfield which removes contaminants and nutrients, via adsorption, to soil organic matter and minerals. Recommendations are provided by SEPA and the EA for suitable conditions for septic tank installation, providing guidance on the distance to surface water, the water table, and the hydraulic properties of the soil (Grant and Moodie, 1997). The location of septic tanks is often determined more by need, however, than by the presence of acceptable conditions. This means that many septic tanks are inappropriately situated and untreated effluent can flow into adjacent water resources, enriching them with nutrients.

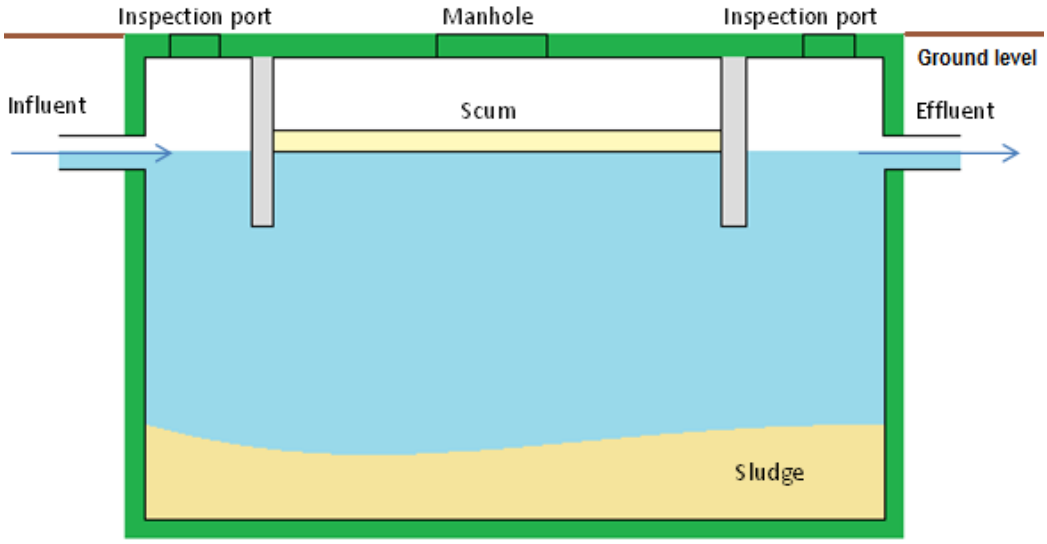

Figure 1.3: Diagram of a septic tank: Influent enters the tank from the left of the diagram with solids settling to the bottom, forming a sludge layer. Light solids float to the top of the tank to form a layer of scum. Effluent leaves the tank to the right and enters a treatment system, typically a leachfield. Inspection ports and manholes allow the septic tank to be examined and sludge to be removed.

Typically, the influent concentration of total phosphorus (TP) to a septic tank is ~25 mg L^{-1}, with 35% as inorganic orthophosphate and the remaining 65% in organic forms (Canter and Knox, 1985). Due to anaerobic bacterial digestion occurring within the septic tank, the majority of the influent P is converted into soluble orthophosphate, with up to 85% of septic tank effluent P in this form. Owing to variations in septic tank operation, and loads entering the system, the effluent P concentration is variable, but is typically 10-15 mg TP L^{-1} (Canter and Knox, 1985).

Upon discharge from a septic tank, P in the effluent is retained by soils in the leachfield. P should thus not enrich ground or surface waters if the leachfield is designed appropriately (Canter and Knox, 1985). In the soil, P ions are chemisorbed onto the surfaces of Fe and Al minerals under acidic to neutral soil conditions and onto Ca under neutral to alkaline conditions (Bouma, 1979). Enfield et al. (1975)

determined that the conversion of orthophosphate to insoluble P compounds by soil is primarily related to concentrations of Fe, Al and Ca.

Septic tanks are not located according to site suitability, however, but where dwellings cannot be connected to sewerage. This means that leachfields may not be appropriate owing to compromises made in terms of available land, soil type or distance from a water course; septic tanks can therefore lead to aquatic P pollution (Viraraghaven and Warnock, 1976; Peavy 1978). Furthermore, septic tanks are often poorly maintained, commonly as a result of infrequent de-sludging which is required every 1-2 years, or as the result of broken pipework affecting the tank's efficiency and leading to pollution incidents. Leachfields can also become saturated with P and therefore P will pass through the leachfield, leading to pollution.

The exact scale of P pollution originating from septic tanks is unknown. For example, in Scotland little is known regarding the number of septic tanks present, their age, size, location or degree of maintenance. A case study of the Loch Leven catchment in Scotland estimated that less than 10% of the septic tanks in the catchment were registered with SEPA (Dudley and May, 2007).

The contribution of septic tanks to the P loading of surface waters is thus also not fully understood, and the only data available are estimates. The contribution of septic tanks to the P loading of all surface waters in Scotland has been estimated as 2.6% (SNIFFER, 2006), whilst the contribution to individual water bodies can be much higher, e.g. 17.5% of P loading to Loch Flemington, Inverness (Frost, 1996) and 22% to Loch Ussie, Ross-shire (May and Gunn, 2000).

In an attempt to gain a better understanding of the number and distribution of septic tanks in Scotland, all such systems must now be registered with SEPA. To ensure registration has occurred, all new septic tanks require authorisation prior to installation (SEPA, 2008). The registration process also facilitates targeted education

about the maintenance requirements for the owners of dwellings with septic tanks, reducing the likelihood that the systems fail and pollute the environment.

Treatment measures do exist for reducing the P concentration in septic tank effluent, such as dosing the septic tank with alum, lime and ferric chloride. The addition of such products lead to the tank needing emptying on a more regular basis which can prove costly however. External filters based upon Fe-sands and Al-muds have been used to treat septic tank effluent with up to 95% of P effluent being adsorbed (USEPA, 2002). However these filters have short lifespans, typically exhausting their capacity within three months to two years and are very expensive, costing US$5,000 to US$11,000. For effective operation of a filter it is essential that the septic tank is working efficiently to remove SS from solution to minimise clogging of the filter.

1.2.2 Wastewater treatment plants

The EC Urban Wastewater Treatment Directive (1991) has the objective of protecting the natural environment from the adverse effects of urban wastewater (EC, 1991). The directive requires the collection and treatment of wastewater produced by an agglomeration of over 2000 population equivalents (p.e.). Secondary treatment is required for WWTPs serving 2000 to 10,000 p.e., with P concentrations in effluent not to exceed 2 mg P L^{-1}. Advanced treatment is required for WWTPs serving more than 10,000 p.e., with P concentrations in effluent not to exceed 1 mg L^{-1}.

Secondary treatment at a WWTP to remove P usually involves biological or chemical processes. Activated sludge is a biological contact treatment process, whereby bacteria and other microorganisms are utilised to remove contaminants. Effective P removal requires the activated sludge to have a high proportion of polyphosphate accumulating organisms; the sludge is aerated to ensure maximum biological growth and therefore P uptake (Junkins et al., 1983). The P removal rate achieved by biological systems is not constant and varies with a number of factors, such as BOD, the P concentration of the influent, and temperature. This variability

in efficiency can often lead WWTP operators to additionally utilise chemical precipitants to ensure that P concentrations in the effluent do not exceed discharge consents.

P precipitation requires the addition of a coagulant, typically lime, alum, sodium aluminate, ferrous sulfate or ferric chloride (Vesilind, 2003). The dose rate of the additive can be altered with influent P concentration to achieve the target effluent concentration. This technique is more reliable than biological treatments in ensuring that discharge consents are met, has a smaller equipment footprint, and is easier to operate. However, the metal salts come at a considerable expense (US$200- US$300 per tonne), are typically a mined raw material and are therefore unsustainable. Another issue with coagulants is the large volume of sludge generated, which will require disposal.

Alternative technologies need to be robust; ensuring P removal from wastewater streams over a range of influent P concentrations, concentrations of competing ions, pH, BOD, and temperature. Even after treatment, WWTPs still provide a point source of P pollution into surface waters, with discharge consents for P from 1 mg P L^{-1} upwards. Further treatment of this effluent could occur prior to discharge into water bodies.

1.2.3 Fish farms

As this research concerns inland surface waters, marine fish farms will not be discussed. Only inland freshwater fish farms which discharge into surface waters are examined here.

With 135 freshwater production units producing 270,000 tonnes in 2007; Scotland is the largest producer of farmed salmon in the EU and the third largest producer globally (Scottish Natural Heritage, 2010). Of other fish farmed in Scotland's inland

waters, the most significant is rainbow trout, of which 7,414 tonnes were produced in 2007, along with smaller amounts of sea trout and Arctic char farmed.

Scottish salmon farms tend to use water from low order headwater streams due to the requirement for clean unpolluted waters; salmonoids are sensitive to low DO levels, intolerant of pollution and their optimum temperature range is 5-15°C (Tello et al., 2009). Fish farms therefore abstract water from these upland streams, returning discharge downstream. They are regulated by SEPA who set abstraction licences and discharge consents. P is produced within the fish farm by direct excretion from the fish (Clark et al., 1985) and via leaching from uneaten food (Brinker and Rosch, 2005). Compliance with discharge consents for P restricts the size and productivity of inland aquaculture. On-site treatment methods to reduce P concentrations in the discharge tend to be low-cost and low-technology based, most often a system of settlement ponds prior to discharge which can prove largely ineffective. A reliable and low-cost treatment mechanism could allow for an enlargement of such fish farms resulting in greater productivity and profitability.

1.2.4 Farmyard runoff

Farmyards, including buildings, livestock gathering areas, access tracks and hardstandings, provide a focal point of farming operations and are a source of various environmental pollutants (Edwards et al., 2008). Soluble P concentrations of 15 - 20 mg P L^{-1} have been measured in runoff originating from a dairy farm (Dunne et al., 2005), whilst the addition of artificial rainfall to cattle yards produced runoff with a P concentration of up to 11.6 mg P L^{-1} (Hively et al., 2005).

Farmyard effluents range in contaminant content but, if originating from areas where faecal matter is stored or deposited, they will contain microbial and pathogenic organisms, high concentrations of nutrients, potentially toxic elements such as pesticides, and metabolic substrates such as labile organic carbon (Edwards et al., 2008). The nature of the effluent will vary not just between sites, but also over

time, with factors such as the nature of farm practices, rainfall and transport pathways affecting the contamination of overland flow (Edwards et al., 2008). The generation of farmyard runoff can also vary over time from episodic storm related events to almost continuous seepage, such as from silage or manure stores.

If the formation of farmyard runoff cannot be prevented, treatment tends to occur in ponds, wetlands or buffer strips (Poe et al., 2003; Dunne et al., 2005; Carty et al., 2008) in which pollutants are removed by a mixture of physical, chemical and biological processes. A variety of these processes can remove P from farmyard runoff. Firstly, P can be removed by physical processes in which particulate bound P can be filtered out of suspension by wetland vegetation acting as a hydrological baffle and optimised by low flows and dense vegetation cover (Carty et al., 2008). Particulate bound P can also settle within a wetland system by gravity if flow velocity and disturbance are low. Within the wetland, P can be removed from solution via biological processes and utilised by plants and micro-organisms for cellular growth. Chemical processes occurring at the soil/sediment-water interface can also remove P by precipitation and sorption onto Fe, Al and Ca (Carty et al., 2008).

Farm ponds can treat a range of contaminants, however large wetland systems are required to reduce P concentrations (Braskerud, 2002). Smaller systems can be used with a P-removing substrate (Drizo et al., 1999) to minimise the required surface area whilst still ensuring low P export.

1.2.5 Golf courses

Golf courses can act as a source of nutrient pollution as they are often fertilised to ensure healthy grass growth and have small streams intersecting them which provide a pathway for P to enter larger watercourses. P export from golf courses is often comparable to that from agricultural land (Winter and Dillon, 2006).

This P export is largely site dependant, however and varies with management. Appropriate treatment of such pollution will thus also vary with site. P concentrations of up to 0.145 mg TP L^{-1}, measured during two years monitoring a small stream running through a golf course, were attributed to poor turf management techniques (Kunimatsu et al., 1999). In another study, P concentrations measured during storm events in the stream draining a small 1.75 ha golf course in South Carolina, USA, had mean and maximum P concentration of 1.07 and 2.44 mg P L^{-1}, respectively (Line et al., 2002). Similar best practices to those recommended for agricultural land could be implemented to reduce P enrichment of surface waters from golf courses. In-stream filter units may also be applicable to treat P pollution originating from golf courses, especially where P concentrations are high and flow rates are low so that an appropriate contact time is provided.

1.2.6 P release from lake and river sediments

Significant P concentrations can occur in a waterbody due to internal loading. Sediments may adsorb various pollutants, such as P, and this can accumulate on the river or lake bed, acting as a pollutant source after the water quality of the overlying waterbody has improved (Lijklema et al., 1993; Kim et al., 2003). Mechanisms of pollutant release from aquatic sediment include advection, molecular diffusion, ion exchange and biologically mediated changes (Kim et al., 2003).

The release rate of P from sediments has been shown in column experiments to be dependent upon a range of factors such as pH, DO and temperature (Kim et al., 2003). The availability of DO greatly affects the P release rate from sediments. Under anaerobic conditions, 105 mg m^{-2} P $week^{-1}$ was released into the overlying water column, whilst only 40 mg m^{-2} P $week^{-1}$ was released under highly aerobic conditions when DO = 7 mg L^{-1}. A fivefold increase in P release rate resulted from an increase in water temperature from 2°C to 35°C, indicating that sediments are most likely to release P during the summer months. This coincides with the time of year when P is more likely to stimulate biological activity and result in eutrophication.

pH can also affect the release of P, although release rates are lowest under normal surface water conditions, pH 7-10. Whilst the effect of temperature cannot be mitigated against, it is suggested that ensuring aerobic conditions and a neutral pH will reduce the release of P from enriched sediments (Kim et al., 2003).

In shallow lakes in summer, an increase in water temperature drives internal loading of P from enriched sediments. In contrast, in stratified deeper lakes the occurrence of anoxic conditions in the hypolimnion due to microbial activity, and a lack of mixing, results in the release of P bound to Fe in the sediment (Petticrew and Arocena, 2001; Lake et al., 2007). Understanding the driving factors responsible for internal loading is crucial for the design of an effective method for reducing the P loading from sediment. Using a Fe dosing system in deep lakes may reduce P loading over winter months, only for it to be re-released under warmer conditions. Alternative P treatment techniques include dosing with Ca (Varjo et al., 2002) or Lanthanum products (Phoslock, 2007). Upon application, these substances remove P from the water column, before forming an adsorbent layer on the top of the lake bed which further inhibits P release.

In shallow lakes, where anoxic conditions do not develop, Fe dosing systems can be utilised to reduce internal loading of P (Deppe and Benndorf, 2002). Fe(II) salts may be preferable in dosing technologies for the removal of P than Fe(III). A combination of laboratory and field experiments demonstrated that the use of Fe(II) salts resulted in delayed floc formation, and a higher P removal potential. Additionally, the buffering capacity of the receiving water is less stressed with the addition of Fe(II) salts, and it is therefore recommended in soft water environments (Deppe and Benndorf, 2002).

1.2.7 Diffuse pollution

Whilst point sources of pollution are clearly identifiable and enter surface waters at a specific point, such as a pipe outfall; diffuse pollution occurs when pollutants

enter surface waters as the result of rainfall, leaching from soils, and surface runoff (EUWFD, 2010). Examples of diffuse pollution include the export of nutrients from agricultural lands via runoff, contaminants from roads and paved areas being washed into surface waters, and the atmospheric deposition of contaminants originating from industry and fossil fuel combustion (EUWFD, 2010).

Agriculture has been identified as a major contributor to inland aquatic pollution in Great Britain, with 20% of P in Great British rivers originating from agricultural land (White and Hammond, 2009). In Scottish rivers, 14.2 % originates from agricultural land, with 56.5 % from households, 17.8 % from industrial sources and 11.6 % present as background concentrations.

Due to the agronomic management of soils, with an emphasis on maximising yields and farm incomes, intensive P fertilisation has occurred in the UK to replace P uptake by crop growth and any losses from the system (Withers et al., 2001). Mis- and over- application of P leads to availability for export from the land, to aquatic systems, via a variety of transport mechanisms.

The loss of P from a soil into surface waters is dependent upon a range of factors, such as land management, rainfall intensity and duration, P form, and P availability (Daniel et al., 1998). Surface runoff, including subsurface flow through tile drains, is the dominant mechanism by which P is exported to surface waters in most catchments. Consequently, P export from agricultural land will be greatest during storm events when surface runoff is most prevalent (D'Arcy and Frost, 2001). Whilst the P content of solution infiltrating through the soil tends to be low due to adsorption of P onto P-depleted sub soils (Daniel et al, 1998).

The majority of P lost from cultivated land to surface waters tends to be in particulate form, either adsorbed to the surfaces of soil particles or associated with organic matter (Sharpley et al., 1992), with any other P exported in a dissolved form.

Runoff from grass and forest dominated land, where erosive rates are low, carry little sediment and therefore P is found predominantly in the dissolved form. Dissolved P tends to be readily available for biological activity, whilst P tends to be slowly released from particulate forms, providing a long term supply of P to an ecosystem (Daniel et al., 1998).

Surface applications of manure and fertilisers can also lead to P being lost from agricultural land without ever becoming part of the soil matrix. This source of P pollution is termed "incidental" losses (Haygarth and Jarvis, 1999) and can account for substantial exports of P from agricultural land. Manures and fertilisers have a high soluble P content and as such, P is readily available for export following application via subsurface and overland flow (Withers et al., 2003). P export due to incidental losses can be controlled by a range of management strategies, e.g. avoiding application of manure to steeply sloping land, incorporating a buffer strip on the agricultural land, and avoiding application to waterlogged soils (Chadwick and Chen, 2002).

Tackling diffuse pollution requires management of the sources and pathways of P export, with opportunities to reduce the P transfer from sources to surface waters by the implementation of best management practices (D'Arcy and Frost, 2001). Up to 90% of the P export from a catchment can occur over a couple of storm events and from relatively small areas of land termed "critical source areas" (Pionke et al., 1997). Identifying these areas, and either removing the source of P, or disconnecting them from hydrological pathways by means of land-use management, are crucial to reducing diffuse pollution.

Attempts to combat point source pollution has proved highly successful in the 1970s and 1980s in the UK, with the introduction of discharge consents allowing polluting bodies and individuals to be held to account for pollution incidents (Baldock and Bennett, 1991). In the case of diffuse pollution, polluters cannot always be easily

identified, however, and therefore diffuse pollution remains a major barrier to achieving non-polluted surface waters.

1.2.8 Groundwater

P pollution is not usually a concern in groundwater systems as P-depleted sub soils have a tendency to adsorb P (Sparks, 2003). This principle is exploited in septic tank leachfields to remove nutrients from effluents prior to discharge into surface waters. Constant loading of P-rich effluents into soils, such as with leachfields and sewage lagoons, can lead to the saturation of sub soils with P, however, thus allowing the transfer of P through soils and into groundwater (Baker et al., 1998). As a result of various sources of pollution, such as septic tanks and leaking sewers, many groundwaters in the UK have median P concentrations above the ecological thresholds for surface waters (Holman et al., 2010).

Permeable reactive barriers (PRBs, Figure 1.4) can be used on sites where the soils are saturated with P to intercept and treat P-enriched through-flow and groundwater. Because the flow rate of groundwater is relatively low, filter systems, such as PRBs, are successful treatment systems. When designed correctly, they can remediate pollution from a site for a number of years, with very little maintenance.

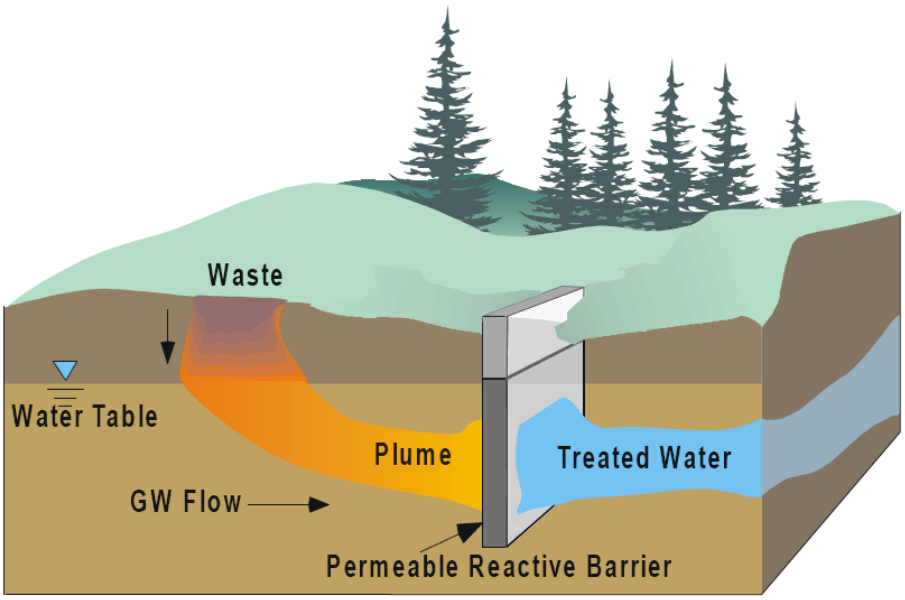

Figure 1.4: The operation of a permeable reactive barrier. A vertical trench is dug and backfilled with a reactive substrate which intercepts the groundwater pollutant flume, treating the water as it infiltrates through the PRB. From USEPA (1998).

Al, Fe and Ca (Baker et al., 1998; Olivera et al., 2010; Miller et al., 2011) based substrates have been proposed for the treatment of P in PRBs. The use of Fe based substrates in PRBs was pioneered in the 1990s (e.g. Blowes and Ptacek, 1994) with continued research since then (Cundy et al., 2008). Of the c.200 PRBs installed worldwide by 2004, 120 of them were Fe based (ITRC, 2005), most containing zero-valent iron, utilised to treat a range of contaminants in groundwater including metal and radionuclide pollution (Cundy et al., 2008). Zero-valent iron cannot typically be used to treat P enriched waters, but of note is the development of a PRB containing basic oxygen furnace slag which has been implemented to treat P pollution from septic tank outlets (Baker et al., 1998; Smyth et al., 2002). Laboratory column experiments with a packed substrate have been used to successfully remove P from solution for a period of eight years, with field scale trials reducing P concentrations in septic tank effluent to less than 0.05 mg P L^{-1} (Smyth et al., 2002).

Long term column experiments investigated the potential of a permeable reactive mixture (containing silica sand, limestone and Fe-oxides) for use as a PRB substrate (Baker et al., 1997). The mixture removed 85-100 % TP from solution over the course of a 3.6 year experiment. The influent (3.3 mg P L^{-1}) was continuously pumped through the column at a flow rate equivalent to that of groundwater, resulting in 1250 pore volumes passing through the column. The P removal mechanisms of the alkaline Fe-oxide mixture were investigated revealing adsorption onto iron oxides and precipitation of hydroxyapatite as the dominant removal mechanisms.

1.3 Ochre formation

Ochre, an iron rich material, is generated when minewater is treated. Due to its high concentrations of Fe, Ca and Al complexes it is suggested as a potential filter substrate for the removal of P from surface waters. The generation of minewater is discussed below in a UK and global context, before describing the formation of ochre. The potential application of ochre to treat P enriched waters is then discussed.

1.3.1 The generation of minewater

Due to the increasingly unprofitable nature of metal and coal mining in the UK during the late twentieth century, the majority of deep mines were closed. During operation, water was pumped from the mines so that the minerals could be exploited. Following abandonment, pumping of water ceased, resulting in the rebound of the water table and the subsequent release of polluted water into surrounding water bodies. The Coal Authority, in partnership with the EA, has identified over 100 polluting discharges which are resultant from coal mining activities. These impact on 141 waterbodies, a total of 2276 km of river, putting them at risk of not achieving "good" status under WFD guidelines (EA, 2008). The same research was also conducted for minewater discharges originating from non-metal mines, finding 315 waterbodies, 2858 km of river reach, at risk of not achieving "good" status (EA, 2008).

Minewater is generated when sulphidic minerals in a mine are exposed to oxygen and water, resulting in the production of acidic waters containing metals and sulphates (Brown et al., 2002). In undisturbed conditions, these minerals are below the water table and under anaerobic conditions, resulting in a slow weathering rate. The process of mining, and subsequent abandonment, leads to the exposure of sulphide minerals to oxygen and water, generating contaminated minewater.

The most common mechanism of minewater generation is through the oxidation of pyrite (FeS_2), whereby pyrite is dissociated (Equation 1.2), and the resulting ferrous iron (Fe^{2+}) is oxidised (Equation 1.3), to ferric iron (Fe^{3+}) (Brown et al., 2002).

$$FeS_{2(s)} + \frac{7}{2}O_2 + H_2O \rightarrow Fe^{2+} + 2SO_4^{2-} + 2H^+ \qquad \text{(Equation 1.2)}$$

$$Fe^{2+} + \frac{1}{4}O_2 + H^+ \rightarrow Fe^{3+} + \frac{1}{2}H_2O \qquad \text{(Equation 1.3)}$$

The creation of H^+ in Equation 1.2 means that mine water tends to be acidic. When the pH of the mine water is above 2.3 to 3.5, the ferric iron is no longer soluble and will precipitate out of the water column (Equation 1.4), (Brown et al., 2002).

$$Fe^{3+}_{(s)} + 3H_2O \rightarrow Fe(OH)_{3(s)} + 3H^+ \qquad \text{(Equation 1.4)}$$

This has the effect of lowering the pH and reducing any ferric iron remaining (Equation 1.5), forming additional acidity and ferrous iron.

$$FeS_{2(s)} + 14Fe^{3+} + 8H_2O \rightarrow 15Fe^{2+} + 2SO_4^{2-} + 16H^+ \qquad \text{(Equation 1.5)}$$

Minewater treatment focuses upon encouraging the oxidation of ferrous iron to ferric iron (Equation 1.4), leading to the formation of a Fe precipitate. The precipitates accumulate as a sludge known as ochre. This contains all of the contaminants that have precipitated out of solution, and any chemicals added to aid

this process. The chemical composition of ochre thus varies with site and treatment method.

The rate determining step in the sequence of equations forming minewater is the oxidation of ferrous to ferric iron (Equation 1.3, Singer and Stumm, 1970). Fe oxidising bacteria, most active between pH 2-4, can accelerate this process by a factor larger than 10^6 (Sobek et al., 1990), whilst bacterial mediation can increase the overall rate of acid generation throughout the weathering process by a factor of 20 (Brown et al., 2002). Following the initial oxidation of FeS_2, subsequent oxidation of pyrite by ferric iron that remains in solution occurs rapidly (Equation 1.5). The weathering of pyrite to produce acidity is self-perpetuating. Whilst the pH of the environment may initially cause $Fe(OH)_3$ to precipitate (Equation 1.4), this reaction produces acidity, lowering pH and allowing more ferric iron to remain in solution. Ferric iron in solution then leads to the further oxidation of pyrite (Equation 1.5), and a decline in pH.

Generation of minewater is highly site-specific and varies with time. Key factors influencing the acidity and metal content of minewater are (Ritcey, 1989):

- Sulphide grain size and surface area
- Porosity and permeability of the deposit
- Nature of the parent material
- Nature of the sulphide ore
- Nature of the acid-consuming minerals
- Various environmental factors influencing the activity of micro-organisms.

Weathering of sulphides will continue to produce contaminated minewater as long as they remain exposed, so contaminated minewater is expected to persist for hundreds of years after mining operations have ceased (Brown et al., 2002). Accurate predictions of the severity and longevity of minewater discharges are

fraught with uncertainty due to the complex geology and hydrogeology of the systems (Younger, 1997).

1.3.2 UK metal mines

Metal mines have existed in the UK from at least Roman times, with production peaking in the 18th and 19th centuries (Brown et al., 2002). Predominantly Pb, Zn, Sn and Cu were mined, as well as lesser amounts of Ag, Si, As and small quantities of other minerals. The mining network is extensive, complex and the full extent is unknown. In addition, unreclaimed spoil heaps are widespread in former mining districts, and are a major source of contaminated minewater. In combination, these sources of contamination have the capability to affect whole catchments (Brown et al., 2002). The impact of abandoned metal mines on watercourses was assessed by the EA (2008) (Table 1.3).

Table 1.3: WFD water bodies impacted by abandoned metal mines (adapted from EA, 2008). 'At risk' indicates that the waterbody is in danger of not achieving WFD good status due to minewater pollution. Omitted River Basin Districts contain no waterbodies at risk.

River Basin District	River water bodies at risk	River length affected (km)	(%)
Scotland	2	18	<1
Solway Tweed	3	38	<1
Northumbria	11	212	6
North West	12	155	3
Humber	8	348	4
Dee	9	105	14
Western Wales	87	687	17
Severn	31	274	4
South East	1	40	2
South West	153	981	14
Total	**315**	**1,858**	**5**

1.3.3 UK coal mines

Major seams of coal have been mined across the UK, most notably in central and northern England, south Wales and central Scotland. Almost all coal mines are now abandoned in the UK. Whilst the exact number is unknown, the Coal Authority reports that there are approximately 10,000 abandoned coal mines in the UK putting 141 water bodies at risk from minewater pollution (Table 1.4).

Table 1.4: WFD water bodies impacted by abandoned coal mines (adapted from EA, 2008). 'At risk' indicates that the waterbody is in danger of not achieving WFD "good status" due to minewater pollution. Omitted River Basin Districts contain no waterbodies at risk.

River Basin District	River water bodies at risk	River length affected (km)	(%)
Scotland	45	436	2
Solway Tweed	3	21	<1
Northumbria	36	494	14
North West	25	383	8
Humber	37	390	4
Dee	1	6	1
Western Wales	18	231	6
Severn	17	310	4
South East	4	18	1
Total	**141**	**2276**	**4**

The UK Coal Authority was founded 1994, under the Coal Industry Act (1994). It has many responsibilities, including licensing coal mining operations, providing information on coal reserves, and implementing minewater remediation schemes. In collaboration with the EA and SEPA, minewater discharges are prioritised and treated under the Coal Authority's minewater treatment programme, initiated in 1996 (Banks, 2003). By August 2002, 15 MWTPs were in operation (Banks, 2003) and a total of 33 were in operation by 2010.

1.3.4 Global minewater

The issue of contaminated minewater is not restricted to the UK and mining operations across the world have associated contaminated minewater issues. In developing countries, the environmental awareness, technology and capital may not be available to restrict the influx of contaminated minewater into the natural environment (Brown et al., 2002). Legislation plays a key role in identifying and tackling minewater pollution, with Canada and the USA forerunners for tackling the issue (Brown et al., 2002). With over 15,000 ha of acid generating mine waste sites, the cost of remediation in Canada is estimated to be US$4 billion over the next 20 years (Brown et al., 2002). In the USA over US$1 million is spent daily to treat contaminated minewater (Kleinmann, 2006), with abandoned mines reducing the quality of over 19,000 km of rivers and over 73,000 ha of lakes and reservoirs (Brown et al., 2002). The production of contaminated minewater is therefore an issue of global environmental concern, which will need sustained investment over the course of future decades, and possibly centuries, in order to remediate.

1.3.5 Minewater treatment

Treatment of contaminated minewater is usually conducted by one of three approaches. The first is to prevent, or restrict, the occurrence of minewater reactions involving the oxidation and hydrolysis of sulphidic minerals. This approach prevents the formation of minewater by eliminating one or more of the components required for the oxidation reactions to occur (Brown et al., 2002). Approaches include controlling the weathering rate of sulphidic material through reducing bacterial activity, or by adjusting pH or temperature.

Secondly, if the generation of contaminated minewater cannot be prevented, then its movement may be controlled by restricting water flow through the sulphidic rocks by diverting surface and ground flows, and preventing infiltration into the rocks (Brown et al., 2002). Whilst this can prove a cost-effective measure, mine workings in the UK are often a complex labyrinth of underground and interconnected

chambers and tunnels. Restricting flow into the area thus often proves unfeasible. Furthermore, mine working maps may be incomplete or inaccurate and thus misleading to the scale of the workings at a site.

The final approach to alleviating contaminated minewater is to collect the minewater, neutralise any acidity and remove any metals that are in solution (Brown et al., 2002). This is conducted at MWTPs, and the two products of the process are treated water and ochre. There are two types of MWTPs: active systems which require continuous inputs of chemicals, energy and maintenance; and passive systems which are designed to be self-sustaining or require a small amount of maintenance, e.g. removal of ochre annually. Whilst passive treatment systems have a larger footprint, they have lower capital and maintenance costs and are therefore often used to treat contaminated minewater originating from abandoned mines.

1.3.6 Ochre formation

Treatment of minewater in passive MWTPs tends to focus upon encouraging the oxidation of ferrous iron to ferric iron, leading to the formation of a Fe precipitate (Equation 1.4). The precipitation of Fe and other metals is enhanced in active treatment plants by implementing techniques such as pH modification or the addition of oxidising agents or flocculants (Heal et al., 2003a). In both active and passive systems, these processes occur in sedimentation tanks or constructed wetlands, allowing deposition of precipitates and accumulation of ochre.

Because it is formed in an aquatic setting, ochre has a high water content (80-95%) which makes it difficult to dispose of, handle, and transport. Ochre can be mechanically or chemically dried, but most commonly it is air-dried in drainage lagoons before centrifuging to remove moisture content prior to disposal. Ochre accumulation in MWTPs across the UK is estimated to be 3.2×10^4 tonnes per annum (Hancock, 2005), highlighting the scale of the issue, and the need for research into alternative uses of ochre. With no current alternative end-use, ochre is disposed to

landfill. A variety of potential end-uses have been proposed for ochre, discussed in Chapter 2, ranging from use as a cement pigment, a raw material in the steel industry, and as a soil amendment.

1.3.7 Ochre as a P-adsorbent: Mechanisms of P removal

There are a variety of mechanisms that can remove P from solution in experimental situations containing ochre. P adsorption onto surfaces of goethite (α-FeOOH) has been suggested as the dominant P removal mechanism (Heal et al., 2003a; Fenton et al., 2009) with ochre containing large amounts of the mineral, as well as other Fe hydroxides, in its composition. Ochre also contains other materials known to remove P, such as Al- and Mg- hydroxides and calcium carbonates (Heal et al., 2003a).

In soil systems, the two main mechanisms of P retention by solids are adsorption and precipitation, collectively defined as sorption (Frossard et al., 1995). A major control on P speciation in soils is the pH of the system (Figure 1.5). Phosphate ions have a negative charge and therefore a high chemical affinity for Al, Fe, Mg and Ca surfaces. These surfaces have variable charge which is determined by the pH of the system. Hydrous oxide surfaces generate increasing amounts of positive charge with declining pH. For example, goethite is positively charged below pH 8-8.5, its point of zero charge (pzc), with charge increasing and thus sites available for adsorption, with decreasing pH. Therefore, under low pH conditions (<6) mechanisms of adsorption onto Al, Fe, Mg and clay surfaces are dominant. Under high pH conditions (>7) P is mostly fixed by precipitation as calcium phosphates (Valsami-Jones, 2004) or adsorption onto calcite surfaces. The continuum between the fixing of P by precipitation or adsorption leads to the requirement of a collective term, sorption.

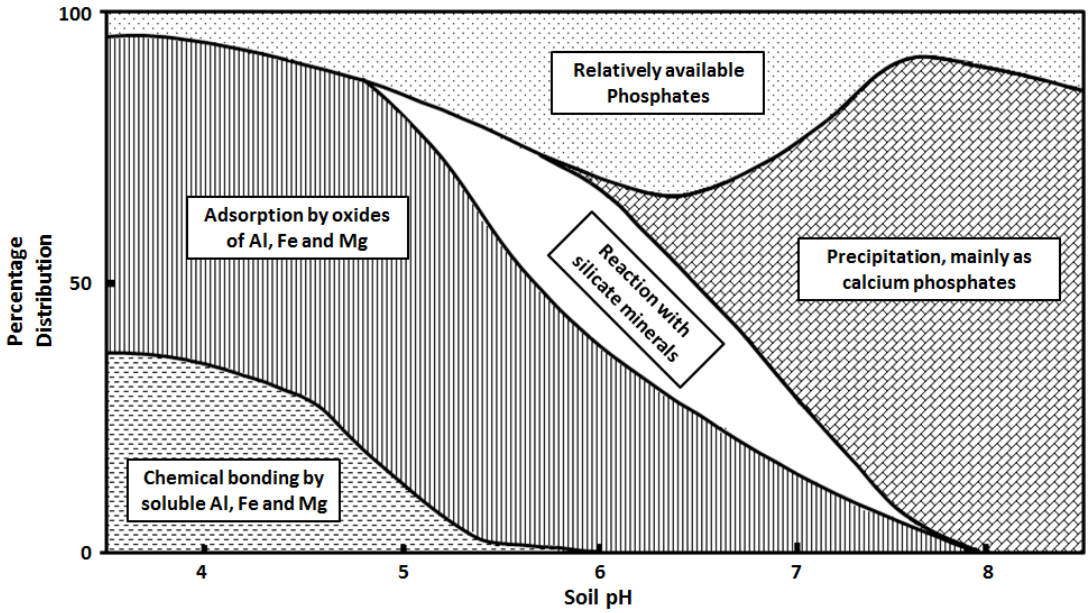

Figure 1.5: Speciation of P in the soil environment: The major phases controlling its availability as a function of pH, adapted from Valsami-Jones (2004).

It is therefore suggested that P sorption by ochre will vary with the composition of the ochre, e.g. predominantly the content of Al- and Fe- hydroxides, and Ca, with the pH of the system acting as a control on the mechanisms removing P. The factors affecting these sorption mechanisms and the conditions under which they operate is discussed in the following sections. Due to the relatively high Ca content previously reported for some of the ochres (Heal et al., 2003a), adsorption onto surfaces of calcite may also occur and the conditions under which this may happen will also be discussed.

1.3.7.1 P adsorption by Fe- and Al- hydroxides

Adsorption by Fe- hydroxides occurs predominantly under acidic pH conditions (Figure 1.5) and has fast kinetics, with P removed from solution within minutes of contact (Parfitt, 1989).

The main mechanism of P adsorption onto Fe- oxides is ligand exchange, with the surface hydroxyl exchanged by a phosphate ion. This process is competitive, with

OH^- ions and other ligands competing with the phosphate for the Lewis acid of the central ion of the Fe- oxide (Stumm and Morgan, 1996). This reaction stoichiometry is discussed in detail in Chapter 5, Table 5.2. Further to this, bidentate ligands can also form, with phosphate ions forming surface chelates, Equation 1.6 (Stumm and Morgan, 1996).

$$\begin{array}{l} \equiv FeOH \\ \quad | \\ \equiv FeOH \end{array} + H_2PO_4^- \leftrightarrow \begin{array}{c} \equiv Fe \quad\quad O^- \\ \quad\quad \backslash \quad / \\ \quad\quad\quad P \\ \quad\quad / \quad \backslash\backslash \\ \equiv Fe \quad\quad O \end{array} + 2\,H_2O \qquad \text{Equation 1.6}$$

Parfitt (1989) notes that the predominant mechanism of P sorption to goethite involves initially "rapid ligand exchange with surface OH^- groups at very reactive sites and the formation of a binuclear bridging complex between a phosphate group and two surface atoms". Following the exhaustion of very reactive sites weaker ligand exchanges occur at less reactive sites whilst over time there is a slow penetration of P into the solid matrix through defect sites and pores (Heal et al., 2003a). Therefore P adsorption onto goethite, and other Fe-hydroxides, can be classified as an initial "fast" period of adsorption on the timescale of a few hours, followed by "slow" period, taking between days and weeks (Parfitt, 1989; Torrent et al., 1992).

The degree of crystallinity of the solid matrix will determine the ability of P to diffuse into the substance, with greater diffusion, and therefore "slow" sorption, of P occurring in amorphous structures (Parfitt, 1989). The mineral structure also affects the adsorption capacity of a material, with amorphous minerals having a higher surface area and therefore more available surfaces sites for P adsorption.

Al-hydroxides have a close association in nature to Fe-hydroxides, with mineralogical similarity and affinity for P adsorption (Douglas et al., 2004). In soil systems, P is associated with Fe- hydroxides at a rate of 4-20 times that of with Al-

hydroxides, however comparative studies of P adsorption onto synthetic Al- and Fe-hydroxides indicate Al-hydroxides to have a substantially higher P adsorption capacity. Natural materials often have higher adsorption capacities than synthetic counterparts, with this attributed to crystal defects and element substitutions in the natural materials (Douglas et al., 2004).

1.3.7.2 P sorption by Ca

As a major component of some soils, calcite has been studied in relation to P availability as P can adsorb onto the surface of the mineral (Suziki et al., 1986) and has subsequently been proposed as an adsorbent to treat P-enriched waters (Karageorgiou et al., 2007). P adsorption onto calcite occurs when P concentrations are relatively low, such as those expected in P-enriched waters (< 10 mg P L^{-1}), contact time is short (< 3 hours) and under basic pH conditions (Karageorgiou et al., 2007; Sø et al., 2011), with adsorption increasing with pH. Therefore, for any ochres which contain calcite, P adsorption onto surfaces of the mineral may occur under the above conditions. P adsorption onto calcite surfaces occurs as a monolayer on a small percentage of the calcite surface area. This can then be followed by nucleation and precipitation of Calcium Phosphate minerals under saturated conditions (Freeman et al., 1981).

Due to the presence of calcium in many ochres, precipitation of calcium phosphates may occur. Calcium phosphates form under neutral to slightly alkaline pH conditions, in the presence of 100 mg Ca L^{-1} and at least 50 mg P L^{-1} (Carlsson et al., 1996). These conditions may occur in laboratory batch experiments resulting in sorption mechanisms removing P which would not be expected under field conditions. This may then give overestimations of adsorption capacity when data is fitted with adsorption isotherms.

1.3.7.3 Adsorption isotherms

The P sorption properties of a material are typically studied in laboratory batch experiments, with the resultant data analysed by the fitting of an adsorption isotherm. The plotting of adsorption isotherms is a common technique to fit a relationship between the concentration of the solute adsorbed and that in solution at a fixed temperature (Cooney, 1999). This is used to investigate the capacity of materials to remove pollutants from wastewater. Previous research into adsorption by ochre, detailed in Chapter 2.2, has utilised the Langmuir (Bozika, 2001; Fenton et al., 2009) and the Freundlich (Wei et al., 2008; Sibrell et al., 2009) adsorption isotherms.

Originally developed to describe the adsorption of gases onto solid phases, the Langmuir equation (Equation 1.7) is used extensively for describing solute adsorption to soils (Bolster and Hornberger, 2007).

$$S = \frac{S_{max}KC}{1+KC} \qquad \text{Equation 1.7}$$

Where S is the adsorbed concentration (mg g^{-1}), S_{max} is the maximum adsorption capacity of the material (mg g^{-1}), K is the Langmuir binding strength coefficient, with higher values indicating a greater affinity of the adsorbate for the adsorbent (L mg^{-1}) and C is the equilibrium concentration (mg L^{-1}).

The equation is based upon four assumptions (Langmuir, 1918):

1. Adsorption occurs at definite local surface sites;
2. Each site can only bond one molecule of the adsorbing species;
3. The strength of the bond created between each site and adsorbing species is the same;
4. There are no forces of interaction between adjacent adsorbed molecules.

There are, therefore, a fixed number of adsorption sites, with adsorption only taking place until every site is occupied, forming a monomolecular layer; multi-layer adsorption is assumed not to occur (Cooney, 1999).

Many alternative adsorption isotherms to the Langmuir exist, although it remains one of the most widely used due to its simplicity. An alternative which is also frequently used is the Freundlich adsorption isotherm (Equation 1.8).This is often better suited to describing adsorption from liquid solutions onto solid surfaces (Cooney, 1999; Sakadevan and Bevan, 1997).

$$S = K_f C^n$$ Equation 1.8

Where S is the adsorbed concentration (mg g^{-1}), C is the equilibrium concentration (mg L^{-1}), K_f is the Freundlich coefficient and n is the Freundlich exponent. The Freundlich coefficient gives a measure of relative P adsorption capacity, with higher values equating to a greater adsorption capacity; the Freundlich exponent is a constant, with a value < 1 (Sakadevan and Bavor, 1997).

The Freundlich isotherm does not impose the condition that adsorption must approach a constant value, equating to a monomolecular layer as solute concentration increases (Cooney, 1999). It assumes that bonding energy can vary between sites, with some sites highly energetic and able to strongly adsorb the solute, whilst others have lower energy and bind the solute weakly. The rate of adsorption therefore varies with the energy of the site, resulting in the possibility of multi-layer adsorption (Cooney, 1999).

Whilst both the above mentioned adsorption isotherms have been utilised to analyse P sorption by ochre, alternative isotherms exist which may provide a better description of P sorption by the material. Ochres contain a variety of adsorbing surfaces, such as Fe- and Al- hydroxides and calcite. Further to this, adsorption onto

Fe hydroxides can occur at different rates, noted by Parfitt (1989) as a period of "fast" initial adsorption followed by a period of a slower rate of adsorption. Therefore an adsorption isotherm which can account for more than one adsorbing surface with differing bonding energies and adsorption capacities should provide an improved model.

The two-surface Langmuir equation provides an excellent model for describing P adsorption from soils, allowing for adsorption onto two types of surface site with differing bonding energies (Holford et al., 1974). For this reason the equation may prove beneficial for modelling P adsorption by ochre. Proposed by Langmuir (1918), the equation can be written as:

$$x = \frac{k' x'_m c}{1+k' c} + \frac{k'' x''_m c}{1+k'' c} + \cdots \qquad \text{Equation 1.9}$$

Where x is the amount adsorbed, x_m is the maximum monolayer adsorption capacity, k the adsorption/ desorption equilibrium constant related to the bonding energy, and c the equilibrium solution concentration.

This isotherm provides an excellent fit for describing P adsorption in a wide range of soils, suggesting that P is adsorbed on two types of surface with contrasting bonding energy: P that is strongly adsorbed with a low dissociation constant, and P that is loosely held with a high dissociation constant and adsorption maxima (Holford et al., 1976). Due to the varying energy of the sites, P is preferentially adsorbed onto high energy sites. The adsorption capacity of the low energy surface is usually at least double that of the high energy one. For these reasons, the two-surface Langmuir equation may make an excellent model for describing P adsorption onto ochres, whereby the differing surfaces would represent either the high and low energy Fe hydroxide surfaces, or in the presence of Al hydroxides, Fe and Al surfaces.

A range of isotherms were utilised to describe P adsorption onto Fe oxides in a study by Zeng et al. (2004). This research found that three parameter equations such as the Redlich-Peterson and Langmuir-Freundlich provided a better fit to data than two parameter equations such as the Freundlich, Langmuir and Temkin. It is therefore suggested that it would be preferable to utilise three parameter equations to describe the adsorption of P by ochre. However, two-parameter isotherms are employed more often due to their easier calculation (Zeng et al., 2004).

1.4 The suitability of different P streams for treatment with ochre filters

Ochre has been applied as a P-adsorbent in the environment as a dosing agent and as a filter substrate. Dosing can rapidly reduce the P concentration of a water column, but there are associated issues with reclaiming the dosing agent from the environment. Dosing technologies, such as Phoslock, discussed in Chapter 2.8.2, remove P from surface waters before settling out of the water column, forming an adsorptive layer on top of the lake bed. Ochre may not be suitable for this purpose as, under anaerobic conditions, it is likely that P would be released from ochre adsorption sites as Fe(III) is reduced to Fe (II).

Ochre has been utilised as a filter substrate in a number of field applications, most notably at Leitholm WWTP, Scotland (Dobbie et al., 2009), discussed in detail in Chapter 2. Whilst the P adsorption capacity of various ochres is high in the laboratory, up to 30.5 mg P g^{-1}, with rapid adsorption kinetics (Heal et al., 2003a), this performance is not replicated under field applications. Dobbie et al. (2009) reported that the ochre filter installed had the highest adsorption rates under a low and constant flow rate, but noted that SS and biofilms could cause future clogging of the filter, leading to a decrease in hydraulic conductivity and a reduction in available adsorption sites.

Sources of P pollution with low and constant flow rates, high P concentrations, low SS concentrations and stable DO concentrations would provide an excellent

candidate for treatment with an ochre filter. The pH of the influent will also affect the P removal capacity of the ochre, investigated in detail in Chapter 4, with the adsorption capacity of many ochres highest at acidic pHs. The effect of competing ions on the adsorption of P by ochre is not well understood and is further investigated in Chapters 4 and 6. Table 1.5 lists relevant characteristics of various P pollutant streams discussed in this chapter that could be alleviated with the installation of ochre filters. Flow rate, TP, DO, suspended sediment (SS) and pH of the pollutant streams are presented, where possible, as these are the key factors that will affect the potential of an ochre filter to alleviate the P pollution.

Table 1.5: Potential sources of P pollution for treatment with ochre: - indicates data not available. *Based upon the design flow rate for a household of four (Grant and Moodie, 1997), [1]Edwards and Withers (2008), [2]Whelan and Titamnis (1982), [3]Boaventura et al. (1996), [4]Gouriveau (2009), [5]Jarvie et al. (2008), [6]Guzzan et al. (2008), [7]Line et al. (2002).

		mg L^{-1} (min-max in brackets)			
Source of P pollution	Flow rate (L s^{-1})	TP	DO	SS	pH
Septic tanks					
Septic tank effluent[1]	0.02*	10.20 (1-22)	-	27.4 (1.5-600)	-
Septic tank effluent – Av. of 5 households[2]	0.02*	17.08	-	22-47	6.96
Fish farms					
Small sized trout farm[3]	72	0.10	9.50	1.80	6.30
Medium sized trout farm[3]	250	0.07	10.50	2.40	6.20
Large sized trout farm[3]	624	0.59	8.40	17.8	6.10
Farmyard runoff					
Farmyard pond influent[4]	-	3.27	-	111	7.51
Farmyard pond effluent[4]	-	1.73	-	40.50	7.89
Farmyard runoff[1]	-	30.8 (0.02-247)	-	982 (690-1284)	-
Track runoff[1]	-	2.69 (0.24-7.30)	-	642 (70-2764)	-
Drainage pipe – cattle shed/ slurry pit[5]	-	0.44	7.00	29	7.09

WWTPs					
WWTPs – 132 sampled[1]	-	2.90 (<DL-13.1)	-	27.4 (1.5-600)	-
WWTP[6]	69.4	(0.6-3.0)	-	-	(6.5-7.7)
Golf courses					
Small stream – storm events[7]	-	1.07	-	202	-
Diffuse pollution					
Stream – High intensity cattle catchment[5]	1.3	0.36	19.20	21.00	6.98
River – Catchment with arable/ sheep farming[5]	1400	0.06	2.50	3.00	7.09
Drainage pipe – cattle shed/ slurry pit[5]	-	0.15	2.40	7.00	7.20
Road runoff[1]	-	0.26 (0.18-0.34)	-	102 (55-149)	-

Septic tanks have low flow rates and relatively high P concentrations. Filter systems are thus suitable, as long as the septic tank is well maintained to remove SS which could otherwise clog the filter. Competing ions may reduce P adsorption by a filter, particularly in the event that biological material leads to the growth of biofilms which covers reactive surfaces.

Ochre filters may be suitable for the treatment of farmyard runoff in some circumstances where flow rates are low and consistent. The presence of high levels of SS is likely to clog filter units, however. Filter units can also be used to treat farm pond effluents, reducing the required land footprint of such ponds and wetlands.

Effluent from fish farms has a relatively low P concentration and associated high flow rates and thus it is not suggested as suitable for treatment utilising ochre packed filters. Further to this, P adsorption by the ochre may be decreased due to the presence of competing ions, or the growth of a biofilm fouling the unit due to the high organic content of the effluent.

It is suggested that ochre filters are of limited use for the treatment of internal loading of P from lake sediments. Ochre dosing may have potential in shallow lakes and rivers with high DO concentrations, but not in deeper waters where anoxia could lead to reducing conditions and the release of P adsorbed to the ochre.

Whilst many WWTPs have discharge consents, effluent P concentrations are still in the order of 1-2 mg P L^{-1}. Although flow rates are likely to be high, part of the waste stream could be treated and the onsite expertise would allow the filters to be maintained and monitored. It is therefore suggested that P-enriched waters from WWTPs are an excellent candidate for treatment by filters of ochre.

The effectiveness of ochre filters in treating P pollution originating from golf courses varies greatly with site. Where golf courses drain into a small channel that intersects

the golf course, ochre filters may be of use to reduce the export of P. However, P pollution from golf courses is associated with episodic runoff events and filter units will be unable to treat the high P loading and volume of discharge associated with such storm events.

Treatment of diffuse pollution by ochre filters is ruled out. Most diffuse P pollution occurs during storm based events so ochre filters will be unable to treat the flow rates involved. Also, as diffuse pollution is generated over a large area, it can be difficult to target a specific site to treat. Even if a site can be identified, the associated flow rates may be too high, and too variable, for treatment using a filter unit.

Slow flow rates of groundwater systems provide high contact times with adsorbent substrates making an excellent candidate for treatment with filter systems such as PRBs. Previous use of Fe in PRBs has used zero-valent Fe and treated pollution streams other than P. Ochre is comprised of ferric iron, and therefore will reduce under anaerobic conditions and may release P that has been adsorbed. If ochre was to be used in a PRB, aerobic conditions would need to be maintained to reduce the risk of release of adsorbed P.

1.5 Research aim and objectives

There remains large gaps in the research of ochre as a filter substrate, discussed in detail in Chapter 2. Various ochres have been utilised as filter substrates following only partial characteristation in laboratory trials, and therefore on a basis of a limited understanding of the chemical and physical properties of the ochre. An improved understanding of these properties and processes is required in order to design effective filter units. The literature review (Chapters 1 and 2) reveals a number of pertinent research questions which will be addressed in this Thesis.

The overall aim of this study is to provide a process-based understanding of P removal by ochre in order to develop effective filters for the treatment of aquatic P pollution. The research objectives outlined below focus on building a greater understanding of ochre, and the processes involved in the removal of P.

Objective 1: Identify potential sources of P pollution for treatment with ochre.

P pollution originates from a variety of sources, discussed in Chapter 1.2. These have different concentrations of P, SS and competing ions, as well as a range of pH and flow characteristics. Pollution streams will be identified and characterised, whilst the capacity of ochre to adsorb P over a range of conditions will be tested.

Objective 2: Select ochres for study and characterise the chemical and physical properties of these ochres.

A greater understanding of the chemical and physical composition of ochre is required to provide critical insight into it's potential for removing P. The compostion of ochre is site specific, and as such varies with the MWTP in which it is formed. Therefore ochres from a variety of MWTPs across the UK and Ireland will be selected and analysed for a range of chemical and physical properties. Where appropriate, comparisons to previous research will be undertaken.

Objective 3: Determine P adsorption isotherms for all selected ochres across a range of pH conditions.

The environmental application of ochre as a filter substrate may require effective adsorption of P over a range of pH, although most likely between pH 6-8 (Table 1.5). In previous studies P adsorption isotherms have been constructed for some ochres, but the effect of pH has not been considered. Using a novel methodology, batch experiments will be conducted for seven ochres, over a sweep of pH, and Freundlich and Langmuir adsorption isotherms fitted to this data.

Objective 4: Investigate the effect of competing ions on P removal by ochre.

Wastewaters contain a range of dissolved ions which may compete with P for adsorption sites on the ochres. This competition has been suggested as a contributing factor to the under-performance of ochre filters at removing P in the field (Dobbie et al., 2009). The majority of batch experiments conducted by previous authors have investigated P removal by ochre with no competing ions in solution. In order to investigate whether the presence of competing ions, in the form of a synthetic sewage, affects P removal by the ochres the batch experiments will be repeated for three of the ochres. The effect of competing ions will also be investigated in column scale experiments.

Objective 5: Investigate the release of potentially toxic elements from ochre during batch experiments.

Ochres are a mixture of elements that have precipitated and settled out of the water column at MWTPs. As such, some ochres have relatively high concentrations of arsenic and other potentially toxic elements (PTEs).The release of PTEs from ochre is a key concern regarding their use for environmental applications, such as in-stream filter units. The release of PTEs from the ochres will be investigated in batch experiments across a range of pH.

Objective 6: Utilise a chemical model to improve understanding of the P removal mechanisms occurring in the batch experiments.

Whilst the fitting of adsorption isotherms can give an indication of the mechanisms involved in P removal, such as the dominance of adsorption or precipitation reactions; chemical equilibrium and speciation models can be utilised to better understand the processes occurring within a particular system, and to quantify the P removal mechanisms.

Objective 7: Investigate P removal by granular ochre under flow-through transport conditions over a range of conditions.

Whilst laboratory batch experiments indicate the potential of ochre to remove P, in-field filter applications will need to cope with flow-through transport conditions. Therein, the kinetics of diffusion and adsorption will play a key role. Laboratory column experiments will be designed to investigate factors which may affect P removal by two granular ochres, namely flow rate, pH conditions, the presence of competing ions, and the effect of a 48 hour resting period between P applications. The transport parameters of the packed columns will be determined by modelling non-reactive tracer experiments in STANMOD, before using these parameters to model P breakthrough.

1.6 Overview of thesis structure

Chapter 1 has identified sources of P pollution, such as diffuse agricultural, septic tanks and fish farms, and indicates which of these may be suitable for treatment using ochre. A brief history of minewater pollution and treatment is included. This focuses upon the creation of the iron rich sludge, ochre, which due to its composition is suggested for use as a P-adsorbent. The research questions, aims and objectives of the thesis have then been outlined.

Chapter 2 examines research conducted on ochre over the last few decades. The P removal capacity of ochre is assessed in relation to other materials currently used for P adsorption. Alternative end-uses for ochre are discussed and evaluated. Gaps in knowledge about the capacity of ochre to remove P are identified.

Three experimental chapters follow. Chapter 3 focuses upon the contrasting ochres from different sites selected for research, and the subsequent physical and chemical characterisation of these ochres.

Chapter 4 examines the potential of these ochres to remove P, as determined under laboratory conditions in batch experiments. Freundlich and Langmuir isotherms are fitted to the adsorption data to determine the adsorption capacities of the ochres. The P removal capacity of the selected ochres in the presence of competing ions is also investigated in Chapter 4, along with the release of PTEs from ochre.

Based upon the data gathered in the experimental chapters, P removal by ochre was modelled using ORCHESTRA (An Object-Oriented Framework for Implementing Chemical Equilibrium Models) in Chapter 5 to provide a greater understanding of the processes and effects of environmental conditions.

In Chapter 6, a series of column experiments examining P removal by two ochres under conditions similar to those expected in the field is presented. The effect of flow rate, competing ions, pH, and resting the column between P applications, on P removal by the ochre substrate was investigated.

In Chapter 7, the major findings of the thesis are outlined and discussed within the context of previous research, highlighting how this study has advanced our understanding of the science of P sorption by ochre. The methods utilised in this thesis are then critiqued and recommendations for their improvement proposed. The implications of this research are then discussed in view of the practical deployment of ochre as a P adsorbent.

Conclusions are presented in the final Chapter.

Chapter 2

Previous ochre research

A considerable amount of research on ochre as a P adsorbent has been conducted over the last decade. This research has explored the chemical and physical characteristics of a range of ochres, the P removal properties of the ochres in batch experiments as well as in field-scale trials. This chapter will identify and explore previous research in order to ascertain the studies already conducted and the gaps in knowledge that persist. Research into the use of P-saturated ochre as a fertiliser will also be examined to understand whether the treatment of P rich streams with ochre yields a commercially viable product – slow-release P fertiliser. A number of other possible end-uses for ochre have also been proposed. These will be introduced as alternatives to its usage as a P-adsorbent, or the current practice of disposal to landfill. Alternative technologies which have been developed to treat P-enriched wastewater streams will be identified and discussed.

2.1 Ochre characterisation

The chemical and physical characteristics of ochre vary with site, and through time, as the factors affecting its formation differ. Knowledge of these characteristics is required in order to assess and understand how ochre removes P from water streams.

2.1.1 Annual UK ochre production

The annual UK production of ochre from minewater was investigated by Hancock (2005). Estimates for MWTPS and untreated mine water discharges were collated by region and aggregated to calculate the UK total (Table 2.1). The estimates are based upon the assumptions of 15% total dissolved solids content in discharge, and 50% of the dried solids is Fe (Hancock, 2005).

Table 2.1: Annual Fe and ochre production by region in the UK (adapted from Hancock, 2005), [1] x 10^3 tonnes.

	Collected in MWTPs			Uncontained at untreated discharges		
Region	**Fe[1]**	**Ochre[1]**	**% total**	**Fe[1]**	**Ochre[1]**	**% total**
NE England	0.93	12.0	39	0.042	0.60	11
NW England	0.22	2.90	9	0.019	0.30	5
Yorkshire/ Derbyshire	0.26	3.40	11	0.088	1.20	23
Fife	0.13	1.70	5	0.041	0.60	11
Mid/East/ West Lothian	0.16	2.10	6	0.000	0.00	0
Ayrshire/ Lanarkshire	0.21	2.80	9	0.044	0.60	12
SW Wales	0.32	4.30	14	0.020	0.30	5
SE Wales	0.17	2.20	7	0.12	1.60	33
Total	**2.4**	**32.0**	**100**	**0.38**	**5.00**	**100**

Hancock (2005) calculated that 32.0 x 10^3 tonnes of ochre is produced annually at MWTPs containing 2.4 x 10^3 tonnes of Fe, with 5.0 x 10^3 tonnes ochre being produced at untreated discharges containing 0.38 x 10^3 tonnes of Fe. 37 x 10^3 tonnes of ochre per annum is therefore produced in the UK. The Fe content of ochres from across the UK was measured and ranged from 6% to 68%, with a mean of 51% (Hancock, 2004). The Fe content of the ochres may give an indication of the potential for each to remove P from solution, although other components, such as Ca, Al and Mg, also play a role in the binding of P.

2.1.2 Ochre chemical composition and physical characteristics

Chemical analysis of ochre deposited near the West Chiverton mine, Cornwall, UK, showed that, whilst fresh sediments consisted of poorly crystalline ferrihydrite and goethite minerals, older sediments were composed only of goethite, which is well crystallized with a rod-shaped morphology (Singh et al., 1999). The colour of the

ochre and the minerals present were correlated. Red to reddish-yellow samples contained poorly crystallized minerals and large amounts of sulphur, whilst brown or yellowish samples contained goethite and smaller amounts of sulphur (Singh et al., 1999, also noted by Brady et al., 1986). Whilst ochre may initially form predominantly as a mixture of ferrihydrite, goethite, hematite and schwertmannite minerals, goethite is ultimately the most stable mineral phase associated with acid mine drainage (Bigham et al., 1996).

Ochre has been collected from depositional beds and the adjacent forest floor at White Bridge, Avoca, Ireland, the site of a Cu-S drainage adit (Fenton et al., 2009). The iron mineralogy was examined by x-ray diffraction (XRD) with the ochre from the beds containing well crystallized goethite, jarosite and hydronium jarosite, with lepidicrocite and ferrihydrite also present. The ochre from the forest floor was composed predominantly of goethite and ferrihydrite.

Two Scottish ochres, from Polkemmet and Minto MWTPs, were air-dried and examined for their chemical composition and physical characteristics (Heal et al., 2003a, b). XRD showed the mineralogy of both ochres to comprise of a mixture of poorly crystalline solids, ferrihydrite and goethite.

Whilst the chemical compositions of Polkemmet and Minto ochre are similar, the physical characteristics differ significantly (Figure 2.1, Table 2.2). Polkemmet dries to a coarse, granular texture with a relatively high hydraulic conductivity whilst Minto dries to a fine powder with a much lower hydraulic conductivity. Whilst it is not clear why the two ochres differ in their particle size distribution, Heal et al. (2003b) suggested that it may be due to the treatment process at Polkemmet MWTP, where hydrogen peroxide and a polymer are added to mine water to encourage oxidation and flocculation.

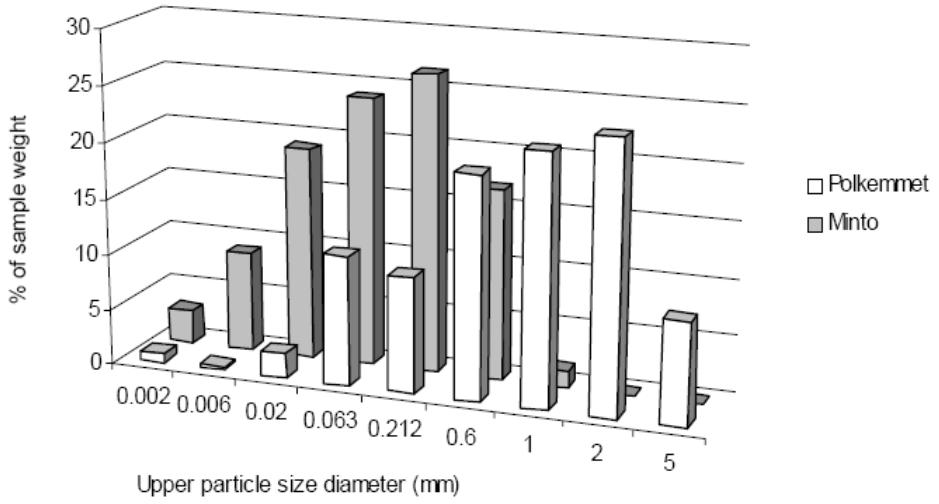

Figure 2.1: Particle size distribution of air-dried Polkemmet and Minto ochres, from Heal et al. (2003b).

Table 2.2: Physical characteristics and chemical composition of Polkemmet and Minto ochres, adapted from Heal et al. (2003b). [1]Mean of triplicate samples ± s.e., determined by atomic absorption spectrophotometry of acid digests.

	Polkemmet	Minto
pH (in distilled water)	7.2	6.9
%Fe[1]	65 ± 0.5	67.5 ± 3
%Al[1]	0.7 ± 0.02	0.1 ± 0.01
%Mg[1]	0.6 ± 0.01	0.8 ± 0.04
%Ca[1]	7.0 ± 0.1	11.8 ± 0.4
Dry bulk density (g cm^{-3})	1.8	0.8
Saturated hydraulic conductivity (m day^{-1})	26-32	0.7-1.7

Physical and chemical characteristics have also been determined for Avoca ochre (Fenton et al., 2009). The particle distribution was (by mass): 21.6% coarse sand, 19.5% fine sand, 22.3% silt and 30.9% clay. The dry bulk density of Avoca ochre was 0.8 g cm^{-3}, the same as Minto ochre, with a saturated conductivity of 0.90-4.80 m d^{-1}

(Fenton et al., 2009). This is slightly higher than for Minto ochre, but lower than for Polkemmet ochre.

The chemical composition (Table 2.3) and P sorption capacity of ochres from six coal mine drainage sites in Pennsylvania, USA, were investigated by Sibrell et al. (2009). Many of these ochres dry to a granular particle distribution, which retains its integrity when rewetted, and are therefore proposed for use in packed beds, marketed as Ferroxysorb (Sibrell et al., 2009).

Table 2.3: Major constituents (in %, 3 s.f.) of various ochres, (adapted from Sibrell et al., 2009). F.H: Friendship Hill, T.C: Toby Creek, B.Ca: Brandy Camp, G.W: Glen White, Ace: Ace ALD, B.Cr: Babb Creek. [1]Loss on ignition, [2]Numbers do not add to total as some minor constituents omitted.

Constituent	**Site of Ochre Collection**					
	F.H.	T.C.	B.Ca.	G.W.	Ace	B.Cr.
SiO_2	8.11	9.72	3.88	19.2	4.1	44.7
Al_2O_3	11.9	19.85	3.51	7.34	0.69	12.4
Fe_2O_3	41.7	36.1	14.4	53.1	72.5	12.0
CaO	6.98	1.63	32.8	0.15	3.63	0.11
MgO	0.43	0.38	6.32	0.30	0.22	0.49
MnO	0.04	0.09	1.93	0.04	1.12	0.03
Na_2O	0.09	0.08	0.03	0.08	0.02	0.14
LOI[1]	28.7	29.8	35.0	18.5	17.5	27.5
Total[2]	98.4	98.0	98.0	100	99.9	100

Ochre collected from Friendship Hill is composed of Fe and Al oxyhydroxides with minor amounts of gypsum and unreacted calcite. Toby Creek ochre contains a higher concentration of Al, reflective of the higher Al concentration in the acid mine drainage source (Sibrell et al., 2009). Brandy Camp ochre is formed with the

addition of lime which, by altering the pH, aids the precipitation of Fe and Mg out of the water column (Sibrell et al., 2009). The effect of this lime dosing can be seen in Table 2.3, where CaO constitutes 32.8% of the ochre. The high SiO_2 content of ochres from Glen White and Babb Creek is attributed to the unlined clay substrate of the settlement ponds in which the ochre accumulate at these sites. This may have become incorporated into the samples taken (Sibrell et al., 2009). The ochre collected from Ace ALD (anoxic limestone drain) has the highest Fe_2O_3 content (72.5%). Ochres originating from coal mining activities, as selected by Sibrell et al. (2009), generally have lower concentrations of PTEs (Table 2.4) than ochres originating from metal mines.

Table 2.4: Concentrations (mg kg^{-1}) of minor elements in acid mine drainage sludge (adapted from Sibrell et al., 2009). F.H: Friendship Hill, T.C: Toby Creek, B.Ca: Brandy Camp, G.W: Glen White, Ace: Ace ALD, B.Cr: Babb Creek.

PTE	**Site of ochre collection**					
	F.H.	T.C.	B.Ca.	G.W.	Ace	B.Cr.
As	46.1	6.5	1.7	11	2.1	10.5
Cd	0.73	0.12	0.88	0.04	0.58	0.04
Co	3	1.9	127	5.1	56.6	6.1
Cr	10	30	20	<10	<10	130
Cu	32	22	20	6	7	31
Ni	<5	<5	246	<5	14	13
Hg	0.023	0.027	0.013	0.113	0.062	0.203
Pb	5	6	<5	23	<5	17
Se	4.1	5.9	2.6	1.3	0.9	2.3
Zn	191	98	547	343	1400	61

Low concentrations of PTEs were measured in all the ochres indicating that they are suitable for disposal by land application according to the U.S. EPA guidelines

(1995), with the exception of Friendship Hill ochre which exceeds the As limit (Sibrell et al., 2009).

Some PTEs, such as As, are mobilised under similar conditions to Fe, therefore when Fe is mobilised into solution from abandoned mine workings, PTEs also transfer into the water column. Upon remediation at MWTPs, Fe settles out of solution and PTEs may adsorb onto the Fe, becoming incorporated in the sludge that forms ochre. A concern of using ochre for water treatment is the release of PTEs, especially if anoxic conditions develop within ochre filters. To address this concern, Hancock (2004, 2005) measured PTEs (As, Be, Cd, Co, Cr, Cu, Hg, Mn, Ni, Pb, V and Zn) by ICP-AES analysis of HCl digests of ochres from 25 MWTPs and eight untreated discharges in the UK.

Some ochres, such as from Ynysarwed and Silkstone contained relatively high As concentrations (746 mg kg^{-1} and 332 mg kg^{-1} respectively), whilst others, such as from Mouse Water had relatively high concentrations of Ni (1545 mg kg^{-1}). Of the Black list metals, substances deemed particularly dangerous that should not be discharged into the environment (EEC, 1976), Cd and Hg were not measured at concentrations higher than 10 mg g^{-1} for any ochre, although the acid digestion procedure used may have led to some losses of Hg (Hancock, 2004). Many of the ochres contained very little PTEs, such as that from Cuthill, or only a significant concentration of one PTE, such as Mn in Polkemmet ochre.

In order to contextualise these results, Hancock (2005) classified the ochres as either hazardous or non-hazardous based upon landfill regulations (Table 2.5). In the first instance, ochres classified as non-hazardous can be considered for use in water treatment. Analysis independent of Hancock (2004) should be conducted on any ochre being used in the natural environment as the composition of ochre is likely to vary with time.

Table 2.5: Classification of ochre by recovery potential and quality (assessed using CAT-Waste[SOIL] tool), adapted from Hancock (2005).

Ochre recovery potential	Non hazardous		Hazardous
High	Bates	Polkemmet	Ynysarwed
	Bullhouse		
Reasonable	Deerplay	Woolley	Elginhaugh
	Minto	Caphouse	
	Old Meadows	Monktonhall	
	Cuthill	Rhymney	
	Fordell Castle	Sheephouse-Wood	
Poor/ None	Taff Merthyr	Kames	Whittle
	Fender	Acomb	Mousewater
	Blaenavan	Lathallan Mill	Mains of Blairin
	Silkstone	Edmonsley	
	Clough Foot	Glyncastle	

2.2 Phosphorus adsorption by ochre determined in batch experiments

Laboratory batch experiments have been employed to determine the P sorption capacity of different ochres. The methodology of batch experiments varies with author, using different conditions such as P concentration in the overlying solution, solid: liquid ratio and shaking time. For most P adsorption batch experiments, adsorption isotherms are plotted to the derived data. From these adsorption isotherms properties of the material under study can be inferred, such as P adsorption capacities and the affinity between adsorbent and adsorbate.

The P adsorption capacities of Polkemmet, Minto and Frances ochres have been determined by batch saturation experiments, in which P-rich solutions were repeatedly added to samples of ochre until adsorption no longer occurred (Bozika, 2001). From this, the adsorption capacities of Polkemmet, Minto and Frances ochres

were calculated as 26, 30.5 and 25 mg P g^{-1} ochre respectively. The adsorption maxima of these ochres were also determined by fitting the Langmuir adsorption isotherm to a series of batch experiments in which the P concentration of the solution was varied between 5 and 1000 mg P L^{-1} (Bozika, 2001; Table 2.6).

Table 2.6: Langmuir parameters for Polkemmet and Minto ochre, where R^2: correlation coefficient, a: a constant of the binding strength, b: the adsorption maximum (from Bozika, 2001 cited in Heal et al., 2003b).

Langmuir parameter	Polkemmet	Minto
R^2	0.98	0.95
a (L mg^{-1})	0.6	1.0
b (mg P g^{-1})	17.8	21.5

The adsorption capacities calculated from the Langmuir isotherm were lower than those derived by saturation experiments. The underlying reason for this may be that ochre does not conform to the assumptions of the Langmuir isotherm, for example it is likely that P adsorption onto ochre does not occur as a monolayer, with P also diffusing into the ochre.

The effect of pH on the adsorption capacity was investigated in a series of batch experiments conducted with Minto and Polkemmet ochre (Heal et al., 2003b). The addition of 100 mg P L^{-1} solutions at pH 4, 5, 7, 8.5 and 10 had no significant effect on P adsorption by the ochres, suggesting the P adsorption capacity of these ochres is pH independent. However the effect the addition had on the system pH was not calculated, with pH not measured at the end of the experiment (Heal et al., 2003b).

Batch experiments, sampled over six hours demonstrate the rapid P sorption by Polkemmet and Minto ochres (Figure 2.2). For Polkemmet ochre, the majority of adsorption occurs in the first hour, after which the experiment reaches equilibrium (Heal et al., 2003a). With a smaller grain size and therefore larger surface area,

Minto ochre has a far higher P adsorption rate, with adsorption equilibrium reached in minutes (Heal et al., 2003a). Independent kinetic studies cited by Heal et al. (2003a) confirm the rapid kinetics of P-adsorption to ochre, with over 98% P sorption in the initial five minutes of batch experiments (Lamont-Black et al., 2001). Whilst these results indicate the potential of ochre to adsorb P, they were conducted using artificial solutions, with no competing ions, and under controlled laboratory conditions.

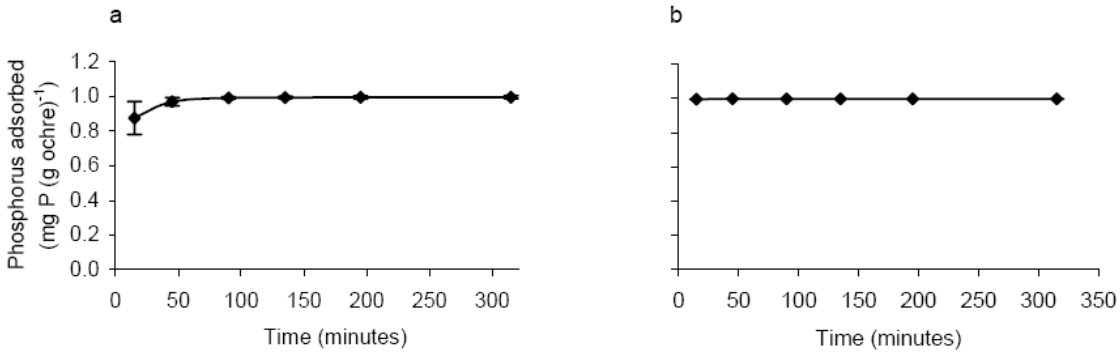

Figure 2.2: P adsorption from artificial solutions (50 mg P L^{-1}) in batch experiments by Polkemmet ochre (a) and Minto ochre (b), from Bozika (2001). Points are the mean of triplicate samples ± s.e.

P sorption by Avoca ochre was assessed by a series of batch experiments (Fenton et al., 2009) using ochre that had been air-dried, ground and passed through a 2 mm-sieve. The samples were not agitated and after 24 hours were centrifuged and the supernatant collected and filtered through a 0.45 μm filter membrane (Fenton et al., 2009). The experiments were repeated using an end-over-end shaker. Shaking improved the P adsorption capacity of Avoca ochre by up to 39 % when high concentration P solutions were used (Fenton et al., 2009). The Langmuir isotherm was fitted to the data from the batch experiments to calculate a P adsorption capacity of Avoca ochre of 21 g P kg^{-1} (Fenton et al., 2009).

The P adsorption kinetics of Avoca ochre were determined in a series of batch experiments (Fenton et al., 2009), with 2.5 g ochre added to 50 mL of P solution

(26.4, 52.3, 108.7 and 188.5 mg P L^{-1}). Experiments were agitated in an end-over-end shaker with samples taken after 1, 5, 15, 30, 60 and 120 minutes. P removal by Avoca ochre was rapid, with >97 % P removed from solution after five minutes. Fenton et al. (2009) relate this to the composition of Avoca ochre coupled with a high surface area for adsorption.

The P adsorption capacity of six ochres from the USA (shown in Tables 2.3 and 2.4) were investigated in a series of batch experiments (Sibrell et al., 2009). Ochre was air-dried and passed through a 0.15 mm sieve. Samples weighing from 0.005 to 0.1 g were then added to 100 mL of 1.0 mg P L^{-1}, in the form of KH_2PO_4 in deionised water, in 125 mL plastic bottles and agitated in an orbital shaker (Sibrell et al., 2009). After two hours, a sample was taken and filtered through a 0.45 μm syringe filter and analysed for P. Freundlich isotherms were fitted to the data to calculate the adsorption capacity of the ochres (Table 2.7).

Table 2.7: Summary of P adsorption characteristics for six ochres calculated by fitting the Freundlich isotherm ($q_e=K_F$ x C^$1/n$) to results of batch experiments, to 2 d.p, adapted from Sibrell et al. (2009).

Ochre	**Freundlich parameters**			**P adsorbed mg g^{-1}**
	1/n	K_F	R^2	
Friendship Hill	0.48	4.38	0.98	23.9
Toby Creek	0.50	4.35	0.83	22.6
Glen White Pond	0.36	3.99	0.97	9.84
Ace ALD	0.37	3.87	0.98	7.41
Brandy Camp	0.40	3.74	0.99	5.53
Babb Creek	0.24	3.26	0.97	1.82

The inferred P adsorption capacity (right-hand column, Table 2.7) varied greatly with ochre type. The capacities of Friendship Hill and Toby Creek ochres were an order of magnitude greater than the others. Sibrell et al. (2009) suggested that this was due to differences in composition between ochres, with some containing more

highly sorbing components, such as Fe and Al hydroxides. Babb Creek ochre had the lowest adsorption capacity and this was attributed to its high Si content and low Al and Fe content. The lowering of P sorption capacities by dilution of the effective adsorbing materials with other substances can also be seen for Glen White ochre which, despite having high concentrations of Fe and Al oxyhydroxides, is contaminated with SiO_2. A dilution is also apparent for Brandy Camp ochre by Ca oxides rather than silica materials, which would be expected to remove P from solution at high pH conditions (Sibrell et al., 2009).

The highest P adsorption capacity was determined in the Friendship Hill and Toby Creek ochres which contain a mixture of Fe and Al hydroxides, rather than in Ace ALD ochre which had the highest concentration of Fe oxides. Sibrell et al. (2009) therefore concluded that ochre containing both Fe and Al oxides has the largest adsorption capacity. This conclusion is supported by Ainsworth et al. (1985) who reported that Al substitution onto goethite led to an increased surface area for P adsorption to occur.

The adsorption characteristics of ochre collected from a MWTP in West Virginia, USA, (from here on referred to as WV ochre) were investigated through a series of batch experiments (Wei et al., 2008) to determine its suitability for wastewater treatment. Like Polkemmet ochre from West Lothian, Scotland, WV ochre originates from coal mine drainage which is actively treated with hydrogen peroxide, along with anhydrous ammonia. Upon collection, WV ochre was sieved through a 0.152 mm screen to remove debris and stored at 4^{o}C for a month prior to experimentation. Elemental analysis of the ochre showed it to be mainly comprised of iron and aluminium hydroxides (Fe 26.1 %, Al 9.5%, Ca 2.6%, Mg 0.6%, Mn 0.2%, Zn 0.2%, Ni 0.1% and Si 4.1%, analysed on a dry weight basis; Wei et al., 2008).The ochre was not dried, but was used in a moist state, with 4.31 % solids by weight and pH 8.1, in order to avoid the energy costs and time required for drying. However, it was hypothesised that drying the ochre could affect surface area and the nature of

surface sites, with rehydration of ochre samples in experiments affecting the number and character of surface sites available for P adsorption (Wei et al., 2008). Whilst moist ochre was used as an adsorbent, application rates are reported in g dry weight^{-1}.

Batch experiments were conducted by adding various masses of ochre to 500 mL P-solution (KH_2PO_4 dissolved in deionised water) and shaking at 150 rpm (Wei et al., 2008). The effect of pH, temperature, P concentration, contact time and adsorbent dose were all examined (Figure 2.3).

The effluent P concentration decreased rapidly when the dose of WV ochre was increased (Figure 2.3a), with a dose of 1.02 g L^{-1} ochre resulting in a 95% reduction in P concentration (Wei et al., 2008). Above this dosage concentration, any increase in P removal is small. A dosing rate of 1 g ochre L^{-1} was therefore recommended. Upon investigating the effect of contact time, rapid removal of P was observed in the first 5 minutes, with 89% P removal in this period (Figure 2.3b). P-removal continued over the next 55 minutes at a much slower rate, with removal after this minimal. Wei et al. (2008) therefore suggested an optimal contact time of 1 hour.

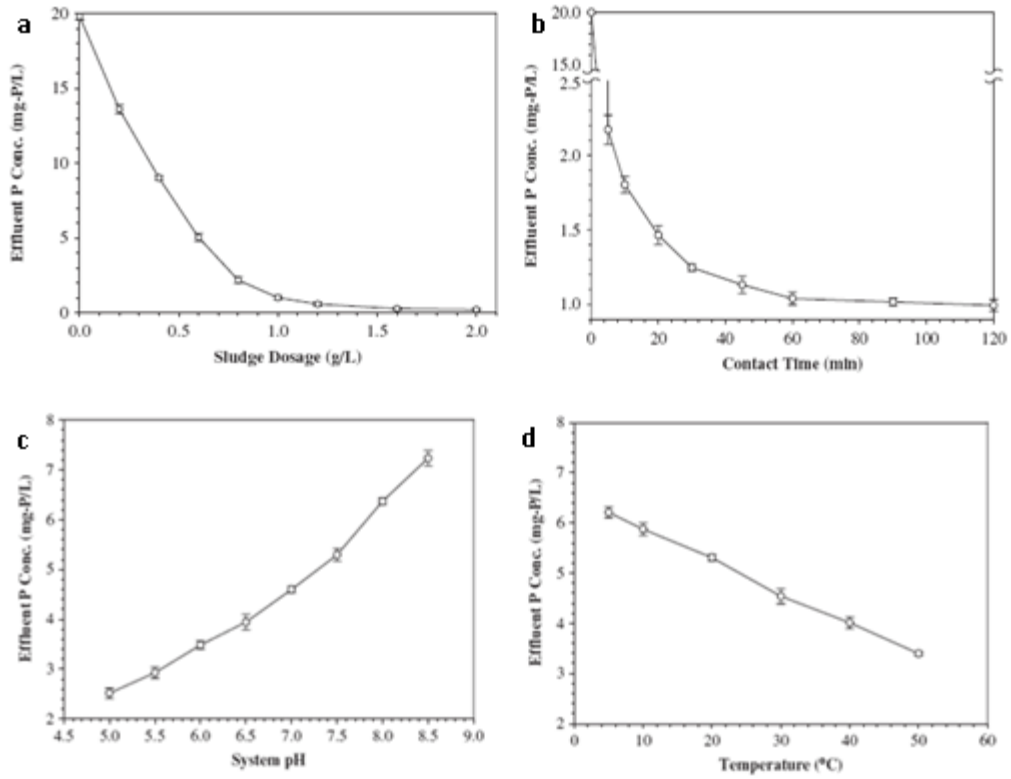

Figure 2.3: P sorption by moist WV ochre over a range of conditions. **a**: alteration of WV ochre dose rate (P concentration 20 mg L^{-1}, 20°C, pH 7.0±0.1, sampled after 1 hour). **b**: contact time (WV ochre dose 1 g L^{-1}, 20°C, pH 7.0±0.1, initial P concentration 20 mg P L^{-1}). **c**: pH (initial P concentration 20 mg P L^{-1}, WV ochre dose 0.6 g L^{-1}, mixing time 1 hour, 20°C). **d**: temperature (initial P concentration 20 mg P L^{-1}, WV ochre dose 0.6 mg L^{-1}, mixing time 1 hour, pH 7.0±0.1). All data points are mean ± 1 standard deviation (adapted from Wei et al., 2008).

P adsorption onto WV ochre was found to be pH dependant (Figure 2.3c) with P removal rates highest under acidic conditions and declining almost linearly with increasing pH. Wei et al. (2008) recommend that P-removal by ochre should occur under neutral or slightly acidic pH conditions, owing to concerns about metal re-solubilisation in conditions with pH <5. Fe and Al hydroxides typically have a point of zero charge between pH 8 and 9 (Cornell and Schwertmann, 2003; Sparks, 2003), therefore in pH conditions below this the surface groups would be positively charged, favouring the adsorption of orthophosphate ions (Wei et al., 2008). In

agreement with Sibrell et al. (2009) a positive relationship between temperature and P removal was found (Figure 2.3d).

The P adsorption capacity of WV ochre was calculated as up to 31.97 mg P g^{-1}, with P adsorption following the Freundlich isotherm model (Wei et al., 2008). The Freundlich constants were similar to those reported by Kang et al. (2003) who used ferrihydrite to adsorb P and, due to this, Wei et al. (2008) concluded that the Fe present in WV ochre is predominantly in the mineral form ferrihydrite, which suggests the ochre is relatively young.

P adsorption capacity is a typically used value to compare substrates when considering applicability for the removal of P. The review of literature in this section reveals that ochre has a relatively high P adsorption capacity, higher than many other materials considered for use as a P removal substrate. Selected ochres identified in this review are compared to a range of materials reviewed by Johansson-Westholm (2006) in Table 2.8.

Table 2.8: Comparison of the P adsorption capacity of ochres to other substrates identified for use as a P removing substrate. [1]Wei et al. (2008), [2]Sibrell et al. (2009), [3]Fenton et al. (2009), [4]Bozika (2001), [5]Johansson (1999), [6]Drizo et al. (2006), [7]Roseth (2000), [8]Mann (1997).

Material	Adsorption capacity (mg g^{-1})
WV ochre[1]	32.0
Friendship Hill ochre[2]	23.9
Toby Creek ochre[2]	22.6
Avoca ochre[3]	21.0
Polkemmet ochre[4]	21.5
Minto ochre[4]	18.2
Limestone[5]	0.0003-0.2
Bauxite[6]	0.61
Shell sand[7]	14-17
Blast furnace slag[8]	0.4
Burnt oil shale[6]	0.65

2.3 Mobilisation of potentially toxic elements from ochre

The possible release of PTEs from ochre is a concern which could prevent the environmental application of an ochre based technology. The mobilization of PTEs was investigated from Avoca forest floor ochre in batch experiments conducted for 24 hours under agitated and non-agitated conditions (Fenton et al., 2009). 5 g samples of ochre, air-dried and sieved < 2 mm, were overlain with distilled water, surface lake water, and dirty water from a dairy farm. PTEs were mobilized under all conditions, with agitation increasing mobilization. Concentrations of Fe, Cu, Mg and Zn in the overlying solution were all above mandatory allowable concentrations for the abstraction of drinking waters (EEC, 1975), with the majority of metal release occurring within the first minute (Fenton et al., 2009). This mobilisation of PTEs may limit the environmental application of Avoca ochre as a P adsorbent as, even without agitation, mobilized metal concentrations exceeded permissible EU guidelines.

Batch experiments similar to those conducted by Fenton et al. (2009) were conducted to examine the release of PTEs from the ochre matrix for six ochres from North America (Sibrell et al., 2009). 0.1 g ochre was added to 100 mL deionised water and shaken for 2 hours at room temperature on an orbital shaker (Sibrell et al., 2009). Only small concentrations of PTEs were released into solution, suggesting ochres originating from coal mine drainage are unlikely to have an adverse effect on the water being treated (Sibrell et al., 2009).

Due to concern regarding the release of metals from WV ochre, batch experiments were conducted over a range of pH, with the overlying solution sampled after 1 hour and analysed for the major constituents of the ochre (Table 2.9).

Table 2.9: Concentrations (mg L^{-1}) of the major constituents of WV ochre following P-adsorption batch experiments at various pH ± 0.1 (initial P concentration; 20 mg P L^{-1}, ochre dosage; 1 g L^{-1}, duration; 1 hour, 20°C), control experiment ~pH 8.1, 0 mg P L^{-1}. Adapted from Wei et al. (2008).

	Fe	Al	Mn	Cu	Ni	Zn
Control	<0.01	<0.1	<0.01	<0.01	<0.01	<0.02
pH 5.0	<0.01	0.1	0.24	<0.01	0.05	0.04
pH 6.0	<0.01	<0.1	0.14	<0.01	0.02	0.01
pH 7.0	<0.01	<0.1	0.01	<0.01	0.01	<0.01
pH 8.0	<0.01	<0.1	<0.01	<0.01	0.01	<0.01
pH 9.0	<0.01	0.3	<0.01	<0.01	0.02	0.01

In comparison to the control, mobilization of some metals occurred in all batch experiments, although only in very small concentrations. Wei et al. (2008) concluded that if WV ochre is dosed at 1 g L^{-1} and used for treating solutions with a pH between 6 and 8, then metal remobilization will not be problematic.

2.4 Pelletisation of fine-grained ochres for filter applications

Whilst fine-grained forms of ochre are acceptable for dosing treatments, they are unsuitable for use in filter units due to their low hydraulic conductivity. A larger grain size is therefore required for the utilisation of many ochres as a filter substrate; this can be achieved through pelletisation. Ochres from several MWTPs in Northern England have been pelletised by Aumônier et al. (permission copy).

For this pelletisation a cement-ochre mixture was used, the proportions of which were based upon preliminary work by Bagot (2002). Near spherical pellets (5.6-9.5 mm diameter), made from ochre from Acomb MWTP, England, were created which were robust, easy to handle, whilst retaining reactivity. The pellets were created by mixing oven-dried ochre with Portland cement, a surfactant and water, and agglomerating in a pan pelletiser before drying at 105^{o}C (Dobbie et al., 2009). The addition of cement caused the pellets to be Ca-, as well as Fe-, rich. The addition of Ca may lead to the P sorption under alkaline conditions by the precipitation of Ca-P minerals and P adsorption onto calcite. Lime has been used as a chemical reagent to precipitate phosphates in sewage waters and industrial effluents (Nriagu and Moore, 1984). Use of Fe oxides and gypsum working simultaneously has occurred previously, and makes for a more robust material for the removal of P; able to remove P at a wider range of pH conditions due to a combination of adsorption and precipitation reactions (Bastin et al., 1999). The pellets produced are under further development to create a commercially viable product, marketed as PhosFate™.

It was concluded that the pelletised ochre retains sufficient physical strength even when wet, that the pellets were durable, and that they had P sorption capacities (21.8 mg P g^{-1}) similar to that of untreated ochre, 26 mg P g^{-1} and 30.5 mg P g^{-1} (Heal et al., 2003b). Pelletisation therefore can be used to create pellets of ochre which have a greater hydraulic conductivity than unpelletised ochre, whilst retaining its P sorption capacity, and are therefore suitable for use as a filter material.

2.5 Larger scale P-removal experiments using ochre

Whilst batch experiments can be indicative of how a material removes P and the adsorption capacity of the material, larger scale trials are required to incorporate the effects of hydraulic scale properties of the ochre and therefore identify whether it is suitable for developing as an effective filter substrate.

2.5.1 Column, trough and tank experiments using artificial P solutions

A continuous adsorption study was conducted by Wei et al. (2008) on ochre from West Virginia, USA, using a continuous stirred tank reactor (CSTR) (Figure 2.4). Three types of influent were tested to investigate the effect of competing ions: 1) synthetic wastewater (P concentration 20 mg P L^{-1}), prepared by dissolving KH_2PO_4 in deionised water; 2) surface water from Monongaheka river, West Virginia, USA, dosed with KH_2PO_4 to 20 mg P L^{-1}; and 3) secondary effluent from a WWTP.

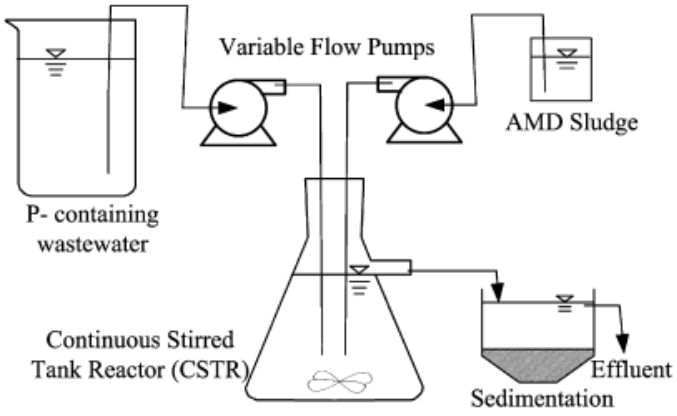

Figure 2.4: Set-up of continuously stirred tank reactor, from Wei et al.,(2008).

At the start of each experiment the CSTR was filled with 2 L of influent. Wastewater was then continuously pumped into the CSTR (2 L hr^{-1}) and ochre was added at a flow rate which delivered the required sludge dosage (0.35, 0.5 or 1.0 g dry weight L^{-1}). The hydraulic residence time in the CSTR (1 or 2 hours) was adjusted by varying the feed rate of the influents (Wei et al., 2008). The experiments were run for 3 to 5 hours and sampled every 10-25 minutes, with the results shown in Figure 2.5.

In all experiments, the P concentration of the solution in the CSTR decreased rapidly over time, with equilibrium typically reached within 3 hours (Wei et al., 2008). The ability of WV ochre to remove P was not inhibited by the presence of competing ions; all three effluents reached equilibrium in a similar manner and timescale (Figure 2.5a). Hydraulic detention time did not significantly affect the eventual equilibrium of the effluent (Figure 2.5b).

The CSTR was also used to examine the effect of varying dose rates of ochre on P removal from synthetic wastewater with a P concentration of 1.8 mg P L^{-1} (Figure 2.5c). Increasing the dose rate of ochre led to a lower P equilibrium concentration in solution, with up to 99% P removal, and allowed equilibrium to be reached quicker (Wei et al., 2008).

Wei et al. (2008) proposed that ochre could be used to treat municipal wastewater, either as a tertiary treatment step using a CSTR, or by injecting ochre into primary effluent prior to the settlement of sludge. Whilst in principle P removal may be possible using ochre in the primary treatment step, it would alter the nature of sewage sludge produced, and may affect other treatment processes in the WWTP. By using ochre as a tertiary treatment step, it could be implemented at currently operational WWTPs, with ochre polishing the effluent.

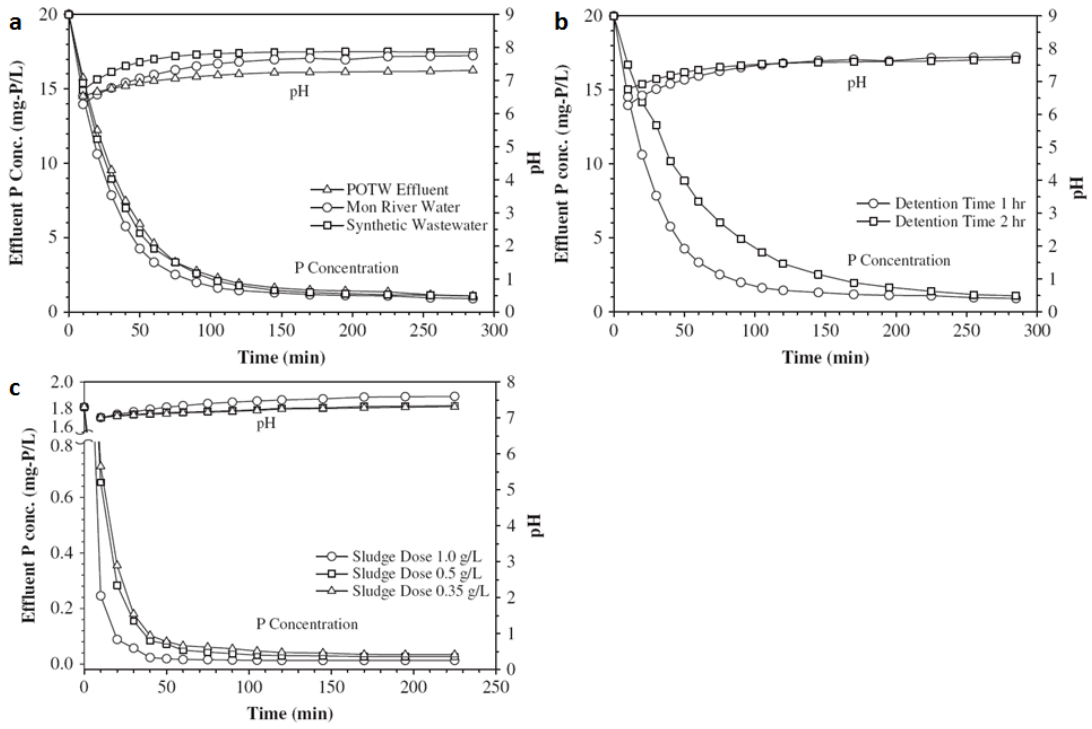

Figure 2.5: P removal by WV ochre during CSTR experimentation, adapted from Wei et al. (2008). **a**) Three types of water sample: feed rate; 2 L hr^{-1}, 20 mg P L^{-1}, ochre dose; 1 g L^{-1}, hydraulic retention time; 1 hour, 20°C. **b**) Detention time: Monongahela River water, feed rate; 1 and 2 L $hour^{-1}$, P concentration; 20 mg P L^{-1}, sludge dose; 1 g L^{-1}, 20°C. **c**) The removal of P by WV ochre when contacted with secondary effluent, feed rate 2 L hr^{-1}, hydraulic retention time; 1 hour, initial P concentration 1.8 mg P L^{-1}, sludge dose 1.0g L^{-1}, 20°C.

Column experiments with ochre from Friendship Hill, Pennsylvania, USA (which dries to a granular texture) were conducted by Sibrell et al. (2009). Preliminary studies indicated that columns packed with ochre adsorbed an increased amount of P from solution when rested between P applications, than when continuous flow was applied (Sibrell et al., 2009). The effect of resting may be to allow intra-particle diffusion of P within the ochre structure (Sibrell et al., 2009), whereby P diffuses from surface sites into the ochre matrix, rejuvenating surface sites for further adsorption. This effect has been noted by various authors (Dzombak and Morel,

1990; Makris et al., 2004), and suggests that intra-particle diffusion plays a crucial role in the adsorption of P onto iron oxyhydroxides.

P solution was pulsed upwards through two parallel columns each 50 cm in length, 2.5 cm in diameter, and packed with 100 g ochre. Solution was passed through one column for 12 hours, at a flow rate of 83 mL min^{-1}, corresponding to an areal flux of 169 L min^{-1} m^{-2}. Flow was then switched to the other column for 12 hours, allowing each column to alternately rest for 12 hours. P solution was made by dissolving KH_2PO_4 in spring water at a concentration of 0.13 mg P L^{-1} which is relatively low compared to other batch and field studies, but represents a typical concentration found in eutrophic surface waters (Sibrell et al., 2009). The experiment was run for 160 days, with effluent sampled periodically. After 40,000 system bed volumes, there was still adsorption capacity for P in the columns, although this decreased linearly from the start of the experiment (Figure 2.6). Sibrell et al. (2009) noted that the ability to remove P may be increased by reducing the flow rate through the columns, allowing a greater contact time for adsorption.

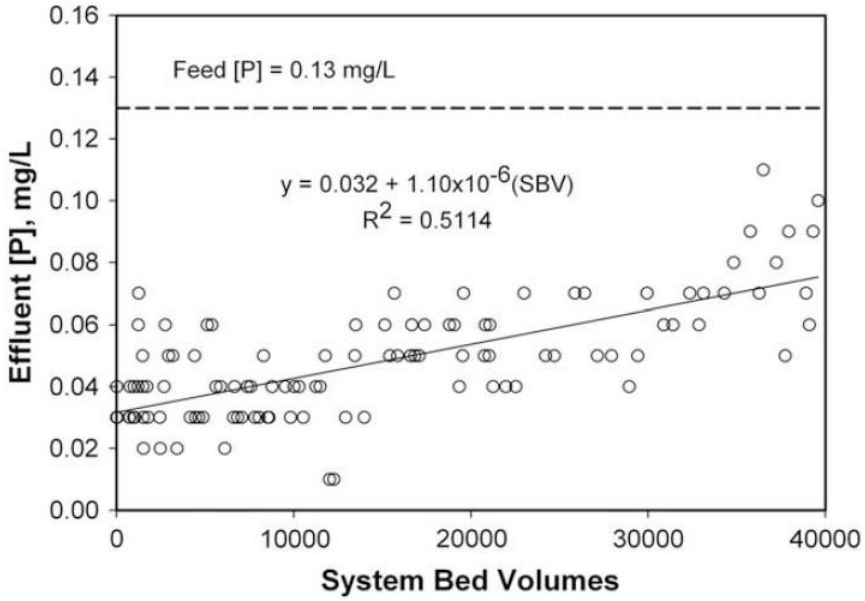

Figure 2.6: The breakthrough curve of Friendship Hill ochre for 40000 pore volumes. Flow directed upwards through a pair of 2.5 cm diameter columns at a flow rate of 83 mL min^{-1}, from Sibrell et al. (2009). The equation of the linear fit is P_{Eff} = 0.032 + 1.10 x 10^{-6} SBV, R^2 = 0.5114.

In a move to scaling up towards field conditions, 20 mg P L^{-1} artificial solution was passed through an inclined trough (2 m length, 0.1 m diameter) packed with 10 kg air-dried Polkemmet ochre (McHaffie et al.,2001, cited in Heal et al., 2003b). The experiment was run continuously for nine months, with the flow rate decreasing over time. The P concentration in solution was measured at 25 cm intervals along the trough and at the outlet. P removal by the trough was high throughout the experiment with the effluent concentration consistently <1 mg P L^{-1} (Figure 2.7). The flow rate of the experiment reduced over the course of the study, from 1.3 L hr^{-1} in December 1999, to 0.35 L hr^{-1} at the end of the experiment and contact time consequently also varied. The P adsorbed is unlikely to be released as only 0.4% was in a plant-available form (McHaffie et al., 2001). Heal et al. (2003b) concluded that Polkemmet ochre is a suitable medium for long term P adsorption in filter units, with potential for treating sewage effluent or agricultural runoff.

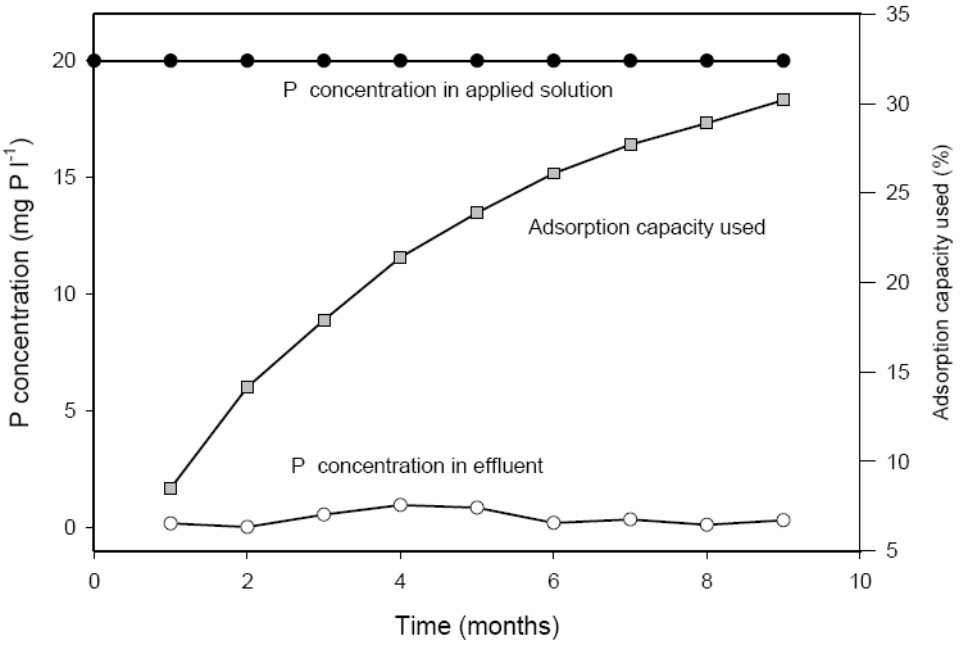

Figure 2.7: Phosphorus removal and ochre P adsorption capacity exhausted (%) over nine months of addition of artificial P solution to a trough packed with Polkemmet ochre (from McHaffie et al., 2001).

McHaffie et al. (2001) highlighted the artificial conditions under which the trough experiment was conducted. Whilst P concentrations were similar to those found in untreated sewage, a possible end use of ochre as a filter material, sewage would have many other chemical constituents that may compete for adsorption sites or impede adsorption. A further trial was conducted using a synthetic sewage (Department of Health, 1981) with a P concentration of 5-6 mg P L^{-1} (McHaffie et al., 2001), a similar concentration to that found in septic tank effluent. This solution was applied for 2 months to an inclined trough of the same aforementioned dimensions filled with 8 kg Polkemmet ochre (McHaffie et al., 2001). The mean flow rate of the experiment was 0.8 L hr^{-1}, approximately that of the previous trial. The mean effluent concentration from the trough was 0.16 mg P L^{-1}, corresponding to a removal rate of c.96%. McHaffie et al. (2001) reported that the addition of nutrients found in synthetic sewage led to increased algal growth and a clogging of the filter, making it difficult to maintain a constant flow rate.

Minto ochre has also been used in filter scale adsorption experiments. Due to its fine-grained nature, Minto ochre has a low hydraulic conductivity and it is not suitable for use as a filter material on its own. To provide a sufficient hydraulic conductivity 4.5 kg Bottom Fly Ash (BFA) was mixed with 0.5 kg Minto ochre, and placed in a 2 m by 0.1 m inclined trough (McHaffie et al., 2001). The trough was supplied with an artificial solution of 20 mg P L^{-1} for three months. The substrate removed P from solution (c.50-80%), but compacted quickly. This resulted in very slow through-flow, with evidence of short circuiting and surface flow occurring (McHaffie et al., 2001).

2.5.2 Use of ochre filters in the field

2.5.2.1 MSc projects

A series of University Masters projects have been conducted to investigate the installation of ochre filters to adsorb P in the field. These projects are often

constrained by cost, time and resources, but they are discussed briefly here as the initial attempts to use ochre under field conditions.

A series of four in-stream installations were conducted by Clarke (2004), Talbot (2006), Nichols (2006), and Carr (2007) in a ditch at Nafferton Farm, Northumberland, which is affected by diffuse agricultural phosphorus pollution. Clarke (2004) installed 44 kg of ochre (of unknown origin) in six permeable bags into the ditch, which had the effect of reducing TP concentrations by a mean of 11.9% across a period of a few weeks.

Talbot (2006) installed 32 hessian bags, each containing 20 kg of Minto ochre, into the stream. A small water sampling effort (only four samples) proved inconclusive. Nichols (2006) improved the design at the site, installing a semi permeable dam immediately upstream from the filter which prevented sediment from clogging the unit. The filter unit consisted of a cascade of box-like structures, made from a semi permeable material, and filled with Polkemmet ochre. Due to a small sampling effort of only four samples, this was again inconclusive. The results did, however, suggest an average P removal of 35% (by concentration) from upstream to downstream of the filter. This filter was washed away during high flows in spring 2007 and was re-designed by Carr (2007). An improved sampling effort showed that the filter reduced TP concentrations by a mean of 15% over a range of flow conditions for a period of six weeks.

Field trials have also been conducted by MSc Students at the University of Edinburgh, notably by Dimoliatis (2002) and Bush (2001). In both such studies, in-stream ochre filters were installed into the River Leet, Berwickshire. These trials were relatively successful, managing to remove P from the nutrient enriched river, and reverting the P concentration to its “natural” state.

2.5.2.2 Leitholm WWTP, Scotland

P adsorption by Polkemmet ochre and Acomb pellets under field conditions was investigated at Leitholm WWTP, Scottish Borders (Dobbie et al., 2009). The site treats 150 population equivalents of sewage per day, and road runoff. Primary treatment of wastewater occurs in a settlement tank before flowing into a biological filter for secondary treatment. The effluent from this passes into a horizontal subsurface flow wetland (175 m^2) planted with common reed in 0.5-0.6 m gravel for tertiary treatment. The water then collects in a settlement tank, which is dosed with Fe salts to ensure that the discharge consent for P is met. The site was monitored from July 2002 until November 2003 to establish the effectiveness of the existing treatment system for removing P. A trough, with dimensions of 0.3 m x 13.55 m x 0.51 m, containing granular air-dried Polkemmet ochre was installed to treat secondary effluent in November 2003, with wastewater from the biological filter pumped into the ochre-filled trough (Dobbie et al., 2009).

Due to the development of preferential flow paths in the ochre, a coarse gravel layer was introduced below the ochre in February 2004 (Figure 2.8). The filter unit was operated in this configuration until March 2005, when the ochre was removed and replaced with ochre pellets. The re-configured trough was operated from May to September 2005. In November 2005, the inlet to the filter was restricted to a flow rate of 0.05 L s^{-1}, and half of the ochre pellets were replaced.

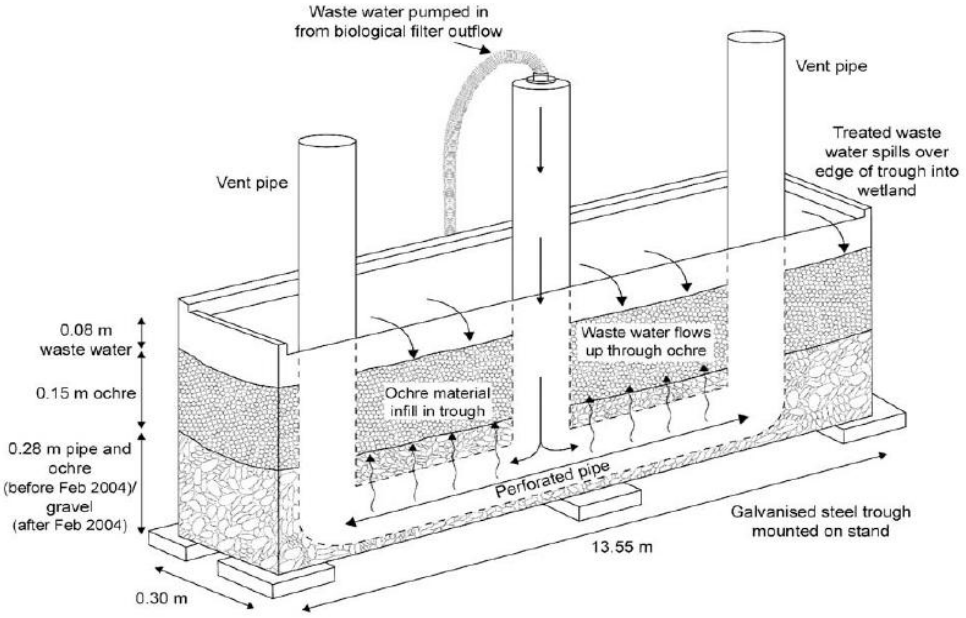

Figure 2.8: Trough installed to treat secondary treatment effluent at Leitholm WWTP (Dobbie et al., 2009).

Whilst the various filter configurations all reduced TP and SRP concentrations in the effluent, only the final filter configuration achieved TP removal rates >40% (Dobbie et al., 2009). For the final filter set-up, TP concentrations were initially reduced by 85% by the trough, although this efficiency decreased over the three month period of operation to c.45% by January 2006 (Dobbie et al., 2009). Whilst P was removed by the on-site filter configurations, removal rates declined rapidly over time. Dobbie et al. (2009) highlight issues that affected performance such as the presence of organic matter, the growth of biofilms, and the effect of hydraulic kinetics on the ability of ochre to adsorb P. These issues need to be addressed to match the potential of ochre that has been demonstrated under laboratory conditions.

2.5.2.3 Windlestone WWTP, England

P adsorption by Acomb pellets under field conditions was investigated at Windlestone WWTP, Northumberland, England (Dobbie et al., 2009). In two consecutive trials, filters containing Acomb pellets were installed on-site, into which the effluent leaving the treatment works was diverted. In comparison to the filter

unit at Leitholm which operated based on upward flow, effluent in the Windlestone filters was introduced to the filter surface. In one filter design (Figure 2.9a) effluent passed through the filter under horizontal saturated flow. Flow was initially through a 0.15 m thick band of gravel (diameter 20-25 mm) and then entered a bed of ochre, containing 1166 kg of Acomb pellets (Dobbie et al., 2009). Flow continued through another band of gravel which was retained by 4 mm mesh, before exiting the filter over a weir. Preferential surface flow paths were restricted by use of a solid barrier, although preferential flow paths may still have developed within the ochre bed. The filter was operated from June to December 2004 with the flow rate restricted during the course of the experiment from 0.75 L s^{-1} to 0.23 L s^{-1} and finally to 0.21 L s^{-1}, giving retention times of 7, 23 and 26 minutes respectively (Dobbie et al., 2009). An alternative filter design utilising vertical saturated flow was tested at the site from December 2004 to February 2005 (Figure 2.9b). A fresh bed of Acomb pellets (1027 kg) was installed above layers of gravel and plastic media, with wastewater applied to the filter through spray bars which distributed the effluent across the surface of the ochre bed. Although a filter was placed on the inflow to reduce clogging, maintenance was required weekly to remove organic matter from the spray bars (Dobbie et al., 2009).

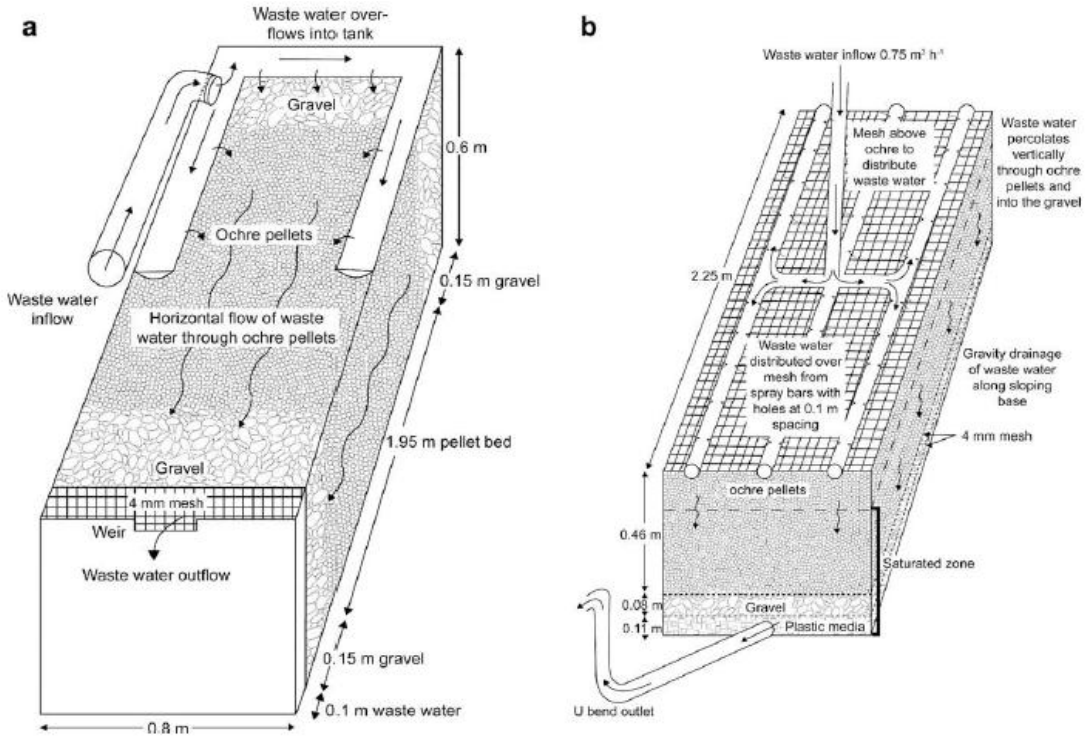

Figure 2.9: Schematic diagrams of the filter units installed at Windlestone WWTP, Dobbie et al. (2009). [a] Filter installed June 2004-December 2004 (horizontal saturated flow), [b] Filter installed December 2004- February 2005 (vertical saturated flow).

For both filter designs installed at Windlestone WWTP, filter inflow and outflow were sampled every 25 hours and analysed for TP. For the horizontal flow filter, initial adsorption rates were high (c.73%) although they declined with time (Dobbie et al., 2009). The restriction of flow led to higher TP removal (c.82%), suggesting that the initially higher flow rate resulted in insufficient contact time for the kinetics of P adsorption.

Under vertical flow conditions, TP removal reached 78% but declined with time, to c.20% TP removal after 42 days of operation (Dobbie et al., 2009). The decline in TP removal rates is attributed to biofilm growth covering the adsorption sites on the ochre pellets (Dobbie et al., 2009). Whilst the overall goal of these filter units is to provide a low-cost solution to treating P enriched waters, periodic cleaning of organic matter was required to ensure permeability of the filter which would have associated costs in a commercial setting (Dobbie et al., 2009).

2.6 Re-use of P-saturated ochre

Phosphorus is a non-renewable resource and there is a growing need to recover P from wastewater streams. A large body of research has focused on the recovery of P from WWTPs in the form of a P-rich mineral, struvite. Since the 1960s the formation of struvite, $NH_4MgPO_4.6H_2O$, has caused operational issues at WWTPs, by coating the insides of pipes and fouling pumps (Stratful et al., 2001). An understanding of struvite formation has led to the design of systems to avoid its precipitation so as to not hinder WWTP processes (Ohlinger et al., 1998). By adapting this knowledge, struvite can be produced to remove P from enriched waters, for example by adding a Mg slurry to wastewater (Münch and Barr, 2000). Struvite can then be marketed as a fertiliser (Ueno and Fujii, 2001) for direct application to land. This has not occurred on a commercial scale as of yet, however. In the current financial climate, the cost of struvite is not competitive with fertilisers derived from P-rich rock, which have a higher P content per unit weight.

2.6.1 The use of P-saturated ochre as a fertiliser

Avoca ochre was evaluated for application to land as a fertiliser following saturation with P, but was rejected owing to the high concentrations of Pb and Cu within this ochre (Fenton et al., 2009). It was suggested, however, that blending of P-saturated Avoca ochre with compost could reduce Pb and Cu concentrations to within permissible standards, thus permitting use of the P-saturated ochre as a fertiliser.

Dobbie et al. (2009) suggest that P-saturated ochre could be employed as a fertiliser due to its high P concentration of up to 30.5 mg P g^{-1}. A similar approach was considered by Hylander and Simàn (2001) and Cucarella et al. (2008) who investigated whether P adsorbed by blast furnace slag was plant-available. Other waste materials, such as steel slag without additionally adsorbed P, have been used as P fertilisers in agriculture (MacNaeidhe, 2001) and forestry (Jandl et al., 2003). Even if materials are rich in P and are proven to provide plant-available P,

application cannot occur if it leads to soil contamination however. Two main issues require addressing before widespread use of P-saturated ochre as a fertiliser can occur. Firstly, whether crop productivity resulting from application of P-saturated ochre matches that from conventional fertilisers; secondly, whether the application of P-saturated ochre leads to soil contamination from any PTEs which may be present within ochre. UK legislation also only permits application of a 'waste' material to land if a benefit can be demonstrated in terms of soil quality, fertility, and crop production.

Dobbie et al. (2005) investigated the ability of Polkemmet ochre to act as a fertiliser in pot and field experiments. Polkemmet ochre was air-dried, coarsely crushed and then saturated with P by soaking it in solutions with high P concentrations until no further P was removed from solution. Plant-available P concentrations were determined in the P-saturated ochre. Pot experiments were conducted using agricultural soil from central Scotland which was air-dried, sieved (4 mm) and mixed with sand to give it the texture of sandy loam. Available P, K and Mg were then measured in the mixture to determine the appropriate fertilizer application (85 kg P_2O_5 ha^{-1} and 90 kg K_2O ha^{-1}).

The pot experiment was conducted for two crop types, barley and grass, with six different treatments: a control treatment where no fertiliser was added, a conventional fertiliser at the recommended application rate, and four treatments using the P-saturated ochre at 0.5, 1, 2 and 5 times the recommended rate. The required P-saturated ochre was mixed with 4 L of soil and used as the growing substrate in a 5 L pot. The experiments were conducted in an unheated greenhouse between July-October 2002.

The field trials were conducted in 3 m x 2 m plots, with three design treatments utilised: conventional fertiliser following an approved application rate, P-saturated ochre with the same P content as the conventional fertiliser, and a control. Barley

and grass were planted in the plots in March 2003, with the trials ending in August 2003 (Dobbie et al., 2005).

The pot experiments showed that there was no significant difference in crop yields between the conventional fertiliser and equivalent P-saturated ochre treatments. Using P-saturated ochre in place of conventional fertilizer resulted in higher P concentrations remaining in the soil at the end of the experiment (Figure 2.10). This may be caused by P that is initially unavailable for plant uptake being converted into plant-available forms due to organic acids released in the root zone dissolving Fe, Ca and Al phosphates (Dakora and Phililips, 2002). In this way, P-saturated ochre acts as a slow release fertiliser, resulting in higher levels of residual P in the soil for the following growing season. The field trial showed that an application rate of 40 t P saturated ochre ha^{-1} supplied enough P for at least two growing seasons, with the relative insolubility of the P bound to the ochre meaning that it is less available for surface run-off than P in conventional fertiliser (Dobbie et al., 2005).

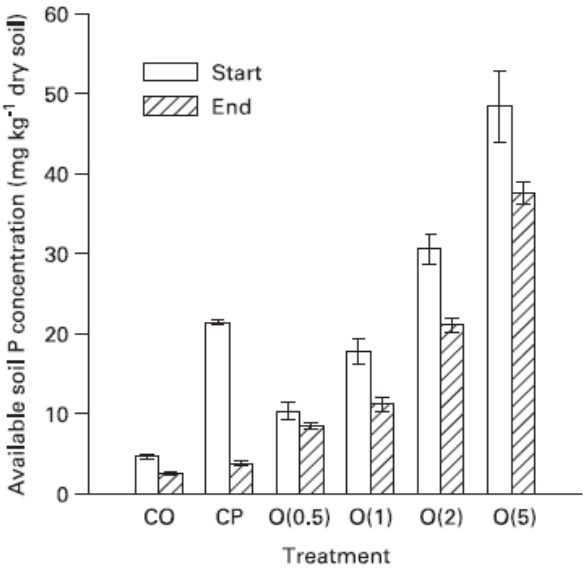

Figure 2.10: Available soil P concentration (± s.e.) in the barley soil at the start and end of the pot experiment. CO=unfertilised control; CP=conventional fertiliser; O(0.5)-O(5)=ochre applied at 0.5-5 times available P in the CP treatment (adapted from Dobbie et al., 2005).

The soil in the pot experiments was analysed before and after the experiment to determine whether the addition of P-saturated ochre led to contamination of the soil with PTEs. With the exception of Ni, soil PTE concentrations did not exceed the maximum permissible standards under the guidelines at that time for the application of sewage sludge to agricultural land (MAFF, 1998). The Ni concentrations in the soil of the ochre treatments, the control, and the conventional fertiliser experiments were not significantly different, however, showing that this excess was not due to the ochre addition (Dobbie et al, 2005). The recommended application rate of 40 t ha^{-1} ochre to soil from the field study would result in soil metal concentrations considerably below the limits set for the application of sewage sludge to agricultural land, again with the exception of Ni (Dobbie et al., 2005). No guidelines are available for maximum Fe application rates and, although the application rate seems high (10.9 t ha^{-1} Fe in 40 t ochre), it would only be equivalent to raising the soil Fe concentration from 2.4 to 2.6% and 3.1 to 3.4% in the field trials (Dobbie et al., 2005). This lies within the range of natural soil conditions for this area of Scotland (Paterson et al., 2003). Potential contamination of the crop by PTEs was examined for the field experiment by measuring the concentrations of Pb and Cd in the barley seeds, since maximum concentrations of these PTEs in foodstuffs are set by the EC (Commission regulation (EC) No. 466/2001). The measured concentrations for barley seeds grown in ochre-amended soils were within permissible standards and were not significantly different from those grown with conventional fertiliser (Dobbie et al., 2005).

2.6.2 Stripping of P from P-saturated ochre

Stripping of P from ochre in which the P sorption capacity is exhausted could provide not only a resource of P but also allow regeneration of ochre for a repeat application as a P-adsorbent. This idea was investigated by Sibrell et al. (2009) by passing an alkaline solution containing 0.1 M NaOH through a column packed with P-saturated Friendship Hill ochre, at a flux of 43 L min^{-1} m^{-2}. After elution for four hours, 76% of the P adsorbed onto the ochre had been stripped into solution. This

solution could then form the basis for the formulation of a product rich in P, and of use to industry. One such approach would be to introduce a source of Ca to the P rich solution to produce Ca-P minerals which could be incorporated into fertiliser. The regenerated ochre can be reused as a P-adsorbent, and the process repeated. The P sorption capacity of regenerated ochre has not been studied and it is unknown how many times such cycling could occur.

2.7 Alternative end uses for ochre

Whilst the potential of ochre to remove P from solution has been shown through batch experiments and field trials, many alternative uses for ochre have been suggested and demonstrated. Hancock (2004) details a number of potential end-uses for ochre, from use in the steel industry, to utilisation as a pigment. The ability of ochre to remove PTEs from solution has also been investigated as an alternative end-use (McHaffie et al., 2001). The potential of possible end-uses will depend upon the needs of the consumer – relating to the required characteristics of the ochre, quantity sought, and whether ochre of a consistent composition is needed.

2.7.1 Ochre as an adsorbent of PTEs

In addition to investigation of their P adsorption capacity, two ochres have been tested for their ability to adsorb PTEs - Fe, Mn, Zn, Cu, Cd, Ni, Cr and Pb (McHaffie et al., 2001). In batch experiments, 10 g of either Polkemmet or Minto ochre were shaken for 24 hours in a solution containing one PTE at a concentration similar to that typically found in landfill leachate (Department of the Environment, 1995) with the foresight that this could be a potential application (McHaffie et al., 2001). PTEs were rapidly removed from solution by Minto ochre with concentrations frequently below the level of detection after 1 minute (Table 2.9). Polkemmet ochre was also efficient at removing PTEs from solution but a slower reaction time was noted, potentially owing to its smaller surface area (McHaffie et al., 2001).

A further batch experiment was conducted using exactly the same method, but with the above PTEs mixed together in a single "cocktail" solution. Pb was omitted, however, as it can cause complications due to precipitation (McHaffie et al., 2001). With the exception of Fe, in the experiment with Polkemmet ochre, the removal of PTEs from the "cocktail" solutions was much slower than in the batch experiments with single PTE solutions (McHaffie et al., 2001; Table 2.10).

Table 2.10: The removal of PTEs from single and cocktail solutions in batch experiments, adapted from McHaffie et al. (2001). Underlined figures correspond to values meeting the requirements of the WHO drinking water guide values or EC Drinking Water Directive standards.

Treatment	**Starting Concentration**	**mg L^{-1} remaining in solution**			
		After 1 minute		After 24 hours	
		Polkemmet	Minto	Polkemmet	Minto
Fe, single	97.5	58.5	0.0	0.0	0.0
Fe, cocktail	116.0	6.7	0.04	0.0	0.0
Mn, single	46.7	40.9	0.7	0.6	0.0
Mn, cocktail	65	64.9	4.4	6.9	0.04
Zn, single	11.8	2.0	0.2	0.0	0.05
Zn, cocktail	22.0	22.0	0.6	0.8	0.2
Cu, single	4.0	0.02	0.0	0.0	0.0
Cu, cocktail	4.4	4.0	0.0	0.0	0.01
Ni, single	5.3	0.7	0.0	0.0	0.0
Ni, cocktail	6.7	6.4	0.1	0.2	0.0
Cd, single	4	0.1	0.0	0.0	0.0
Cd, cocktail	5.9	5.2	0.03	0.1	0.0
Cr, single	5.2	0.02	0.03	0.0	0.0
Cr, cocktail	5	3.84	0.0	0.03	0.0

Column experiments were also conducted to investigate PTE removal by Polkemmet and Minto ochres under conditions of different hydraulic conductivities (McHaffie et al., 2001). 30 cm long columns with a cross sectional area of 4.3 cm^2, were filled with 50 g bottom furnace ash placed above a 0.5 mm mesh. This was

followed by 100 g of one of the ochre mixtures shown in the header row of Table 2.10 to achieve different hydraulic conductivities.

100 mL PTE cocktail solution was passed through each column daily, with hydraulic conductivity calculated from the time taken for the 100 mL solution to pass through the column. Flow rates for all columns decreased over the six day experiment, most notably for columns packed with Polkemmet ochre (Table 2.11). McHaffie et al. (2001) attributed this reduction to the disintegration of ochre into a finer state, and potentially the precipitation of PTEs in pore spaces.

Table 2.11: Time taken for 100 mL PTE cocktail solution to flow through the packed columns (adapted from McHaffie et al., 2001). Column substrate <100% indicates mixing ochre with BFA.

	100 % Polkemmet	**80 % Polkemmet**	**100 % Coarse Minto**	**20 % Minto**	**100 % Minto**
Day	Time (minutes)				
1	20	10	26	28	90
2	45	55	60	77	120
3	120	180	75	85	150
4	310	200	75	85	170
5	540	480	96	120	190
6	1200	720	85	110	180

The results from the column experiments demonstrate that ochre can reduce the concentrations of many of the PTEs to below WHO drinking water guidelines. Fe and Cu concentrations were reduced in all columns below the guideline figures of 0.2 mg L^{-1} and 0.25 mg L^{-1} respectively. The columns were less effective for Mn removal, with only the coarse Minto column reducing concentrations below the guideline. All columns reduced Zn concentrations to below the WHO guideline except for the 10% Minto column wherein, initially the effluent concentration was within the target guidelines, but exceeded them after 340 column volumes had

passed through, possibly due to saturation of Zn adsorption sites (McHaffie et al., 2001).

Whilst the coarse Minto and the 100% and 80% Polkemmet, columns reduced Cd below guideline concentrations, the 20% and 10% Minto columns did not. Ni concentrations were reduced to below target guidelines by all columns, although the 100% Polkemmet ochre column became saturated after 190 column volumes. The Polkemmet columns and the coarse Minto column removed Cr from solution to below the guideline concentration. Cr concentration in effluent from the 20% Minto column failed to achieve the guideline concentration on one occasion, whilst for the 10% Minto column the effluent Cr concentration always exceeded the guideline (McHaffie et al., 2001).

Overall, whilst the removal of various PTEs by ochre is very high in column experiments, adsorption capacities are rapidly achieved, and flow rates through the columns very rapidly reduced – although much more so for the Polkemmet columns. Whilst McHaffie et al. (2001) propose ochre could be used as an active geochemical barrier for landfill sites, it is acknowledged that the acidic pH of these leachates will decrease PTE adsorption by ochre.

2.7.2 Ochre for use in steel making

Iron ore used in the steel industry is predominately from mined hematite, although other sources of Fe are also appropriate, such as goethite (O'Neill, 1998). The use of ochre in the steel industry is an issue of quality and economics; ochre should have a similar purity as mined hematite, and be available at a lower or equal price (Hancock, 2004). The steel industry already recycles scrap metal to obtain Fe and therefore recognises the value of materials often regarded as wastes. As noted by Hancock (2004), however, the use of ochre for the production of steel is unlikely as the mass of Fe processed by a single steel plant is much higher than the total ochre produced in the UK per annum.

2.7.3 Ochre as a flocculant for sewage treatment

Ochre has been used as a flocculant in sewage treatment since the late nineteenth century (Banks et al., 1997). The variability of PTE concentrations in ochre, however, may result in flocculant producers being unlikely to use ochre due to the prohibitive cost of frequent testing of ochres for PTEs and subsequent removal (Dudeney, 2003; Hancock, 2004). This could be addressed by only using ochres with consistently low PTE concentrations.

2.7.4 Ochre for use in cement production

The Coal Authority has previously marketed ochre as a cement feed stock (Dudeney et al., 2003). Ochre could either be used as bulk filler material owing to its high Fe concentration, or as a pigment (Hancock, 2004).

2.7.4.1 Ochre as a bulk filler material

In 2004 Glacier-ARM sourced approximately 33,000 tonnes of 'iron replacement components' for use in cement manufacture from 23 industrial sludge producers (Hancock, 2004), so have a proven record in recycling industrial by-products. A batch experiment was conducted by Glacier-ARM, a subsidiary of Lafarge Cement UK, to examine the suitability of ochre from Caphouse MWTP for use in the cement industry. Hancock (2004) reported that the results of experiments conducted by Glacier-ARM showed ochre to be suitable for its requirements, but with a few concerns. Most notably, the potential presence of PTEs in the ochre may lead to damage to equipment and the release of atmospheric pollutants during the cement refining process. PTEs of particular concern to Glacier-ARM were As, Cd, Cl, Hg, Pb and Zn, all of which have been found in various ochres at low concentrations (Hancock, 2004). Due to the temporal and spatial variation in ochre composition, PTE concentrations would need to be determined in every batch of ochre. Any ochres found to have unsuitably high concentrations of a PTE could be blended with other 'iron replacement components' until a satisfactory PTE concentration was achieved (Hancock, 2004). With an annual UK production of 22,000 tonnes

Hancock (2004) concludes that ochre could provide a satisfactory material for use in the cement industry.

2.7.4.2 Ochre as a pigment

Since synthetic iron oxides are produced for the colouration of cement, Hancock (2004) suggested that ochre could be an alternative source material for pigments. A precedent for this had been set, with ochre from a MWTP in Pennsylvania, USA, being processed to produce a pigment trademarked EnvironOxide™ (Hedin, 2003). The ochre was screened, dewatered and blended with other iron oxides to produce a marketable pigment (Hedin, 2003). The company responsible for this product also noted alternative end-uses for it, including phosphate retention and soil remediation.

The suitability of ochres for use as a pigment would need to be assessed on a site specific basis. Hedin (2003) noted that the two most important factors for the use of ochre as a pigment are colour, with red and yellow shades being more marketable than browns; and tinting strength, that is, the amount of ochre that would be required to produce a depth of colour. Ochre such as from Polkemmet, Scotland, may not be marketable as a pigment, for example, due to its dark brown appearance. This is possibly the result of a high concentration of black hematite produced from the dosing of hydrogen peroxide in the mine water treatment process. With a precedent already set, a few simple heating and paint drawdown tests could be conducted to assess the potential of different ochres for use as pigments.

2.7.5 Ochre for use in soil amendment and remediation

When combined with composts and wood chips, ochre sludge can provide a medium for plant growth (Dudeney et al., 2004). As shown by Dobbie et al. (2005), if these ochre-blended soils were dosed with P they could provide a suitable growing substrate. Ochres originating from the wetland stage of a MWTP will be of

particular interest as they will already have a relatively high organic content, making them more suitable as soils and less suitable for other purposes. Hancock (2004) proposed that contaminated or derelict soils could be replaced with ochre soils blended with compost, which could utilise large volumes of ochre.

Ochre has the ability to adsorb a range of PTEs, such as Cu, Cr and Zn (McHaffie, et al., 2001), and as such it has been proposed that ochre could be used in soil remediation (Doi et al., 2005). As mentioned previously, EnvironOxide™ is predominately marketed as pigment, although another suggested use from the manufacturer is for soil remediation.

2.8 Alternative technologies for P-adsorption

Many alternative technologies are available for the purpose of removing P from water, primarily from WWTPs, in order to recover P with an economic value for use in fertiliser production but also to find lower-cost methods of achieving water quality targets.

2.8.1 Experimental technologies

A large number of substances show potential for use as a filter substrate for P removal from wastewater streams; ranging from minerals and rocks (e.g. Dolomite, Limestone and Wollasonite), soils rich in Al, Ca or Fe, marine sediments (e.g. maerl and shell sand) and industrial by-products. A review of the P removal properties of these substances in batch and column experiments has been conducted by Johansson-Westholm (2006), highlighting the need for continued research to understand how these substrates will operate outside of the laboratory in real life applications.

Industrial waste products which have a high Fe content have shown promise for removing high concentrations of P. Blast furnace slag has a high Fe content and has been identified as a suitable material for use in constructed wetlands for the

purpose of P removal (Grüneberg and Kern, 2001; Johansson, 1999). Based upon the known high affinity of Fe and Al for P, some synthetic Fe and Al oxide based materials have been developed (Bastin et al., 1999; Biswas et al., 2007). Research into filter materials containing Fe and Al has been conducted by Ayoub et al. (2001) and Codling et al. (2000). Aluminium based materials have also been used successfully to remove P from wastewater (Codling et al., 2000; Huang and Chiswell, 2000; Tanada et al., 2003).

2.8.2 Lime, Fe and Al salts

WWTPs which have a discharge consent for the P concentration of effluent tend to rely on dosing systems, whereby Fe or Al salts, typically ferric chloride or aluminium sulphate, are added to primary or secondary effluents. The salts react with P and form insoluble precipitates, with the dose rate depending upon the influent P concentration (Noyes, 1991). Another commonly employed technique is dosing with lime. When added to effluent with pH > 10.5, precipitation of Ca-P occurs, removing P from solution. These techniques can be expensive, however, and yield large quantities of sludge which is either sent to landfill or applied to land as fertiliser.

2.8.3 Phoslock™

Phoslock™ is a P-adsorbing material aimed at remediating lakes enriched with P. Developed at the Land and Water Division of Australia's CSIRO (Commonwealth Scientific and Industrial Research Organisation), Phoslock™ comprises bentonite clay enriched with lanthanum in the form of $La_2(CO_3)_2$ which is strongly bound within the clay. The clay is not active and allows the product to settle through the water column. Lanthanum, the active ingredient (c.5% dry weight) for P adsorption, is also used in the pharmaceutical industry for removing P from blood. Upon adsorption to Phoslock™, P is no longer bio-available, which can reduce algal growth in a waterbody. Phoslock™ has an adsorption capacity of 11 mg P g^{-1} and

can operate in waters with a wide range of pH (c.4-11), and even under anoxic conditions (Phoslock, 2007).

For application, Phoslock™ is mixed with water so that it can be sprayed over the target water body. Phoslock™ then settles through the water column, adsorbing up to 95% SRP present in the water, with the potential to reduce SRP concentrations to 0.01 mg P l^{-1} (Phoslock, 2007). Based on suggested application rates, Phoslock™ settles on the aquatic bed forming a 1-3 mm deep layer which continues to adsorb P as it is released from aquatic sediments (Phoslock, 2007).

Phoslock™ has been available in a granular form since 2004, making it easy to handle and transport. Prior to this, it was available as a slurry – the resultant state from the formation process of La exchange in solution. Batch experiments showed rapid P sorption by the Phoslock™ slurry from a range of waters, including river waters, sewage, and piggery effluent (Douglas et al., 1999). After the initial batch experiments Phoslock™ was applied to the nutrient enriched Canning River in Australia. This resulted in the removal of at least 95% SRP from aquatic sediments and the water column (River Science, 2001).

Upon producing granular Phoslock™, further batch experiments were conducted to investigate its P adsorption isotherms over a range of pHs (Table 2.12). From the high correlation coefficients it was concluded that the Langmuir adsorption isotherm fitted the batch experiment results well, suggesting that P removal by Phoslock™ follows the assumptions set out by the Langmuir equation. The adsorption capacity (Q) of Phoslock™ declined as pH increased. Haghseresht (2006) also investigated the effects of anoxic conditions and microbial activity on P adsorption by Phoslock™ and showed that these factors did significantly reduce its P adsorption capacity.

Table 2.12: Parameters of the modified Langmuir adsorption equation fitted to the results of batch experiments using granular Phoslock™ conducted at a range of pH. Q is the adsorption capacity of the material and b, the Langmuir constant, a measure of the affinity of the solute to the adsorbent. Adapted from (Haghseresht, 2006).

	Modified Langmuir parameters		
Solution pH	Q (mg g^{-1})	b (L g^{-1})	R^2
5.0	10.14	26	0.99
6.0	10.19	19	0.99
6.0	9.47	53	0.99
7.0	9.34	134	0.99
7.5	8.76	33	0.99
8.0	7.69	41	0.99
9.0	7.19	696	0.99

The success of the Canning River trial, combined with the development of Phoslock™ into a granular form, led to a commercially viable product that has been applied in more than 100 water bodies across 20 countries. The lanthanum clay for Phoslock™ is mined in China, with associated transport costs and sustainability issues. The cost to of applying Phoslock™ to a water body, including the freight and application, is £1700 per 1000 kg. Assuming that Phoslock™ has a P adsorption capacity of 11 mg P g^{-1} the cost of recovering 1 kg P is £155.

Whilst Phoslock™ has been used successfully across Europe and Australia for the treatment of bathing lakes, its cost is likely to prove prohibitive for use under most "polluter pays" scenarios in the UK.

2.9 Summary of findings

It is estimated that over $32x10^3$ tonnes of ochre is produced annually (Hancock, 2005), with no currently defined end use. Various ochres have been investigated in batch experiments for their P removal properties, with most ochres having a high P adsorption capacity and rapid kinetics of adsorption. Larger scale column and field

trials have been conducted utilising ochre as a reactive substrate, with P removal notably less successful than in the batch experiments. Research in this thesis will focus upon improving process based understanding of P removal by ochre in batch experiments, in order to garner understanding as to why larger scale trials have not been as successful.

It has been noted that some of the ochres contain PTEs such as As. Within the selection of ochres for this study, some of those containing PTEs will be chosen to investigate PTE release during laboratory experiments.

Whilst most ochres form as fine-grained powders, Polkemmet ochre forms with a relatively coarse particle size distribution. For this reason, Polkemmet ochre will be selected for further investigation in this research. An experimental pelletisation approach has developed pellets of ochre formed from fine-grained Acomb ochre. Samples of this pelleted ochre will also be requested for use in this study as filter systems will require ochres with a high hydraulic conductivity.

A range of alternative technologies for P removal from surface waters have also been highlighted. These range from accepted technologies, such as dosing with lime or Fe- and Al- salts, to experimental technologies such as Phoslock™, or utilising industrial by-products, minerals and rocks, and red mud (Johansson-Westholm, 2006). P removal by ochre will be compared to these alternative technologies in order to assess its potential for treating surface water.

Chapter 3
Ochre characterisation

Based upon the review of previous research on ochre in Chapter 2, ochres suitable for the purpose of this research were selected. Ochre was collected from four sites in the UK, air-dried, and then each batch mixed to produce homogeneous samples. A further three ochres were selected which had been previously researched as P-adsorbents.

This chapter presents the methods and results for the characterisation of these seven ochres in order to garner an understanding of their chemical and physical properties. The pH of the ochres in deionised water was measured, along with the B.E.T. surface area. The elemental properties of the various ochres were determined from acid digestion and ammonium oxalate extraction, and their mineralogy was investigated using XRD analysis. Two ochres, chosen for experimentation due to their coarse nature and thus suitability as a filter substrate, were examined for particle size distribution; all ochres were analysed for particle density.

3.1 Ochre selection

The treatment of minewater tends to focus on encouraging the oxidation of ferrous iron (Fe^{3+}, in solution) to ferric iron ($Fe(OH)_3$), leading to the settlement of Fe out of the water column, forming a precipitate. The resultant sludge is known as ochre, containing all the contaminants that precipitate out of solution and any chemicals added to aid this process. The chemical composition of ochre will therefore vary with site, treatment method, and over time.

A number of factors were considered when selecting ochres as suitable adsorbents of P. Research has been conducted on various ochres from Scottish MWTPs, notably Polkemmet and Minto ochres (Bozika, 2001., Heal et al., 2003b). These ochres have been characterised in terms of their physical characteristics, adsorption rate, and

have been tested in a variety of in-stream filter units. Whilst both of these ochres have been studied in some detail, this has not been exhaustive. Including these ochres also enables this research to be compared with that of the previous authors.

Whilst fine-grained ochres are acceptable for dosing treatments, they are unsuitable for use as in-stream filter units due to their low hydraulic conductivity. A larger grain size is therefore required for utilisation of ochre as a filter substrate, although this can also be achieved through pelletisation of fine-grained ochres. Ochre from several MWTPs in Northern England has been pelletised by Aumônier et al. (permission copy). A pelleted form of ochre from Acomb MWTP was selected for analysis, along with the ochre in its original fine-grained state.

Ochre from Avoca, Ireland, was also selected due to a common concern regarding ochres – namely the mobilisation of PTEs from the ochre matrix. In addition to having been recently researched, and having available samples, Avoca has been shown to contain a relatively high Arsenic (As) concentration. It will therefore be used to study whether As is mobilised under experimental conditions. Ochres from Ynysarwed and Silkstone MWTPs were also selected for the same purpose, having been shown previously to contain relatively high concentrations of As (Hancock, 2004). All the ochres selected for study are listed in Table 3.1.

Table 3.1: Ochres selected for research, organised by treatment system and the presence of PTEs, [1]ochre in a granular form, [2]ochre formed in a wetland.

	Minewater Treatment	
	Active	**Passive**
No PTEs	Polkemmet[1]	Acomb[2] Acomb pellets[1,2] Minto
PTEs	Ynysarwed	Silkstone[2] Avoca

The origin of the different ochres is described in detail below as this information is crucial to interpreting characterisation results, and also for predicting the properties of ochres from other MWTPs. The locations of the MWTPs selected for study in this thesis are displayed in Figure 3.1.

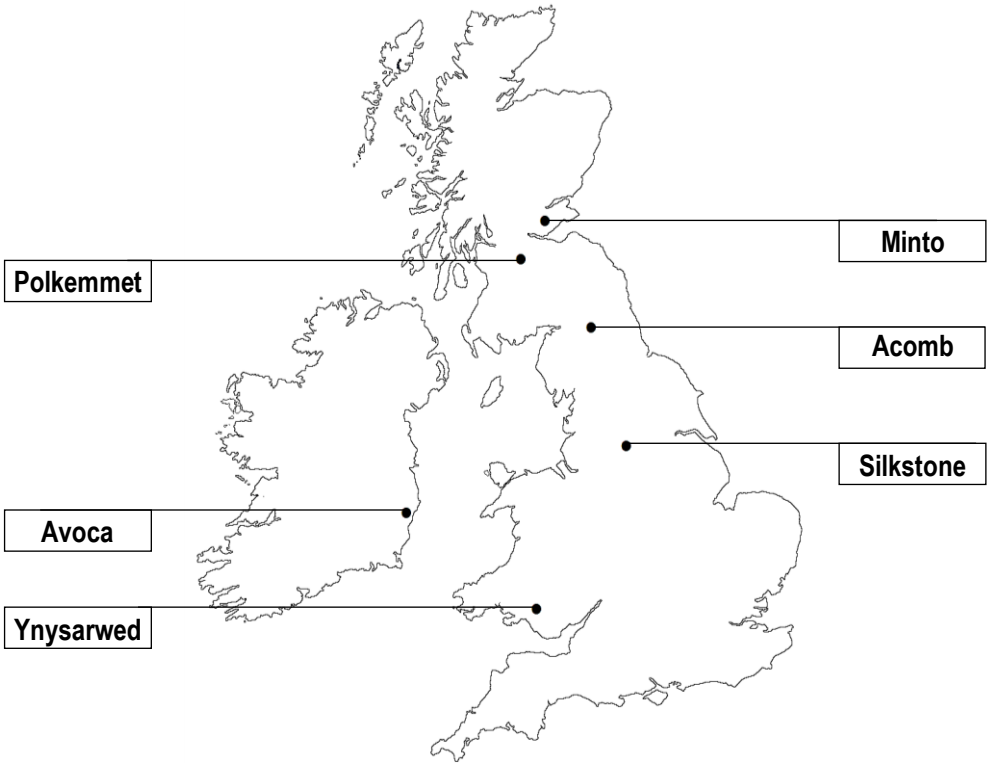

Figure 3.1: Location of MWTPs where ochre samples were collected from.

3.1.1 Polkemmet ochre

The colliery at Polkemmet, Scotland (NS 93678, 64035), was closed in 1984 and pumping of subsurface water ceased in 1986. The rebound of the water table led to the hydrolysis of exposed pyrite minerals and consequently the production of Fe^{2+} rich minewater. The site was targeted for remediation by SEPA as a top priority; an investigation commissioned by the Coal Authority in 1998 concluded that the site could potentially pollute the nearby River Almond (Brown et al., 2002). A minewater treatment scheme was implemented in 1998 before being altered to its present design in 1999. Minewater is pumped from the Polkemmet shaft and dosed with a 35 % H_2O_2 solution which acts as a coagulant. The flow is split into two streams and a polymer flocculant added before being directed into parallel

settlement lagoons where the majority of precipitation and settlement occur, forming ochre (Figure 3.2). Flow continues onto a further settlement lagoon before the effluent is polished in a wetland prior to discharge into surface waters (Brown et al., 2002).

Figure 3.2: Settlement lagoon, Polkemmet, Scotland.

Ochre is removed periodically from the settlement lagoons and transferred to a storage lagoon, where the ochre is air-dried prior to disposal. Samples were taken from these drying beds in December 2007, dried in an unheated greenhouse for six weeks and then mixed to homogenise the ochre. The ochre was orange and brown in colouration upon collection and dried to a dark brown colour with a coarse granular form, as previously reported by McHaffie et al. (2000). The granular nature of the ochre makes it suitable for use as a filter substrate, which has thus been the focus of previous research. A coarse texture is unusual, with most ochres drying to a fine powder; the reason for this is unclear but can perhaps be attributed to the active nature of the treatment system and the addition of polymer flocculant.

3.1.2 Minto ochre

A passive treatment reed bed was installed by the Coal Authority in 1998 to treat polluted discharge originating from the former Minto colliery, Fife, Scotland (NT 20329, 94885). Minewater originating from the mine workings was impacting upon the environmental quality of the River Ore, with precipitates forming upon the bed and inhibiting biological activity.

Minewater is now diverted to an aeration cascade to oxygenate the water, with the flow then split into two streams that enter parallel reed beds (Brown et al., 2002). The flow re-joins before again being split to flow into another set of reed beds (Figure 3.3). The vegetation in the reed beds encourage the sedimentation of ochre by filtering out precipitates and creating favourable conditions for microbial activity.

Figure 3.3: Minto MWTP: One of the four reed beds which treat Minto minewater.

Ochre was collected at this site from the edge of the treatment wetlands in December 2007. It was then dried in an unheated greenhouse for six weeks, drying to a fine rich orange coloured powder, and was then mixed to create a homogeneous sample.

Minto ochre was selected for this research as it is typical of many types of ochre in that it is formed in treatment wetlands and is fine-grained. Previous research on

Minto ochre has found it to have a large P adsorption capacity with rapid adsorption kinetics (Heal et al., 2003b).

3.1.3 Silkstone ochre

A passive system is used to treat minewater originating from the abandoned Silkstone coal mine, England (SE 29065, 05604). It incorporates a lagoon, to encourage settlement of Fe precipitates and PTEs, and a meandering constructed wetland. In February 2008, samples of ochre were taken from the wetland (Figure 3.4). Vegetation from the surface of the wetland was removed using shears, and samples of ochre dug out using a spade. The ochre was then air dried in an unheated greenhouse for six weeks before mixing manually to form a homogenous sample. Like Minto ochre, Silkstone ochre is an example of a wetland-generated ochre originating from coal mine workings. It differs from Minto ochre, however, as it has been shown to have a high concentration of As: a result of the relatively high As concentration of the minewater (Hancock, 2005).

Figure 3.4: Silkstone wetland. Ochre was sampled from an area of the wetland from which vegetation had been removed.

3.1.4 Acomb ochre and Acomb pellets

A passive system, completed in 2001, is used to treat minewater originating from the abandoned Acomb drift coal mine, Northumberland, England (NY 92590, 66143). The water is aerated and then flows through two settlement lagoons containing a mix of vegetation which encourages settlement of PTEs out of solution (Figure 3.5). The water then flows through two wetlands containing a mix of *Typha latifolia, Iris pseudacorus* and *Scirpus lacustris* (Brown et al., 2002). The ochre used for this research comprised Acomb ochre, sampled from the settlement lagoons, which had been air-dried to form a fine-grained powder, and Acomb ochre in a pelleted form, made available to The University of Edinburgh in 2007.

Figure 3.5: Settlement lagoon at Acomb from which ochre was taken (L), Acomb pellets (R).

The procedure for the pelletisation of the pellets is documented in Chapter 2.4. The pellets are robust, with a high hydraulic conductivity, and the high P removal capacity of the ochre is maintained.

3.1.5 Avoca ochre

During the mining of Cu-S ore in the Avoca catchment, Ireland (SG 16993, 30766), settling pits were used to allow Fe and other PTEs to deposit out of the water column (Gallagher and O'Conner, 1999). Water from the mine, abandoned in 1982, also discharges into the River Avoca, leading to ochre deposition on the river bed.

The installation of a MWTP is required at this site to treat the polluted discharge which in turn would produce large quantities of ochre (Fenton et al., 2009).

Samples of ochre which had been present for a minimum of a few decades in the settling pits, detailed in Fenton et al. (2009), were provided by Dr Owen Fenton (TEAGASC, Agriculture and Food Development Authority, Ireland). They were oven-dried at 95°C for 24 hours, any vegetation within the samples was removed manually, and the ochre was sieved <2 mm (Figure 3.6). Initial analysis showed the ochre to have a high P adsorption capacity, 16-21 mg P g^{-1}, similar to other ochres chosen for this research, but a low pH in distilled water of 3 (Fenton et al., 2009).

Chemical analysis of Avoca ochre by Fenton et al. (2009) showed that it has high concentrations of many PTEs such as As. The potential release of these PTEs during P adsorption needs to be understood before the ochre can be used in environmental applications.

Figure 3.6: Avoca ochre: Ochre settling pits from which samples were taken (L), Avoca ochre after drying (Image courtesy of Dr. Owen Fenton) and vegetation removal (R).

3.1.6 Ynysarwed ochre

Drainage in an adit from the former Ynysarwed Cu-S, South Wales (SN 80856, 01715) is net acidic, with pH as low as 3.5 and a Fe concentration of up to 400 mg L^{-1} (Brown et al., 2002). It has been treated since 1993 by a combination of active and

passive processes to raise the pH, and precipitate out the metals in solution to form ochre, before entering the Neath canal.

The active stage includes mechanical aeration with the addition of lime and a polymer flocculent in a large tank. Lamella plate separators then aid the settlement of precipitates out of the water column. Sludge is drawn off the bottom of the tanks and pumped to a settlement lagoon (Figure 3.7) where it is stored before mechanical dewatering via centrifuge, and then disposal to landfill. Owing to the presence of vegetation overhanging the settlement lagoon some organic matter may be present in the ochre.

Figure 3.7: Settlement lagoon at Ynysarwed.

Treated minewater, with a Fe concentration of 3-5 mg L^{-1} is piped to a 1 ha constructed wetland to further reduce PTE concentrations before discharge into a canal and subsequently the River Neath (Brown et al., 2002).

Dewatered ochre was collected from the active treatment works in February 2008 from skips which were awaiting landfill. It was then air-dried for six weeks and prepared in the same way as the other ochres. Ynysarwed ochre has a high

concentration of As (Hancock, 2004) and as such is of interest to examine whether PTEs are released from the ochre matrix during P adsorption.

3.2 Ochre pH

The pH of ochre is important for two main reasons. Firstly, the relationship between pH and P-adsorption capacity of various materials (Figure 3.8) indicates that substances with a high pH tend to have a higher P adsorption capacity, whilst materials with pH <6 have a low P adsorption capacity (Cucarella and Renman, 2009). Secondly, reducing conditions can lead to the release of P from the ochre matrix, a concern with the use of ochre for many environmental applications. An extensive release of P is considered unlikely even under reducing conditions if ochre has an alkaline pH and a high Ca content (Dobbie et al., 2009).

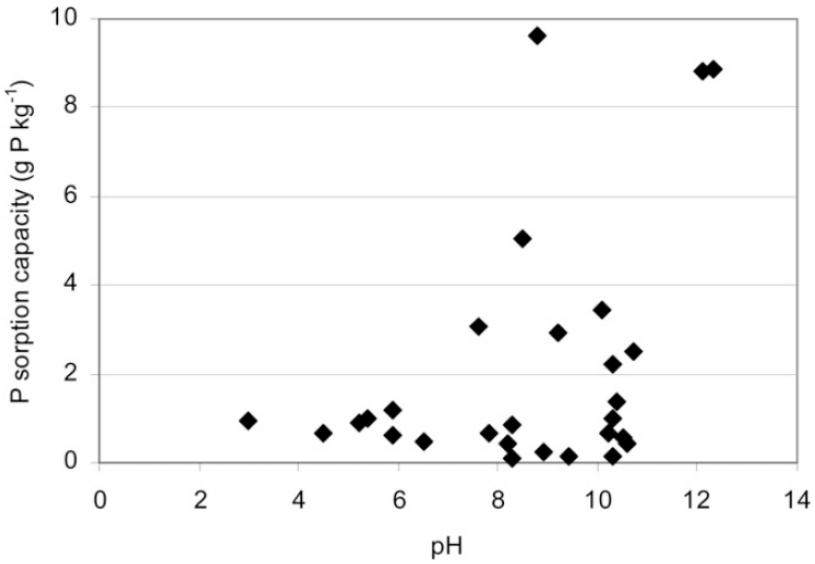

Figure 3.8: Relationship between pH and P adsorption capacity of various materials suggested for P adsorption, from Cucarella and Renman (2009).

In this study pH was determined in deionised water based upon the British Standard ISO 10390 (2005) method, using air-dried ochres that had been passed through a 2 mm sieve. Two types of Acomb pellets were investigated: pellets less than 2 mm in diameter and pellets > 2 mm which had been crushed and passed

through a 100 μm sieve. pH was determined for three separate samples of each ochre. 5 mL ochre was measured into a 50 mL centrifuge tubes and 25 mL deionised water was added to obtain a 1:5 volume ratio. The centrifuge tubes were sealed, shaken in a cabinet shaker at 150 rpm for 60 minutes and then removed and allowed to stand upright for 1 hour. The pH was measured using a temperature compensated bench-top pH probe calibrated with pH 4.01, 7.01 and 10.01 buffer solutions and recalibrated after every 20 samples. The results from the experiment are shown in Table 3.2.

Table 3.2: Mean and standard deviation of the pH measured in the ochres (n=3).

Ochre	pH	
	Mean	σ
Acomb	7.81	0.006
Acomb pellets	9.68	0.045
Acomb pellets (crushed)	11.20	0.032
Avoca	2.31	0.015
Minto	7.37	0.081
Polkemmet	7.52	0.035
Silkstone	6.97	0.032
Ynysarwed	9.30	0.083

The pH of most ochres was in the range ~7-9, apart from Acomb pellets (pH 9.68 and 11.20) and Avoca ochre (pH 2.31). The pH of Minto and Polkemmet ochre has been previously determined as 6.9 and 7.2 respectively (Heal et al., 2003b). Whilst the results presented here support that the pH of Polkemmet ochre is higher than that of Minto ochre, the values are higher than reported previously. This may indicate that conditions at the MWTPs have changed in the time between samples being taken.

Whilst minewater at Minto is treated passively in a wetland system, Polkemmet minewater is treated actively using 35% hydrogen peroxide solution as a coagulant and a polymer flocculant to encourage sedimentation. The addition of 35%

hydrogen peroxide (~pH 4.6) is unlikely to be the controlling factor in producing an ochre with a pH of 7.52; the treatment conditions may lead to formation of an ochre dominated by goethite minerals, the most stable mineral phase associated with acid mine drainage (Bigham et al., 1996). Polkemmet ochre is a dark brown colour, previously correlated to a high concentration of goethite, whilst Minto ochre is a dark red-orange colour, suggestive of poorly crystalline minerals, such as ferrihydrite (Brady et al., 1986). This difference in the mineralogy of the two ochres may account for the differing pH results, with weathering reactions generating different amounts of H^+ during the experiment.

Silkstone and Acomb ochres, like Minto, are formed within a passive wetland treatment system. It is therefore expected that they will have a similar pH, and any differences can be accounted for by the composition of the minewater treated. Of the three wetland ochres, the pH of Silkstone (6.97) is the lowest, and Acomb ochre has the highest pH (7.81).

Pelletising Acomb ochre renders the pH of the material more alkaline, probably due to the addition of Portland cement in the pelletisation process which has a high pH in water. This is due to the dissolution of Ca, Na and potassium hydroxides. The pH of Acomb pellets increased from 9.68 to 11.2 when crushed to a smaller grain size. This is attributed to the creation of a greater surface area of ochre which may increase the rate of Ca, Na and potassium hydroxide dissolution.

Ynysarwed ochre has a pH of 9.30, the highest of all the ochres in their 'unprocessed' form. This is attributed to the addition of lime to minewater at the Ynysarwed MWTP, before a polymer is added as a flocculant.

Avoca ochre had a strongly acidic pH of 2.31. The pH of the ochre had been previously reported to be around 3, although this measurement was conducted after the ochre had been saturated with P (Fenton et al., 2009). Avoca ochre has a P

adsorption capacity lower than other ochres, ~16-21 mg P g^{-1}. This corresponds to the correlation that P adsorption capacity increases with adsorbent pH. The formation of Avoca ochre differs from the others studied as it was deposited in settling pits a number of decades prior to excavation. The properties of the ochre may therefore have been altered by weathering reactions since deposition.

3.3 Ochre surface area determination

Total surface area is an important characteristic to determine for assessing the potential of a material to be a successful adsorbent in wastewater treatment (McKay, 1996). Based upon the assumption that adsorption sites are equally distributed across the surface of an adsorbent, larger surface areas correspond to materials with a greater adsorption capacity. The surface areas of the ochres were determined using the B.E.T. method (Brunauer et al., 1938). B.E.T. surface area is an aggregate of the internal and external surface areas of a material. Whilst the external surface area of an adsorbate defines the contact time with the adsorbent and therefore influences the kinetics of adsorption, it is internal surface area that determines the amount of adsorption that occurs at equilibrium (Cooney, 1999).

All ochres were passed through a 100 μm sieve in order to obtain comparable particle size fractions across ochres. Acomb pellets were crushed with a pestle and mortar before sieving to 100 μm. Care was taken not to grind the pellets as this may create new surfaces for adsorption thus resulting in an overestimate of surface area.

3.3.1 B.E.T theory and calculation

Calculating the surface area of a substance using gas adsorption allows the entire surface to be investigated including pore interiors and irregularities. The amount of gas adsorbed is also a function of temperature, pressure and the intrinsic strength of attraction between the solid and gas. By keeping temperature constant, and varying pressure, the amount of adsorbate adsorbed varies. Different types of adsorption

occur at different pressures, and from this the surface area can be determined (Figure 3.9).

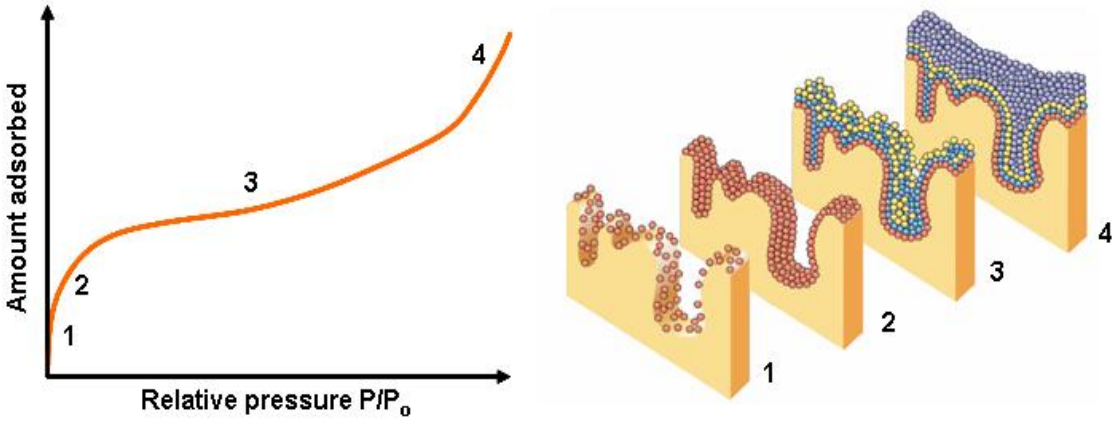

Figure 3.9: Relationship between amount of adsorbate adsorbed and relative pressure during BET analysis. 1: Filling of micropores with adsorbate. 2: Formation of a monolayer on the material. 3: Multilayer condensation, 4: Capillary condensation. (R) adapted from Micromeritics (2001).

B.E.T surface area analysis was conducted using a Micromeritics Gemini 2370 surface area analyser at the "Archaeological, Forensic & Environmental Scientific Services" laboratories, University of Reading. This uses a flowing gas technique whereby the analysis gas flows simultaneously into a tube containing the sample and a balance tube; both are immersed in a liquid nitrogen bath to maintain isothermal conditions. Analysis gas (N_2) is delivered to both tubes using servo valves connected to a differential pressure transducer. This measures the pressure difference between the two tubes which is caused by adsorption of N_2 onto the sample. As adsorption occurs, the pressure drops in the sample tube and the servo valve delivers more N_2 into the sample tube to maintain equal pressure in the two tubes.

Samples were degassed using a Micromeritics FlowPrep 060 overnight at 60°C in a flow of nitrogen, to ensure they were free of moisture and other contaminants prior to analysis. For quality control an internal standard, Montmorillonite (Mont-33),

with a known B.E.T surface area was also analysed. One replicate of each sample was analysed at five different pressures with the BET transformation (B_I) calculated for each pressure (Equation 3.1).

$$B_I = \frac{Prel_I}{(1.0 - Prel_I)(Nads_I)} \qquad \text{Equation 3.1}$$

Where B_I = BET transformation (g $cm^{-3)}$, $Prel_I$ = relative pressure adsorbed after equilibrating I^{th} dose (cm^3 STP) and $Nads_I$ = volume of gas adsorbed.

B_I values were plotted against relative pressure and a linear trend-line fitted (see Figure 3.10 for an example). The slope of the line, y-intercept, error of the slope, error of the y-intercept, and the correlation coefficient, were all calculated and used to determine BET surface area (SA_{BET}) in m^2 g^{-1} (Equation 3.2).

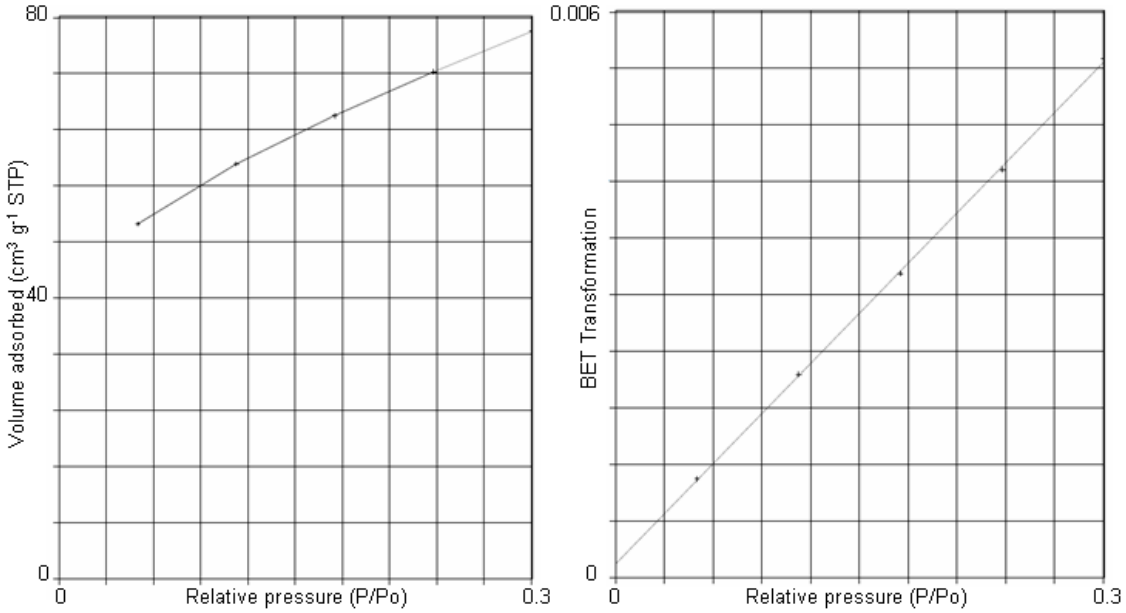

Figure 3.10: Calculating BET surface area for Silkstone ochre: Left: Volume of analysis gas (N_2) adsorbed plotted against relative pressure. Right: BET transformation (B_I) plotted against relative pressure.

$$SA_{BET} = \frac{(CSA)(6.023 \times 10^{23})}{(22414\,cm^3\ STP)(10^{18}\,nm^2/m^2)(S + Y_{INT})}$$ Equation 3.2

Where: CSA= analysis gas (N_2) cross-sectional area (nm^2), S = slope (g cm^{-3} STP) and Y_{INT}= y-intercept (g cm^{-3} STP)

3.3.2 B.E.T surface area results

B.E.T surface area varies with ochre type (Table 3.3). Silkstone ochre has the largest surface area, 243.41 $m^2\ g^{-1}$, and Avoca ochre the smallest, 55.93 $m^2\ g^{-1}$. Acomb and Minto ochre are formed under similar conditions to Silkstone ochre, from the passive treatment of coal mine drainage in wetlands, but have smaller B.E.T surface areas, 184.50 $m^2\ g^{-1}$ and 113.29 $m^2\ g^{-1}$ respectively. The B.E.T surface area of Acomb ochre reduced to 103.87 $m^2\ g^{-1}$ following the pelletisation of the ochre.

In comparison to many other materials used as P adsorbents, such as bauxite and zeolite, the ochres studied had a higher B.E.T surface area (Table 3.3). Materials with a higher B.E.T surface area tend to be expensive. Activated carbon, for example, has a much higher potential surface area for adsorption than the ochres analysed but costs US$700-1480 per tonne.

The P adsorption maximum of adsorbent materials has been shown to correlate positively with surface area (Fontes and Weed, 1996), therefore ochre with a larger surface area is expected to have a higher P adsorption capacity. The P adsorption capacities of Minto, Polkemmet and Avoca ochre have been previously determined as 30.5, 26 and 20 mg P g^{-1} respectively (Bozika, 2001; Fenton, 2009). This supports the hypothesis that surface area and P adsorption capacity are positively correlated as, of these three ochres, Minto has the highest surface area and Avoca the lowest.

Table 3.3: B.E.T surface area of the ochres and, for comparison, other materials used as P adsorbents (3 s.f). The B.E.T surface area of the Mont-33 was within the expected range for the standard. [1]Cooney (1999), [2]Drizo et al. (1999), [3]Jeong et al., (2007), [4]Unob et al. (2006).

Adsorbing Material	B.E.T Surface Area (m^2 g^{-1})
Acomb ochre	184
Acomb pellets	104
Avoca ochre	56
Minto ochre	113
Polkemmet ochre	98
Silkstone ochre	243
Ynysarwed ochre	220
Mont-33	55
Activated carbon(1)	600-2000
Bauxite(2)	6.80
Burnt oil shale(2)	8.30
Fe_2O_3(3)	5.05
Iron hydroxide coated silica gel(4)	236
Limestone(2)	7.40
Shale(2)	19.9
Zeolite(2)	31.4

3.4 Total metal analysis

The elemental composition of the ochres was determined from a strong acid digestion (HCl-HNO_3) that dissolves both crystalline and amorphous mineral structures, but not elements strongly bound in silicate structures, which are not normally mobile within the natural environment. Previous analysis of the composition of Polkemmet and Minto ochre using the same HCl-HNO_3 acid digest method showed that they comprise elements known to adsorb P, such as Fe, Al, Ca and Mg (Heal et al., 2003b).

3.4.1 Methodology

Triplicate sub-samples of all seven ochres, and a Fe-rich certified reference material (CRM) NCS DC 73308, were acid digested. 20 g ground ochre was oven dried for 24

hours at 105°C to remove any moisture. 5 g oven-dried ochre was then ashed in a muffle furnace at 430°C for 6 hours, cooled in a desiccator, and reweighed.

Crucibles containing 1 g ashed samples were placed on a water bath, set at 40°C. 5 mL concentrated HCl was added to the crucibles before they were covered with watch glasses and left to warm for 15 minutes. The watch glasses were rinsed into the crucibles using a small amount of distilled water and 1 mL concentrated HNO_3 was added to each. The crucibles were left for an hour or until evaporated when 1 mL 1:1 HCl was added to each crucible. Following this, deionised water was added to the crucibles which were then heated on the water bath. The crucibles were removed and allowed to cool to room temperature. The digests were then filtered into a 50 mL volumetric flask using 0.45 μm cellulose filter paper, rinsing out the crucibles with deionised water. The filtered solution was made up to 50 mL using deionised water and analysed by ICP-OES in the laboratories of the James Hutton Institute in Aberdeen for concentrations of Al, As, B, Ca, Cu, Fe, K, Mg, Mn, Na, Ni, Pb, S, Si, Sr and Zn. Blank experiments were also conducted, using the same methodology as above but without any solid material. The concentrations of the analytes in these blank experiments were all below the detection limits.

3.4.2 Results

The composition of the CRM, determined by acid digestion, compared to the certified values is shown in Figures 3.11 and 3.12. Of the major constituents of the CRM – the acid digest concentrations and certified values are not statistically different for Ca (2-tailed z-test, $p>0.05$). The acid digest calculated and certified values are significantly different, however, for the other major constituents (Al, Fe, K and Mn).

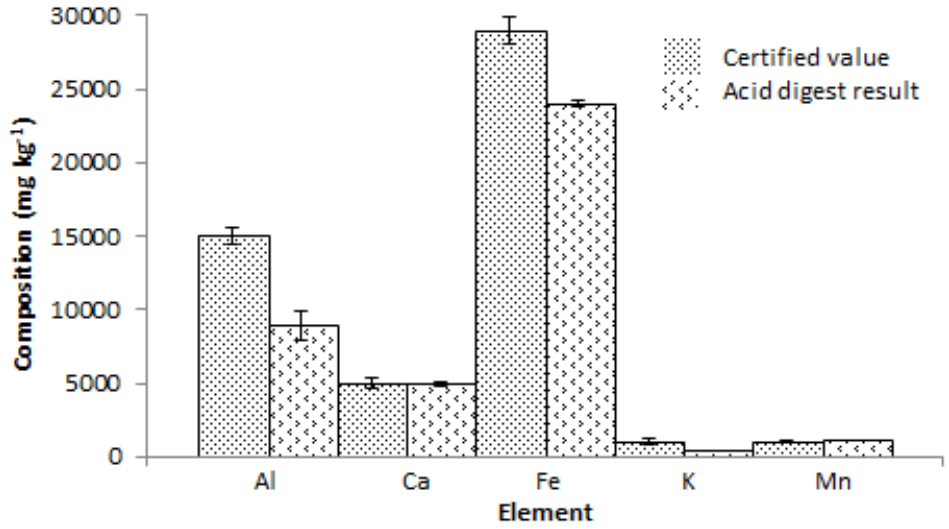

Figure 3.11: Major constituents of CRM: Certified values and those determined by acid digest (n=3),bar indicates the mean value, error bars ± 1 s.d.

Of the minor constituents of the CRM – there was no significant difference between the Cu concentration determined by acid digestion and the certified value. The difference in concentrations determined from acid digestion and certified values were significantly different, however, for the other minor constituents (As, B, Mg, Na, Ni, Pb, S, Sr and Zn).

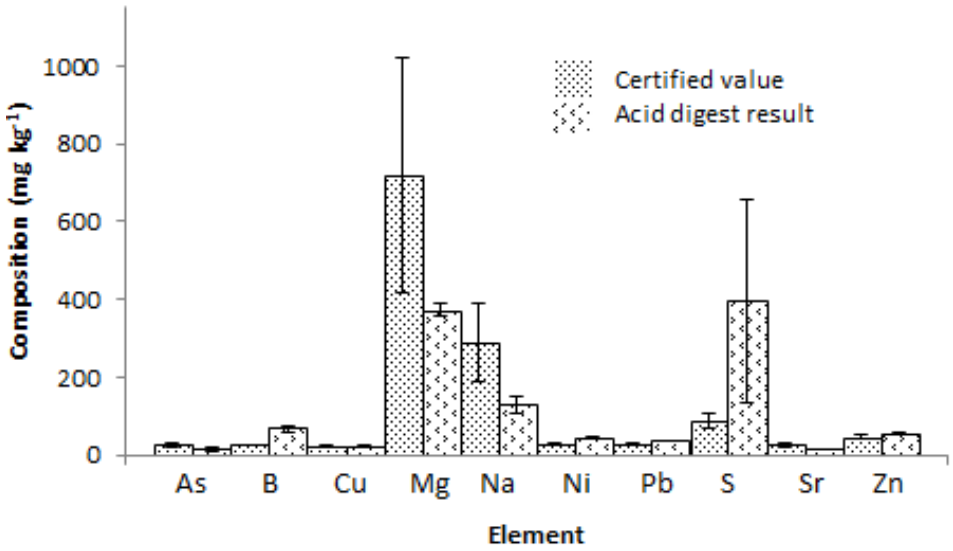

Figure 3.12: Minor constituents of CRM: Certified values and those determined by acid digest (n=3),bar indicates the mean value, with error bars ± 1 s.d.

Due to the large discrepancy between many of the certified values and those measured by the acid digestion for the CRM, a correction factor (CF) was applied to the results garnered from the acid digest. CF was calculated as the percentage difference between the certified values of the CRM and those measured in the acid digest; e.g. for Al, the certified value had a higher concentration by 69 %, therefore the CF is 1.69. The adjusted ochre composition with associated CFs is shown in Table 3.4.

Table 3.4: Constituents of ochre, % by dry weight, determined by HCl-HNO_3 acid digest, analysis by ICP-OES, to 3 s.f. (Polk: Polkemmet, Yny: Ynysawred, Silk: Silkstone, AcP: Acomb pellets).

Element		**Ochre**						
	CF	**Avoca**	**Polk**	**Yny**	**Minto**	**Silk**	**Acomb**	**AcP**
Al	1.69	0.715	3.40	0.627	0.169	0.468	0.328	3.63
As	1.68	0.0257	<0.001	0.0554	<0.001	0.0119	<0.001	<0.001
Ca	1.00	0.0577	0.963	1.56	1.27	0.442	2.91	10.8
Cu	1.00	0.0567	0.00385	0.000502	0.00149	0.00459	0.00118	0.00530
Fe	1.21	50.4	44.6	31.8	60.9	41.0	56.9	31.5
Mg	1.93	0.359	0.461	34.4	0.552	0.170	0.243	2.82
Mn	0.90	0.00733	0.106	0.0470	0.221	0.410	0.0456	0.113
Ni	0.69	0.00314	0.00449	0.00445	0.00578	0.00433	0.00419	0.00218
Pb	0.73	0.138	0.00934	0.00383	0.00788	0.00617	0.00788	0.00450
S	0.23	0.759	0.125	0.0849	0.0750	0.0299	0.0518	0.124
Zn	0.79	0.0293	0.00924	0.00423	0.000924	0.00776	0.0127	0.00675

The composition of the ochres determined from the HCl-HNO_3 acid digest (Table 3.4) is highly variable, although all ochres have high Fe concentrations (Figure 3.13). Minto ochre has the highest Fe content at 60.9 %. The other ochres formed within wetland treatment systems, Acomb and Silkstone ochre, contain 56.9 and 41.0 % Fe

by dry weight, respectively. The pelletisation of Acomb ochre reduces the Fe content to 31.5 % as the ochre is diluted with additives. Avoca ochre, formed in settling pits, contains 50.4 % Fe by dry weight whilst the two ochres treated actively, Polkemmet and Ynysarwed, contain 44.6 and 31.8 % Fe, respectively.

The concentration of other elements, aside from Fe, with a high P adsorption capacity in the ochres, namely Al, Ca and Mg, is far lower. Notable concentrations of Al are present in Polkemmet ochre and Acomb pellets. The higher Al content of Acomb pellets, 3.63 %, compared to only 0.328 % in Acomb ochre is a result of the pelletisation process which involves the addition of calcium alumina-silicates. Acomb pellets also have a far higher Mg concentration, 2.82 % by dry weight, than Acomb ochre due to another additive used in the pelletisation process. Acomb pellets have the highest Ca concentration by dry weight, 10.8 %, reflecting the addition of a Ca-rich material during pelletisation (Aumônier et al., permission copy).

Materials containing high concentrations of both Al and Fe tend to have the highest P adsorption capacity (Ainsworth et al., 1985; Sibrell et al., 2009). Consequently, whilst Polkemmet ochre has a relatively low Fe content in comparison to the other ochres studied, an Al content of 3.40 % by dry weight may increase the adsorption capacity of this ochre.

Ynysarwed ochre has a Mg content of 34.4 % by dry weight which could be due to high Mg concentrations in the untreated minewater. The addition of Mg may also occur when a polymer is added during active treatment, however. pH adjustment occurs at Ynysarwed MWTP by the addition of lime, as is reflected in the relatively high Ca concentration measured in this ochre.

Of the elements associated with P removal (Al, Ca, Fe and Mg) Ynysarwed contains the highest combined concentration, 68.4 % (Figure 3.13), largely due to a high Mg

content. Silkstone ochre has the smallest combined concentration of these elements, 42.0 %, and is therefore expected to have a lower P adsorption capacity. The remaining ochres have combined concentrations of Al, Ca, Fe and Mg between 48.8 and 62.9 %.

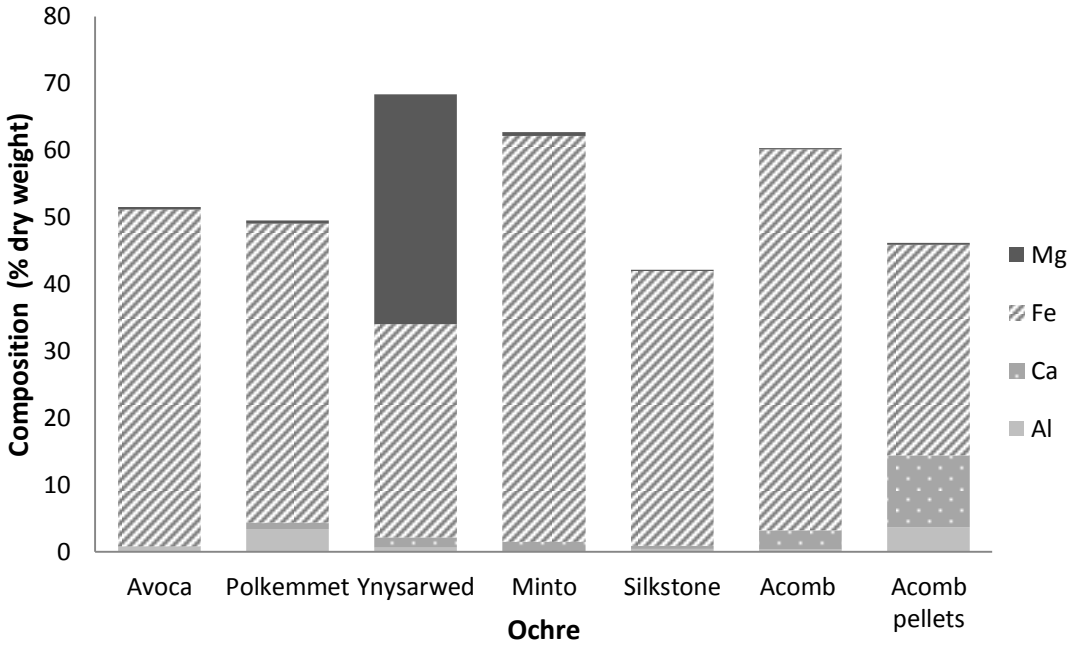

Figure 3.13: Corrected Al, Ca, Fe and Mg elemental composition of ochres, determined by HCl-HNO_3 acid digest, analysis by ICP-OES.

The concentration of Al, Ca, Fe and Mg in Minto and Polkemmet ochre has been previously determined using the same methodology utilised here (Heal et al., 2003b). The composition of ochre is known to vary with time due to changes in treatment and minewater conditions (Brown et al., 2002). Therefore, whilst the ochre analysed by Heal et al. (2003b) originated from the same MWTPs, it was collected about eight years prior to the ochre samples analysed here and hence its composition may have changed. In comparison to Heal et al. (2003b, values in brackets), this study measured lower concentrations of Ca (7.0 % and 11.8 %), Fe (65 % and 67.5 %) and Mg (0.6 % and 0.8 %), with higher concentrations of Al (0.7 % and 0.1 %) for Polkemmet and Minto ochre respectively.

Avoca, Ynysarwed, and Silkstone ochre were selected for this study in part due to their high As concentrations: 0.0162, 0.0746 and 0.0332 % by dry weight, respectively (Fenton et al., 2009; Hancock, 2004). The concentration of As in Avoca ochre was measured here as 0.0257 % by dry weight, higher than that determined by Fenton et al. (2009), possibly because the ochre digested by Fenton et al. (2009) had been saturated with P prior to analysis. Lower As concentrations were found for Silkstone and Ynysarwed ochre than previously reported (Hancock, 2004). Ynysarwed has the highest As concentration of the ochres examined, 0.03554 % by dry weight, with Silkstone containing 0.0119 %. Arsenic was only detected in the three ochres previously identified to have a relatively high As content.

3.5 Acid ammonium oxalate extractable Fe

Whilst total elemental concentrations determined from acid digestion indicate the P adsorption capacity of ochres, the form of Fe in the ochre, whether crystalline or amorphous, is also an important control on the P adsorption capacity as amorphous forms of Fe have a larger surface area for adsorption. An ammonium oxalate extraction was conducted to determine the amorphous Fe in the seven ochres.

3.5.1 Methodology

To calculate the Fe concentration contained within amorphous minerals the ochres were extracted with acid ammonium oxalate, using the method proposed by McKeague and Day (1966) and modified by Farmer et al. (1983).

Acid ammonium oxalate solution was made by mixing 700 mL 0.2 M ammonium oxalate solution with 535 mL 0.2 M oxalic acid. The pH of the solution was adjusted to 3.0 by adding small amounts of either solution as required. 40 mg of air dried ochre, <0.1 mm, was weighed (to 4 decimal places) into a 50 mL centrifuge tube. 20 mL acid ammonium oxalate solution was pipetted into the tube which was then sealed and placed in a cardboard box to exclude light, and rotated for 4 hours at 120 rpm in a cabinet shaker. All experiments were conducted in triplicate. The tubes

were then removed and centrifuged at 3500 rpm for 10 minutes, and the supernatants analysed for Fe content by ICP-OES at the James Hutton Institute laboratories, Aberdeen.

The maximum P sorption capacity of the amorphous Fe content of the ochres was calculated from Equation 3.3.

$$Q_m = \alpha_m M \qquad \text{Equation 3.3}$$

Where; Q_m is the maximum sorption capacity (mmol P kg ochre^{-1}), M the extractable Fe (mmol kg^{-1}) and α_m the fraction of M than can bind P (Moelants et al., 2011).

As suggested by Moelants et al. (2011), α_m, the coefficient which describes the proportion of Fe in contact with solution, was set at 0.5 and the P sorption capacity of the ochres calculated, with figures converted to mg P g^{-1} ochre.

3.5.2 Results

The concentration of ammonium oxalate extractable Fe in the ochres is shown with the total Fe content determined by HCl-HNO_3 for comparison in Table 3.5. The amount of ammonium oxalate extractable Fe varied for the ochres between 8.2%, for Polkemmet ochre, to 23.9 % for Silkstone ochre. Whilst it was determined in the HCl-HNO_3 digest that Minto ochre had the highest total Fe content of all the ochres, most of this Fe is in crystalline forms, with only 14.8 % of the total Fe content in amorphous forms. In contrast, whilst only 31.8 % of Ynysarwed ochre was found to be Fe by HCl-HNO_3 digest, most of this Fe (74.5 %) is in the amorphous state, as determined by the ammonium oxalate extraction.

Table 3.5: Ammonium oxalate extractable Fe content (by % dry weight) for the seven ochres under study (3 s.f.) and the maximum P sorption capacity associated with this (Equation 3.3). Digest results are the mean values from triplicate experiments.

Ochre Type	Ammonium oxalate	$HCl\text{-}HNO_3$	P sorption capacity	Fe in amorphous state
	Fe content (%) as extracted by digest		(mg g^{-1})	(%)
Acomb	14.8	56.9	41.0	26.0
Acomb pellets	10.1	31.5	27.0	32.1
Avoca	18.6	50.4	51.5	36.9
Minto	9.0	60.9	25.0	14.8
Polkemmet	8.2	44.6	22.7	18.4
Silkstone	23.9	41.0	66.3	58.3
Ynysarwed	23.7	31.8	65.8	74.5

The maximum P sorption capacity was determined using Equation 3.3 and is presented in Table 3.5. As this derived maximum P sorption capacity is a function of ammonium oxalate extractable Fe, the highest value corresponds with Silkstone ochre, 66.3 mg P g^{-1}, and the lowest with Polkemmet ochre, 22.7 mg P g^{-1}. These theoretical maximum sorption capacities are larger than have been previously determined, 21.5 mg P g^{-1} and 18.2 mg P g^{-1} for Polkemmet ochre and Minto ochre respectively (Bozika, 2001) and 21 mg P g^{-1} for Avoca ochre (Fenton et al., 2009). Moelants et al. (2011) note that this calculation often overestimates the P sorption capacity of materials. It should thus only be used as a guideline. The P sorption capacities of the ochres under study are also calculated from P adsorption batch experiments in Chapter 4.

3.6 Ochre Mineralogy

Ochre mineralogy was determined using x-ray diffraction (XRD). The rate and capacity of P adsorption by Fe varies with mineral form. Mineral structure affects not only the available surface area for adsorption, but the number and distribution of reactive surface sites.

3.6.1 Methodology

Ochres were crushed to a fine powder using a pestle and mortar, and passed through a 100 μm sieve. The ochre powder was then poured into a plastic receptacle for use in the analytical equipment, and excess powder removed by scraping. Care was taken not to compress the powder as the method relies on mineral structures being randomly orientated in the sample. The ochre was then rotated under a beam of x-rays and the diffracted radiation counted using an x-ray detector. The amount of x-rays diffracted at each angle can be used to interpret the mineral forms in the sample by comparing the diffraction patterns to those of standards. Samples were analysed using a Panalytical Xpert-pro theta-theta diffractometer. Nickel filtered Copper radiation was utilised, counting for 300 seconds at a 0.17 degree step. A position sensitive Xcellerator detector was used to count the x-rays diffracted by the sample.

3.6.2 Results

Data from the XRD experiment is presented in Figures 3.14, 3.15 and 3.16. These figures are annotated to highlight some of the major peaks which indicate the presence of various minerals. It is important to note that the relative intensity of a peak is not directly proportional to quantity. For example, quartz gives a high peak at around 27 2ϕ, however this is due to the crystalline structure of the mineral resulting in a high level of diffraction. The interpreted results of the XRD are displayed in Table 3.6. All the ochres were found to contain goethite (FeOH), previously determined as a major component of Polkemmet and Minto ochres (Heal et al., 2003b).

Table 3.6: Mineral components of the ochres under study determined by XRD.

Ochre	Major components	Minor components
Acomb	Goethite, Quartz	Calcite
Acomb pellets	Calcite, Goethite	Quartz
Avoca	Chlorite, Quartz	Goethite, Jarosite
Minto	Goethite	
Polkemmet	Quartz, Goethite	Kaolinite
Silkstone	Labradorite	Quartz, Goethite
Ynysarwed	Brucite	Goethite, Calcite, Double-layered hydroxide.

Quartz was found is many of the samples and reflects that most ochres are formed in treatment wetlands or in the natural environment. Quartz is the second most abundant mineral on the planet and its presence in the samples is detrital.

The major mineral component of Acomb ochre was determined as goethite (54 %), with the ochre containing minor amounts of calcite (14 %) and quartz (32 %; Figure 3.14). The presence of calcite is in agreement with the relatively high Ca concentration of the ochre determined in the acid digest analysis. Acomb pellets were found to be mainly comprised of goethite (35 %) and calcite (52 %). This is reflective of the Acomb ochre used in the pellets, which contained these minerals. More calcite is present in the pelleted ochre due to the addition of Ca during the pelletising process.

Avoca ochre contains large amounts of chlorite (39 %) and quartz (31 %) with minor amounts of goethite (20 %) and jarosite (10 %; Figure 3.14). Fenton et al. (2009) found Avoca ochre to be primarily comprised of goethite with ferrihydrite, jarosite, and quartz also present in the sample. Whilst the ochre compared here is from the same sampling effort, the ochre in this study was examined two years later. Ferrihydrite is associated with younger sediments and is known to transform into goethite with time (Singh et al., 1999). It is therefore proposed that any ferrihydrite

present in the ochre when sampled has transformed into goethite in the two years prior to analysis in this study. The quartz and chlorite in the samples of this study are most likely detrital.

Minto ochre was found to be 100 % goethite (Figure 3.15) and unlike previous research, ferrihydrite was not present in the sample (Heal et al., 2003b). As with Avoca ochre, it may be that ferrihydrite was present in the ochre upon formation, but in the time between collection and analysis this ferrihydrite has transformed into goethite (Singh et al., 1999).

Polkemmet ochre is mainly comprised of goethite (35 %), as previously reported by Heal et al. (2003b), but whereas the previous research report the presence of ferrihydrite, this study found quartz (40 %) and kaolinite (25 %; Figure 3.15)). The ochre collected for this study had been in-situ in a drying lagoon for more than six months prior to collection and, as such, any ferrihydrite present upon formation may have transformed into goethite when the sample was analysed (Singh et al., 1999). The presence of kaolinite in the ochre reflects the high Al concentration determined in the ochre by acid digest (Chapter 3.4). Silkstone ochre contains 58 % Labradorite ($(Ca,Na)(Al,Si)_4O_8$), a feldspar mineral probably reflecting detrital material as a result of the ochre forming in a treatment wetland. Further to this, Silkstone ochre contains 26 % quartz and 16 % goethite, Figure 3.15.

The major component of Ynysarwed ochre was found to be brucite (61 %; Figure 3.16). This corresponds to the results of the acid digest, with Ynysarwed containing 34.4 % Mg by dry weight. Magnesium hydroxide is added to the minewater in the MWTP as an active treatment step (Geroni et al., 2010) resulting in the presence of brucite in the ochre. The ochre also contained goethite (16 %), calcite (11 %) and a double layered hydroxide (12 %), most likely a pyroaurite compound containing Fe and Mg (Drits and Bookin, 2001).

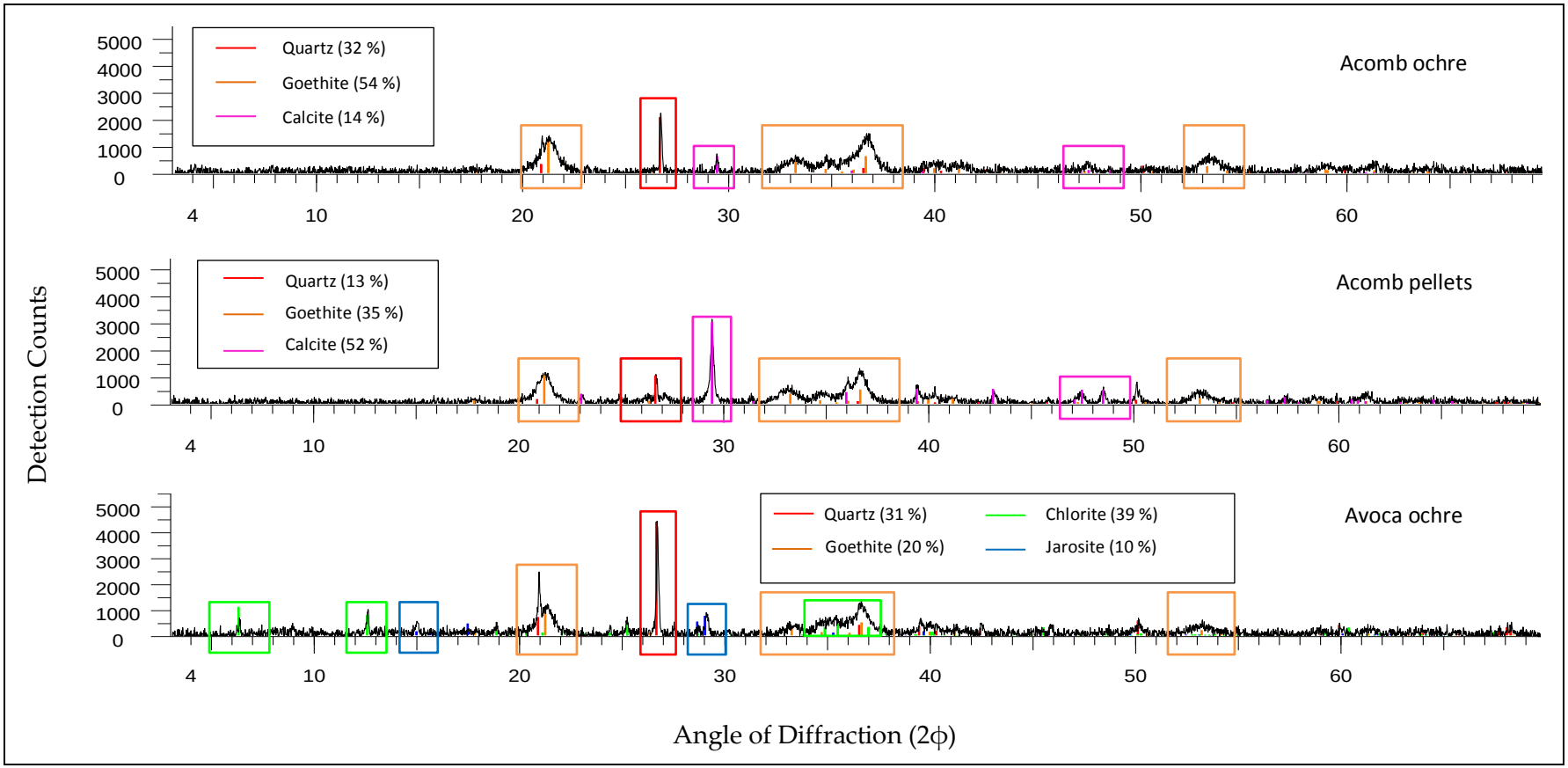

Figure 3.14: Background subtracted x-ray counts detected from the XRD experiment for Acomb ochre, Acomb pellets and Avoca ochre. Position and magnitude of peaks interpreted to determine mineral phases present in the ochre and from this the estimated mineral content.

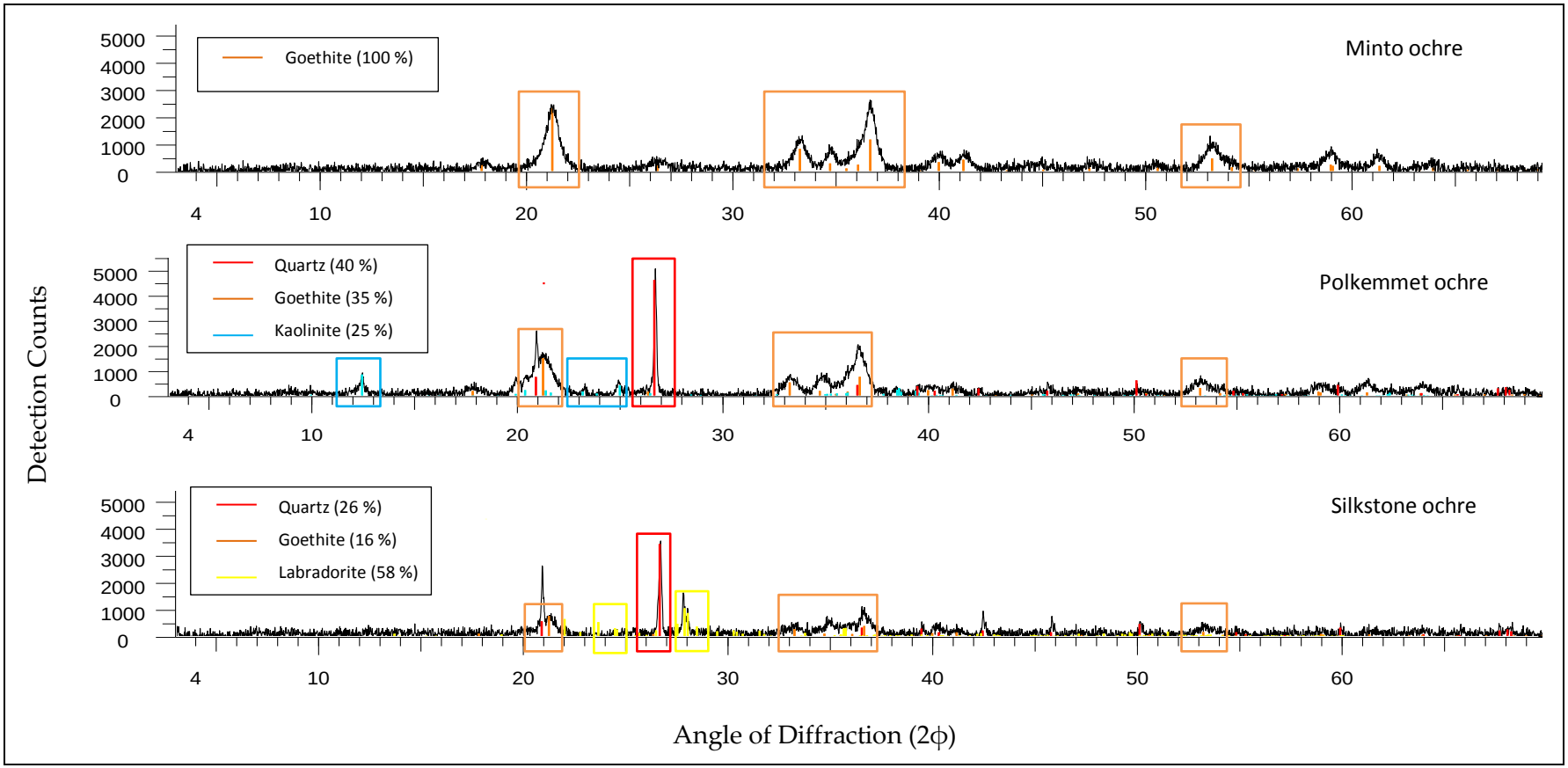

Figure 3.15: Background subtracted x-ray counts detected from the XRD experiment for Minto, Polkemmet and Silkstone ochre. Position and magnitude of peaks interpreted to determine mineral phases present in the ochre and from this the estimated mineral content.

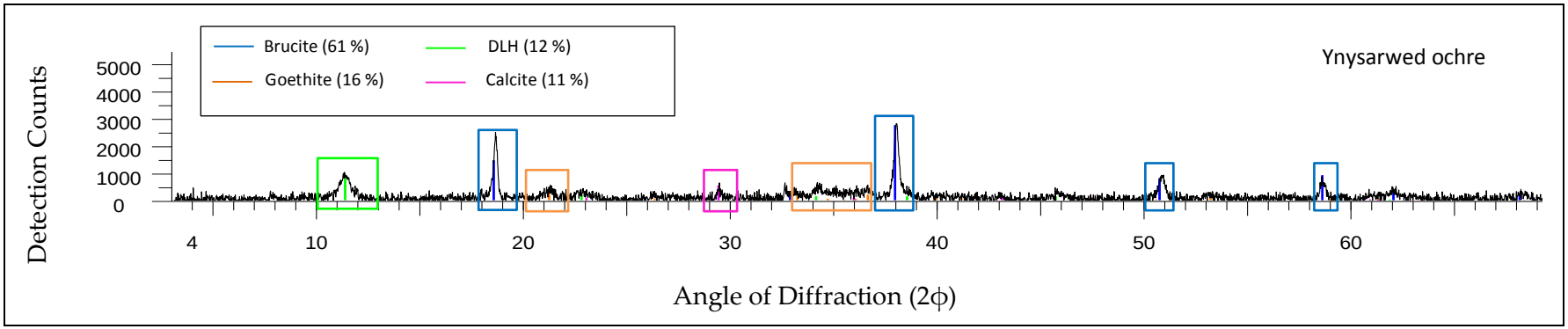

Figure 3.16: Background subtracted x-ray counts detected from the XRD experiment for Ynysarwed ochre. Position and magnitude of peaks interpreted to determine mineral phases present in the ochre and from this the estimated mineral content.

3.7 Particle size distribution

Particle size distribution was determined for both of the coarse-grained ochres under study, Polkemmet and Acomb pellets, in order to assess suitable size fractions for use as filter substrate. Approximately 5 kg of each ochre was mechanically shaken through a set of sieves with mesh sizes 8, 4, 2, 1, 0.5, 0.25, 0.125 and 0.063 mm for one hour. The weight of ochre collected in each sieve was then measured to calculate the particle size distribution (Figure 3.20).

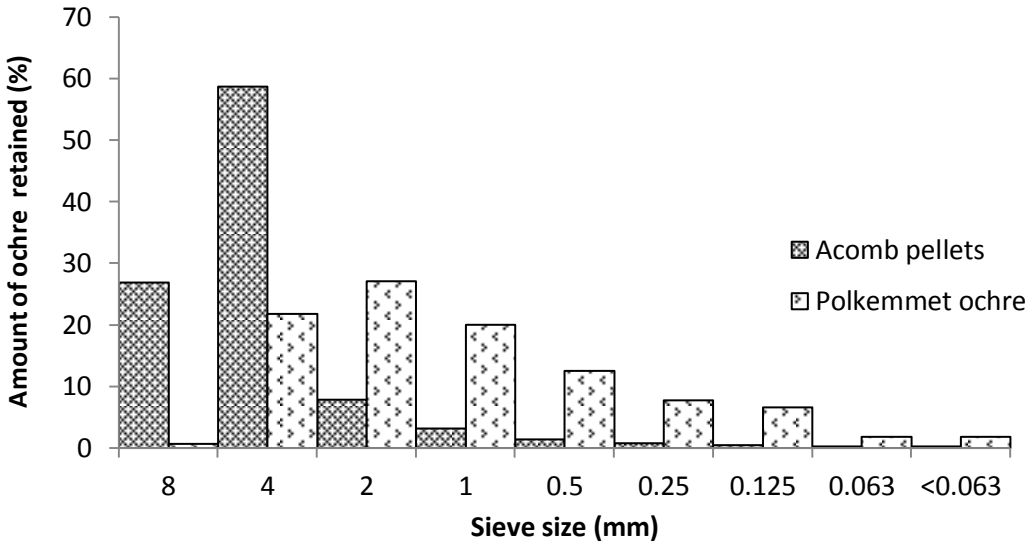

Figure 3.17: Particle size distribution of Acomb pellets and Polkemmet ochre.

The pelletisation process for Acomb pellets produces a particle size distribution whereby over 90% of the pellets have a diameter greater than 2 mm, and over half have a particle size between 4 and 8 mm. The aim of the pelletisation process was to create pellets in two size fractions, 4.0-5.6 mm and 5.6-9.5 mm. The particle size distribution suggests that the target particle sizes have been achieved, and these size fractions will be utilised for investigation into Acomb pellets as a filter substrate.

Polkemmet ochre contains a more distributed range of particle sizes, with more than 10% occurring in all the size fractions between 0.5 mm and 4 mm. A similar particle size distribution for Polkemmet ochre was reported by Bozika (2001). Polkemmet

ochre will therefore be considered for use in filter units in two particle sizes which approximately divide the coarse available material: 1.0- 2.8 mm and 2.8 – 8.0 mm.

3.8 Particle density

The particle density of all the ochres was measured following the BS 733: Part 2 (1987) guidelines. For Polkemmet ochre and Acomb pellets the particle density was determined on the size fractions likely to be utilised in filter units. Two types of pycnometers were used to determine particle density, Gay-Lussac and Hubbard. Gay-Lussac bottles have a narrow neck and are suitable for particles <0.5 mm in diameter whilst the Hubbard pycnometer is suitable for larger diameter particles.

3.8.1 Methodology

Pycnometers and stoppers were thoroughly cleaned with de-ionised water and dried in an oven at 60°C prior to each use. After cleaning, pycnometers were only handled using gloves. Both pycnometers were calibrated following the BS 733: Part 2 (1987) guidelines.

Particle density was determined for five samples of each ochre. For each sample, approximately 1-3 g of ochre was placed in the pycnometer and weighed to 0.1 mg (m_1). The pycnometer was then filled with deionised water, a fine wire was used to remove any air bubbles from within the bottle, and then it was stored at 4°C. The pycnometer was then brought up to test temperature (20°C) by placing it, up to the neck, in a 20°C water bath for 30 minutes. The stopper was then inserted and allowed to sink under its own weight, with any excess water removed from the top of the stopper with one wipe of the hand. The pycnometer was removed from the water bath, dried using lint-free cloth and then weighed to the nearest 0.1 mg (m_2). The particle density of the sample was then calculated using Equation 3.4.

$$\rho_c = \frac{m_1 - m_0}{m_c - m_{0-m_2+m_1}}$$ Equation 3.4

Where, ρ_c = particle density of the sample (g cm^{-3}), m_1 = mass (g) of the pycnometer when part filled with sample, m_0 = mass (g) of the pycnometer when empty, m_c = mass (g) of the pycnometer when filled with water at calibration temperature; 20°C, m_2 = mass (g) of pycnometer when filled with sample and water at experimental temperature.

3.8.2 Results

The particle size densities measured for all the ochres are similar, ranging from 2.07-2.53 g cm^{-3} (Table 3.7). Of the ochres studied, Minto ochre has the highest density, 2.53 g cm^{-3}, and Acomb pellets the lowest density, 2.07-2.12 g cm^{-3}. Whilst Acomb ochre has a density of 2.50 g cm^{-3}, Acomb pellets have a far lower density due to the incorporation of additives and porosity during pelletisation.

Polkemmet ochre and Acomb pellets were examined in two size fractions that would be suitable for filter units, as well as a ground sample. The density of the ochre was expected to be lower when it was in a granular form, as opposed to ground, due to the removal of internal pore space, but this was not the case for Polkemmet ochre. This ochre contains small rock fragments, the result of the surrounding construction/ earth moving activities, and whilst these are included in the larger particle size distributions, these do not pass through a 100 μm sieve. The rock fragments were not removed for determination of particle density as they only make up a small component of the ochre and are unlikely to be extracted were Polkemmet ochre to be used as a filter substrate.

Table 3.7: Ochre particle density: Mean and s.d. of ochre particle densities (n=5). Where particle size is not noted, ochre was sieved to <100 μm, (2d.p).

Ochre	Particle density	
	Mean (g cm^{-3})	s.d. (g cm^{-3})
Polkemmet (2-4 mm)	2.43	0.09
Polkemmet (1-2 mm)	2.43	0.10
Polkemmet (Ground, <100 μm)	2.15	0.11
Acomb pellets (5.60-9.52 mm)	2.10	0.01
Acomb pellets (4.00-5.60 mm)	2.07	0.03
Acomb pellets (Ground, <100 μm)	2.12	0.05
Acomb	2.50	0.12
Avoca	2.51	0.02
Minto	2.53	0.11
Silkstone	2.19	0.04
Ynysarwed	2.13	0.07

3.9 Summary of Findings

A range of chemical and physical properties of the ochres selected for study were determined in this Chapter. These will be drawn upon throughout the thesis to interpret the results of batch and column experiments.

The pH of the ochres selected for research were found to vary from 2.31 to 11.20. Avoca ochre had a very low pH of 2.31, whilst high pH values were found for Acomb pellets, 11.20, and Ynysarwed ochre, 9.30.

B.E.T surface area of the ochres was higher than many other substances previously proposed as P adsorbents. Surface area is strongly linked to P adsorption capacity, as a higher surface area tends to have more adsorption sites. Silkstone ochre was found to have the highest surface area, 243 m^2 g^{-1}, with Ynysarwed ochre also high, 220 m^2 g^{-1}. Whilst Avoca ochre has the lowest B.E.T surface area of the ochres under

study, 56 m^2 g^{-1}, this is still higher than most substances previously proposed as a filter substrate, such as Bauxite: 6.8 m^2 g^{-1} (Drizo et al., 1999).

The ochres were found to be largely composed of elements with a known sorption capacity for P: Al, Ca, Fe and Mg. Silkstone has the lowest composition of these elements, 42 % by dry weight, with Ynysarwed the highest, 68.4 % by dry weight. The effect of pelletesing Acomb ochre was to increase the Ca and Al content but decrease the Fe content. Ynysarwed ochre was found to have a large Mg content, 34.4 % by dry weight, probably owing to the addition of Magnesium hydroxide at the WWTP as part of the active treatment. The ochres were also examined for ammonium oxalate extractable Fe to investigate the Fe content of the ochres in an amorphous state. Oxalate extractable Fe content varied in the ochres between 8.2-23.9 % composition by dry weight, equating to 14.8-74.5 % of the total Fe in the amorphous state.

The mineral content of the ochres was investigated by XRD. All ochres were found to contain goethite, with it being a major component in Acomb ochre (54 %), Minto ochre (100 %), Polkemmet ochre (35 %) and in the Acomb pellets (35 %). Calcite was a minor component of Acomb (14 %) and Ynysarwed (11 %) ochre and a major component of Acomb pellets (52 %).

The following Chapter principally investigates the P adsorption capacity of the ochres through a series of batch experiments at a range of pH conditions. The chemical properties of the ochres derived in this Chapter will be fundamental to the interpretation of the results.

Chapter 4

The P adsorption capacity of ochre and the release of potentially toxic elements

Batch experiments were conducted to calculate the P adsorption capacity of the ochres under study. Experiments were designed to allow data to be fitted to adsorption isotherms and were conducted over a range of pH in order to investigate the effect of pH on P removal by ochre. The fitting of adsorption isotherms by various authors does not typically account for pH. This is a key factor in P removal by materials, however, and can vary greatly in batch experiments due to the variation in P concentrations added to different trials and the sorption reactions occurring. In this experiment pH was accounted for with a novel approach that allowed adsorption isotherms to be plotted at selected pH conditions.

The effect of competing ions was also investigated by repeating the batch experiments for three of the ochres, Acomb, Polkemmet and Acomb pellets, in the presence of synthetic sewage.

A concern with utilising ochre for environmental applications is the possible release of potentially toxic elements (PTEs) from the ochre. The mobilisation of Al, As, Cu, Fe, Mn, Ni, Pb and Zn from ochre was investigated through a series of batch experiments, over a range of pH conditions.

4.1 pH equilibrium study

In order to conduct batch experiments to assess the P removal characteristics of ochre over a range of pH, a preliminary study was required to determine the concentration of acid (HCl) or base (NaOH) needed to induce the required pH conditions within the experiment. The length of time required to reach pH equilibrium was also determined from this preliminary study.

To ensure comparable ochre particle size distributions for the equilibrium study, all the ochres were crushed using a pestle and mortar and passed through a 100 μm sieve. 3 g ochre was added to 200 mL 0.01 M $NaNO_3$ and stirred on a magnetic stirrer for 30 minutes, producing a homogeneous suspension of 15 mg ochre mL^{-1}. Suspension concentration was checked over the course of the experiment by oven-drying 5 mL samples that were pipetted into pre-weighed dishes. The experiments were repeated if the ochre concentration was ± 10% the target ochre concentration.

5 mL ochre suspension was pipetted into a 50 mL centrifuge tube with 25 mL 0.01 M $NaNO_3$ which formed the matrix for the experiment. 1 mL of either acid or base, at varying concentrations, was added to induce a range of pH conditions, targeting pH values 3, 4.5, 6, 7.5, 9, 10. The centrifuge tubes were placed in a cabinet shaker (120 rpm) and equilibrated for 250 hours at room temperature. pH was measured at the start of the experiment and daily using a Mettler-Toledo portable pH meter with automatic temperature compensation, calibrated with three appropriate pH buffers after every 30 samples. Figure 4.1 shows the pH measured over time for different acid/base additions to a suspension of Polkemmet ochre. The equilibrium pH values were plotted against the concentration of acid or base addition to determine the required dose to achieve the target pH values for the P adsorption experiments; this can be seen for Polkemmet ochre in Figure 4.2. The experiment was run for 11 days, with pH not varying by ± 0.1 over a 24 hour period after 8 days.

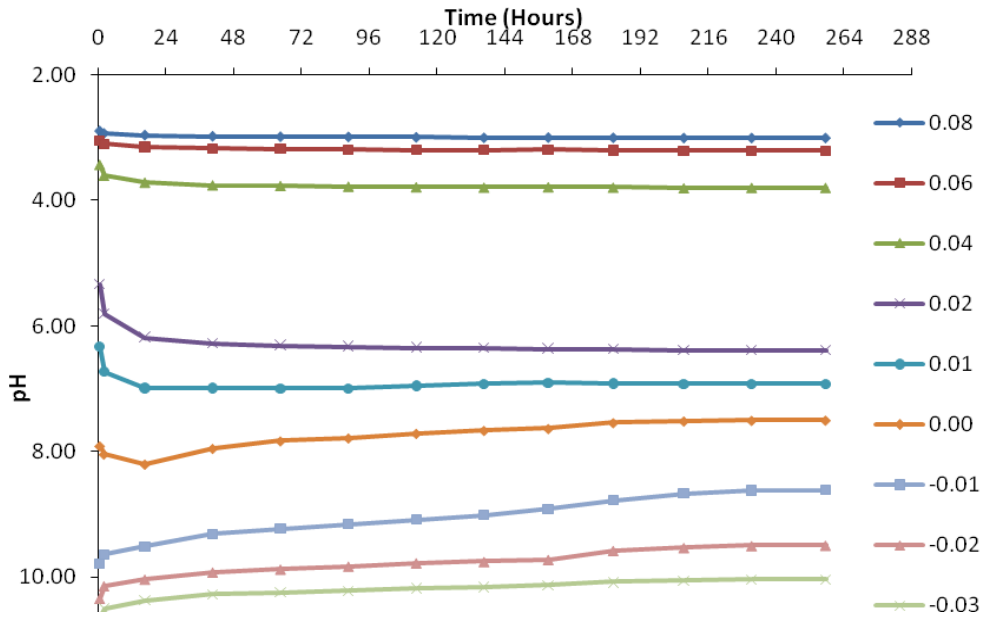

Figure 4.1: Polkemmet ochre pH equilibrium batch experiments. Molar strength of the 1 mL addition of acid or base at the start of the experiment is shown in the key. Positive values indicate the addition of HCl and negative values, NaOH. e.g. 0.08 represents 1 mL 0.08 M HCl addition. Each data point is the mean of triplicate experiments.

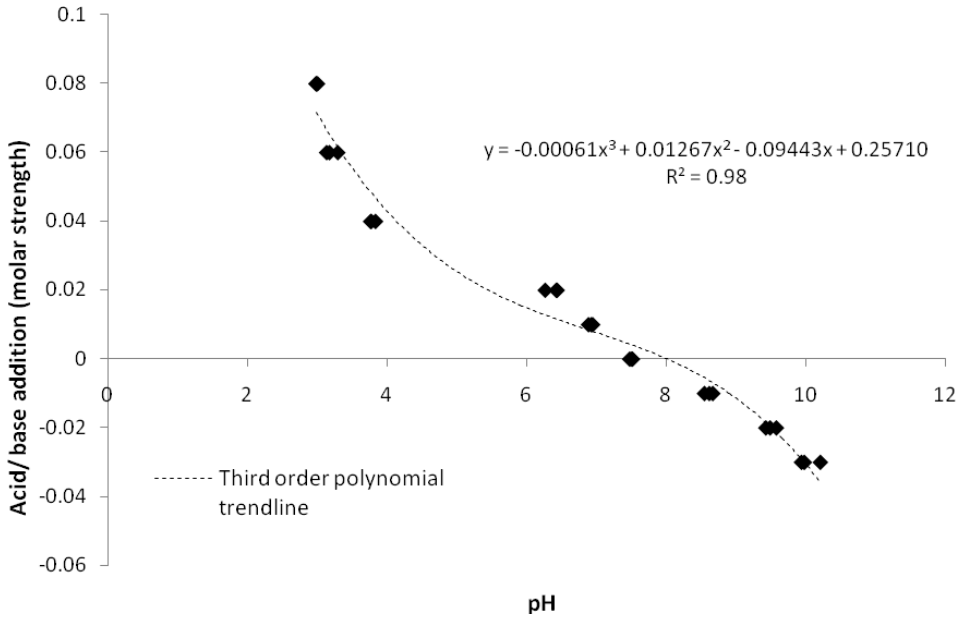

Figure 4.2: Determination of the acid or base addition required to induce pH equilibrium conditions in batch experiments: Polkemmet ochre.

4.2 P adsorption batch experiments

The P adsorption capacity of ochre has been previously calculated, as described in Chapter 2, and has found to be high, ~20-30 mg P g^{-1} (Heal et al., 2003a). Whilst the end use of ochre as a P adsorbent is yet to be defined, most environmental applications would involve the treatment of P enriched water with a pH between 6 and 8. A larger range of pH was investigated here to gain further understanding of the effect of pH on P removal by ochre. Adsorption isotherms were fitted to the results to calculate P adsorption capacities. Other parameters, such as ochre particle size, solid to liquid ratio and contact time, were kept consistent for all P adsorption batch experiments to ensure comparable results.

4.2.1 Batch experiment design

The P adsorption capacity of materials is strongly influenced by surface area and thus particle size. Materials should therefore be tested in laboratory conditions at the expected particle size distribution of the field application (Drizo et al., 1999). That said, using the different particle size distribution of each ochre may yield results which cannot be compared to infer the effect of the other differing characteristics of the ochres on P adsorption capacity, such as chemical composition, mineralogy and BET surface area. All ochres were therefore sieved to < 100 μm for the batch experiments.

The methodology was developed to be conducted in 50 mL centrifuge tubes, to be compatible with the centrifuge facilities available. Decisions concerning the ochre addition (g) and overlying solution (mL) thus had to be made within this constraint. The amount of ochre used in each batch experiment needs to be representative of the ochre composition. A typical amount to use in batch experiments investigating P adsorption is 0.5-3 g, with an overlying solution volume of 30-100 mL (Cucarella and Renman, 2009). However, ochre has a high P adsorption capacity and therefore the more ochre that is added, the higher the required solution P concentration to ensure saturation. As the solution P concentration increases, the pH of the solution

decreases, affecting the conditions of the P adsorption experiment. High concentrations of added P can therefore alter the experimental pH conditions and affect the amount and rate of P removal (Cucarealla and Renman, 2009).

High P concentrations in the overlying solution (200-1000 mg P L^{-1}) create equilibrium conditions which do not occur at lower P concentrations such as those expected under field conditions (0.1 to 15 mg P L^{-1}). For example, high P concentrations can lead to precipitation reactions occurring, whilst at lower P concentrations adsorption reactions, expected to be the main process of P removal from P enriched waters by ochre, are dominant (Cucarella and Renman, 2009; Søvik and Kløve, 2005). The amount of ochre in each batch experiment thus needs to be carefully considered to ensure it can be saturated by the overlying P solution without using high P concentrations which affect the P sorption processes occurring.

75 mg ochre, <100 μm grain size, was selected as a representative sample of ochre for each experiment. Based upon previous calculations of the P adsorption capacity, this would require c.1.875 mg P in the overlying solution for saturation to occur. This mass of P would not result in high P concentrations in the overlying solution and thus the effect of the P addition on experimental pH and sorption processes would be minimal. Six different P additions were selected for the batch experiments: two for which the ochre should remove all the P from solution, and four which should result in ochre saturation with P remaining in solution.

Potassium dihydrogen phosphate, KH_2PO_4, was used to make up the P solution since it is commonly used in P adsorption batch experiments (Cucarella and Renman, 2009). Adding P in this form creates an artificial situation whereby P is isolated as PO_4^{3-} and available for adsorption. This is in contrast to field conditions, where P is present in a variety of forms, each competing for adsorption sites

(Cucarella and Renman, 2009). Consequently, the P adsorption capacity of ochre will be higher in batch experiments than would be expected under field conditions.

An electrolyte in the overlying solution was used to maintain a constant ionic strength. Electrolytes containing Ca, such as $CaCl_2$, were not used as Ca can precipitate with P. Commonly used electrolytes for P adsorption batch experiments include KCl (Mann and Bavor, 1993; Li et al., 2006) and $NaNO_3$ (Johansson, 1999). 0.01 M $NaNO_3$ L^{-1} was selected for this study.

The solid to liquid ratio of the batch experiments was 1:427 (75 mg ochre in 32 mL solution). This ratio is low compared to batch experiments conducted in other studies to determine the P adsorption capacity of other materials, which typically used a ratio between 1:10 and 1:50 (Cucarella and Renman, 2008). The ratio selected in this study ensures that the P concentration in overlying solution is not greater than 200 mg P L^{-1}. If a higher ratio was used, e.g. 1:20, 1:50, a far greater concentration of P in the overlying solution would be required to ensure the saturation of ochre.

Although such a low solid: liquid ratio will increase the time taken for adsorption maxima to be obtained, the experimental tubes were kept well agitated and the P adsorption kinetics of ochre have been shown to be rapid (Heal et al., 2003a). Following P addition, which occurs after the system has reached pH equilibrium, 24 hours contact time was allowed for P removal. This contact time is identical to other similar studies (e.g. Mann and Bavor, 1993; Xu et al., 2006; Boujelben et al., 2008). In batch experiments the experimental tubes are typically agitated and at 20-25^{o}C (Cucarella and Renman, 2008), therefore here the tubes were agitated in a cabinet shaker at 120 rpm, ensuring ochre is kept in suspension, at room temperature (c.20°C).

4.2.2 P adsorption batch experiment methodology

A 15 mg mL^{-1} ochre suspension in a 0.01 M $NaNO_3$ matrix was made up in a 500 mL beaker and kept in suspension using a magnetic stirrer. Suspension concentration was checked over the course of the experiment by oven-drying 5 mL samples that were pipetted into pre-weighed dishes. The measured suspension concentration was then used in subsequent data analysis.

5 mL ochre suspension was pipetted into a 50 mL polypropylene centrifuge tube containing 25 mL 0.01 M $NaNO_3$. 1 mL of HCl or NaOH of varying concentration was added depending upon the target pH conditions of the experiment. The centrifuge tubes were then sealed and placed in a cabinet shaker set at 120 rpm for 8 days at room temperature (~20°C), after which time it was assumed that the samples were at equilibrium based upon the pH equilibrium experiment. Samples were checked daily to ensure ochre remained in suspension.

After 8 days, the tubes were opened and the pH measured with a Mettler-Toledo portable pH probe prior to P addition. In order to fit adsorption isotherms, varying concentrations of P were added to ensure the P adsorption maximum of the ochres was exceeded. An adsorption capacity of 25 mg P g^{-1} ochre was assumed for the basis of these calculations. Calculated from the formula weight of KH_2PO_4, and the atomic weight of P, 8.23 mg KH_2PO_4 is required to saturate the 75 mg ochre in each tube. Six concentrations of P were added: two which would not saturate the ochre, 0.5 and 1 mg P; and four that should, 2, 3, 4, 6 mg P, corresponding to overlying solution concentrations of 15.625, 31.25, 62.5, 93.75, 125 and 187.5 mg P L^{-1}. These masses of P were added to the corresponding centrifuge tubes in 1 mL of solution made with deionised water as the solvent. Whilst these were the target P additions, the actual P concentration of additions to each experiment varied slightly. The actual, rather than design, additions are used in the data analysis. The centrifuge tubes were then agitated at 120 rpm for a further 24 hours before taking a final pH measurement. The experiments were then centrifuged at 4500 rpm for 30 minutes

and filtered through 0.45 μm cellulose filter paper to remove any suspended P and ochre. All experiments were conducted in triplicate and blank experiments were run with only electrolyte and acid or base added to the solution, i.e. no ochre or P solution. The average P concentration of the blanks was subtracted from the P concentrations determined in the batch experiments. Samples were stored at 4°C and analysed within 2 weeks of being collected.

The supernatant was decanted and analysed for total orthophosphate concentration at the James Hutton Institute, Aberdeen. Analysis was conducted using a Konelab 20 discrete analyser and a method based upon that of Murphy and Riley (1962). The method was adapted so that standards were made up in the same matrix as that used in the experiments, 0.01 M $NaNO_3$. The technique is based on the principle that orthophosphate reacts with ammonium molybdate and antimony potassium tartate under acidic conditions. The resultant complex is reduced with ascorbic acid which produces a blue coloured liquid, with the intensity of colour proportional to the concentration of orthophosphate. This colour intensity is measured within the Konelab analyser spectrophically at a wavelength of 880 nm.

The analyser was calibrated daily with a range of solutions between 0-10 mg P L^{-1} in order to calculate a relationship between colour intensity and total orthophosphate concentration. After every 12 samples were run in the analyser low and high checks were run to ensure the calibration was still valid. In the event that calibration was no longer valid, the analyser was recalibrated and the samples re-analysed. The total orthophosphate concentration of samples was accepted if they were within the range of concentrations the analyser was calibrated to, 0-10 mg P L^{-1}. This resulted in most of the samples requiring dilution to ensure a valid result due to concentrations > 10 mg P L^{-1}.

4.2.3 Data Analysis

The mass of P removed from solution was calculated from the P concentration measured in the supernatant at the end of the batch experiment. Whilst the initial pH conditions of the experiments were controlled by the addition of acid or base, the various concentrations of P added to the experiments and the sorption processes occurring led to changes in the final pH of the experiments (Figure 4.3).

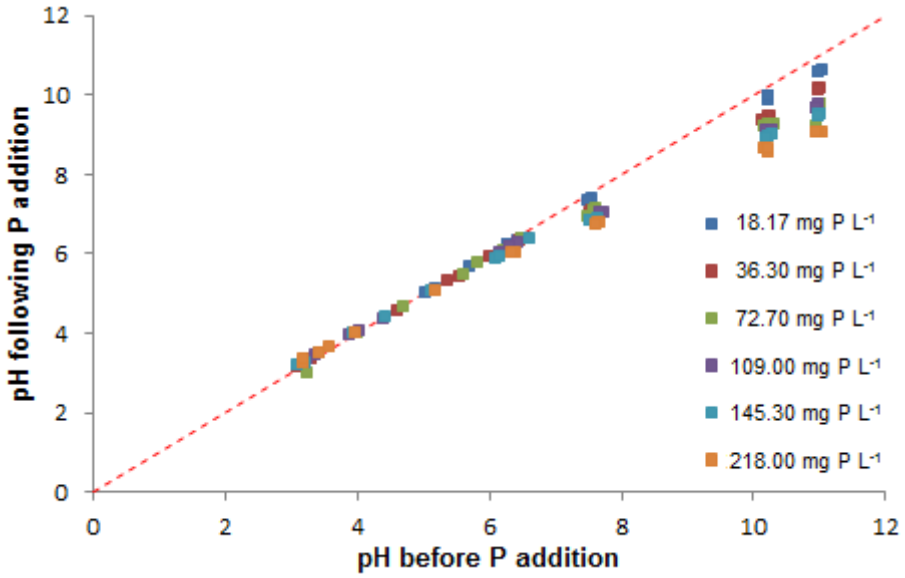

Figure 4.3: The effect of P addition and P removal on the pH of batch experiments for Acomb ochre. Dashed line indicates y=x.

P was added to the experiments in the form of $H_2PO_4^-$, with the speciation of orthophosphate dependent on pH (Figure 4.4). Therefore when $H_2PO_4^-$ is added to experiments with high pH conditions, it may deprotonate to HPO_4^{2-}, leading to a decrease in pH as H^+ ions are released. This effect is increased at higher initial pH conditions and with increasing P addition.

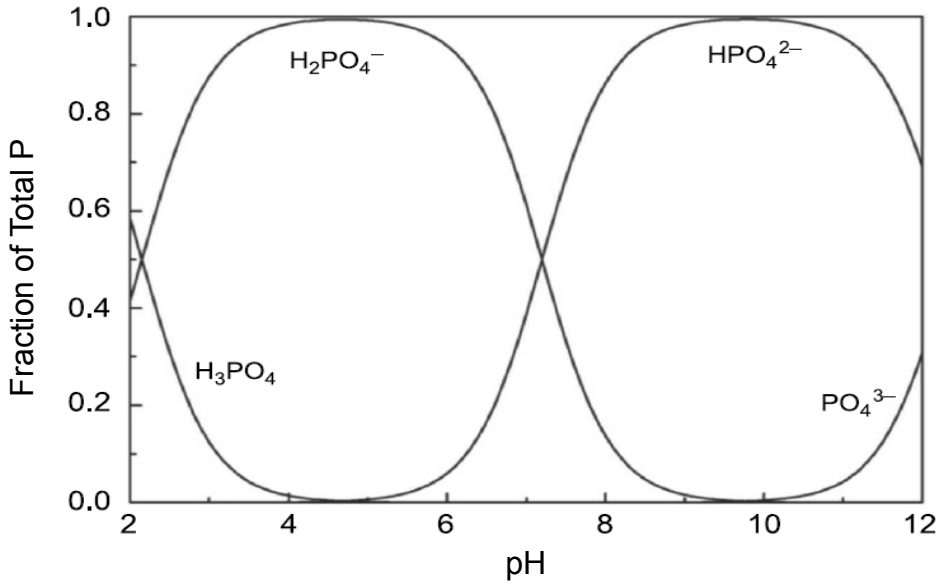

Figure 4.4: Effect of pH on the speciation of orthophosphate. Adapted from Oliveira et al. (2011).

An association between increasing the P concentration of experiments and a resultant decrease in pH conditions has been previously noted by Holford et al. (1974). Many of the adsorption reactions of phosphate ions onto goethite, a major component of many of the ochres, result in the release of protons (Zhong et al., 2006). These adsorption reactions may be monodentate, such as ligand exchange, or bidentate (as introduced in Chapter 1.3.7.1). Therefore, the higher the P addition, the more adsorption may occur and the greater the decline in pH from the resultant release of H^+, as can be seen in Figure 3.3.

Any change in pH from initial conditions is significant as P adsorption by Fe occurs mainly under acidic conditions (Valsami-Jones, 2004). The addition of high concentration P solutions which reduce the experimental pH will therefore lead to a greater than expected amount of adsorption. This was corrected for in order to plot adsorption isotherms at constant pH conditions. Datasets were sorted by concentration of P added to factor out its influence, with P removed g^{-1} ochre plotted against pH measured at the end of the experiment, as shown in Figure 4.5 for Acomb ochre experiments. Third order polynomial trend lines were fitted to

each of the datasets as these gave consistently high values for the coefficient of determination (R^2). From the equation of these trend lines, mg P g^{-1} ochre can be calculated for any pH value within the pH range of the dataset, and thus the P concentration remaining in solution can also be derived. Adsorption isotherms were plotted to these corrected values of P removed in order to determine the P adsorption capacity of the ochres at discrete pH values.

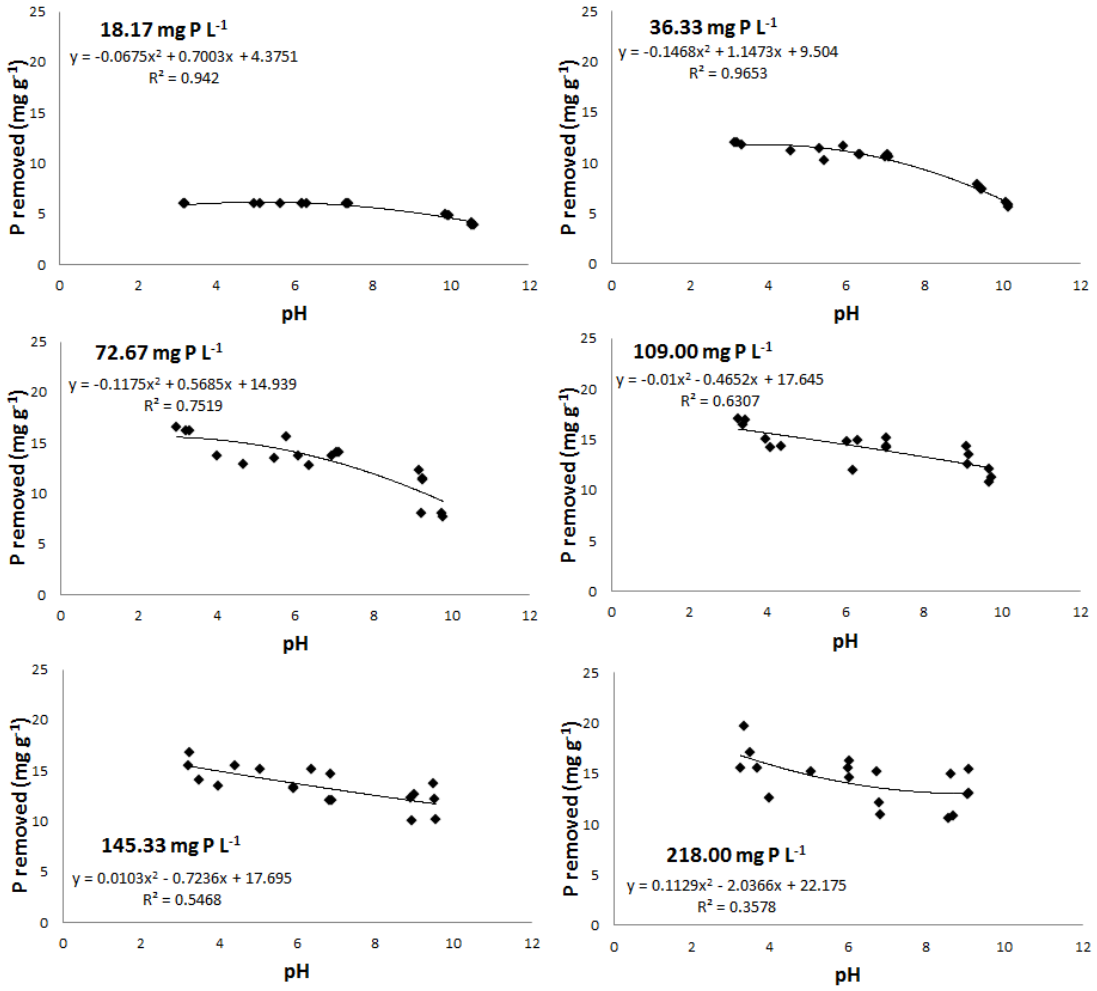

Figure 4.5: P removed plotted against pH for Acomb ochre, data sorted by P addition. Trend lines were fitted to the datasets and from the resultant equations P removed at any pH for the range of the dataset can be calculated.

4.2.4 Fitting Langmuir and Freundlich adsorption isotherms

Two adsorption isotherms, the Freundlich and Langmuir, were used to infer the adsorption capacity and binding energy of P to ochre, each of which make different assumptions about the adsorption process, discussed in detail in Chapter 1.3.7. Whilst three parameter isotherms, such as the Langmuir-Freundlich or Redlich-Peterson, may give a better fit to P adsorption onto Fe- oxides data, two parameter isotherms are more often utilised due to their easier derivation. Previous batch experiments analysing P adsorption by ochre have used the Langmuir and Freundlich isotherms and thus these were selected for comparative reasons.

As the Langmuir equation is nonlinear, fitting it to data requires an iterative approach. Using a linearised version of the Langmuir equation can avoid this step, but although it is equivalent mathematically, this technique reduces the accuracy with which adsorption data can be modelled (Bolster and Hornberger, 2007). Consequently, in this research, the non-linear Langmuir equation was fitted to the data derived from the P adsorption batch experiments with an iterative approach in Microsoft Excel using an open source model and the Solver function to inform the iteration process (Bolster and Hornberger, 2007).

As with the Langmuir adsorption isotherm, fitting the Freundlich equation to a dataset requires an iterative process due to its nonlinear nature. An open source model developed in Microsoft Excel and available online (Bolster, 2010) was utilised.

The two models operate iteratively to solve the Langmuir and Freundlich equations, estimating parameters by minimising an objective function – a metric of the difference between modelled and observed data. The models use a least squares regression, the square of the standard errors (SSE), to fit the equations to the observed data, Equation 4.1 (Bolster and Hornberger, 2007).

$$SSE = \sum_{i=1}^{N}[S_i - \bar{S}_i]^2 \qquad \text{Equation 4.1}$$

Where SSE is the objective function, N is the number of observations, S_i and $\bar{S}_i$ are the *i*th observed and modelled values of the dependant variable.

The model efficiency (E, Equation 4.2), proposed by Nash and Sutcliffe (1970), was calculated to indicate the overall fit of the model to the dataset.

$$E = 1 - \frac{\sum_{i=1}^{N}(S_i - \bar{S}_i)^2}{\sum_{i=1}^{N}(S_i - \bar{S})^2} \qquad \text{Equation 4.2}$$

Where N is the number of observations, S_i and $\bar{S}_i$ are the *i*th observed and modelled value of the dependant variable, respectively, and $\bar{S}$ is the mean of the dependant variable.

The statistic E ranges from -∞ to 1, with a value of 1 indicating a perfect model fit to the dataset and values <0 signifying that taking the average value of all the data points would give a better prediction than the model. Whilst other statistics can be calculated, E is often considered to give the best overall indication of model fit (Mayer and Butler, 1993; Bolster and Hornberger, 2007).

In order to ascertain whether the Langmuir or Freundlich equation is a better fit to the data, the corrected Akaike's Information Criterion (AIC) was calculated for each isotherm (Equation 4.3).

$$AIC = N\ln\left(\frac{SSE}{N}\right) + 2(p+1) + \frac{2(p+1)(p+2)}{N-p-2} \qquad \text{Equation 4.3}$$

Where N is the number of observations, SSE is the sum of the squared errors and p is the number of fitting parameters.

AIC requires the number of observed data points to exceed the number of fitting parameters by three or more (Bolster and Hornberger, 2007). The AIC values calculated for the Langmuir and Freundlich fits can be compared, and the model

with the lower value is considered to be the more accurate (Bolster and Hornberger, 2007). By comparing the AIC values of the two adsorption isotherms, the certainty that the model with the lower AIC score is optimal can be calculated, Equation 4.4.

$$P = \frac{\exp(0.5\Delta)}{1 + \exp(0.5\Delta)}$$ Equation 4.4

Where Δ is the absolute difference in AIC between the two models and P is the certainty, expressed as a probability, that the model with the lower AIC value is optimal.

4.2.5 P adsorption isotherm results

In this section, the adsorption isotherms fitted to the results of P adsorption batch experiments, conducted for all seven ochres under study, are presented and discussed. The ochres are largely comprised of Fe, with smaller, variable amounts of Al, Ca and Mg (calculated in Chapter 3.4). Al, Fe and Mg have a high affinity for adsorbing P under acidic conditions in soil. The ochres containing the highest amounts of these elements are therefore expected to have the highest P adsorption capacity under acidic conditions. The removal of P by ochre under alkaline conditions is expected to be dominated by adsorption onto calcite, and is only expected to occur for ochres containing this mineral, e.g. Acomb ochre, Acomb pellets and Ynysarwed ochre. Some precipitation of calcium phosphates may occur under high pH conditions in the experiments with the highest P additions.

The shape of adsorption isotherms is indicative of the predominant P removal mechanism. Steeply sloping isotherms with high values of Langmuir K indicate that adsorption onto sites with a high affinity for P is the dominant mechanism, with high P removal rates at low P concentrations. Isotherms with low gradients, and thus low values of K, indicate that adsorption is occurring onto sites with a weaker affinity for P, e.g. onto surfaces of calcite.

4.2.5.1 Acomb ochre

P removal by Acomb ochre is dependent on whether the system pH is greater or less than 8. Removal was highest under acidic conditions, > 15 mg P g^{-1} at pH 3 for the four highest P additions (Figure 4.6). Between pH 4 and 8, the amount of P removed remained almost constant for each P addition, and then decreased above pH 8.

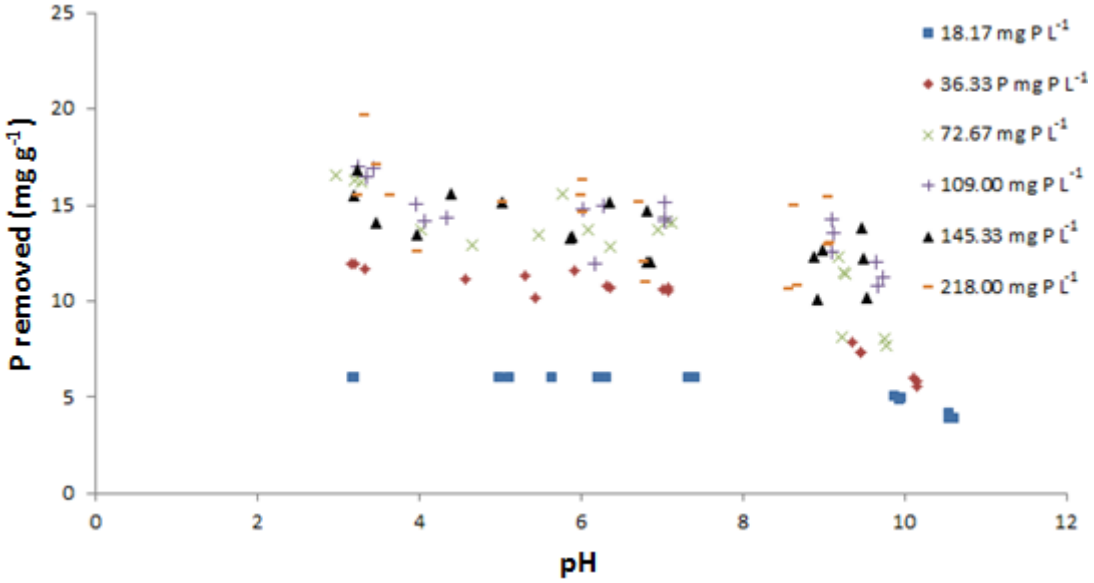

Figure 4.6: P adsorption batch experiment results for Acomb ochre. Each replicate is shown as a separate data point.

Whilst it appears that higher concentration P additions were not conducted under the most alkaline pH conditions (Figure 4.6), this is not the case. A decrease in pH conditions occurred for the highest P additions due to factors outlined in Chapter 4.2.3, i.e. the speciation of $H_2PO_4^-$ and the release of H^+ during adsorption reactions.

The dataset for each P addition was fitted with a polynomial line of best fit to describe the relationship between P removed and pH, Figure 4.5. The fit of the trend lines to the data (R^2) is high at the low P additions, but decreases with increasing P addition.

From these trend lines the mass of P removed and equilibrium P concentration in the overlying solution was calculated for pH values 4 to 9. Adsorption isotherms were then fitted to this derived data (Figure 4.7). The Langmuir and Freundlich isotherms further show that P removal by Acomb ochre is pH dependant, with P adsorption capacity (S_{max}, K_f) increasing with decreasing pH (Figure 4.7, Table 4.1, Table 4.2). The Freundlich isotherm fits the Acomb ochre dataset better than the Langmuir isotherm, with lower values of AIC for all datasets except pH 8. The goodness of fit (E) for the Freundlich isotherm is above 0.73 at all pHs and SSE consistently low. The Langmuir isotherm fitted the datasets well at high pHs, with low values of SSE and high values of E, but did not fit the data as well at pH values 4-6.

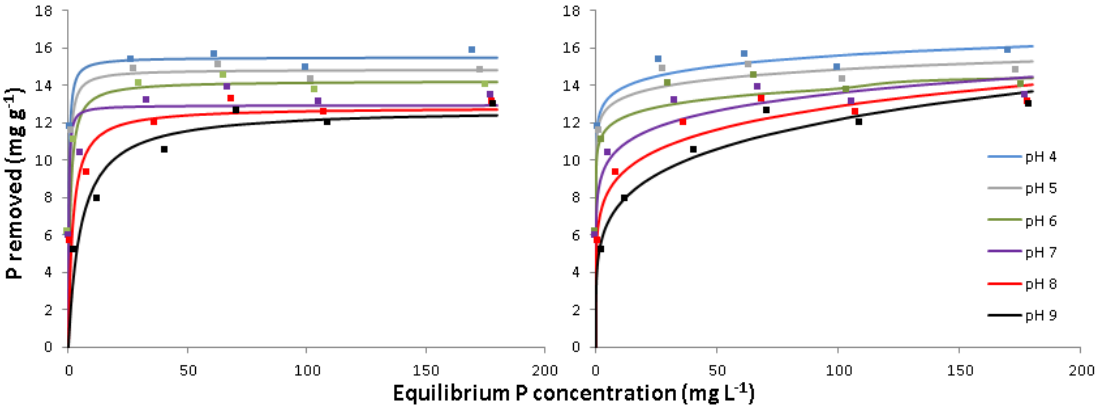

Figure 4.7: P adsorption isotherms derived from fitting the Langmuir (L) and Freundlich (R) isotherms to the Acomb ochre P adsorption batch experiment data.

The higher the Langmuir K value, the greater the affinity between P and ochre resulting in P adsorption occurring. Other than a spurious result at pH 7, when K=5.77 L mg^{-1}, K decreases with increasing pH from 3.79 L mg^{-1} at pH 4 to 0.19 mg L mg^{-1} at pH 9. This suggests that adsorption is occurring onto sites with a high affinity for P, such as Fe- hydroxides at low pH conditions. Acomb ochre is 54 % goethite, and as such it is suggested that adsorption onto these surfaces is occurring under the above conditions. At higher pH conditions, the lower value of K suggests that adsorption is occurring onto sites with a lower affinity for P. Acomb ochre

contains 14 % calcite and as such adsorption onto these surfaces is suggested as the dominant P removal mechanism under higher pH conditions.

Table 4.1: Langmuir parameters and goodness of fit for Acomb ochre derived from model runs (2 d.p).

		pH					
		4	**5**	**6**	**7**	**8**	**9**
Goodness of fit	**SSE**	37.57	38.65	38.21	6.17	3.10	3.95
	E	0.49	0.37	0.27	0.87	0.93	0.92
	AIC	29.01	29.18	29.11	18.12	14.03	15.49
S_{max} (mg g^{-1})	**Value**	15.51	14.86	14.25	12.95	12.84	12.77
	S.E.	1.57	1.61	1.67	0.57	0.47	0.64
K (L mg^{-1})	**Value**	3.79	2.63	1.30	5.77	0.57	0.19
	S.E.	4.44	3.54	1.86	2.31	0.16	0.06

Table 4.2: Freundlich parameters and goodness of fit for Acomb ochre derived from model runs (2 d.p).

		pH					
		4	**5**	**6**	**7**	**8**	**9**
Goodness of fit	**SSE**	1.38	1.78	2.02	3.99	4.02	2.73
	E	0.88	0.79	0.73	0.92	0.91	0.94
	AIC	23.56	24.84	25.46	15.55	15.60	13.27
K_f	**Value**	12.22	11.85	11.02	8.41	6.57	4.86
	S.E.	0.62	0.76	0.92	0.69	0.76	0.62
N	**Value**	0.05	0.050	0.05	0.11	0.15	0.20
	S.E.	0.01	0.02	0.02	0.02	0.03	0.03

The better fit of the Freundlich isotherm to the observed data suggests that P adsorption onto Acomb ochre does not occur in a monolayer and that adsorption

sites have varying amounts of binding energy. Acomb ochre has a high Langmuir isotherm P adsorption capacity of 12.84-14.25 mg P g^{-1} between pH 6 and 8, the conditions typical of P-enriched waters. The value of Langmuir K is low in these pH conditions, however, suggesting adsorption onto surfaces of calcite. The low gradients of the adsorption isotherms indicate that Acomb ochre will not be suitable for removing P from solution at the relatively low P concentrations, expected under field conditions, 0.1-15 mg P L^{-1}.

4.2.5.2 Acomb pellets

P removal by Acomb pellets varies with pH in a parabolic manner, with the largest amounts of P removed below pH 5 and above pH 8 (Figure 4.8). P removed in some experiments exceeded 30 mg g^{-1} i.e. when the P addition was greater than 100 mg P L^{-1} and when pH> 7. P removal is lowest around pH 5.

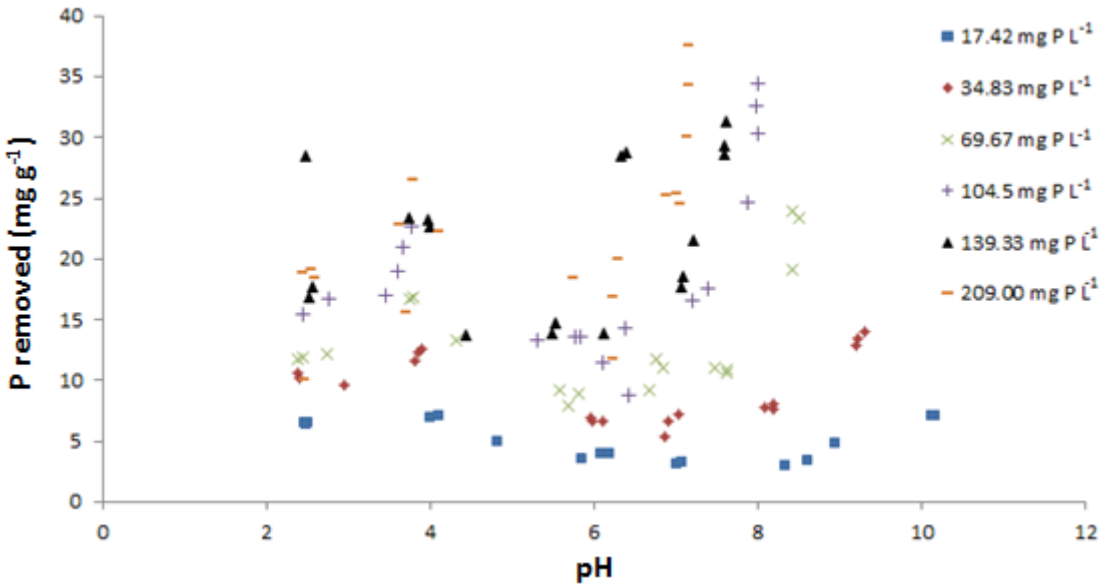

Figure 4.8: P adsorption batch experiment dataset for Acomb pellets. Each replicate is shown as a separate data point.

The dataset for each P addition was fitted with a polynomial line of best fit (Figure 4.9) to describes the relationship between pH and P removed. The fit of the trend lines is relatively good for the four lower P additions, with $R^2 > 0.46$, but is less

successful at higher P additions with R^2 values of 0.27 and 0.37. From these trend lines, the mass of P removed and equilibrium P concentration in the overlying solution were calculated for pH values 3 to 7 and adsorption isotherms were fitted to this data (Figure 4.10). Isotherms could not be calculated for pH >7 as the dataset for 209 mg P L^{-1} addition did not exceed pH 7.

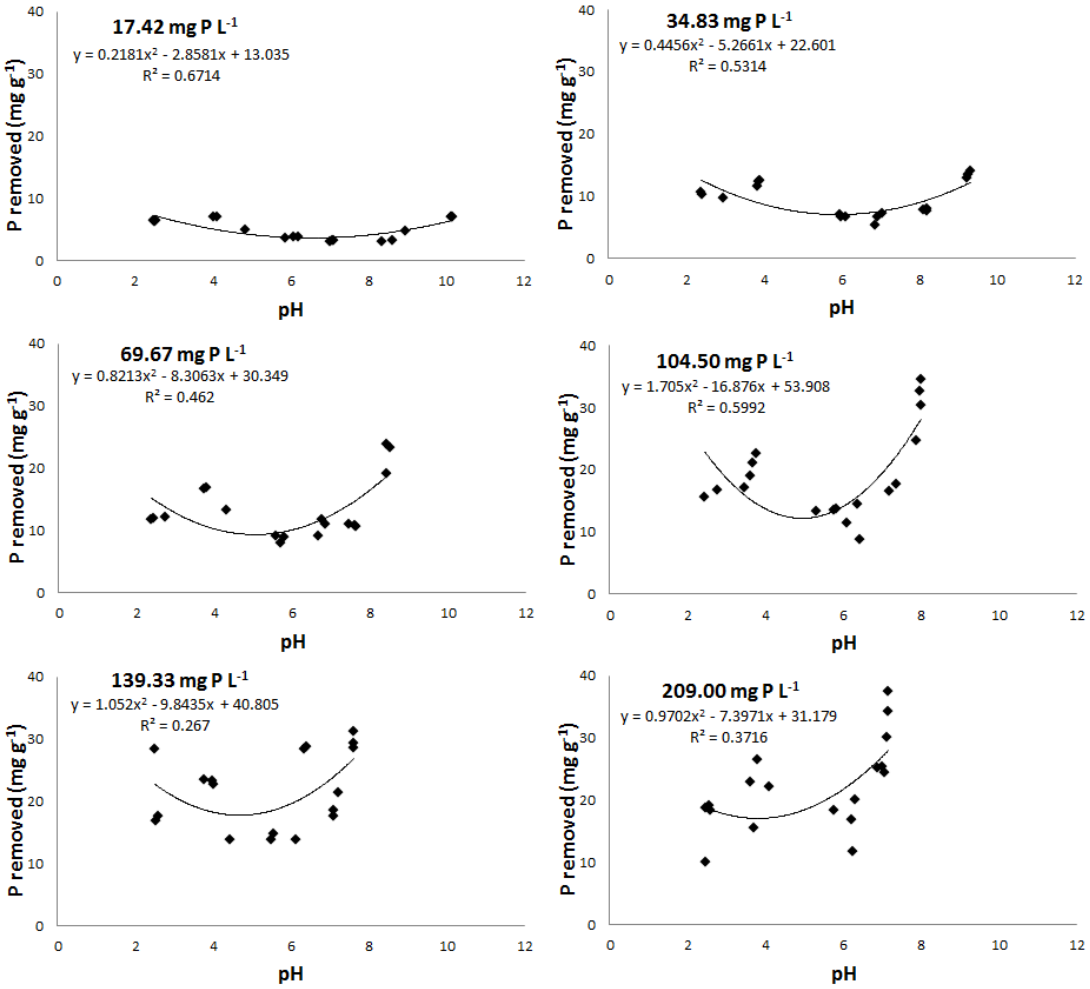

Figure 4.9: Curve fitting to P removed by Acomb pellets over a range of pH. Data sorted by P addition.

A difference in the shapes of the Langmuir and Freundlich isotherms at low and high pH values is apparent in both plots. At low pH, the initial gradient of the isotherm is steep, and P adsorption maxima occur at lower equilibrium concentrations. At pH 6 and 7, P adsorption maxima are not met, even at an

equilibrium concentration of 180 mg P L^{-1}. The differences in isotherm shape indicate that adsorption onto high affinity sites is dominant at the lower pH values, most probably onto the surface of goethite. Under higher pH conditions, it is suggested that P is adsorbing onto surfaces of calcite, with Acomb pellets containing 52 % calcite. Some calcium phosphate precipitates may also be forming at the higher P concentrations. The P adsorption capacity (S_{max}) of Acomb pellets under high pH conditions is the largest of all the ochres under study.

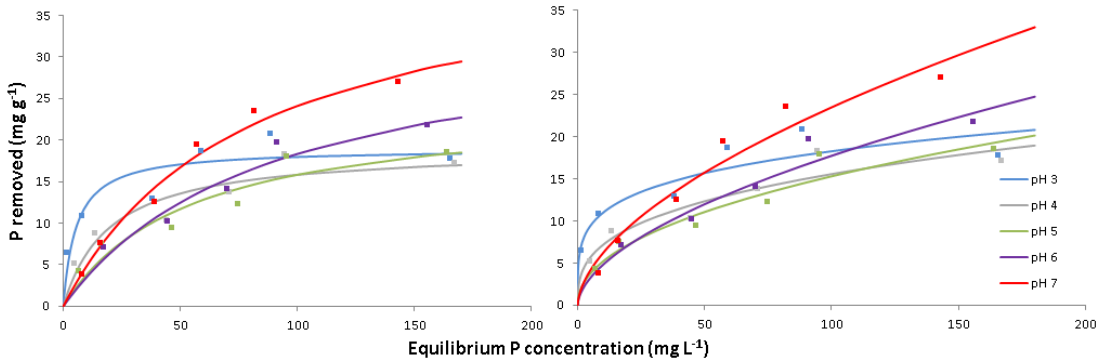

Figure 4.10: P adsorption isotherms derived from fitting the Langmuir (L) and Freundlich (R) isotherms to the Acomb pellets P adsorption batch experiment data.

The AIC values show that the Freundlich isotherm provides a better fit to the data between pH 3 and 5, with the Langmuir optimal at pH 6 and 7 (Table 4.3 and Table 4.4). Both isotherms fit the data well, with E above 0.81 for all model runs. SSE decreases with increasing pH for both the Langmuir and Freundlich isotherms, with the exception of pH 7 for the Freundlich isotherm.

The Langmuir isotherms indicate that the adsorption capacity (S_{max}) of Acomb pellets increases with pH from 18.96 mg P g^{-1} at pH 3, to 43.12 mg P g^{-1} at pH 7. However the Freundlich isotherms show the opposite trend, with the relative adsorption capacity, K_f, decreasing with increasing pH from 6.62 at pH 3 to 1.31 at pH 6, with a small increase to 1.64 at pH 7.

Table 4.3: Langmuir parameters and goodness of fit for Acomb pellets derived from model runs (2 d.p).

		pH				
		3	**4**	**5**	**6**	**7**
Goodness of fit	**SSE**	28.43	18.69	17.74	10.73	8.02
	E	0.81	0.86	0.89	0.96	0.98
	AIC	27.34	24.82	24.50	21.49	19.74
S_{max} (mg g^{-1})	**Value**	18.96	18.98	24.39	34.54	43.12
	S.E.	1.82	2.46	5.05	6.55	5.37
K (L mg^{-1})	**Value**	0.18	0.05	0.02	0.01	0.01
	S.E.	0.10	0.03	0.01	0.01	0.01

The value of Langmuir K is low for all pH conditions suggesting that adsorption onto calcite surfaces is the dominant P removal mechanism by Acomb pellets. Langmuir K is slightly higher at pH 3 and 4 suggesting adsorption onto higher affinity sites such as Fe hydroxides occurring under these conditions.

Table 4.4: Freundlich parameters and goodness of fit for Acomb pellets derived from model runs (2 d.p).

		pH				
		3	**4**	**5**	**6**	**7**
Goodness of fit	**SSE**	26.63	14.23	13.16	11.03	20.87
	E	0.82	0.89	0.92	0.96	0.95
	AIC	26.94	23.18	22.71	21.65	25.48
K_f	**Value**	6.62	3.32	1.78	1.31	1.64
	S.E.	1.79	1.06	0.70	0.47	0.62
n	**Value**	0.22	0.37	0.47	0.57	0.58
	S.E.	0.06	0.07	0.09	0.08	0.08

Between pH 6 and 8, the conditions of most P enriched wastewaters, the dominant P removal mechanism by Acomb pellets is adsorption onto surfaces of calcite. The shape of the adsorption isotherms at these pH values indicate that Acomb ochre will not be efficient at removing P from solution at low P concentrations, such as those expected under proposed field conditions, 0.1-15 mg P L^{-1}.

4.2.5.3 Avoca ochre

P removal by Avoca ochre correlates very strongly with pH (Figure 4.11). P removed is highest at low pH conditions, with up to 34 mg P g^{-1} adsorbed at pH 3, then decreases almost linearly with increasing pH to below 5 mg P g^{-1} at ~pH 10.

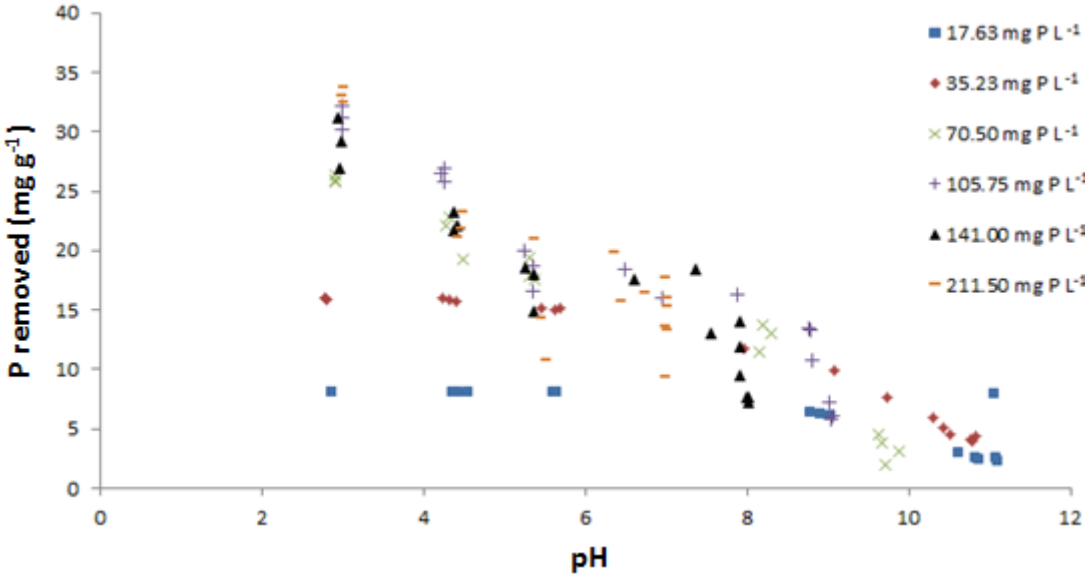

Figure 4.11: P adsorption batch experiment dataset for Avoca ochre. Each replicate is shown as a separate data point.

Data was sorted by P addition and polynomial trend lines were fitted to each dataset to describe the relationship between pH and P removed (Figure 4.12). The strength of fit (R^2) was high (>0.85) for all the trend lines. These equations of fit were used to calculate mg P g^{-1} adsorbed at a range of pH from 3 to 7 with adsorption isotherms fitted to this data (Figure 4.13). Data could not be derived from the trend

lines for values above pH 7 as the datasets for the higher P additions did not extend above this pH value.

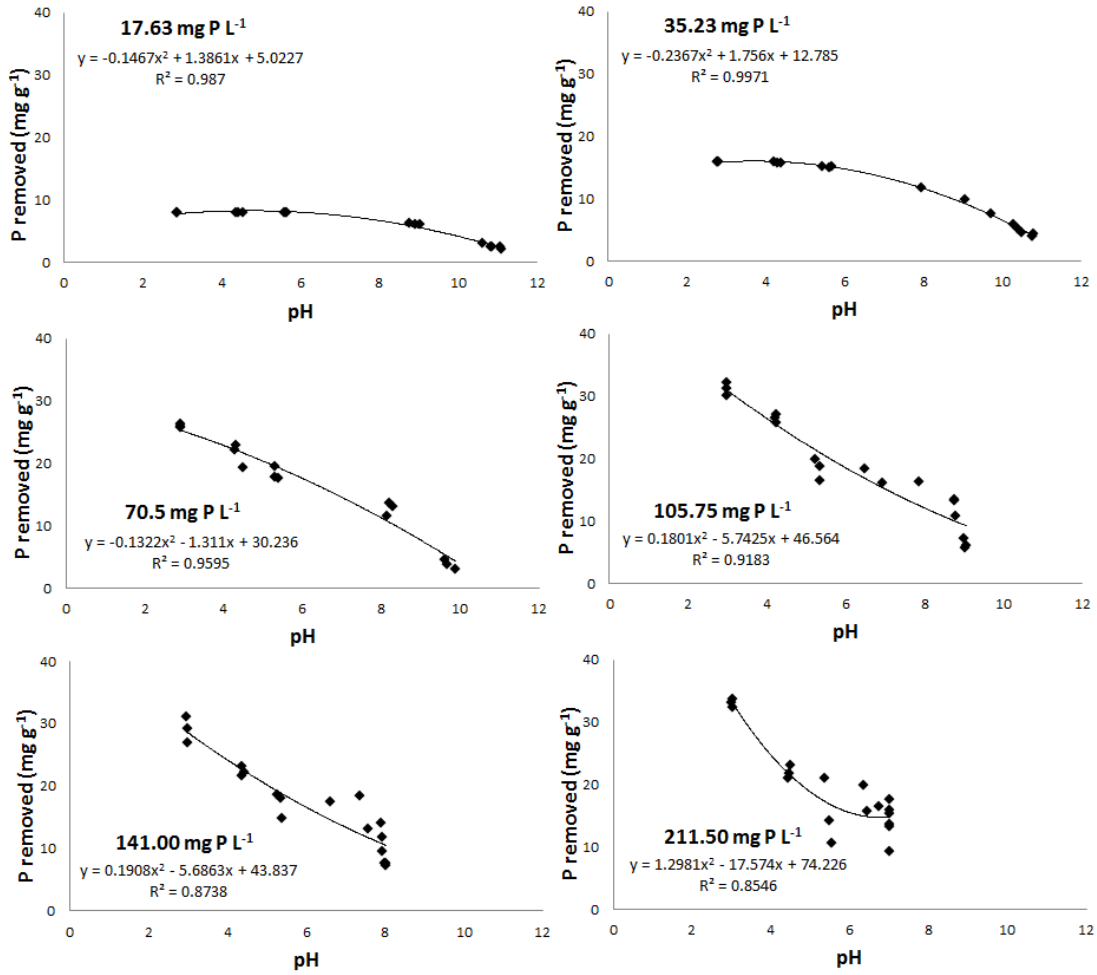

Figure 4.12: Curve fitting to P removed by Avoca ochre over a range of pH. Data sorted by P addition.

The Langmuir isotherms indicate that the P adsorption capacity of Avoca ochre is pH dependant, with S_{max} largest at pH 3, 29.76 mg P g^{-1}, decreasing with increasing pH to 14.79 mg P g^{-1} at pH 7 (Table 4.5). This is not replicated with the Freundlich isotherm, however, wherein the P adsorption capacity (K_f) is highest at pH 4, 20.76, rather than pH 3 and then decreases with pH to 9.69 at pH 7 (Table 4.6).

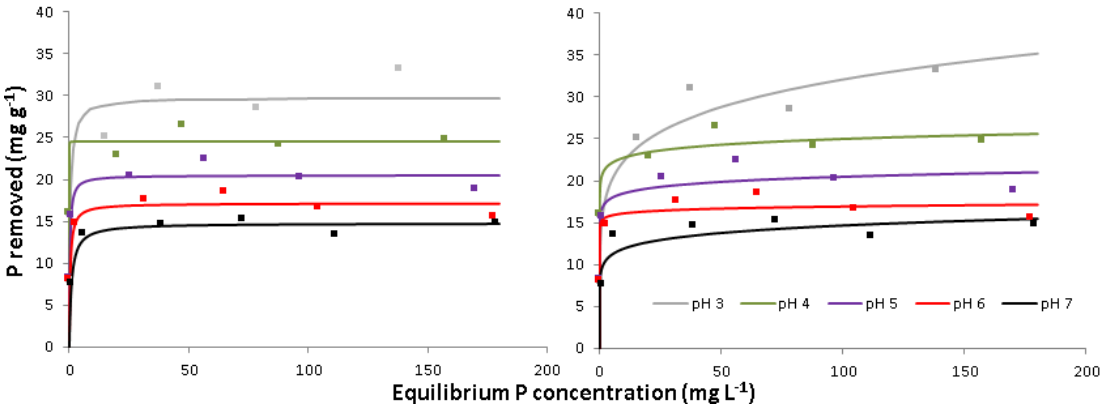

Figure 4.13: P adsorption isotherms fitted to Avoca ochre data: Langmuir (L), Freundlich (R).

The Langmuir isotherm fits the data better than the Freundlich isotherm at pH 7 (P>99%), but apart from this there is little difference in the two models in terms of AIC. There is a strong goodness of fit (E) for the isotherms at pH 3, 4 and 7 (>0.65), but E is very low at pH 6 with a slight improvement at pH 5 for both the Langmuir and Freundlich isotherms. SSE values are consistently lower for the Freundlich isotherm than for the Langmuir isotherm, with the exception at pH 7.

Table 4.5: Langmuir parameters and goodness of fit for Avoca ochre derived from model runs (2 d.p). Note: spurious result for K at pH 4.

		pH				
		3	**4**	**5**	**6**	**7**
Goodness of fit	**SSE**	90.77	74.26	75.28	70.60	2.73
	E	0.81	0.69	0.42	0.00	0.93
	AIC	34.30	33.09	33.18	32.79	13.29
S_{max} (mg g^{-1})	**Value**	29.76	24.55	20.52	17.16	14.79
	S.E.	2.46	2.15	2.22	2.23	0.42
K (L mg^{-1})	**Value**	2.31	920.91	3.93	2.46	1.10
	S.E.	1.17	749.98	5.04	6.05	0.25

Langmuir K has an exceptionally high value of 920.91 at pH 4. This spurious result is an artefact of the batch experiment results in which P removal by Avoca ochre was higher at P addition 105.75 mg P L^{-1} than at an addition of 141 or 211.5 mg P L^{-1} (see Figure 4.11).

The relatively high values of K suggest that adsorption onto high affinity sites is the dominant P removal mechanism. With a goethite and jarosite content of 20 % and 10 % respectively, it is suggested that adsorption is occurring onto these surfaces. The low amount of calcite in Avoca ochre results in very little P removal occurring at higher pH values and hence the P adsorption capacity is particularly dependent on pH for this ochre.

Table 4.6: Freundlich parameters and goodness of fit for Avoca ochre derived from model runs (2 d.p).

		pH				
		3	**4**	**5**	**6**	**7**
Goodness of fit	**SSE**	59.96	6.35	12.44	8.02	14.09
	E	0.86	0.90	0.50	0.15	0.65
	AIC	31.81	31.19	34.56	32.37	23.12
K_f	**Value**	15.66	20.76	16.77	15.35	9.69
	S.E.	2.34	0.82	1.85	1.92	1.46
n	**Value**	0.16	0.04	0.04	0.02	0.09
	S.E.	0.04	0.01	0.03	0.03	0.04

The P enriched waters likely to be treated with ochre have a pH between 6 and 8. Whilst S_{max} could not be calculated at pH 8, the ochre has a high adsorption capacity of 14.79-17.16 mg P g^{-1} between pH 6-7, similar to that calculated by Fenton et al., (2009); 16-21 mg P g^{-1}. The dominance of adsorption reactions makes Avoca ochre suitable for the removal of P from water with a P concentration of 0.1-15 mg P L^{-1}.

4.2.5.4 Minto ochre

P removal from solution by Minto ochre is relatively constant between pH 3.5 and 6 and declines above pH 6 (Figure 4.14). At the highest P addition, 212.75 mg P L^{-1}, P removal is greater than 15 mg g^{-1} between pH 4 and 6.

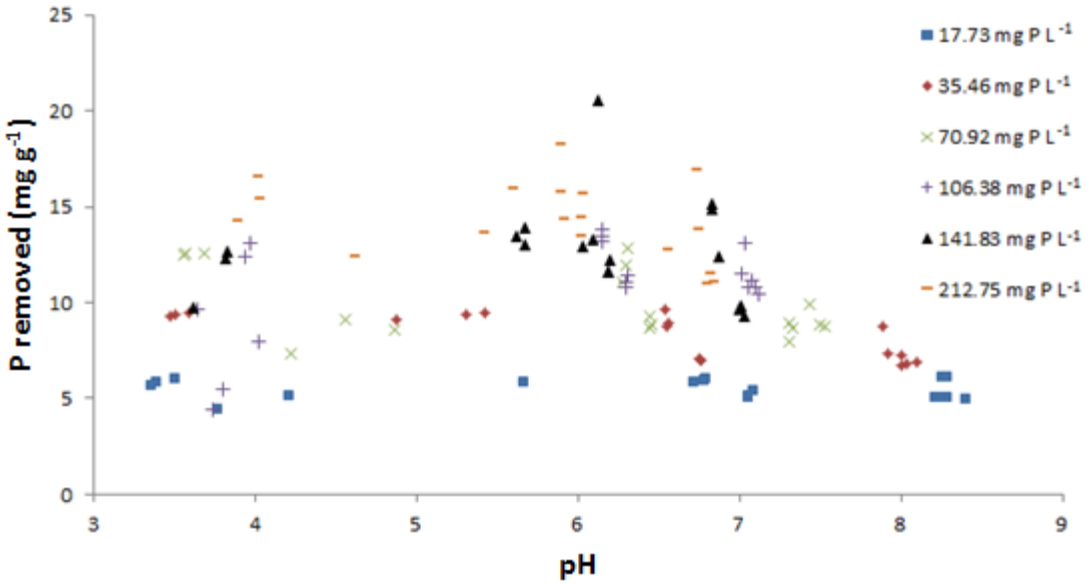

Figure 4.14: P adsorption batch experiment dataset for Minto ochre. Each replicate is shown as a separate data point.

Data was sorted by P addition, with P adsorbed plotted against equilibrium concentration, to which polynomial trend lines were fitted (Figure 4.15). Whilst the goodness of fit of many of these trend lines is low, they describe the general trend of the data well. They were used to calculate P adsorbed between pH 4 and 7 (the pH range of results in the high P addition batch experiments) to which adsorption isotherms were fitted (Figure 4.16).

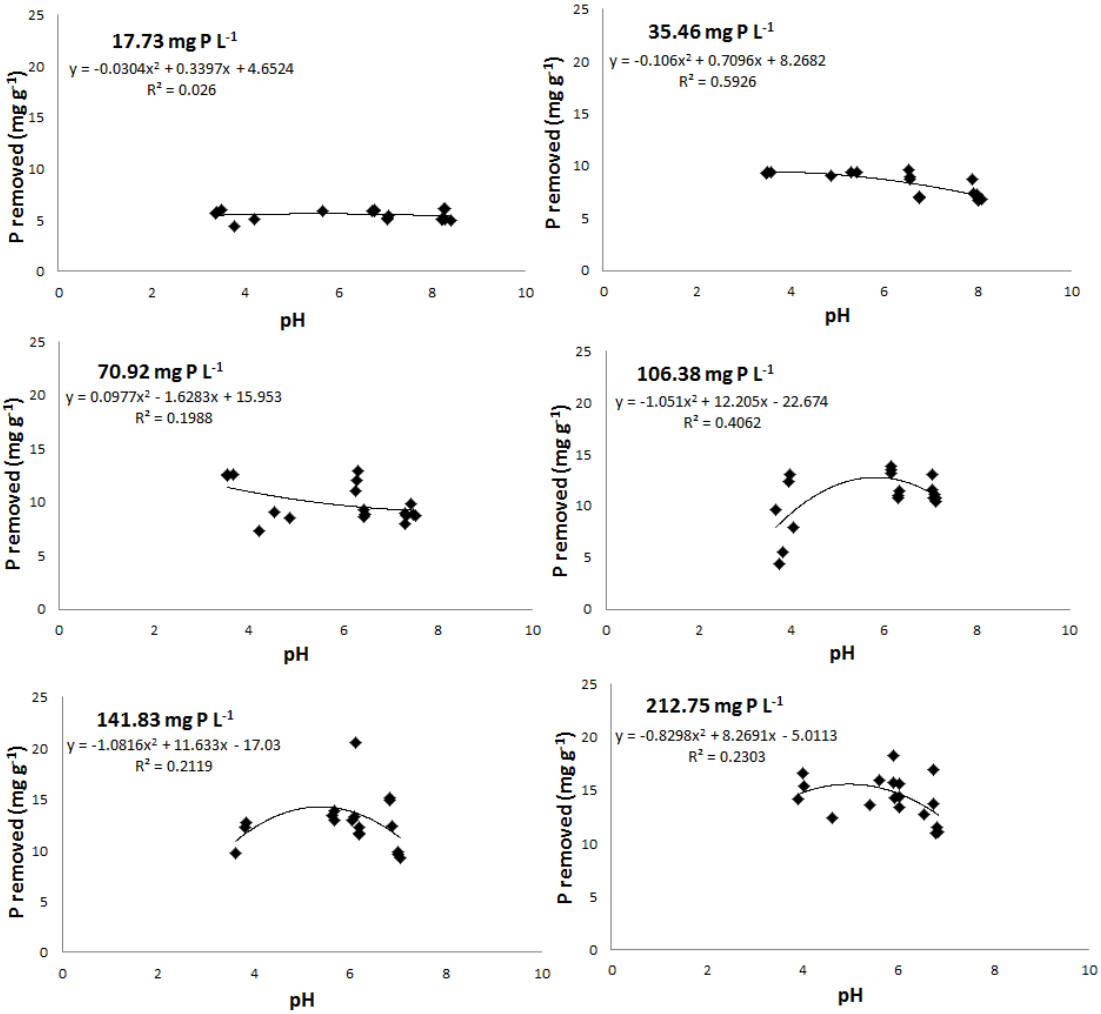

Figure 4.15: Curve fitting to P removed by Minto ochre over a range of pH. Data sorted by P addition.

Freundlich isotherms produced a better fit to the data than Langmuir isotherms, with consistently lower values of AIC (Table 4.7 and Table 4.8). For all model runs the goodness of fit was above 0.73 and SSE values were low.

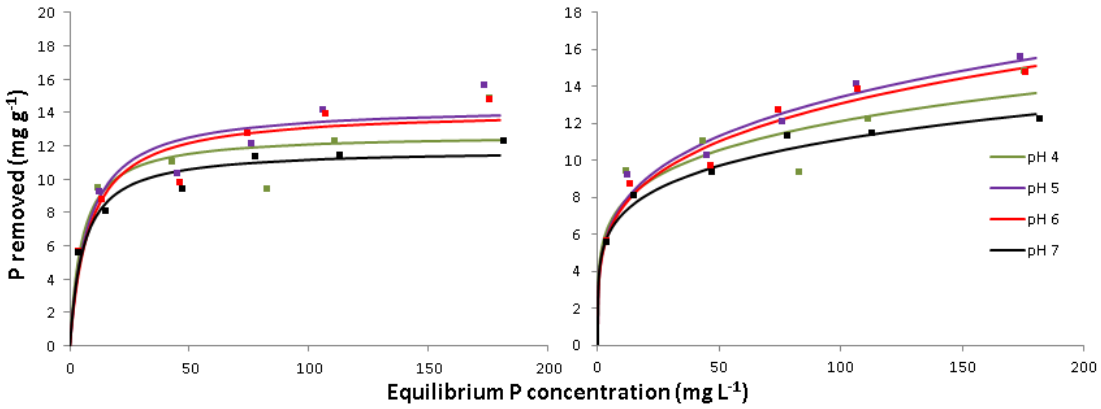

Figure 4.16: P adsorption isotherms fitted to Minto ochre data: Langmuir (L), Freundlich (R).

The P adsorption capacity of Minto ochre is not very pH dependant between pH 4 and 7 with the highest S_{max} of 14.41 mg P g^{-1} at pH 5 not dissimilar from the lowest value of 11.79 mg P g^{-1} at pH 7. The Freundlich isotherm also indicates little variability in P adsorption capacity at different pHs, with K_f highest at 4.83 for pH 4, and lowest, 4.24, at pH 6. Visual analysis of Figure 4.14 suggests that P removal declines with pH above pH 7, therefore Minto ochre may not be suitable for treatment of water with pH >7. Fitting the Langmuir isotherm to the data produced low values of K, 0.12 to 0.18 L mg^{-1}, suggesting there is a low affinity between P and Minto ochre.

Table 4.7: Langmuir parameters and goodness of fit for Minto ochre derived from model runs (2 d.p).

		pH			
		4	**5**	**6**	**7**
Goodness of fit	**SSE**	13.32	9.69	8.73	3.00
	E	0.73	0.85	0.86	0.91
	AIC	22.79	20.88	20.25	13.85
S_{max} (mg g^{-1})	**Value**	12.70	14.41	14.15	11.79
	S.E.	1.16	1.11	1.08	0.56
K (L mg^{-1})	**Value**	0.12	0.13	0.12	0.18
	S.E.	0.11	0.05	0.05	0.05

Table 4.8: Freundlich parameters and goodness of fit for Minto ochre derived from model runs (2 d.p).

		pH			
		4	**5**	**6**	**7**
Goodness of fit	**SSE**	10.47	2.50	2.50	0.83
	E	0.79	0.96	0.96	0.97
	AIC	21.34	12.74	12.74	6.15
K_f	**Value**	4.83	4.32	4.24	4.51
	S.E.	1.24	0.55	0.56	0.36
N	**Value**	0.20	0.25	0.25	0.20
	S.E.	0.06	0.03	0.03	0.02

The P adsorption capacity of Minto ochre, 11.79-14.41 mg P g^{-1} is lower than the previously reported value, 21.5 mg P g^{-1} (Bozika, 2001; Heal et al., 2003b), which was calculated from fitting the Langmuir equation to batch experiment data in a similar manner to this study. The lower P adsorption capacity of Minto ochre determined in this study may be due to the lower Ca concentration of the ochre sampled (1.27 %

by dry weight) compared to the previous study (11.8 % by dry weight). It is therefore likely that P removal mechanisms associated with Ca such as adsorption onto calcite and the formation of calcium phosphates occurred in the previous study and was the cause of the higher P adsorption capacity.

4.2.5.5 Silkstone ochre

P removal by Silkstone ochre is pH dependant, with P removed generally decreasing as pH increases (Figure 4.17). At the higher P additions, P removal exceeds 20 mg P g^{-1} below pH 6, but decreases to ~15 mg P g^{-1} between pH 6 and 8.

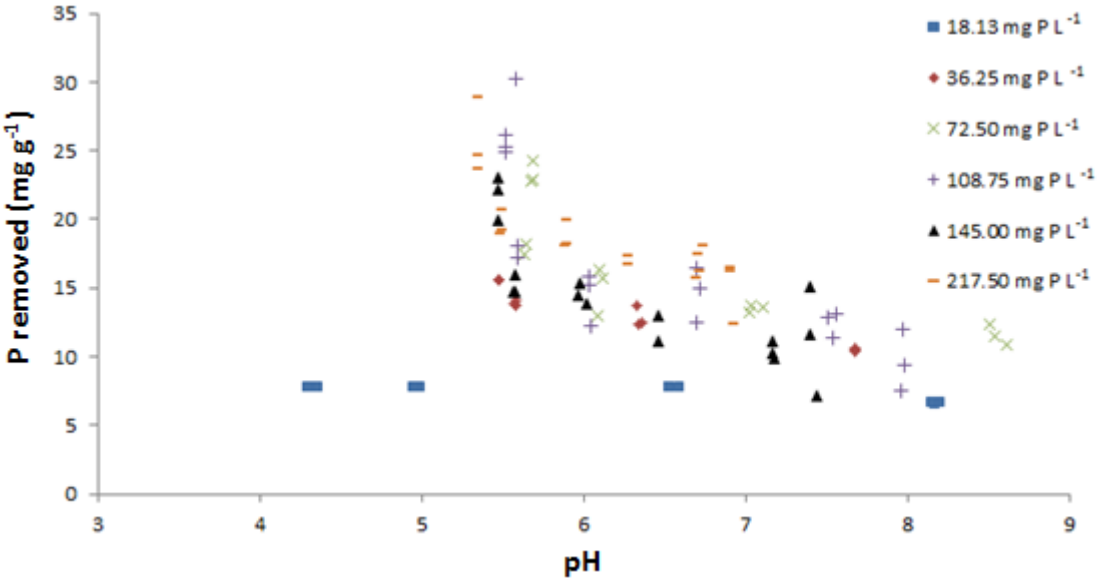

Figure 4.17: P adsorption batch experiment dataset for Silkstone ochre. Each replicate is shown as a separate data point.

For each P addition, the dataset was fitted with a polynomial trend line to describe the relationship between P removed and pH (Figure 4.18). The fit of these trend lines is high, with $R^2 \geq 0.70$. From these trend lines, P removed was calculated for the pH range 5.5-7.0 and adsorption isotherms fitted to this data (Figure 4.19).

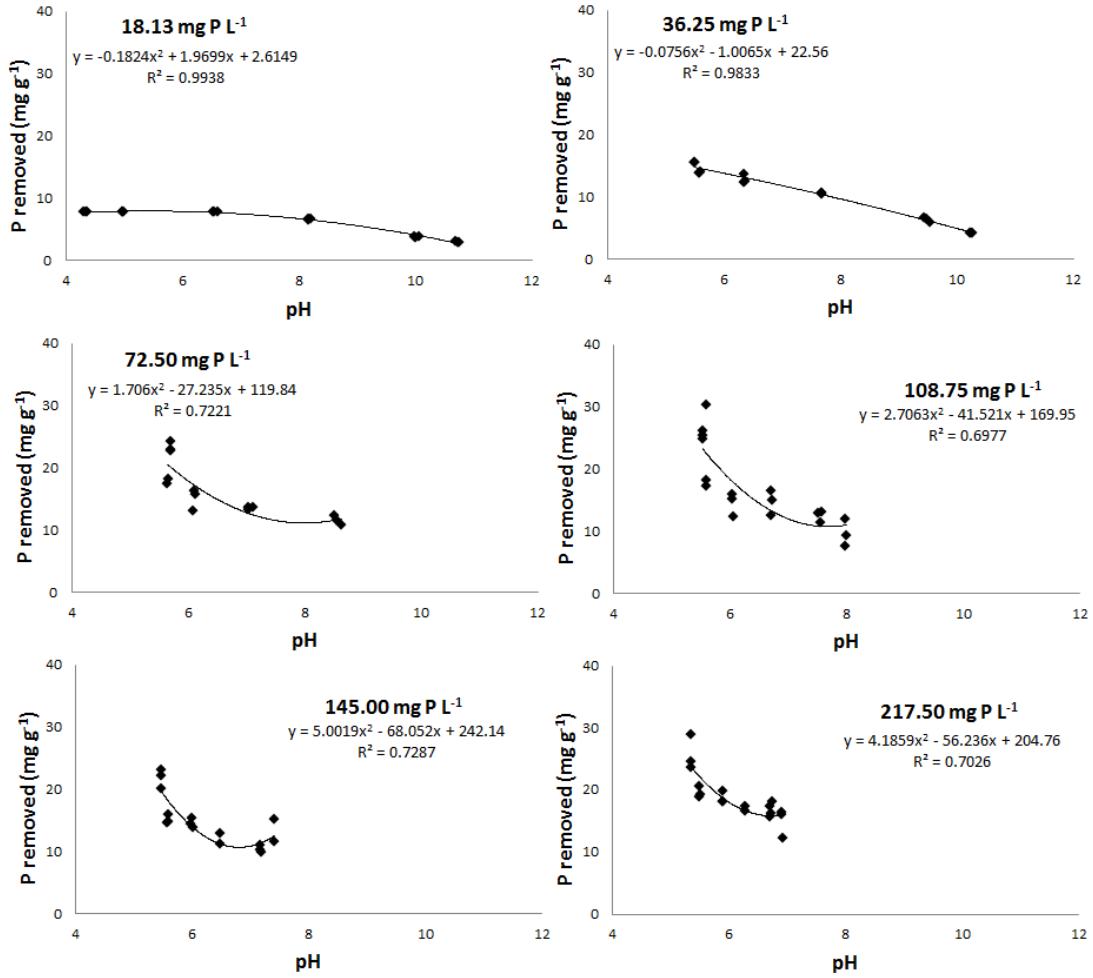

Figure 4.18: Curve fitting to P removed by Silkstone ochre over a range of pH. Data sorted by P addition.

The adsorption isotherms show that the P adsorption capacity of Silkstone ochre increases with decreasing pH (Figure 4.19, Table 4.9 and Table 4.10). S_{max}, determined from the Langmuir isotherm, is highest at pH 5.5 (21.95 mg P g^{-1}) and decreases to 12.97 mg P g^{-1} at pH 7.0. Similarly, K_f, calculated from fitting the Freundlich isotherm, is highest at pH 5.5 at 15.56 and decreases to 8.40 at pH 7.0. The Langmuir isotherm fits the data better than the Freundlich isotherm, with consistently lower AIC values. The model efficiency (E) is similar for both isotherm models, however, with values of 0.55-0.69 recorded at all pHs except pH 6 wherein lower values were calculated of 0.07 and 0.21 for the Langmuir and Freundlich isotherms, respectively.

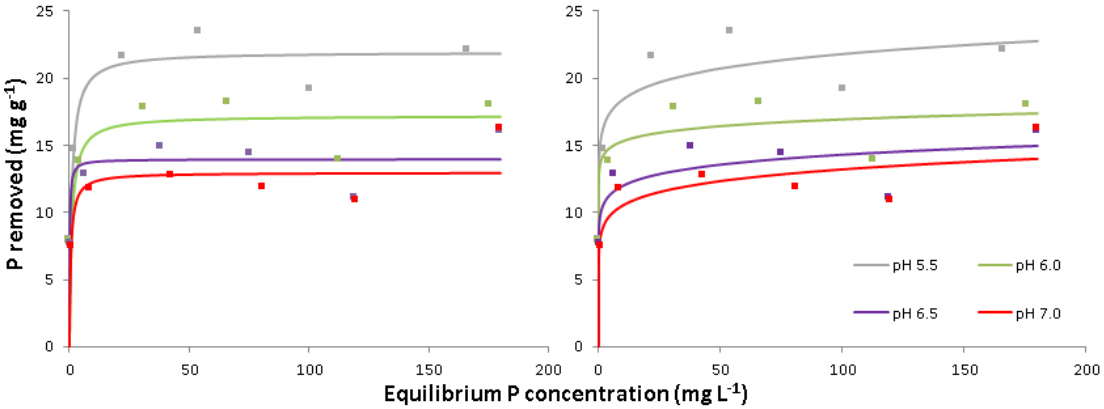

Figure 4.19: P adsorption isotherms fitted to Silkstone ochre data: Langmuir (L), Freundlich (R).

The overall better fit of the Langmuir isotherm to the results suggests that it provides a better description of the adsorption of P by Silkstone ochre, i.e. with adsorption occurring at definite surface sites, each site bonding with only one P molecule, the same strength of bond between each surface site and P molecule, and no forces of interaction between adjacent adsorbed P molecules.

Table 4.9: Langmuir parameters and goodness of fit for Silkstone ochre derived from nonlinear Langmuir model runs (2 d.p).

		pH			
		5.5	**6.0**	**6.5**	**7.0**
Goodness of fit	**SSE**	73.53	75.80	14.33	16.05
	E	0.57	0.07	0.69	0.60
	AIC	33.04	33.22	23.22	23.91
S_{max} (mg g^{-1})	**Value**	21.95	17.21	13.96	12.97
	S.E.	2.33	2.42	0.86	0.96
K (L mg^{-1})	**Value**	1.09	1.06	6.99	1.75
	S.E.	1.08	2.04	3.98	1.16

The Langmuir K values are high for Silkstone ochre, ranging from 1.06 to 6.99, suggesting adsorption onto sites with a high affinity for P such as Fe- hydroxides. As the ochre contains 16 % goethite, it is suggested that P adsorption onto these surfaces is the dominant P removal mechanism. The high K values suggest that Silkstone ochre will be suitable for adsorbing P from P-enriched waters with relatively low P concentrations of ~0.1-15 mg P L^{-1} and below.

Table 4.10: Freundlich parameters and goodness of fit for Silkstone ochre derived from model runs (2 d.p).

		pH			
		5.5	**6.0**	**6.5**	**7.0**
Goodness of fit	**SSE**	21.20	16.81	18.03	15.53
	E	0.55	0.21	0.61	0.61
	AIC	37.22	36.06	24.60	23.70
K_f	**Value**	15.56	13.85	10.06	8.40
	S.E.	2.65	2.95	1.48	1.55
n	**Value**	0.07	0.04	0.08	0.10
	S.E.	0.04	0.05	0.04	0.04

P enriched waters, which are potential targets for remediation with ochre, tend to have a pH between 6 and 8. The P adsorption capacity of Silkstone ochre has been shown to decline with increasing pH; it has a P adsorption capacity of 17.21 mg P g^{-1} at pH 6, declining to 12.97 mg P g^{-1} at pH 7. The batch experiment results for the lower P concentration additions, which extend beyond pH 7, indicate that P adsorption continues to decrease with increasing pH. Thus, the P adsorption capacity of Silkstone ochre will be lower at pH 8 than pH 7.

4.2.5.6 Polkemmet ochre

At low P additions, P removed by Polkemmet ochre has a very small pH dependant relationship (Figure 4.20). At P addition 18.16 mg P L^{-1}, P removal is >5 mg P g^{-1} between pH 3 to 6, declining to 3.5 mg P g^{-1} above pH 7. This relationship is less distinct at the higher P additions where data is only available between ~pH 3-6 due to a drift in pH following the addition of P.

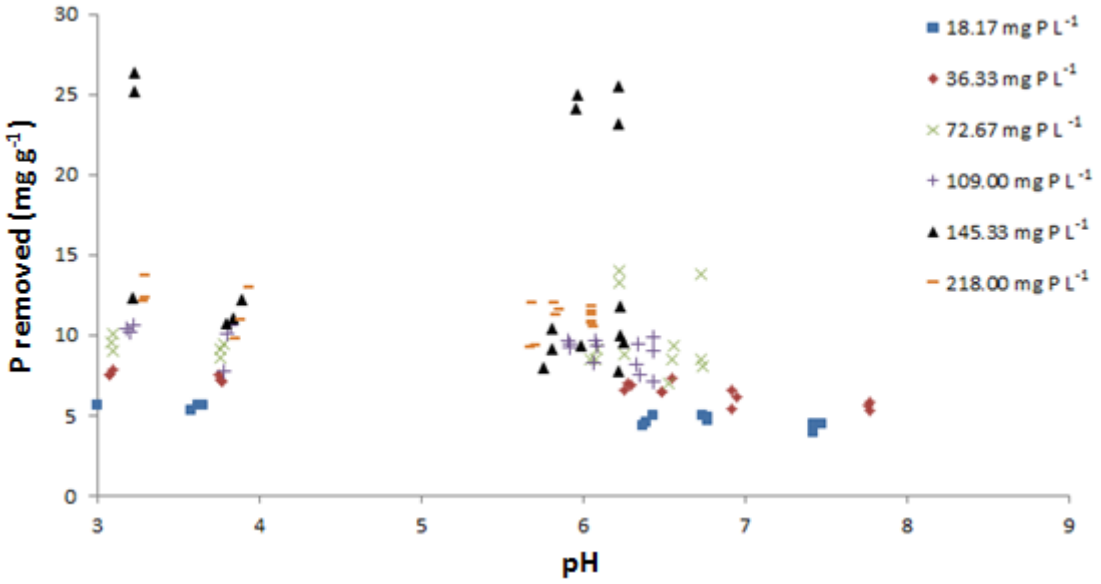

Figure 4.20: P adsorption batch experiment dataset for Polkemmet ochre. Each replicate is shown as a separate data point.

A gap in the dataset is evident between pH 4 and 5.5 (Figure 4.20). This is because samples which were at equilibrium pH 5 drifted to a final pH value below 4 following P addition. The dataset for each P addition was fitted with a polynomial trend line to describe the relationship between pH and P removal by Polkemmet ochre (Figure 4.21). The strength of fit (R^2) at the two lowest P additions is high (>0.78) but low for the other P additions. The variability of the data for P addition 145.33 mg P L^{-1} led to it being excluded from further calculations as the data was deemed unreliable. The remaining trend lines were utilised to derive P removal data between pH 3.5 to 6, to which adsorption isotherms were fitted (Figure 4.22, Table 4.11 and Table 4.12).

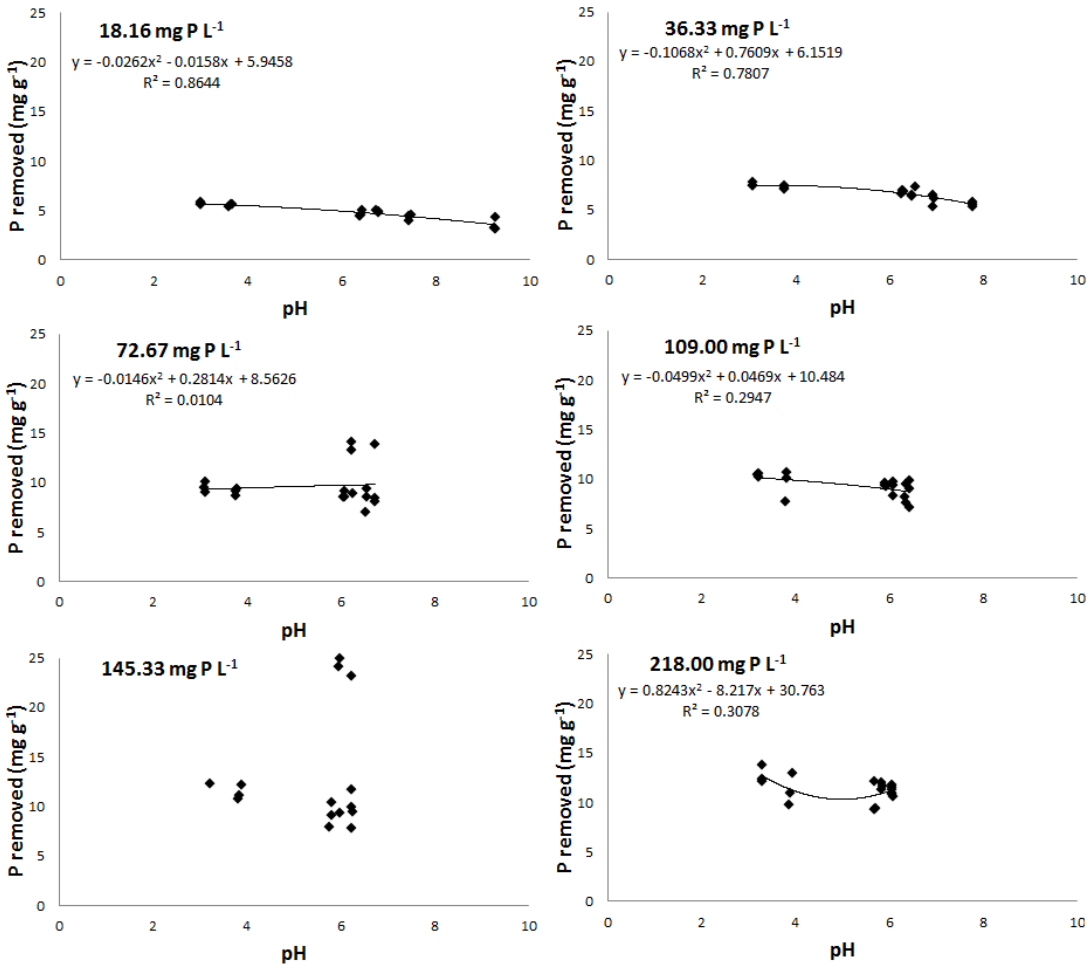

Figure 4.21: Curve fitting to P removed by Polkemmet ochre over a range of pH. Data sorted by P addition.

S_{max}, derived from the Langmuir isotherm, decreases from 11.51 mg P g^{-1} at pH 3.5 to 10.56 mg P g^{-1} at pH 5 before increasing at pH 5.5 and 6.0. The P adsorption capacity of Polkemmet ochre is therefore not pH dependant across this range of conditions. This is also indicated from the close overlap of the adsorption isotherms across pH 3.5-6.0 (Figure 4.22).

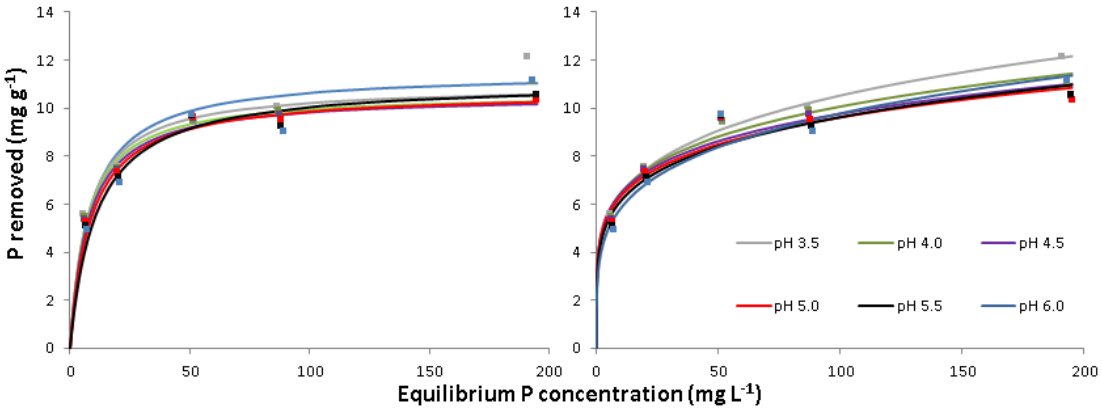

Figure 4.22: P adsorption isotherms fitted to Polkemmet ochre data: Langmuir (L), Freundlich (R)

For pH 3.5 and 4.0 the Freundlich isotherm provides a better fit for the data, with lower values of AIC, whilst for pH conditions 4.5 to 6.0 the Langmuir isotherm provides a better fit. Efficiency (E) is high for all isotherm plots (>0.89) with SSE also low for each model fit. The better fit of the Langmuir isotherm at pH 4.5 and above suggests that P adsorption occurs in a monolayer in these pH conditions, with multilayer adsorption occurring at lower pH, as reflected in the improved fit with the Freundlich isotherm.

Table 4.11: Langmuir parameters and goodness of fit for Polkemmet ochre derived from model runs (2 d.p).

		pH					
		3.5	**4.0**	**4.5**	**5.0**	**5.5**	**6.0**
Goodness of fit	**SSE**	2.65	0.84	0.38	0.46	0.86	1.96
	E	0.89	0.96	0.98	0.97	0.96	0.92
	AIC	26.83	21.06	17.15	18.09	21.20	25.32
S_{max} (mg g^{-1})	**Value**	11.51	10.96	10.65	10.56	10.70	11.12
	S.E.	0.78	0.42	0.28	0.32	0.45	0.73
K (L mg^{-1})	**Value**	0.12	0.14	0.14	0.13	0.12	0.09
	S.E.	0.04	0.03	0.02	0.02	0.02	0.03

Table 4.12: Freundlich parameters and goodness of fit for Polkemmet ochre derived from model runs (2 d.p).

		pH					
		3.5	**4.0**	**4.5**	**5.0**	**5.5**	**6.0**
Goodness of fit	**SSE**	0.11	0.65	1.43	1.96	2.16	2.36
	E	1.00	0.97	0.92	0.89	0.89	0.90
	AIC	10.95	19.83	23.75	25.32	25.80	26.25
K_f	**Value**	3.89	4.17	4.27	4.19	3.93	3.49
	S.E.	0.15	0.40	0.62	0.72	0.73	0.71
n	**Value**	0.22	0.19	0.18	0.18	0.19	0.22
	S.E.	0.01	0.02	0.03	0.04	0.04	0.05

The value of Langmuir K remained relatively constant between pH 3.5 and 6.0, ranging between 0.09 and 0.14. This means that whilst the affinity between P and ochre is relatively low, it does not vary greatly with pH. The Langmuir K value for Polkemmet ochre has previously been reported as 0.6 (Heal et al., 2003b), which would suggest adsorption occurring onto sites with a high affinity for P, e.g. goethite.

The P adsorption capacity of Polkemmet ochre has previously been determined as 17.8 mg P g^{-1} by fitting the Langmuir isotherm to batch experiment data (Bozika, 2001., Heal et al., 2003b). The higher P adsorption capacity in the previous study may be due to a difference in ochre composition, since the ochres from Polkemmet had been sampled eight years apart and there has been a change in the operation of the ochre drying beds during this time period (Chapter 3.1.1). Whilst Polkemmet ochre was found in this study to have a higher Al content than determined previously, it contained significantly lower amounts of Fe and Ca (44.6 and 0.96 %, compared to 65 and 7 % in the previous studies). The lower measured Fe and Ca contents may account for the lower P adsorption capacity calculated in this study.

P enriched waters suitable for remediation by ochre will likely have pHs between 6 and 8. Whilst adsorption isotherms could only be plotted up to pH 6, the adsorption of P between pH 6 and 8 remained at a near constant level for the two lowest P additions (Figure 4.20). Thus, the P adsorption capacity is expected to be similar to that at pH 6, ~11 mg P g^{-1}. Langmuir K was low at the range of pH tested, this means that Polkemmet ochre may not prove effective at removing P from waters with P concentrations between 0.1 and 15 mg P L^{-1}.

4.2.5.7 Ynysarwed ochre

P removal by Ynysarwed ochre was highest at pH 3, and up to 25-30 mg P g^{-1} for the four highest P additions (Figure 4.23). A small decline in P removal occurred between pH 3 and 9, and there was a rapid decline in P removed above pH 9. The apparent lack of response to pH for the two lowest P additions up to pH 9 is due to the fact that all the available P in solution was removed by the ochre at this range of pH conditions. A gap in the dataset is evident between pH 3 and 6.5 (Figure 4.23). This is because the samples at pH equilibrium had a poor distribution of pH values (pH 3, 7, 8, 8.8, 9.5 and 10). It was noted in previous batch experiments using other ochres that the pH of the experiments converged towards ~pH 4.5 following P addition. The experiments using Ynysarwed ochre were therefore continued with the expectation that the range of pH values would decrease following the P addition. Despite this not occurring, the dataset still provides valuable information regarding P removal across a range of pH and P additions and will be used to calculate adsorption isotherms.

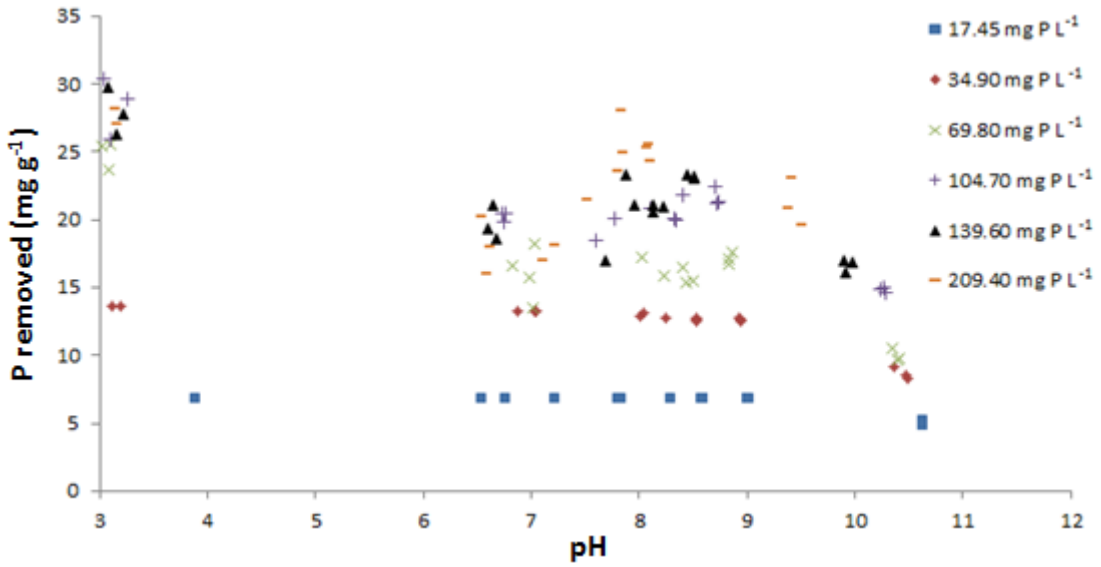

Figure 4.23: P adsorption batch experiment dataset for Ynysarwed ochre. Each replicate is shown as a separate data point.

The dataset for each P addition was fitted with a polynomial trend line to describe the relationship between pH and P adsorbed by the ochre (Figure 4.24). The trend lines represent the data well, with $R^2 > 0.62$ for all P additions, apart from for the highest addition (209.40 mg P L^{-1}), for which $R^2 = 0.22$. Although goodness of fit was low for the highest P addition, the trend line was still utilised as it captures the general trend of the dataset. For each trend line, P removed was calculated from pH 4 to 9, and adsorption isotherms plotted to this data (Figure 4.25, Table 4.13 and Table 4.14).

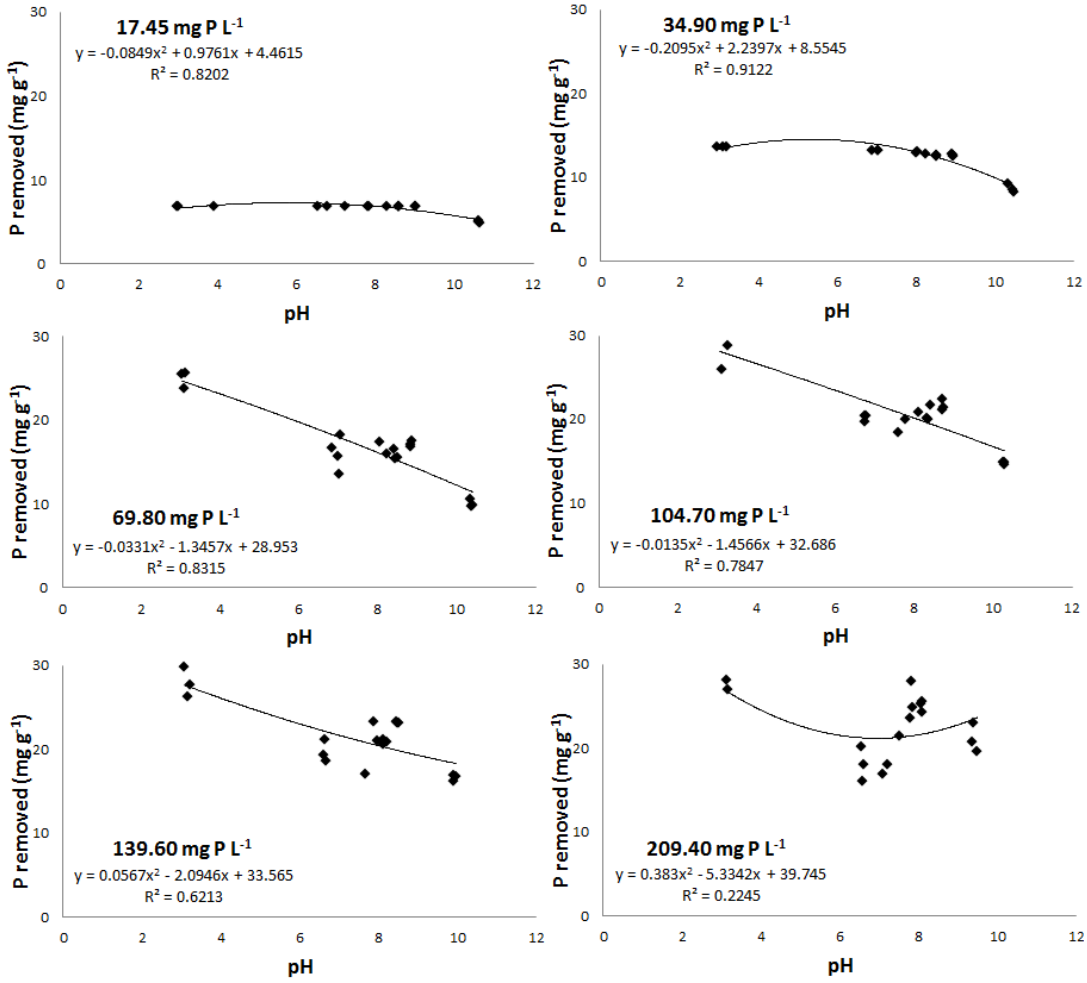

Figure 4.24: Curve fitting to P removed by Ynysarwed ochre over a range of pH. Data sorted by P addition.

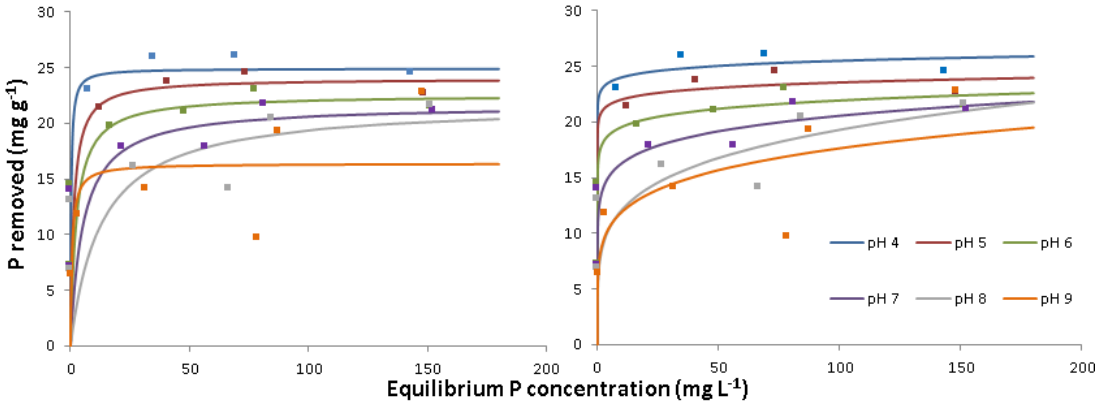

Figure 4.25: P adsorption isotherms fitted to Ynysarwed ochre data: Langmuir (L), Freundlich (R)

The adsorption isotherms show that the P adsorption capacity of Ynysarwed ochre is pH dependant. It is highest at pH 3 (25.84 mg P g^{-1}) and lowest at pH 9 (16.39 mg P g^{-1}). Between pH 4 and 8 the adsorption capacity of Ynysarwed ochre is consistently high at over 20 mg P g^{-1}. Fitting the Freundlich isotherm shows a similar trend, with the P adsorption capacity (K_f) highest at pH 4 and then declining with increasing pH.

Table 4.13: Langmuir parameters and goodness of fit for Ynysarwed ochre derived from model runs (2 d.p).

		pH					
		4	**5**	**6**	**7**	**8**	**9**
Goodness of fit	**SSE**	251.90	265.27	263.57	251.90	241.11	102.40
	E	0.18	-0.15	-0.48	-0.72	-0.67	0.45
	AIC	40.42	40.73	40.70	40.42	40.16	35.02
S_{max} (mg g^{-1})	**Value**	25.84	24.02	22.57	21.67	21.83	16.39
	S.E.	5.55	6.24	6.90	7.81	9.93	2.55
K (L mg^{-1})	**Value**	1.16	0.74	0.41	0.19	0.08	1.50
	S.E.	5.11	3.81	1.93	0.68	0.20	1.99

Table 4.14: Freundlich parameters and goodness of fit for Ynysarwed ochre derived from model runs (2 d.p). – indicates AIC could not be calculated.

		pH					
		4	**5**	**6**	**7**	**8**	**9**
Goodness of fit	**SSE**	4.23	3.90	2.81	4.88	18.65	74.91
	E	0.32	0.29	0.51	0.61	0.50	0.60
	AIC	-	-	-	-	-	33.15
K_f	**Value**	22.63	20.60	17.44	12.91	7.58	8.04
	S.E.	2.42	2.76	2.55	3.22	4.80	2.97
n	**Value**	0.03	0.03	0.05	0.10	0.20	0.17
	S.E.	0.03	0.03	0.04	0.06	0.14	0.08

The fitting of the Freundlich equation to a dataset is only possible for data points which have an equilibrium concentration greater than 0 mg P L^{-1}. For some of the P additions (17.45 and 34.90 mg P L^{-1}) all the P was removed from solution, resulting in calculated P equilibrium concentrations of 0 mg P L^{-1}. These data points therefore could not be included in the dataset for fitting the Freundlich equation. The requirements to calculate AIC were consequently not met between pH 4 and 8. However, from comparison of the values of model efficiencies (E), the Freundlich isotherm gives a better fit to the data. Between pH 5 and 8 the Langmuir isotherm gives such a poor fit to the dataset ($E < 0$), that taking the average P adsorbed value of the observed data would give a closer fit than the modelled result.

The Freundlich isotherm is more successful than the Langmuir for describing P adsorption by Ynysarwed ochre. This suggests that adsorption does not occur in a monolayer, and that adsorption sites have varying amounts of bonding energy. The high P adsorption capacity of Ynysarwed ochre suggests it is suitable for the removal of P from P-enriched waters, which are expected to have pH conditions of between 6 and 8.

4.3 P adsorption batch experiments in the presence of competing ions

The successful application of ochre for the remediation of P enriched waters will require preferential P removal in the presence of other ions competing for adsorption sites. In an attempt to simulate more realistic field conditions, further batch experiments were conducted to determine the adsorption isotherms of three ochres in the presence of competing ions. Polkemmet ochre and Acomb pellets were selected as they are the most likely candidates for use as a filter substrate due to their high hydraulic conductivity. Acomb ochre was also selected as a comparison to determine the effect of the pelletisation process.

The same P adsorption batch experiment methodology was used as before across a range of pHs (Chapter 4.2), with the addition of competing ions in the form of

synthetic sewage (SynS), due to the intended end-use of ochre for wastewater treatment. The SynS was made up following the Department of the Environment (1981) guidelines – 1 L SynS comprising 160 mg peptone, 110 mg meat extract, 30 mg urea, 7 mg sodium chloride, 4 mg calcium chloride dihydrate and 2 mg magnesium sulphate heptahydrate dissolved in 1 L tap water.

The experiments were set-up and allowed to equilibrate for 8 days, agitated in a cabinet shaker at 120 rpm. The pH at equilibrium was then measured. A 1 mL addition was then made to the experiments: containing the required P concentration in a solution of 32 times concentrated SynS. The concentrated dose is because the SynS dose will be diluted in the 32 mL total volume in each centrifuge tube to the guideline SynS concentration. The centrifuge tubes were then agitated for 24 hours before the final pH was measured and they were centrifuged at 4500 rpm for 30 minutes and filtered through 0.45 μm cellulose filter paper into polypropane containers. The supernatant was analysed for PO_4-P concentration using a Konelab 20 discrete analyser at the James Hutton Institute, Aberdeen using the same methodology as documented in Chapter 4.2.2. Samples were stored below 4°C and were analysed within two weeks of sample collection. All experiments were conducted in triplicate, and blank experiments were run which did not include the addition of ochre suspension or the P-enriched SynS solution. The results of these blanks were analysed for P concentration, with the average of this subtracted from the results of the batch experiments.

4.3.1 P adsorption isotherms in the presence of competing ions

Data generated from the batch experiments in the presence of competing ions was analysed in the same manner as the P adsorption batch experiments. Trend lines were plotted through the experimental datasets to calculate equilibrium P concentrations and P removed by ochre at discrete pH values. P adsorption isotherms were then fitted to this derived data.

4.3.1 Acomb ochre

For the three lowest P additions, P removal by Acomb ochre in the presence of competing ions is pH dependant; the highest amount of P is removed under acidic conditions, decreasing with increasing pH (Figure 4.26). This trend occurred in the P adsorption batch experiments with Acomb ochre for all P additions, but was not apparent in this dataset for the higher P additions.

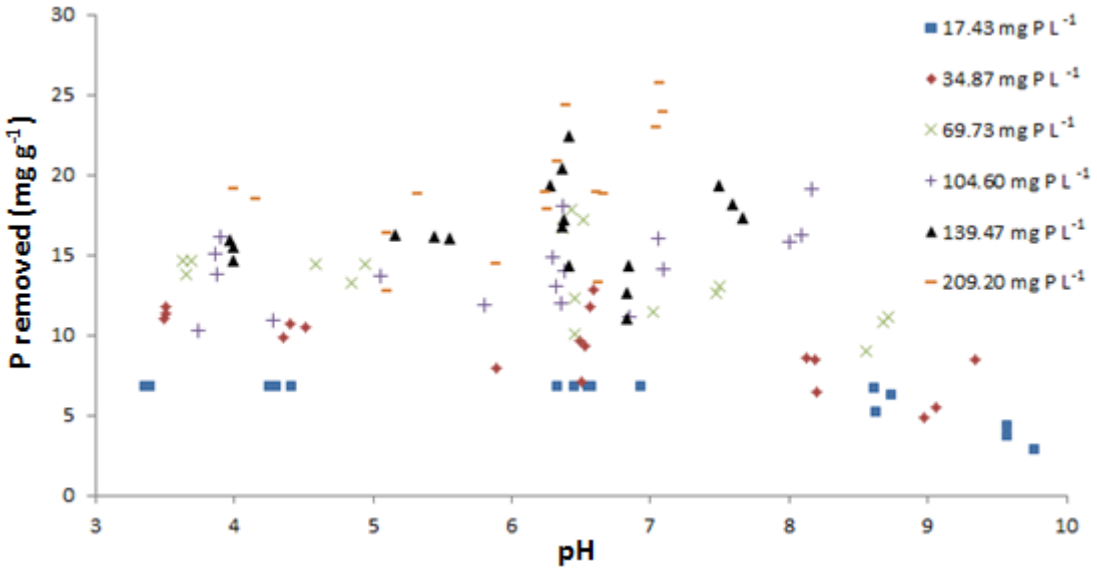

Figure 4.26: P removal by Acomb ochre in the presence of competing ions dataset. Each replicate is shown as a separate data point.

The data was fitted with trend lines (Figure 4.27) with the goodness of fit (R^2) ranging from 0.04 to 0.83. The worst fit occurred for the 139.47 mg P addition. The trend line for this P addition represents the data below pH 6 well due to limited variability of the data. The data between pH 6 and 7 is highly variable however, with P removal ranging between 10-22 mg g^{-1}, resulting in the the low value of R^2.

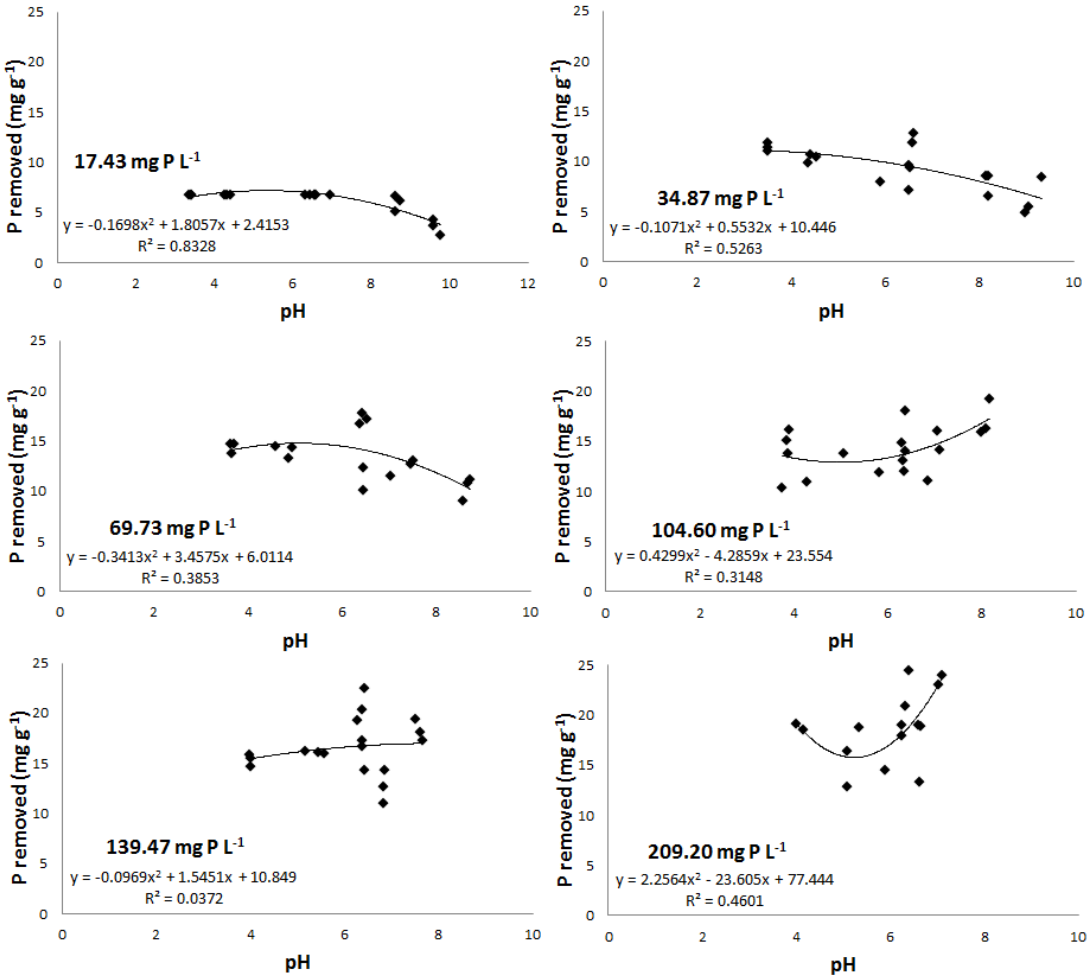

Figure 4.27: Curve fitting to P removed by Acomb ochre over a range of pH in the presence of competing ions. Data sorted by P addition.

All trend lines were utilised to derive the data required for fitting adsorption isotherms between pH 4 and 7 (Figure 4.28). In the P adsorption batch experiments (Chapter 4.2.5.1), P removal by Acomb ochre was pH dependant, with P removed decreasing as pH increased. In the presence of competing ions, a relationship between P removal and pH is not apparent, with P removal highest at pH 7. In the presence of competing ions, as in the P adsorption batch experiments, the Freundlich isotherm provides a better fit to the dataset than the Langmuir isotherm. The former has lower values of AIC, and the efficiency values (E) for each model run were above 0.69 (Table 4.15 and Table 4.16).

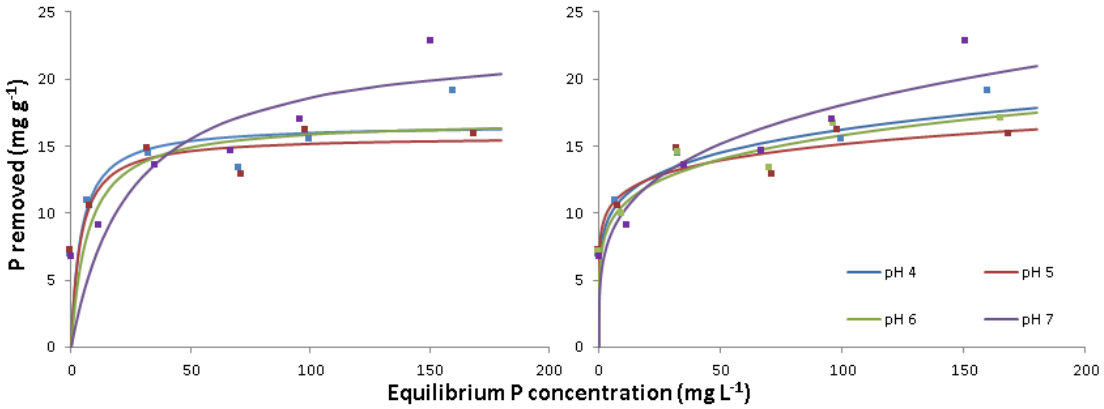

Figure 4.28: P adsorption isotherms for Acomb ochre in the presence of SynS: Langmuir (L) Freundlich (R)

Table 4.15: Langmuir parameters and goodness of fit for Acomb ochre in the presence of competing ions derived from model runs (2 d.p).

		pH			
		4	**5**	**6**	**7**
Goodness of fit	**SSE**	62.99	57.82	56.93	61.87
	E	0.27	0.05	0.25	0.62
	AIC	32.11	31.59	31.50	32.00
S_{max} (mg g^{-1})	**Value**	16.62	15.75	16.96	23.16
	S.E.	2.64	2.56	2.94	5.62
K (L mg^{-1})	**Value**	0.25	0.26	0.15	0.04
	S.E.	0.30	0.34	0.16	0.04

Table 4.16: Freundlich parameters and goodness of fit for Acomb ochre in the presence of competing ions derived from model runs (2 d.p).

		pH			
		4	**5**	**6**	**7**
Goodness of fit	**SSE**	8.22	6.83	5.77	23.24
	E	0.77	0.69	0.83	0.86
	AIC	32.49	31.56	30.72	26.12
K_f	**Value**	7.72	8.73	7.13	5.64
	S.E.	1.79	1.85	1.52	1.72
n	**Value**	0.16	0.12	0.17	0.25
	S.E.	0.05	0.05	0.05	0.07

To assess whether the presence of competing ions has affected the P adsorption capacity of Acomb ochre, a two-tailed t-test was utilised to compare S_{max} and K_f calculated in these experiments with that in the P adsorption batch experiments.

P adsorption capacity (K_f), determined by fitting the Freundlich isotherm in the presence of competing ions, is lower for all pH values than was found in the P adsorption batch experiments (Chapter 4.2). There is only a statistical difference for the two sets of data at pH 4, however, where the P adsorption capacity is significantly lower in the presence of competing ions (Table 4.17). In contrast, S_{max} calculated from the Langmuir isotherm is higher at each pH than for the P adsorption batch experiment, although not to a statistically significant level.

Table 4.17: Summary statistics for t-tests comparing P adsorption capacity for Acomb ochre in batch experiments conducted with and without competing ions. *indicates that the test result is statistically significant ($p<0.05$). df (degrees of freedom) was calculated from the combined number of derived data points used to calculate the adsorption isotherms for each pH condition minus 2 (n+n-2).

P adsorption isotherm	t-test result	pH			
		4	**5**	**6**	**7**
Langmuir (S_{max})	t value	0.36	0.29	0.88	1.81
	df	10	10	10	10
	Two-tailed P value	0.73	0.77	0.44	0.10
Freundlich (K_f)	t value	2.38	1.56	2.19	1.50
	df	8	8	8	10
	Two-tailed P value	**0.05***	0.16	0.06	0.17

Whilst the results of fitting the Langmuir isotherm indicate that the presence of competing ions does not reduce the P adsorption capacity of Acomb ochre, the Freundlich isotherm, which has a better fit, suggests that the presence of competing

ions reduces the P adsorption capacity of the ochre, but only significantly at pH 4 ($p=0.045$).

4.3.2 Polkemmet ochre

From the P adsorption batch experiments, P removal by Polkemmet ochre was found to be independent of pH, with P removed ~11 mg P g^{-1} between pH 3.5 and 6. In the presence of competing ions there is no clear relationship between P removal and pH for Polkemmet ochre from the experimental results. A slight negative relationship is apparent for the two lowest P additions, however (Figure 4.29). A gap is evident in the data between pH 4 and 6. Batch experiments prepared at a pH equilibrium of 3 drifted to pH ~4 following the P addition, and experiments prepared with a pH equilibrium of ~4.5 drifted to pH 6 following P addition.

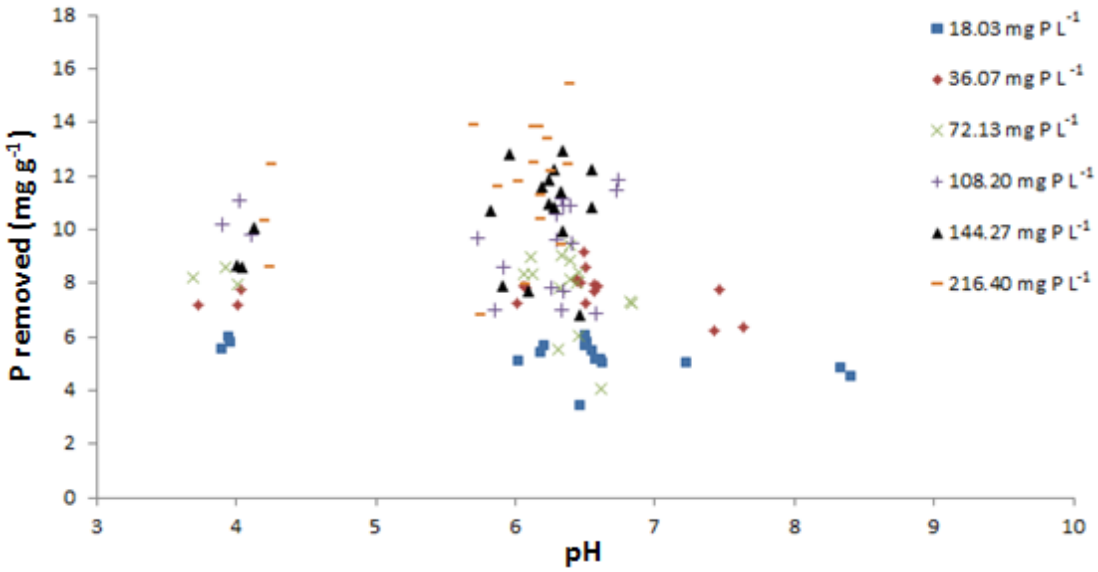

Figure 4.29: P removal by Polkemmet ochre in the presence of competing ions dataset. Each replicate is shown as a separate data point.

The dataset for each P addition was fitted with trend lines to determine the relationship between P adsorbed and pH (Figure 4.30). Whilst the goodness of fit for these trend lines is low (R^2 = 0.21-0.41), they still represent the data well and were therefore used to calculate P removed by Polkemmet ochre in the presence of competing ions between pH 4.5 to 6.

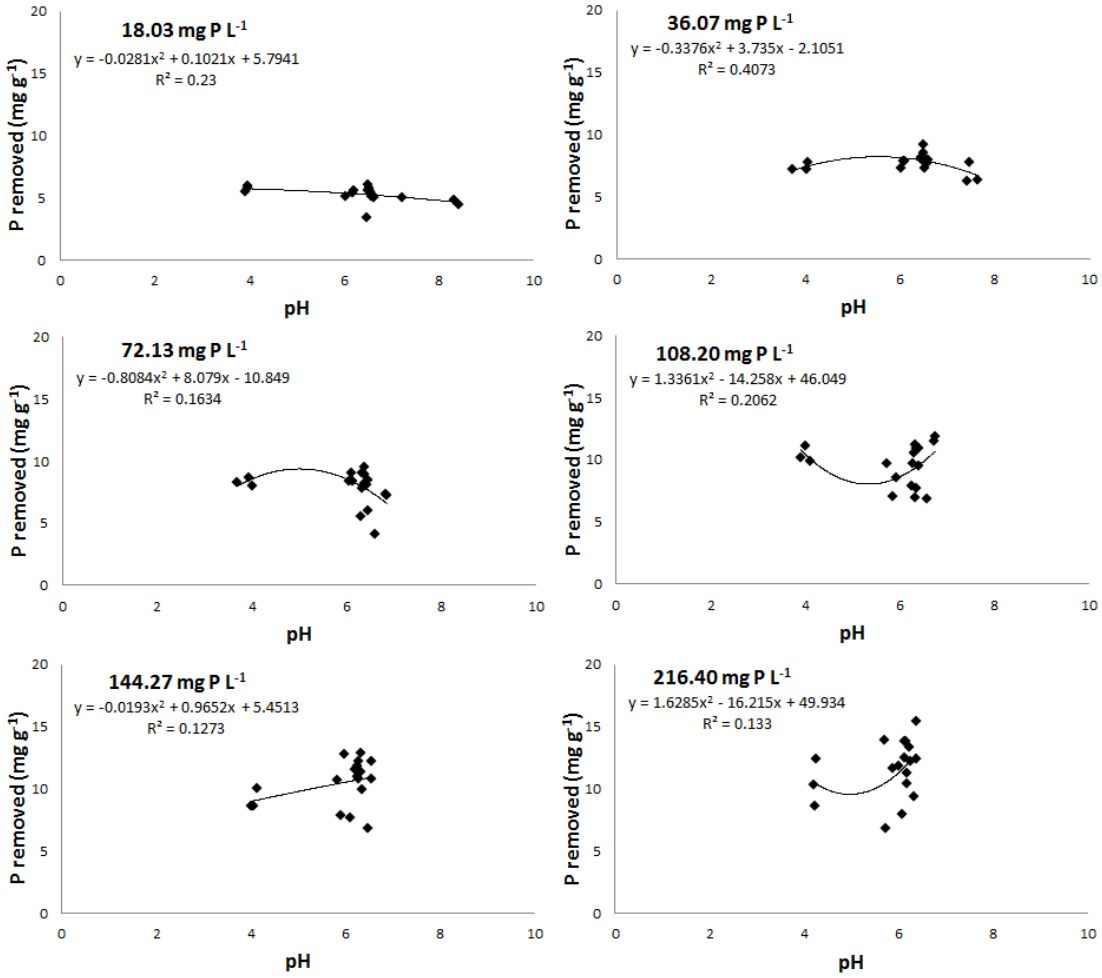

Figure 4.30: Curve fitting to P removed by Polkemmet ochre over a range of pH in the presence of competing ions. Data sorted by P addition.

Langmuir and Freundlich isotherms were fitted to the data generated from the trend lines (Figure 4.31, Table 4.18 and Table 4.19). The overlap of the P adsorption isotherms indicates that P adsorption by Polkemmet ochre is not pH dependant. In the P adsorption batch experiment the Freundlich isotherm provided a better fit to the data between pH 3.5 to 4, with the Langmuir isotherm giving a better fit between pH 4.5 to 6 (Chapter 4.2.5.6). In the presence of competing ions, the Freundlich isotherm provides a better fit for P adsorption for all pH values investigated (except pH 5.0) based on the AIC values calculated. The model

efficiency (E) was high at all pH values for both adsorption isotherms. The lowest value (0.73) corresponds to the fitting of the Langmuir isotherm at pH 6.0.

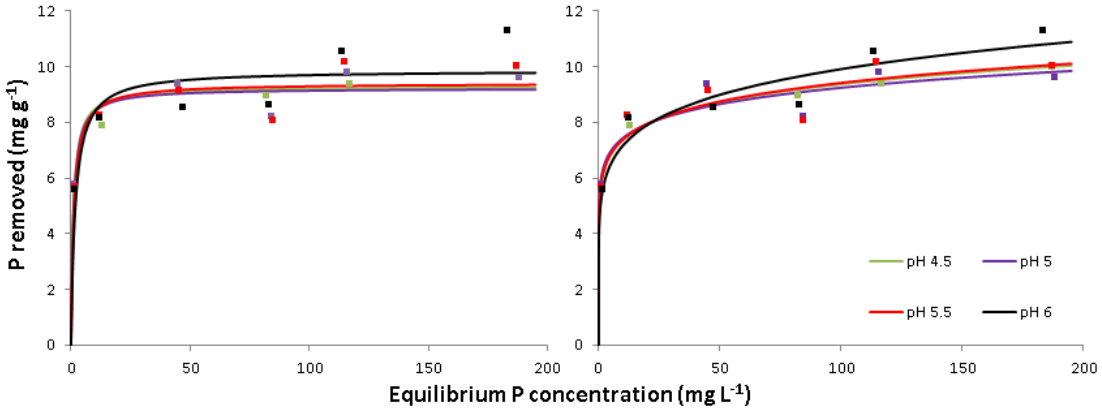

Figure 4.31: P adsorption isotherms for Polkemmet ochre in the presence of SynS: Langmuir (L) Freundlich (R)

There is no apparent relationship between pH and P adsorption capacity (S_{max}, K_f) as was noted in the P adsorption batch experiments with Polkemmet ochre. In the presence of competing ions, S_{max} was highest at pH 6.0 (9.87 mg P g^{-1}) and lowest at pH 5.0 (at 9.23 mg P g^{-1}), whilst the highest value of K_f was 5.98 at pH 5.0 and the lowest was 5.18 at pH 6.0.

Table 4.18: Langmuir parameters and goodness of fit for Polkemmet ochre in the presence of competing ions derived from model runs (2 d.p).

		pH			
		4.5	**5.0**	**5.5**	**6.0**
Goodness of fit	**SSE**	1.26	1.74	2.78	5.34
	E	0.89	0.85	0.80	0.73
	AIC	8.66	10.56	13.39	17.30
S_{max} (mg g^{-1})	**Value**	9.29	9.23	9.41	9.87
	S.E.	0.28	0.33	0.42	0.60
K (L mg^{-1})	**Value**	1.05	1.03	0.83	0.57
	S.E.	0.28	0.33	0.32	0.28

Table 4.19: Freundlich parameters and goodness of fit for Polkemmet ochre in the presence of competing ions derived from nonlinear runs (2 d.p).

		pH			
		4.5	**5.0**	**5.5**	**6.0**
Goodness of fit	**SSE**	0.47	2.19	2.69	2.27
	E	0.96	0.81	0.80	0.89
	AIC	2.74	11.96	13.19	12.13
K_f	**Value**	5.83	5.98	5.79	5.18
	S.E.	0.29	0.64	0.71	0.63
n	**Value**	0.10	0.09	0.11	0.14
	S.E.	0.01	0.03	0.03	0.03

The results of statistical comparison of the S_{max} and K_f values for Polkemmet ochre derived from bath experiments with and without competing ions are shown in Table 4.20. The P adsorption capacity of Polkemmet ochre determined from fitting the Langmuir isotherm was significantly lower at pH 4.5 and 5.0 in the presence of competing ions than in the original P adsorption batch experiments (Chapter 4.2.5.6). In contrast, P adsorption capacity determined using the Freundlich isotherm was significantly higher in the presence of competing ions at pH 4.5 ($p = 0.05$). This only occurred at this pH however.

Table 4.20: Summary statistics for t-tests comparing P adsorption capacity for Polkemmet ochre in batch experiments conducted with and without competing ions. *indicates that the test result is statistically significant ($p<0.05$). df (degrees of freedom) was calculated from the combined number of derived data points used to calculate the adsorption isotherms for each pH condition minus 2 (n+n-2).

P adsorption isotherm	t-test result	pH			
		4.5	**5.0**	**5.5**	**6.0**
Langmuir (S_{max})	t value	3.46	2.92	2.10	1.32
	df	10	10	10	10
	Two-tailed P value	**0.01***	**0.02***	0.06	0.22
Freundlich (K_f)	t value	2.27	1.86	1.82	1.79
	df	10	10	10	10
	Two-tailed P value	**0.05***	0.09	0.10	0.10

There is therefore some evidence that the presence of competing ions reduces the P adsorption capacity of Polkemmet ochre. There is also evidence to the contrary however. Overall, the Freundlich isotherm was found to be a better fit to the derived data in the presence of competing ions. For this isotherm, P adsorption capacity (K_f) was also higher in the presence of competing ions at all pH conditions, and significantly so at pH 4.5.

4.3.3 Acomb pellets

P removal by Acomb pellets in the presence of competing ions appears to have a similar, parabolic, relationship with pH as that described by the P adsorption batch experiments (Chapter 4.2.5.2). P removal is high at ~pH 3 and at higher pH conditions (Figure 4.32).

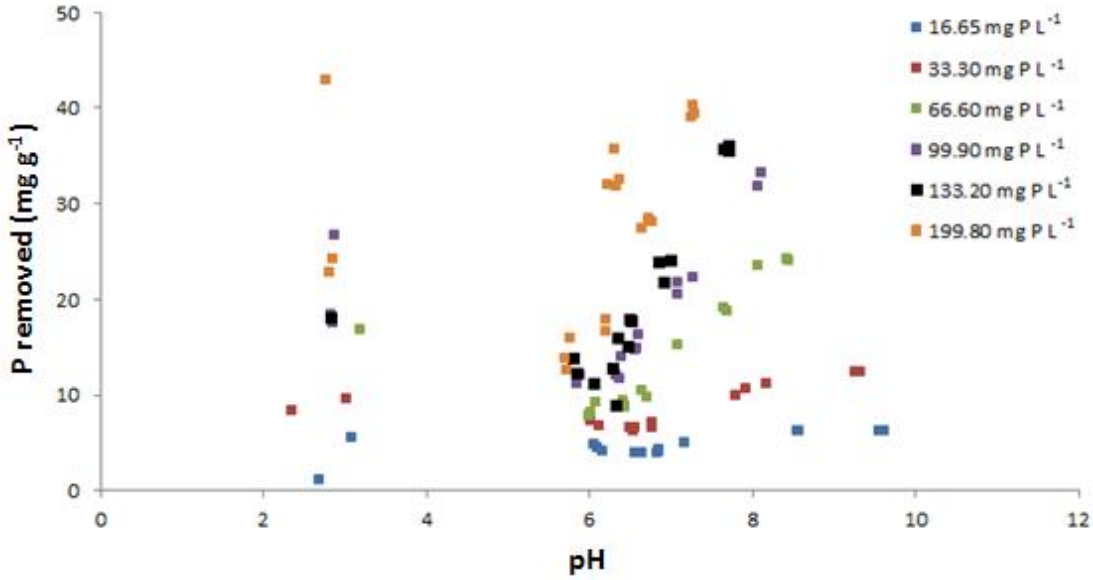

Figure 4.32: P removal by Acomb pellets in the presence of competing ions dataset. Each replicate is shown as a separate data point.

The data was sorted by P addition and fitted with trend lines to describe the relationship between P adsorbed and pH (Figure 4.33). The trend lines describe the datasets well. The lowest R^2 value is 0.57 for the 199.80 mg P L^{-1} addition, with R^2 ≥0.81 for all other P additions.

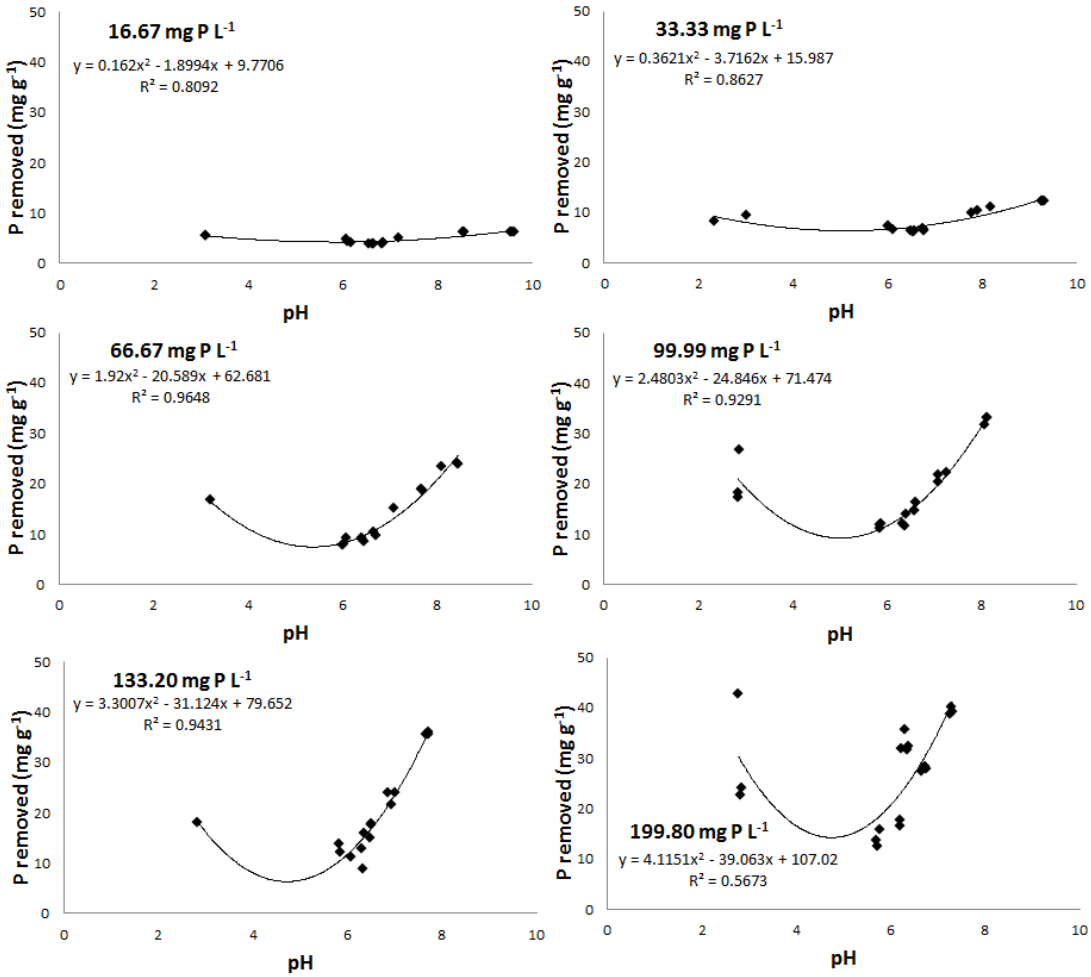

Figure 4.33: Curve fitting to P removed by Acomb pellets over a range of pH in the presence of competing ions. Data sorted by P addition.

The trend lines were utilised to calculate P removed by ochre at discrete pH conditions between pH 3 and 7, to which P adsorption isotherms were fitted (Figure 4.34). The adsorption isotherms have a similar shape to those from the P adsorption batch experiments, with P removal greatest under the highest and lowest pH conditions.

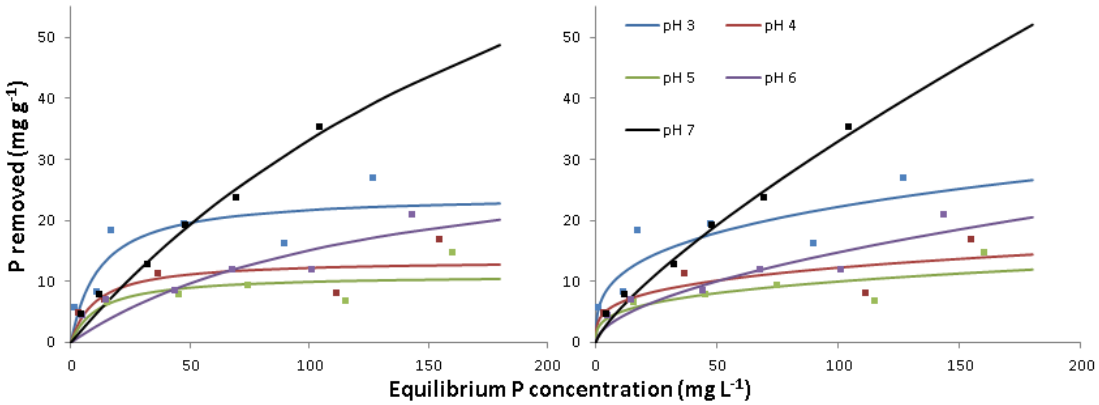

Figure 4.34: P adsorption isotherms for Acomb pellets in the presence of SynS: Langmuir (L) Freundlich (R)

In the presence of competing ions, the Freundlich isotherm provides a better fit to the dataset than the Langmuir isotherm as the AIC values are lower at all pHs (Table 4.21 and Table 4.22). This suggests that P adsorption occurs in a multilayer with adsorption sites having varying amounts of bonding energy. The model efficiency values (E) for the Freundlich isotherm are high, with the lowest value 0.60 at pH 5. SSE values for both models are highest at pH 3 and decrease with increasing pH. In contrast, a combination of the Langmuir and Freundlich isotherms best described the data from the P adsorption batch experiments for Acomb pellets.

Table 4.21: Langmuir parameters and goodness of fit for Acomb pellets in the presence of competing ions derived from model runs (2 d.p, values for K to 3 d.p).

		pH				
		3	**4**	**5**	**6**	**7**
Goodness of fit	**SSE**	85.95	37.42	32.75	36.86	14.66
	E	0.72	0.58	0.48	0.78	0.98
	AIC	33.97	28.98	28.18	28.89	23.36
S_{max} (mg g^{-1})	**Value**	24.27	13.49	11.09	34.40	117.85
	S.E.	4.61	2.57	2.42	20.81	55.13
K (L mg^{-1})	**Value**	0.084	0.095	0.085	0.008	0.004
	S.E.	0.065	0.087	0.088	0.008	0.002

Table 4.22: Freundlich parameters and goodness of fit for Acomb pellets in the presence of competing ions derived from model runs (2 d.p).

		pH				
		3	**4**	**5**	**6**	**7**
Goodness of fit	**SSE**	80.31	33.28	25.12	22.90	7.59
	E	0.74	0.63	0.60	0.86	0.99
	AIC	33.57	28.28	26.59	26.04	19.41
K_f	**Value**	5.43	3.48	2.47	1.13	0.92
	S.E.	2.59	1.80	1.57	0.73	0.24
n	**Value**	0.31	0.27	0.30	0.56	0.78
	S.E.	0.11	0.13	0.14	0.14	0.06

The presence of competing ions did not lead to a statistically significant decrease in the P adsorption capacity of Acomb pellets between pH 3 and 7, with the exception of S_{max} derived from the Langmuir equation at pH 5, where the adsorption capacity of ochre was significantly lower in the presence of competing ions (Table 4.23).

Table 4.23: Summary statistics for t-tests comparing P adsorption capacity for Acomb pellets in batch experiments conducted with and without competing ions. *indicates that the test result is statistically significant ($p<0.05$). df (degrees of freedom) was calculated from the combined number of derived data points used to calculate the adsorption isotherms for each pH condition minus 2 (n+n-2).

P adsorption isotherm	t-test result	pH				
		3	**4**	**5**	**6**	**7**
Langmuir (S_{max})	t value	1.07	1.54	2.38	0.01	1.35
	df	10	10	10	10	10
	Two-tailed P value	0.31	0.15	**0.04***	0.99	0.21
Freundlich (K_f)	t value	0.38	0.07	0.40	0.21	1.08
	df	10	10	10	10	10
	Two-tailed P value	0.70	0.94	0.70	0.84	0.30

4.4 The release of potentially toxic elements (PTEs)

Ochre is an aggregate of substances which have precipitated out of minewater and therefore it may contain PTEs. An important concern regarding the use of ochre as a filter substrate in the environment is whether PTEs can be remobilised and ochre itself becomes a point source of pollution. Consequently, the release of PTEs (As and Mg) and the major constituents of ochre (Al, Ca and Fe) into solution was monitored in the pH equilibrium batch experiments. Samples were taken after 30 minutes and at the end of the eleven day experiment. PTE release from selected ochres, Polkemmet ochre and Acomb pellets, was also examined in the P adsorption batch experiments, whereby the release of Al, As, Ca, Cu, Fe , Mn, Ni, Pb, and Zn was measured under three pH conditions.

4.4.1 pH equilibrium study

Two pH equilibrium experiments were run, a pilot lasting 30 minutes and a long term one over the course of 11 days (see Chapter 4.1 for the method). PTE release for all seven ochres was investigated for the above timescales: 30 minutes, a suggested application time for environmental application, and when the experiments had reached pH equilibrium, 11 days. Following the completion of the pH equilibrium studies, the tubes were centrifuged and the supernatant analysed by ICP-OES at the James Hutton Institute, Aberdeen, for the main constituents of ochre, Al, Ca, Fe and Mg, and As concentrations also analysed. The As concentration did not exceed the detection limits, 0.03 mg L^{-1} and is therefore not plotted. However, it should be noted that the World Health Organisation (WHO) drinking water standard has been revised to 0.01 mg L^{-1} (WHO, 2011) and thus more detailed analysis may be required of As-rich ochres prior to use in environmental applications.

4.4.1.1 Acomb ochre

The acid digest results (Chapter 3.4) reveal that Acomb ochre is largely comprised of Fe, 56.9 % by dry weight (D_{wt}) and 2.91 % Ca, with smaller amounts of Al and Mg, 0.328 % and 0.170 % D_{wt} respectively.

The largest elemental concentration in solution in both the 30 minute and pH equilibrium experiments was Ca (Figure 4.35). A negative correlation between Ca in solution and pH after thirty minutes exists. At pH equilibrium, a solubility edge can be noted for Ca, the concentration is constant at ~55 mg L^{-1} between pH 3-7, before dropping sharply to 5 mg L^{-1} at pH 9. Under equilibrium conditions, Mg shows a similar trend to Ca, with the concentration in solution relatively constant between pH 3-6 at ~0.65 mg L^{-1}, before decreasing to 0 mg L^{-1} at pH 8. Fe concentrations in solution are low after 30 minutes <pH 4, increasing with acidity to 0.63 mg L^{-1} at pH 2.89. At pH equilibrium, the Fe concentration in solution at pH 3 is almost 7 mg L^{-1}, but decreases sharply with pH, with no Fe in solution at pH>5. Al concentrations above the detection limit, 0.01 mg L^{-1}, were only detected at pH 3 and below in the equilibrium experiment.

Targeted wastewaters are expected to have a pH between 6 and 8; across this range, Fe and Al will not be released into solution. Mg may be released into solution, especially if pH is less than 7 whilst Ca will be released into solution, with the amount released dependent upon pH.

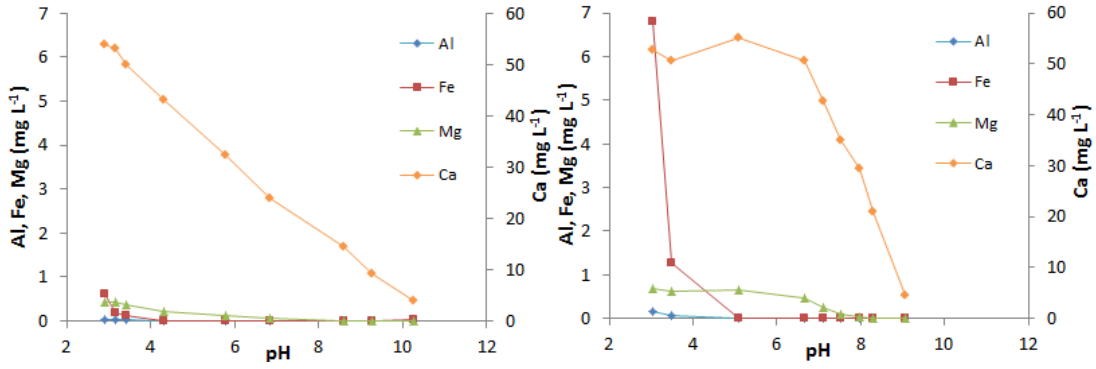

Figure 4.35: Al, Ca, Fe and Mg released into solution from Acomb ochre; data points are the mean of triplicate experiments: Solution concentration after thirty minutes (L), and at pH equilibrium (R).

4.4.1.2 Acomb pellets

Acomb pellets have a higher concentration of Al, Ca and Mg in its composition and a lower concentration of Fe than Acomb ochre (Chapter 3.4). The release of Ca was the highest concentration in solution of these four elements in both the 30 minute and pH equilibrium study. As with Acomb ochre, Ca is rapidly released into solution over the initial 30 minute study, with a positive relationship between acidity and Ca concentration (Figure 4.36). Increased amounts are released into solution at equilibrium; at pH 6 after 30 minutes Ca concentration was ~100 mg L^{-1}, rising to 200 mg L^{-1} at equilibrium.

Fe was measured in solution in detectable concentrations at pH<4; 0.689 mg L^{-1} at pH 3.6 after 30 minutes. Fe was recorded in solution during the pH equilibrium experiment, though the pH of the final solution did not reach pH condition less than 5.7. Similar to this, Al was only recorded in solution below pH 5. The high Al concentration in solution below pH 4 after 30 minutes, 10-22 mg L^{-1}, does not occur for Acomb ochre. This suggests Al released into solution is a result of the addition of calcium alumina-silicates during the pelletisation process. Al concentration in solution increases as pH tends to acidic conditions. The pelletisation process also results in the pellet composition having a higher concentration of Mg which is released into solution, with ~4 mg Mg L^{-1} at pH 6 after 30 minutes, approaching 20 mg L^{-1} at equilibrium.

The release of Ca and Mg from Acomb pellets is high between pH 6 to 8. Therefore if Acomb pellets were used to treat P enriched waters, Ca and Mg would be released into the system.

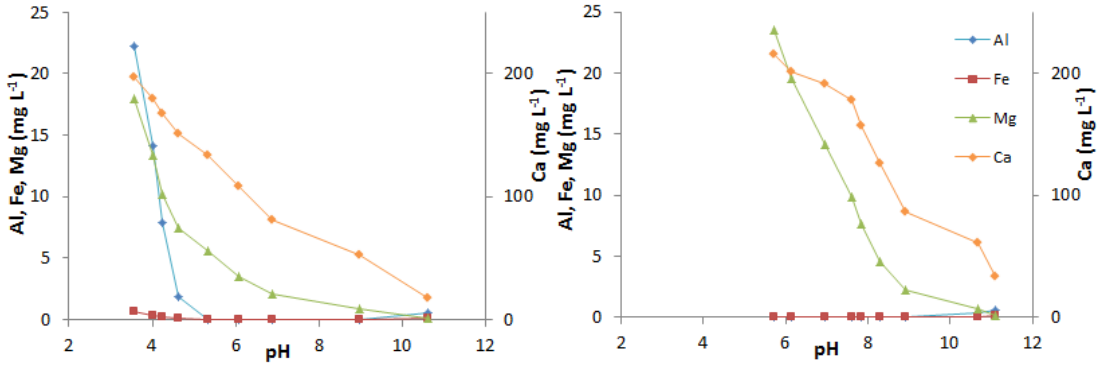

Figure 4.36: Al, Ca, Fe and Mg released into solution from Acomb pellets; data points are the mean of triplicate experiments: Solution concentration after thirty minutes (L), and at pH equilibrium (R).

4.4.1.3 Minto ochre

The acid digest determined Minto ochre contains 60.9 % Fe and 1.27 % Ca D_{wt}, with smaller amounts of Mg and Al, 0.552 and 0.169 %. The release of these elements into solution follow similar trends as noted for Acomb ochre. After 30 minutes, high Ca concentrations were measured in solution, with a negative relationship between Ca concentration and pH (Figure 4.37). Below pH 5.5, more Ca was found in solution in the 30 minute experiment than at pH equilibrium. At equilibrium, the Ca concentration of the overlying solution was found to be ~ 10 mg L^{-1} between pH 3 and 7 and declined with increasing pH.

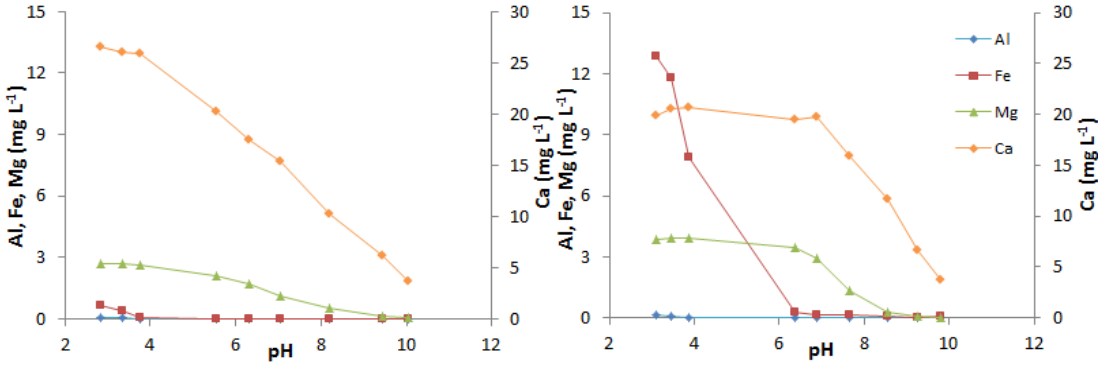

Figure 4.37: Al, Ca, Fe and Mg released into solution from Minto ochre; data points are the mean of triplicate experiments: Solution concentration after thirty minutes (L), and at pH equilibrium (R).

Whilst low Fe concentrations are detected after 30 minutes below pH 4, these increase greatly at pH equilibrium with Fe concentrations > 12 mg L^{-1} detected below pH 4. Mg concentration is fairly constant at pH equilibrium at around 3.5 mg L^{-1} between pH 3-6, declining to undetectable concentrations between pH 6 and 9. The majority of Mg released is in solution after 30 minutes, showing that it is rapidly mobilised under these pH conditions. Al was only found in solution at very low pH and at just above the detection limits for both experiments.

Between pH 6 and 8, the expected conditions of targeted P enriched waters, no Al or Fe is released into solution but Ca and Mg are rapidly mobilised and released into solution.

4.4.1.4 Silkstone ochre

The acid digest revealed that Silkstone ochre has the lowest Mg concentration, 0.170 % D_{wt}, and a comparatively low concentration of Fe, 41.0 %, to the other ochres under study. The ochre also contains 0.442 % Ca and 0.468 % Al D_{wt}.

Ca is rapidly released into solution from Silkstone ochre with almost all the Ca in solution at pH equilibrium released in the 30 minute experiment, indicating the rapid rate of Ca solubilisation from the ochre (Figure 4.38). During the 30 minute experiment, Fe was detected in solution at low pH, exceeding 1 mg L^{-1} at ~pH 3. A similar result was noted for Acomb and Minto ochres, though at equilibrium these ochres release higher Fe concentrations into solution. This did not occur for Silkstone ochre where the Fe concentration decreased at equilibrium.

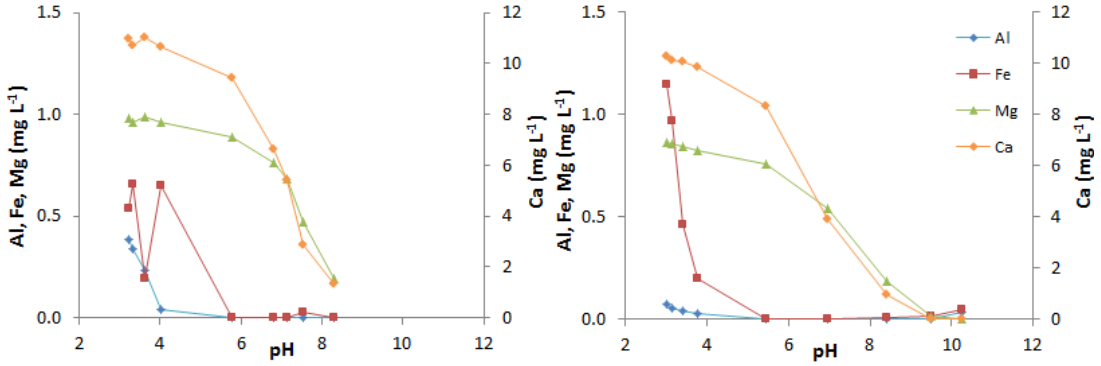

Figure 4.38: Al, Ca, Fe and Mg released into solution from Silkstone ochre; data points are the mean of triplicate experiments: Solution concentration after thirty minutes (L), and at pH equilibrium (R).

Mg is rapidly released into solution from Silkstone ochre, with the majority of Mg released under acidic conditions in solution after 30 minutes. At pH equilibrium, a solubility curve is apparent, with Mg concentration in solution declining gradually between pH 3 and 7 from 1 to 0.8 mg L^{-1}. Under alkaline conditions, Mg concentration declines rapidly approaching 0 mg L^{-1} by pH 9. Low Al concentrations occur in solution below pH 4 and above pH 10 during the 30 minute experiment. Lower Al concentrations were detected at equilibrium and, due to a drift in pH over the course of the experiments, the Al concentration at pH conditions higher than 8.3 is unknown.

Silkstone ochre has a relatively high As content, 0.0119 % D_{wt}, and the potential release of As is a potential barrier to the application of ochre in the natural environment. Throughout both the 30 minute and pH equilibrium experiments, As in solution did not exceed the detection limit, 0.03 mg L^{-1}. The adsorption behaviour of As onto Fe-oxides (Dixit and Hering, 2003) is similar to P. Therefore under neutral to acidic conditions the release of As into solution would not be expected. Any As desorption would predominantly occur under alkaline conditions, but concentrations above the detection limit were not measured.

Between pH 6 and 8, the conditions expected of P enriched waters, Al and Fe concentrations were not found above the detection limit, whilst relatively low concentrations of Ca and Mg were found in solution between pH 6 and 8, declining with increasing pH.

4.4.1.5 Polkemmet ochre

Of the ochres examined, Polkemmet contains the second most Al, 3.40 % D_{wt}, after Acomb pellets. The ochre also contains 44.6 % Fe, 0.963 % Ca and 0.461 % Mg, determined by acid digest (Chapter 3.4). As with the other ochres, Ca is released rapidly in the thirty minute experiment into solution under acidic pH and has by the far the highest concentration of the four elements in solution (Figure 4.39). At pH equilibrium, the Ca concentration in solution has increased at neutral pHs, producing a solubility curve with a similar shape to that observed for other ochres, such as Minto and Acomb.

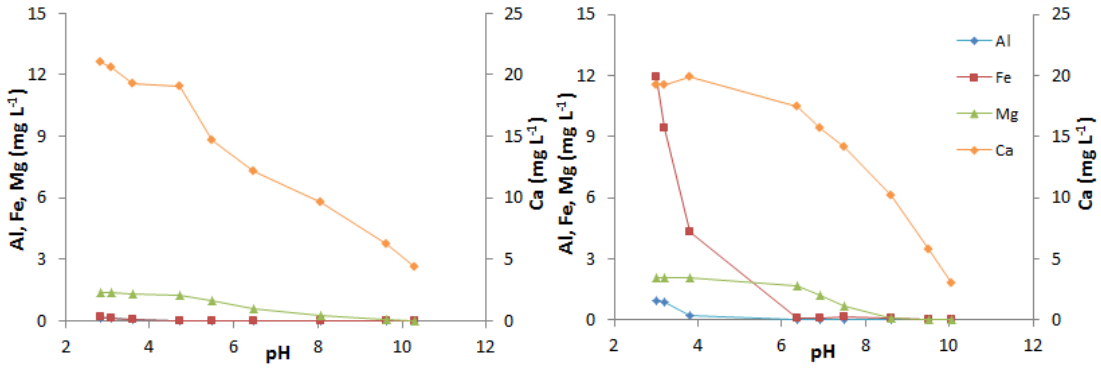

Figure 4.39: Al, Ca, Fe and Mg released into solution from Polkemmet ochre; data points are the mean of triplicate experiments: Solution concentration after thirty minutes (L), and at pH equilibrium (R).

The release of Fe and Mg from Polkemmet ochre in both the thirty minute and pH equilibrium experiment is similar to Acomb ochre. Very little Fe is present in solution after thirty minutes, with high concentrations of Fe present in solution at pH equilibrium under acidic conditions; 11.9 mg L^{-1} at pH 3.0. Mg is rapidly released into solution, with over half the Mg in solution at pH equilibrium present

after thirty minutes. At pH equilibrium, Mg concentration is relatively constant between pH 3-6 at 2 mg L^{-1}. Above pH 6 a near linear decline in Mg concentration occurs to less than the detection limit by pH 9.

Al was not detected during the thirty minute experiment, but was recorded in solution at pH equilibrium at highly acidic pH conditions, reaching 0.963 mg L^{-1} at pH 3.0. Between pH 6 and 8, conditions typical of P enriched waters, Fe and Al is not expected to be released into solution. The Mg concentration is highly variable across this pH range, decreasing from ~2 mg L^{-1} at pH 6 to ~0.3 mg L^{-1} at pH 8. Ca will also be released into solution, with the amount dependent upon the pH of the systems, with a negative relationship between pH and Ca solubility.

4.4.1.6 Ynysarwed ochre

Ynysarwed ochre contains a much higher Mg concentration, 34.4 % D_{wt}, in its composition than the other ochres under study. With the exception of Acomb pellets, Ynysarwed ochre contains the lowest Fe concentration of the ochres studied, 31.8 % D_{wt}. The ochre also contains 0.627 % Al and 1.56 % Ca.

For Ynysarwed ochre, Mg was detected in solution at the highest concentrations, rather than Ca as was the case for the previous five ochres in this study. Mg was released rapidly into solution over the initial thirty minutes of the study, with a negative relationship between pH and concentration (Figure 4.40). At pH equilibrium, the Mg concentration in solution declines gradually between ~pH 3-8 from 110 mg L^{-1} to 100 mg L^{-1}, before dropping sharply approaching 0 mg L^{-1} at pH 10.

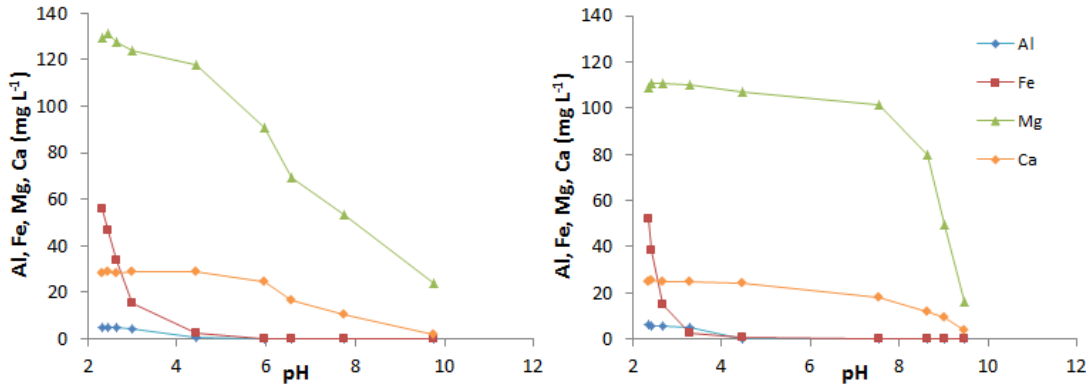

Figure 4.40: Al, Ca, Fe and Mg released into solution from Ynysarwed ochre; data points are the mean of triplicate experiments: Solution concentration after thirty minutes (L), and at pH equilibrium (R).

Al, Ca and Fe are all released rapidly into solution, with little difference in concentration between the thirty minute experiment and pH equilibrium. Very low amounts of Fe and Al are found in solution above pH 4.

Ynysarwed ochre was chosen for study due a high As concentration; 0.0746 % D_{wt} (Hancock, 2004), with the As content determined as 0.0554 % D_{wt} in this study (Chapter 3.4). Arsenic concentrations did not exceed the detection limit, 0.03 mg L^{-1}, during the thirty minute experiment or at pH equilibrium. It is therefore not expected that the application of Ynysarwed ochre will lead to the pollution of wastewaters with As.

Between pH 6 and 8, conditions typical of P enriched waters, Ynysarwed ochre releases a large amount of Mg into solution along with a smaller concentration of Ca. Very little Al or Fe will be released into solution in this pH range. This release of Mg into the overlying solution may prohibit the use of Ynysarwed ochre for environmental applications.

4.4.1.7 Avoca ochre

The acid digest conducted on Avoca ochre revealed it has the lowest Ca content of the ochres under study, 0.0577 % D_{wt}. Avoca ochre is 50.3 % Fe, with smaller amounts of Al, 0.715 %, and Mg, 0.360 %.

The release of Ca into solution in both the thirty minute and pH equilibrium experiments is far lower than for any of the other ochres (Figure 4.41). This is due to the low amount of Ca in the ochre composition. During the thirty minute experiment, Fe was detected in solution at pH 4 and below and also above pH 10. The pH equilibrium experiment did not have any trials above pH 7.5, thus only the release of Fe under acidic pH can be compared. The Fe content of the overlying solution can be seen to rise rapidly with decreasing pH up to 2.48 mg L^{-1} at pH 2.74. Al is detected in solution for both experiments below pH 4 and at pH 11 in the thirty minute trial. Mg enters into solution rapidly with the concentrations after thirty minutes matching those at pH equilibrium closely.

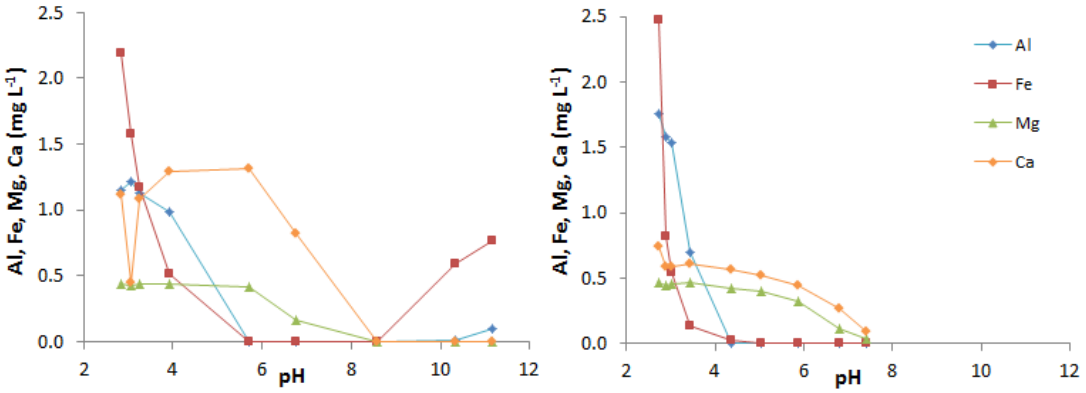

Figure 4.41: Al, Ca, Fe and Mg released into solution from Avoca ochre; data points are the mean of triplicate experiments: Solution concentration after thirty minutes (L), and at pH equilibrium (R).

Avoca was selected for research due to its high As content, determined as 0.0162 % D_{wt} (Fenton et al., 2009) and 0.0257 % D_{wt} in this study (Chapter 3.4). Arsenic

concentrations were not measured above the detection limit, 0.03 mg L^{-1}, for any of the samples taken in the thirty minute or pH equilibrium experiments.

Of all the ochres under study, Avoca releases the lowest concentrations of Al, Ca, Fe and Mg into solution between the pH range 6-8, with only small amounts of Mg and Ca being released into solution. On the basis of this, Avoca would be preferential to the other ochres under study for use under environmental applications.

4.4.2 PTE release during P adsorption batch experiments

PTE concentrations were determined in selected samples from the P adsorption batch experiment. Polkemmet ochre and Acomb pellets were chosen as they are the most likely candidates for use in full-scale filters due to their coarse particle size distributions. Three target pHs were examined, acidic (pH 2.5-3), neutral (pH 7-7.5) and alkaline (pH 10.5-11), with all six P additions tested in duplicate. Following the centrifuging of batch experiments, the sample was split into two, half of which was analysed for P concentration (Chapter 4.2) with the other half analysed for PTEs: Al, As, Cu, Fe, Mn, Ni, Pb and Zn and the major constituents of ochre Ca and Mg by ICP-OES. Samples were stored at 4^{o}C and analysed within two weeks of collection.

4.4.2.1 Aluminium, Calcium, Iron and Magnesium

As with the release of these four elements from ochre during the pH equilibrium experiment, the largest release occurred under acidic conditions, with a decline in solubility with increasing pH (Figure 4.42). For Polkemmet ochre, Ca concentration in solution is high in comparison to the other elements, although it is lower in the P adsorption batch experiment than the pH equilibrium experiment at all pHs.

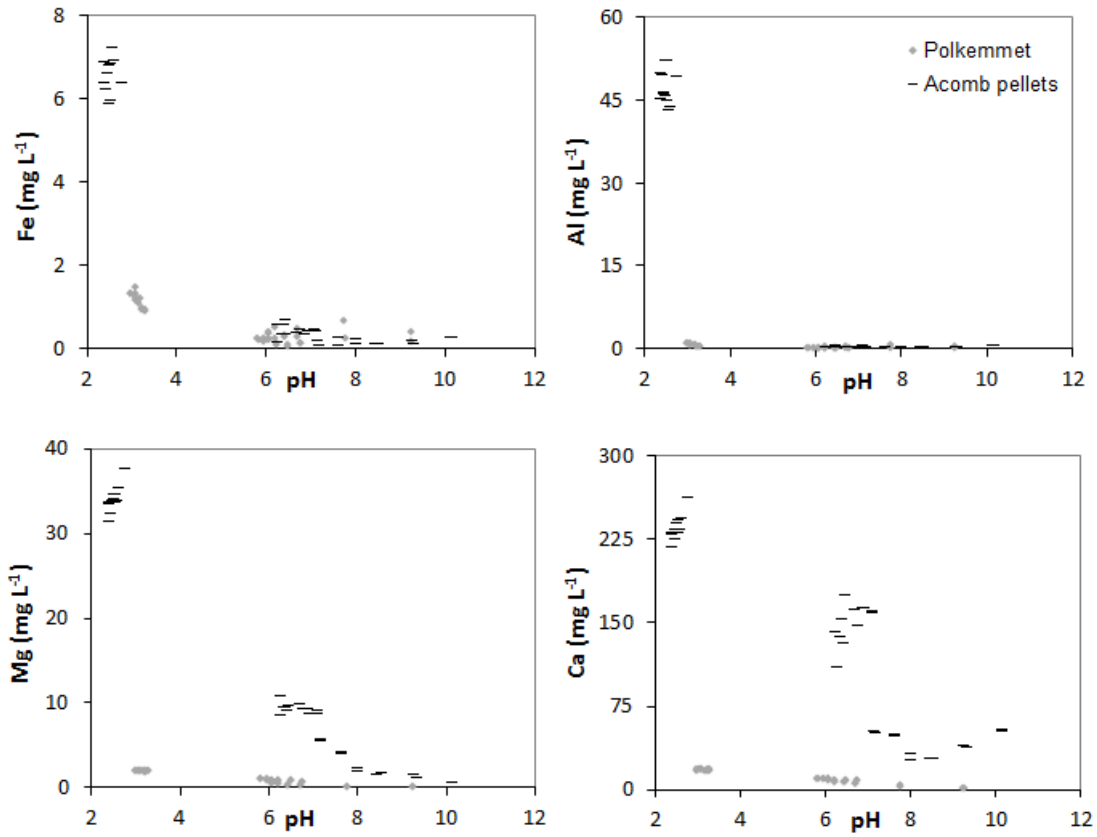

Figure 4.42: The concentration of Fe, Al, Mg and Ca in solution at the completion of P adsorption batch experiments.

For Acomb pellets, a comparison cannot be made with the pH equilibrium experiment results for acidic conditions as pH conditions only down to ~pH 6 were achieved in the experiment, though for pH 7 the concentration of Ca in solution for the P adsorption batch experiments is lower, possibly due to the precipitation of Ca-P out of solution. This effect is not apparent under alkaline conditions, where the Ca concentration is higher in the pH equilibrium experiment.

Al concentrations exceed WHO (2011) guidelines, 0.1 mg L^{-1}, under acidic conditions, however Al concentrations were below the detection limits of the analytical equipment, 0.01 mg L^{-1}, for the experiments with pH conditions >6, and thus should not cause an issue for the treatment of wastewater streams with a pH between 6 and 8.

4.4.2.2 Manganese and Zinc

The largest concentrations of Mn occurred under acidic conditions, ~1.8 and 0.25 mg L^{-1}, for Acomb pellets and Polkemmet ochre, respectively, with much lower concentrations released under neutral and alkaline pH conditions (Figure 4.43). A pH dependant relationship can also be seen for Zn, with concentrations increasing as pH decreases.

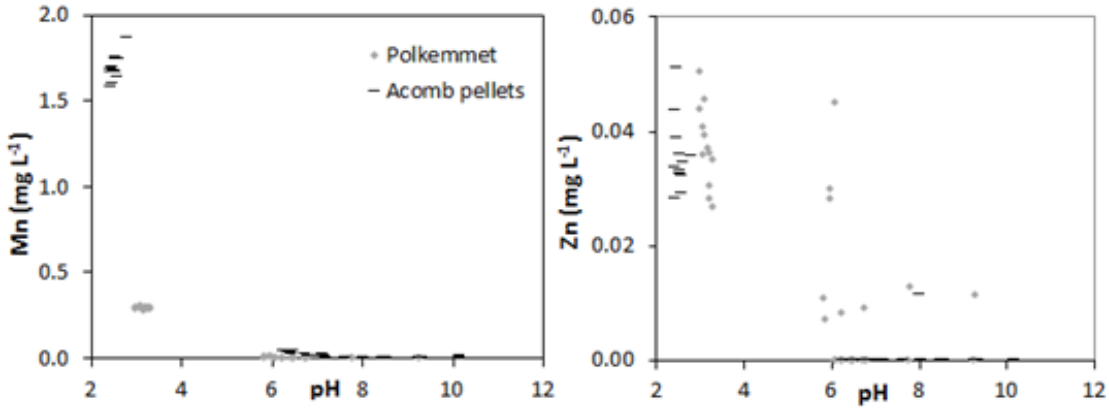

Figure 4.43: The concentration of Mn and Zn in solution at the completion of P adsorption batch experiments.

4.4.2.3 Arsenic, Copper, Nickel and Lead

Concentrations of As and Ni did not exceed the detection limits of 0.03 and 0.09 mg L^{-1}, respectively, in any of the samples. Concentrations of Cu and Pb also rarely exceeded the detection limits of 0.04 and 0.02 mg L^{-1}, respectively, except on two occasions in acidic conditions when concentrations were just above the detection limits. None of these PTEs were detected in solution between pH 6 and 8, the conditions typical of P enriched waters.

4.5 Summary Discussion

The P removal capacity of ochre was found to vary both with ochre type and with the pH conditions at which it was determined. Whilst the P adsorption capacity of some of the ochres varied little with pH, such as for Acomb ochre (12.77-15.51 mg P g^{-1} between pH 4-9), it declined with increasing pH for other ochres e.g. Avoca and Ynysarwed ochre, and had a parabolic relationship with pH for Acomb pellets.

The mechanisms of P removal also vary with ochre type and for different pH conditions. Values of Langmuir K were semi-quantitatively analysed, with low values at high pH conditions suggesting adsorption onto surfaces of calcite, whilst high values suggest adsorption reactions onto high affinity sites such as Al- Fe-hydroxides. It is also suggested that Ca-P minerals may form in some of the batch experiments at the higher P additions, such as the experiments utilising Acomb pellets, which have a high Ca content. The P removal mechanisms occurring in the batch experiments will be examined in greater detail in Chapter 5 by modelling the observed datasets in a chemical model.

For the treatment of wastewaters, ochres with a high P adsorption capacity over the intended pH range of treatment (to maximise filter lifespan) and a high affinity for P are preferable. Based upon these criteria, Silkstone and Avoca ochres are suggested for use to treat P enriched waters. Both have a relatively high P adsorption capacity at pH 6 and 7, with associated high values of Langmuir K.

The effect of competing ions on P removal was investigated in Chapter 4.3 for three ochres: Acomb ochre, Acomb pellets and Polkemmet ochre. Competing ions in the SynS solution include weakly adsorbing sulphate and organic forms of P. Therefore the presence of these ions in solution should not be expected to have a large impact on P adsorption by the experiments. In the presence of competing ions, the Freundlich isotherm fitted the datasets better, suggesting adsorption is occurring in a multilayer. The presence of competing ions does not statistically reduce P

adsorption capacity for the ochres, but in some cases led to a significant increase in P adsorption capacity. This may suggest that competing ions are adsorbing onto the surface of the ochre, and are providing adsorption sites for P removal.

The release of the major components of ochre, and the PTE As, into solution was investigated in Chapter 4.4. Between the pH range expected of potential environmental application (pH 6-8) Ca and Mg were released into solution for most of the ochres, with concentrations declining with increasing pH. Arsenic was not measured in solution for any of the ochres above the detection limit, however. Whilst detected at lower pH conditions, Al was not in solution between pH 6-8.

P adsorption batch experiments using Acomb pellets and Polkemmet ochre were also investigated for the release of the major constituents of ochre and PTEs into solution. These results mirrored those above, with Ca and Mg released into solution between pH 6-8. Of the PTEs, only Zn was detected in solution above the analytical detection limit between pH 6-8 (0.01 mg L^{-1} for both ochres).

Whilst improvements can be made to the P adsorption batch experiment methodology, the results of the experiment indicate the importance of calculating P adsorption capacity of materials at a range of pH conditions. One such improvement would be to alter the pH of the P addition to that of the batch experiment to minimise the drift in pH conditions of the experiments from those that were targeted. The scale of the experiments could also be increased so that a larger, and potentially more representative, sample of ochre is utilised in the experiments. This may help reduce any variability that was observed in the datasets in this Chapter.

Chapter 5
Chemical modelling of the P adsorption batch experiments

Fitting adsorption isotherms to the P adsorption batch experiments (Chapter 4) indicated the P adsorption capacity of the seven ochres under study as well as the potential sorption mechanisms that are occurring. Chemical equilibrium and speciation models can be utilised to better understand the processes and P removal mechanisms occurring within a particular system.

A diffuse double layer model (also known as the generalized two layer model) was utilised for the modelling of the P adsorption batch experiments. The model used was developed by Dzombak and Moral (1990) to describe adsorption onto the surfaces of hydrous ferric oxide, which is expected to be the dominant P removal mechanism of the Fe-rich ochres in this study. The modelling software ORCHESTRA (Objects Representing Chemical Speciation and Transport models) was utilised to create a model for each ochre to describe P removal from solution.

5.1 Modelling approach

Three main types of reaction are responsible for the removal of P at the solid solution interface; adsorption, precipitation and absorption (Haworth, 1989). The interpretation of batch experiments to indicate which of these mechanisms is responsible for observed P removal requires a modelling approach. In Chapter 4 two empirical models, the Langmuir and Freundlich equations were utilised to describe the removal of P from solution by the ochres. The results broadly indicated adsorption reactions occurring onto high affinity sites under low pH conditions and adsorption onto low affinity sites occurring in some of the ochres at high pH conditions. Precipitation reactions may also occur in batch experiments containing ochres with high Ca contents at high P additions. Whilst empirical models can be used indicatively, they lack theoretical basis (Goldberg, 1995). Alternatively,

chemical models provide a molecular description of the adsorption of a system using an equilibrium approach.

In surface complexation models (SCM), adsorbing ions in solution are considered to react chemically with surface groups on the solid phase. For hydrous oxide minerals, the surface sites are hydroxyls, represented by ≡S-OH^0 in model nomenclature, where ≡S represents the adsorbing species e.g. Fe (Lumsdon, 1995). The protonation reactions of surface groups account for the development of surface charge and are most commonly represented in SCM as the dissociation of a diprotic acid site (Davis and Kent, 1990., Lumsdon, 1995). Thus, when a surface is in water, three surface sites can be present: ≡S-OH_2^+, ≡S-OH^0 and ≡S-O^-, with the proton dissociation constants represented by Equation 5.1 and 5.2.

$$\equiv SOH_2^+ \leftrightarrow \equiv SOH^0 + H^+ \qquad \text{Equation 5.1}$$

$$\equiv SOH^0 \leftrightarrow \equiv SO^- + H^+ \qquad \text{Equation 5.2}$$

Where ≡S is a metal ion surface site, and H^+ relates to the proton activity of the bulk solution (Lumsdon, 1995).

SCM aim to characterise adsorption at surface sites by accounting for chemical and electrostatic interactions (Haworth, 1989). SCM have many similarities with techniques utilised for solving complex equilibria problems, primarily that the reactions which describe the formation of surface species are described by mass action equations and are subject to the constraint of mass balance (Equation 5.3, Lumsdon, 1995). Differences arise due to the fact that ligand surface groups are electrically charged, thus requiring the introduction of an electrostatic component into the mass action equations (Lumsdon, 1995). To solve the mass action equations, a charge balance equation is required. This equation differs with the SCM utilised, with Equation 5.4 used for the double diffuse layer model.

$$[\equiv SOH]_{TOT} = [\equiv SOH_2^+] + [\equiv SO^-] + [\equiv SOCd^+] \quad \text{Equation 5.3}$$

Where; Cd^{2+} is representative of an adsorbing species.

$$-\sigma^s = \sigma_d = 0.1174 I^{0.5} \sinh\left(\frac{F\varphi_d}{2RT}\right) \quad \text{Equation 5.4}$$

Where; σ^s (C m^{-2}) is the surface charge, σ^d (C m^{-2}) is the diffuse layer charge, I is the ionic strength of the system (mol dm^{-3}), F is the Faraday constant (C mol L^{-1}), φd is electrical potential in the diffuse layer, R is the gas constant (8.315 J mol^{-1} K^{-1}), and T is temperature in kelvin (K).

SCM such as the constant capacitance model, the diffuse double layer model and the triple layer model differ in their structural representation of the solid: solution interface, leading to differences in the location and hydration status of the adsorbed species (Goldberg, 1995).

The Diffuse Double Layer Model (DDLM), proposed by Stumm et al. (1970) and Huang and Stumm (1973) and developed by Dzombak and Moral (1990), is selected for use in this study. The model has a consistent internal thermodynamic database and is becoming a standard approach for the modelling of adsorption onto the surface of Fe-oxides (e.g. Ali and Dzombak, 1996; Dijkstra et al., 2009). In the DDLM adsorbed ions form inner-sphere complexes (strong complexes, either ionic or covalent bonding; Sposito, 1984), containing no water bonds between the surface and the adsorbing species, developing a surface charge, σ_s (Lumsdon, 1995). The surface charge is balanced by ions in the diffuse layer (Figure 5.1). In the interfacial region there are two sections: the surface plane for adsorption of H^+, OH^- and specifically adsorbed solutes (σ_s to σ_d), and the diffuse layer which represents the closest distance of approach of counter ions (Davis and Kent, 1990).

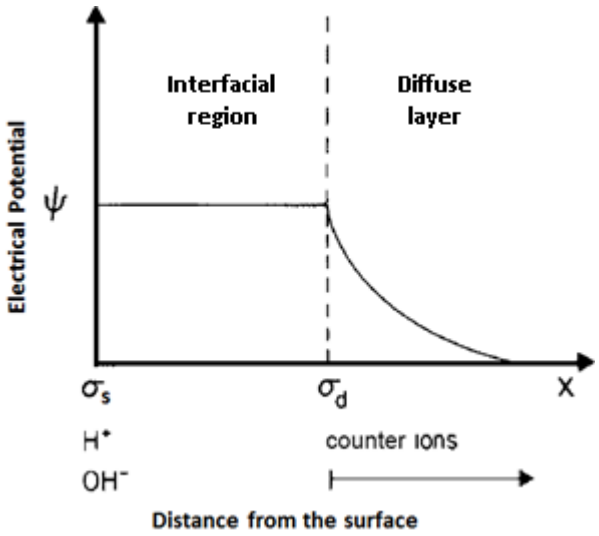

Figure 5.1: Structure of the surface: solution interface for the DDLM. Illustrative of the decay of electrical potential with distance from the surface. (After Dzombak and Moral, 1990).

The Gouy-Chapman theory is applied to determine the charge-potential relationship in the diffuse layer (Equation 5.4), with the electrical potential decreasing exponentially with distance from the surface (Figure 5.1).

Dzombak and Moral (1990) provide an extensive set of modelling parameters for hydrous ferric oxide (HFO) surfaces for use in the DDLM and thus it is this model that is selected for the purpose of this research, with adsorption onto HFO surfaces the predicted dominant removal mechanism in the batch experiments.

5.2 Geochemical Software

A DDLM was utilised in the software ORCHESTRA (Objects Representing Chemical Speciation and Transport models). ORCHESTRA is not a specific model, but a toolbox that allows users to develop their own geochemical speciation models (Meeussen, 2003). ORCHESTRA consists of two main parts; a generic calculation kernel, which is in the form of a Java executable providing the user with a general user interface (GUI), and a text file which contains basic model object definitions (Meeussen, 2003). This text file is also referred to as the object database, containing

the definitions of model elements, such as components, species and sites. This object database allows ORCHESTRA to be utilised in a similar manner to other chemical speciation models such as PHREEQC and MINTEQ.

ORCHESTRA differs to other models, such as PHREEQC and MINEQL, as the structure of the models developed is object orientated, meaning that each primary entity (object) entered in the model has associated functions which can be applied to the object, with objects having relationships between them. Objects are classified as one of three types; entities, reactions and phases; these form the basis for model development. Equations are contained within the text file which is read by ORCHESTRA during model runs, making them accessible and editable rather than them being contained within the model source code as with PHREEQC and MINEQL (Meeussen, 2003). ORCHESTRA has been further developed since its initial publication with the incorporation of a much improved GUI. For the purpose of this research, a version of ORCHESTRA which was published in June 2008 will be utilised (Meeussen, 2011).

As ORCHESTRA can only model adsorption onto one surface, the anticipated dominant surface for adsorption, HFO, will be modelled and not adsorption onto calcite, which would only occur for ochres with a high calcite content under high pH conditions.

5.3 Model reactions

Within the model a range of aqueous speciation, mineral formation and HFO (Hydrous ferric oxide) adsorption reactions were allowed to occur. For most of the ochres, the aqueous species were kept constant but the minerals allowed to form were altered to improve the fit of the model to the observed dataset. The amount of P adsorption onto HFO surfaces was also controlled in the model by altering the HFO surface area (HFO-SA) to optimise fit between the model and the observed dataset.

5.3.1 Aqueous species

A list of aqueous species allowed to form in the model is presented in Table 5.1 with the associated activity coefficients.

Table 5.1: List of aqueous species allowed to form in the model developed in ORCHESTRA. logK is the activity coefficient of the reaction.

Reaction stoichiometry				Aqueous Species	logK
1 Al^{3+}	- 1H^+	+ 1H_2O	⇔	$AlOH^{2+}$	-4.997
1 Al^{3+}	- 2H^+	+2 H_2O	⇔	$Al(OH)_2^+$	-10.094
1 Al^{3+}	- 3H^+	+3H_2O	⇔	$Al(OH)_3$	-16.791
1 Al^{3+}	- 4H^+	+ 4H_2O	⇔	$Al(OH)_4^-$	-22.688
2 Fe^{3+}	- 2H^+	+2H_2O	⇔	$Fe_2(OH)_2^{4+}$	-2.854
3 Fe^{3+}	- 4 H^+	+4 H_2O	⇔	$Fe_3(OH)_4^{5+}$	-6.288
1 Fe^{3+}	- 1 H^+	+ H_3PO_4	⇔	$FeH_2PO_4^{2+}$	2.1305
1 Fe^{3+}	- 2 H^+	+ 1 H_3PO_4	⇔	$FeHPO_4^+$	0.571
1 Fe^{3+}	+ 1 NO_3^-		⇔	$FeNO_3^{2+}$	1
1 Fe^{3+}	- 1 H^+	+ 1 H_2O	⇔	$FeOH^{2+}$	-2.187
1 Fe^{3+}	- 2H^+	+2 H2O	⇔	$Fe(OH)_2^+$	-4.594
1 Fe^{3+}	- 3 H^+	+ 3 H_2O	⇔	$Fe[OH]_3$	-12.56
1 Fe^{3+}	- 4 H^+	+ 4 H_2O	⇔	$Fe[OH]_4^-$	-21.588
1 Ca^{2+}	- 1 H^+	+ 1 H_3PO_4	⇔	$CaH_2PO_4^+$	-0.798
1 Ca^{2+}	- 2 H+	+ 1 H_3PO_4	⇔	$CaHPO_4$	-6.686
1 Ca^{2+}	1 NO_3^-		⇔	$CaNO_3^+$	0.5
1 Ca^{2+}	- 1 H^+	+ 1 H2O	⇔	$CaOH^+$	-12.697
1 Ca^{2+}	- 3 H^+	+ 1 H_3PO_4	⇔	$CaPO_4^-$	-15.261
-1 H^+	+ 1 H_3PO_4		⇔	$H_2PO_4^-$	-2.148
-2 H^+	+ 1 H_4SiO_4		⇔	$H_2SiO_4^{2-}$	-23.04
-1 H^+	+ 1 H_4SiO_4		⇔	$H_3SiO_4^-$	-9.84
-2 H^+	+ 1 H_3PO_4		⇔	HPO_4^{2-}	-9.346
-2 H^+	+ 1 H_3PO_4	+ 1 Na^+	⇔	$NaHPO_4^-$	-8.276
- 1 H^+	+1 H_2O		⇔	OH^-	-13.997
-3 H^+	+ 1 H_3PO_4		⇔	PO_4^{3-}	-21.721

5.3.2 Adsorption onto HFO surface sites

In the model, Fe (oxy)hydroxide mineral surfaces were modelled using data for a hydrous ferric oxide surface (Dzombak and Morel, 1990), since the surface chemistry of this phase is likely to be representative of the ochre's reactive Fe phase. HFO was defined with a specific surface area of 600 m^2g^{-1} and a surface site density of 2.31 sites nm^{-2} (Table 5.2). The surface area of HFO (600 m^2 g^{-1}), will be used for initial model runs but will then be altered to optimise the fit between the model and the observed data.

Table 5.2: Surface complexation constants (log K) for proton and phosphate adsorption on hydrous ferric oxide sites (≡$FeOH^0$) using the DDLM in ORCHESTRA. Ionic strength = 0.

Reaction stoichiometry			Log K
≡$FeOH^0$ + H^+	⇔	≡$FeOH_2^+$	7.29
≡$FeOH^0$	⇔	≡FeO^- + H^+	-8.93
≡$FeOH^0$ + PO_4^{3-} + $3H^+$	⇔	≡$FeH_2PO_4^0$ + H_2O	31.29
≡$FeOH^0$ + PO_4^{3-} + $2H^+$	⇔	≡$FeHPO_4^-$ + H_2O	25.39
≡$FeOH^0$ + PO_4^{3-} + H^+	⇔	≡$FePO_4^{2-}$ + H_2O	17.72

The solid phase concentration of HFO present in each ochre sample was calculated from the oxalate extractable Fe by a factor of 1.7, a value suggested by Parfitt and Childs (1988).

5.3.3 Mineral formation

A range of minerals with a component of P (Table 5.3) were allowed to form in the model if they improved the fit to the observed dataset. For most ochres the addition of these minerals did not alter or decrease the goodness of fit between the model and the observed dataset. However, for some ochres the inclusion of one or more of these minerals greatly improved the fit with the model observed dataset.

Table 5.3: List of minerals utilised to improve the fit between the ORCHESTRA model and the observed datasets. logK is the activity coefficient of the reaction.

Mineral	Reaction stoichiometry					logK
$Ca_3(PO_4)_2$(beta)	+6 H^-	⇔	+3 Ca^{2+}	+2 H_3PO_4		-14.522
$Ca_4H(PO_4)_3.3H_2O$	+8 H^-	⇔	+4 Ca^{2+}	+3 H_2O	+3 H_3PO_4	-18.083
$CaHPO_4.2H_2O$	+2 H^-	⇔	+1 Ca^{2+}	+2 H_2O	+1 H_3PO_4	-2.726
$CaHPO_4$[s]	+2 H^-	⇔	+1 Ca^{2+}	+1 H_3PO_4		-2.446
$Mg_3(PO_4)_2$	+6 H^-	⇔	+3 Mg^{2+}	+2 H_3PO_4		-20.162
$MgHPO_4.3H_2O$	+2 H^-	⇔	+1 Mg^{2+}	+1 H_3PO_4	+ 3 H_2O	-3.546

5.4 Model inputs: Ochre properties

The objective of this Chapter is to better understand the P removal mechanisms involved in the batch experiments (Chapter 4). A project folder was set-up for each of the ochres containing an executable for the ORCHESTRA model. Using this executable a number of primary entities were added to chemistry input file for the model. The GUI allows primary species to be added into the model in the chemistry tab, the concentrations of which are updated by reading an input file when the model is run. Within the chemistry tab, the concentrations of the primary entities can either be set at a fixed activity throughout the model runs or allowed to vary with the conditions that the model predicts. The primary entities entered into the model are used either to describe the system conditions (pH, Na^+ and NO_3^-) or the additions to the system of P (H_3PO_4) and ochre (Al^{3+}, Ca^{2+}, Cu^{2+}, Fe^{3+}, $H_2SiO_4^{2-}$, Mg^{2+}, Mn^{2+}, Ni^{2+}, Pb^{2+}, SO_4^{2-} and Zn^{2+}). For each model run the concentrations of the primary entities are read from an input file. The concentration of Na^+ and NO_3^- are the same for all experiments as this is the electrolyte which was used; 0.01 M $NaNO_3$. The P concentration varied with experiments, with six different P additions for each ochre. The primary entities associated with the ochre in the system were calculated using the figures from the acid digest (Chapter 3). The value of pH is set as fixed activity to that measured at the end of the batch experiment, meaning that the value of pH is constrained and not allowed to change within the model.

When a primary entity is entered into the model, associated functions can be selected within the model; this can be used to allow mineral phases to form, reactions to occur and various chemical species to be present. Within the GUI, these functions are selected in the Reactions tab, within the Chemistry tab, and will be altered throughout the modelling process to optimise the fit of the models to the batch experiment data.

Data to be inputted into the model (Table 5.4) was collated in a Microsoft Excel spreadsheet. This was then copied and pasted into the input tab of the model, which was exported to create an input file. This file is read by the model to define the initial concentrations of the primary entities before the model is run whereby the equilibrium conditions of the system are calculated by using the selected object relationships. Following the model run, the equilibrium concentration of selected parameters are displayed in the output tab of the ORCHESTRA GUI. The variables displayed in this output file need to be entered as headers into the output file before running the model. The output data was then copied into a Microsoft Excel spreadsheet so that the modelled result could be compared to the observed dataset using graphical tools and statistical analysis. This analysis informs the modelling process with the objective of being able to accurately model the P equilibrium conditions of the batch experiments.

Table 5.4: System inputs to ORCHESTRA calculated from the P adsorption batch experiments, acid digest and ammonium oxalate extraction. L: S is the liquid to solid ratio of the various batch experiments. Data inputted into the model but not included in Table are HFO-SA, which was initially set at 600 $m^2\ g^{-1}$, Na^+ and NO_3^- set at 0.01 M, and ionic strength set at 0.01. pH was entered for each batch experiment when fitting the model, with the model run for a sweep of pH when it was optimised. The P adsorption batch experiments were run at six different P additions and thus P inputs were altered in the model accordingly. For the molarity values, e indicates x10^.

Ochre	**Input to ORCHESTRA**												
	L: S	HFO	Al^{3+}	Ca^{3+}	Cu^{2+}	Fe^{3+}	$H_2SO_4^{2-}$	Mg^{2+}	Mn^{2+}	Ni^{2+}	Pb^{2+}	SO_4^{2-}	Zn^{2+}
	$L\ kg^{-1}$	$kg\ kg^{-1}$	Molarity										
Acomb	331.1	0.2513	3.68e-4	2.19e-3	5.62e-7	3.07e-2	7.00e-4	3.03e-4	2.51e-5	2.15e-6	1.15e-6	4.67e-5	5.87e-6
Acomb pellets	409.9	0.1716	3.29e-3	6.57e-3	5.87e-7	1.38e-2	2.58-3	2.83e-3	5.04e-5	9.07e-7	5.30e-7	9.44e-5	2.52e-6
Avoca	454.5	0.3156	5.82e-4	3.17e-5	1.96e-5	1.98e-2	5.10e-5	3.25e-4	2.93e-6	1.18e-6	1.46e-5	5.22e-4	9.85e-6
Minto	454.6	0.1530	1.38e-4	6.96e-4	5.15e-7	2.40e-2	1.15e-4	5.00e-4	8.87e-5	2.16e-6	8.35e-7	5.15e-5	3.11e-7
Polkemmet	454.5	0.1944	2.78e-3	5.82e-4	1.33e-6	1.76e-2	5.11e-5	4.17e-4	4.25e-5	1.68e-6	9.93e-7	3.12e-6	3.12e-6
Silkstone	429.5	0.4062	4.03e-4	2.57e-4	1.68e-6	1.71e-2	9.67e-4	1.63e-4	1.74e-4	1.72e-6	6.93e-7	2.17e-5	2.76e-6
Ynysarwed	371.1	0.4034	6.26e-4	1.05e-3	2.13e-7	1.54e-2	8.73e-4	3.81e-2	2.30e-5	2.04e-6	4.99e-7	7.15e-5	1.74-6

5.5 Statistics

To assess the difference between the equilibrium P concentrations in the observed and modelled datasets, a weighted version of the sum of the squared errors was calculated, Equation 5.5, with minimising this, the target of the optimisation process.

$$\sum_{i=1}^{N}([S_i - \bar{S}_i]^2/W_i) \qquad \text{Equation 5.5}$$

Where SSE is the objective function, N is the number of observations, S_i and $\bar{S}_i$ are the *i*th observed and modelled values of the dependant variable (P) and W_i is the weighted function of the *i*th value.

The value of the weighted function varied with the model run, with W_i equal to the P addition (mg L^{-1}) of the batch experiment. This ensured that the SSE was standardised removing any bias in fitting the model towards the experiments with higher P additions. SSE was calculated for each P addition within the dataset as well as for the dataset as a whole. This gives a calculation of the overall fit of the model to the observed dataset, but also allows the fit of individual P additions to be quantified to identify where the model is not performing well.

Further to this the goodness of fit of the model to the observed dataset was assessed by calculating the model efficiency (E, Chapter 4.2.3.3) with a value of 1 indicating a perfect model fit. Values <0 indicate a poor fit and that the mean value of the observed dataset would give a better prediction than the model.

5.6 Initial model runs

For the initial model runs, the reactions occurring in the model were restricted. The major P removal mechanism involved was the HFO adsorption model, with all P mineral forms such as Ca-P not allowed to form in the model. Dissolved P species

were allowed to form (Table 5.1). Each ochre was modelled separately, with the HFO-SA value altered to determine the effect this had on the model efficiency.

An example of the first set of model runs where only the HFO-SA was adjusted is detailed for Ynysarwed ochre. The total SSE (ΣSSE) decreased with increasing HFO-SA for Ynysarwed ochre, with ΣSSE lowest at 258.1 for a surface area of 750 m^2 g^{-1} (Table 5.5). In the model, the HFO-SA parameter is multiplied by the amount of HFO to give a total surface area available for adsorption. Therefore the better fit that occurs with increasing HFO-SA may mean that either; the HFO has a higher surface area than suggested by the literature, or that the calculated value of HFO was underestimated in the experiment. Also, it may be that the increased amount of adsorption is compensating for removal mechanisms which have not been put into the model at this stage.

The model for each ochre was run increasing the HFO-SA in increments of 50 from 450 m^2 g^{-1} to 750 m^2 g^{-1}. Whilst this is a relatively large increase for each model run, a higher resolution could lead to over training the model. Of these model runs, the four with the lowest ΣSSE were utilised for further model development. Model efficiency (E) was negative for all the model runs for Ynysarwed ochre (Table 5.5), indicating that taking the mean of the observed dataset would provide a better prediction than the modelled result. Model efficiency improved with increasing HFO-SA.

Table 5.5: Model fit to the observed dataset for Ynysarwed ochre when adjusting HFO-SA. Underlined ΣSSE figures indicate the HFO-SA values which will be utilised for subsequent model runs.

P addition (mg L^{-1})		**HFO surface area (m^2 g^{-1})**						
		450	500	550	600	650	700	750
17.5	SSE	32.4	30.1	28.4	26.9	25.5	24.0	22.5
34.9		92.3	76.8	64.2	53.8	45.5	38.5	33.0
69.8		88.7	71.9	59.6	51.0	44.5	39.8	36.8
104.7		130.7	109.8	93.0	80.2	71.2	65.7	63.4
139.6		99.5	83.7	71.4	62.4	56.8	54.5	55.3
209.4		72.0	61.8	54.1	48.8	45.9	45.4	47.2
	ΣSSE	515.6	434.2	370.7	<u>323.1</u>	<u>289.3</u>	<u>267.9</u>	<u>258.1</u>
17.5	E	-9.4	-8.7	-8.1	-7.7	-7.1	-6.7	-6.2
34.9		-8.8	-7.2	-5.8	-4.7	-3.7	-3.1	-2.5
69.8		-1.6	-1.1	-0.8	-0.5	-0.3	-0.2	-0.1
104.7		-5.9	-4.8	-3.9	-3.2	-2.7	-2.4	-2.3
139.6		-7.5	-6.1	-5.1	-4.3	-3.8	-3.6	-3.7
209.4		-8.6	-7.2	-6.2	-5.5	-5.1	-5.0	-5.3

Modelled runs were also compared to the observed dataset graphically (Figure 5.2). This Figure is typical for many of the model fits for the various ochres following the initial model runs. The model fits well at low pH, where adsorption by HFO is high, and poor at high pH where very little P is being removed by the model.

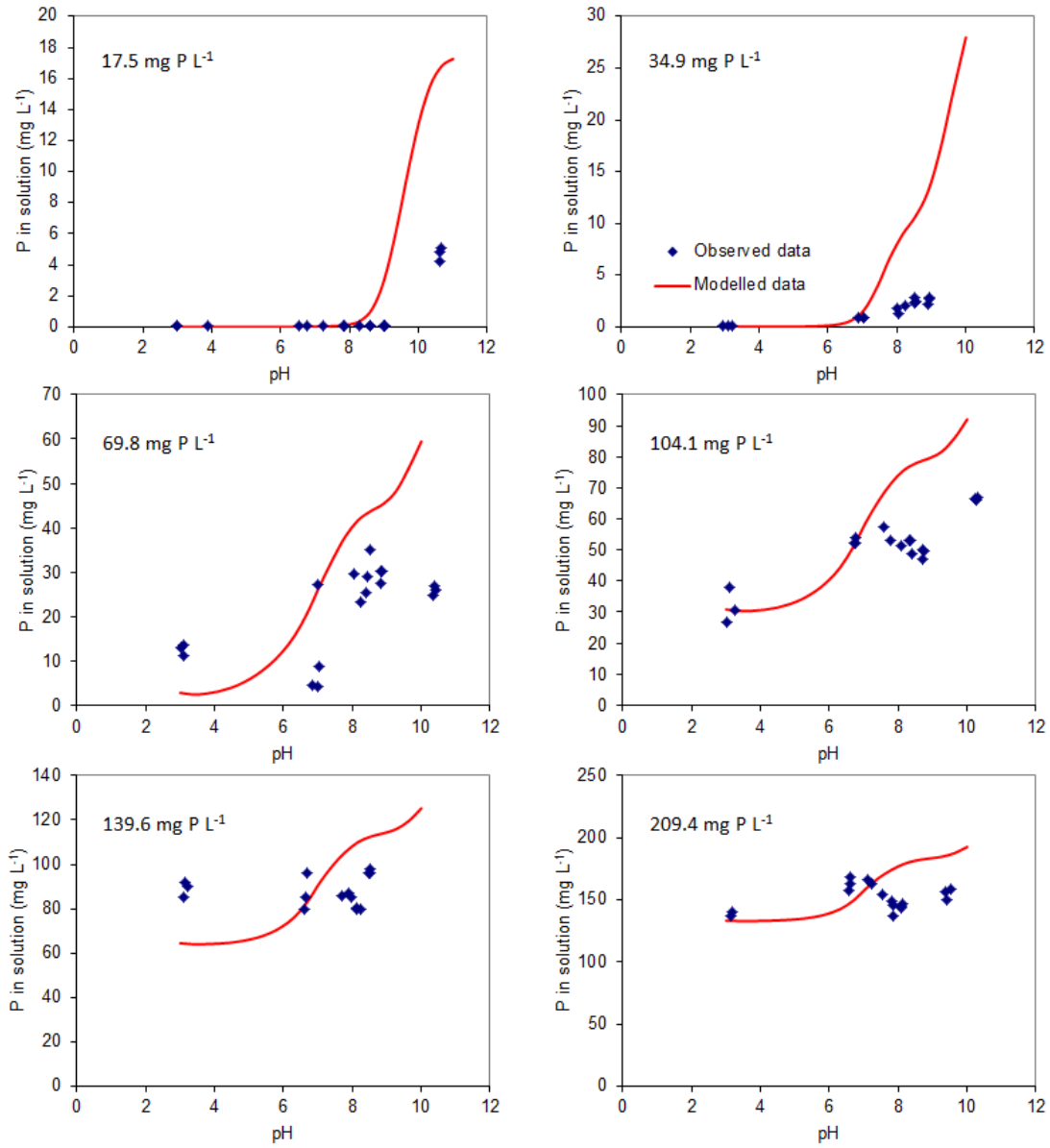

Figure 5.2: Initial model fits to observed data for Ynysarwed ochre. HFO-SA = 600 m^2 g^{-1}. P addition of the observed datasets noted on each graph.

Summary results for varying the HFO-SA for each ochre can be seen in Table 5.6. The four best model fits to the observed datasets are underlined and these will be utilised for subsequent model runs. The range of ΣSSE varies with ochre, with model fits for Avoca showing a good fit between modelled and observed datasets, 77.2-166.9, and model fits relatively poor for Acomb pellets, 557.3-803.3.

Table 5.6: Summary results for model runs varying HFO-SA for all seven ochres. Underlined ΣSSE figures indicate the HFO-SA values which will be utilised for subsequent model runs.

Ochre Type		HFO-SA (m^2 g^{-1})						
		450	500	550	600	650	700	750
Acomb ochre	ΣSSE	214.4	175.5	152.4	144.1	149.9	168.7	199.8
Acomb pellets		803.3	743.9	692.4	648.6	611.76	581.6	557.3
Avoca		166.9	124.2	95.6	80.1	77.2	86.4	107.4
Minto		339.7	281.9	231.3	187.7	150.8	120.5	95.5
Polkemmet		232.0	195.2	165.3	141.4	123.1	110.5	100.3
Silkstone		61.7	83.5	125.7	186.5	264.5	357.6	464.0
Ynysarwed		515.6	434.2	370.7	323.1	289.3	267.9	258.1

5.7 Model optimisation

Following the initial model runs, each ochre was considered on a separate basis. Various adjustments were made to each model in order to improve fit to the observed data, such as allowing Ca-P minerals to form.

5.7.1 Acomb ochre

Initial model fits to the observed data for Acomb ochre were relatively good, with ΣSSE as low as 144.1. For these initial model runs, a better fit occurred under low pH conditions than at higher pH conditions, with the model predicting higher P concentrations in solution at high pH conditions than in the observed data. Therefore a removal mechanism needs to occur under higher pH conditions to improve the model fit. To this effect the Ca minerals brushite and octacalcium phosphate (OCP) were allowed to form in the model by selecting them in the ORCHESTRA chemistry tab. The result of introducing these Ca minerals into the model led to an increase in the ΣSSE for the model (Table 5.7), as the mineral formation removed too much P at high pH conditions. Therefore these minerals were left out of the finalised model. The optimum model set-up utilises a HFO-SA

of 600 m^2 g^{-1} (Figure 5.3), which corresponds to the HFO surface area suggested by Dzombak and Morel, (1990).

Table 5.7: The effect on ΣSSE of introducing Ca minerals into the model for Acomb ochre.

Ca mineral		**HFO surface area (m^2 g^{-1})**			
		550	600	650	700
None	ΣSSE	152.4	144.1	149.9	168.7
OCP		225.6	248.3	282.2	326.6
Brushite		204.0	219.7	246.3	281.8
Both Ca minerals		228.4	252.1	286.9	331.8

The optimal set-up of the model suggests that the dominant mechanism of P removal in the batch experiments for Acomb ochre is adsorption onto HFO. Under high pH conditions, the model consistently predicts more P in solution than was observed (Figure 5.3). The mineral calcite was detected in the XRD analysis of Acomb ochre as a minor component (Chapter 3.6) and it is suggested that P adsorption onto calcite may be responsible for the difference in the observed and modelled datasets under high pH conditions. Whilst it was outside of the scope of this study to add calcite adsorption into the ORCHESTRA model, appropriate techniques are under development (Sø et al., 2011).

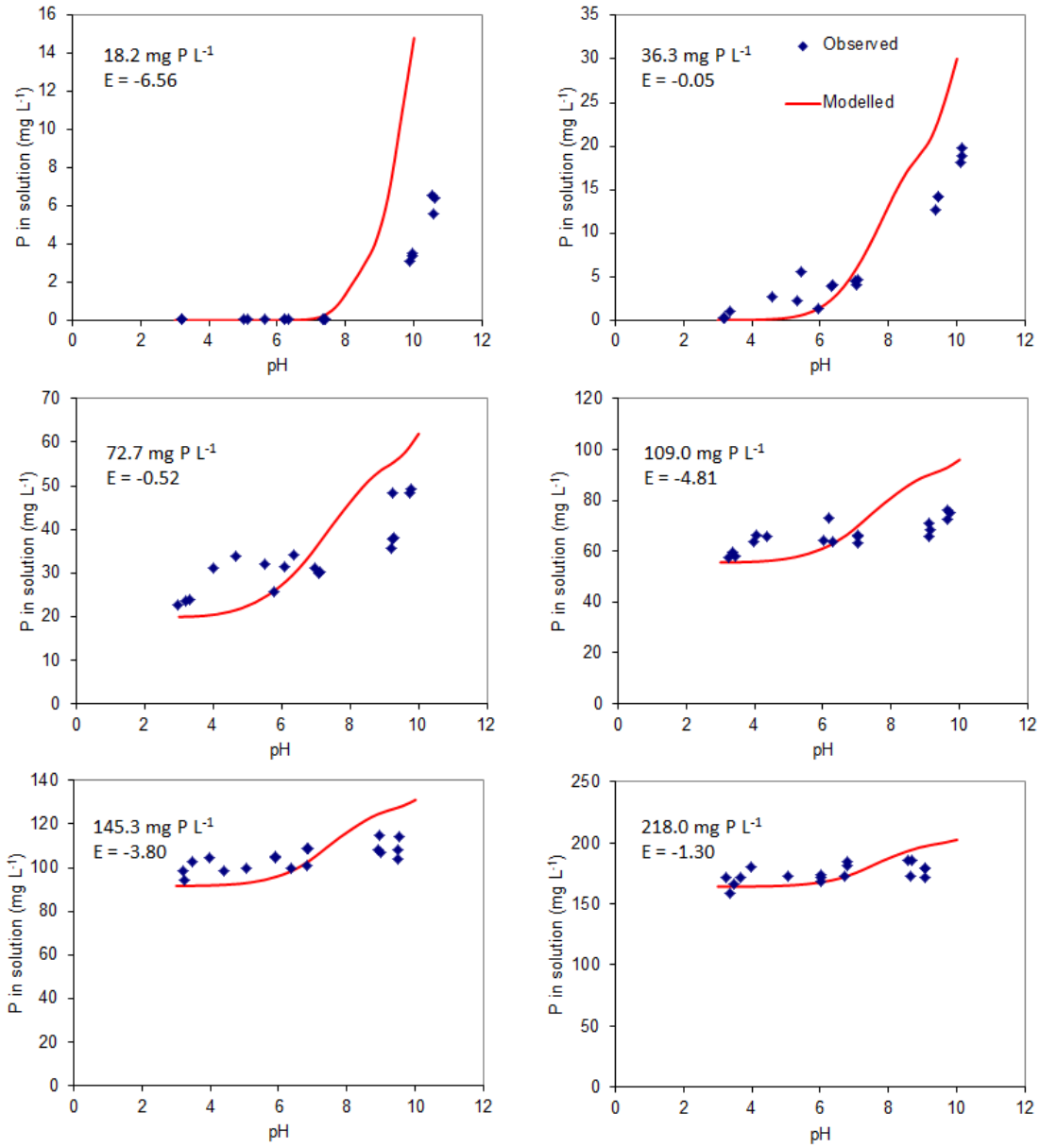

Figure 5.3: Final model fits to observed data for Acomb ochre. HFO-SA = 600 m^2 g^{-1}. P addition of the observed datasets and model efficiency (E) is noted on each graph.

All P removed from solution in the model runs occurred by adsorption onto HFO and this is therefore suggested as the main P removal mechanism for Acomb ochre. Whilst the model efficiency (E) is negative for all P additions, this is the optimal fit that could be determined using the chemical model. An improved model fit would see higher P removal under high pH conditions, possibly due to calcite adsorption.

5.7.2 Acomb pellets

The initial model fits for Acomb pellets had the highest values of ΣSSE for any of the ochres and as such the observed dataset is not that well described by the initial model set-up. The introduction of Ca minerals does not improve the models, leading to a large increase in ΣSSE. The poor fit of the model to the observed data was due to the model removing too much P from solution. The fit of the model was improved by removing dissolved species containing P and either Ca or Mg (e.g. $CaPO_4^-$), with the optimal fit when both were removed from the model. Whilst constraining the model in this way is unrealistic, Acomb pellets contain a large amount of Ca and Mg (10.8 and 2.82 % by dry weight respectively, determined in Chapter 3.4) and the model may be allowing more of this to go into solution than did in the batch experiments. Magnesium phosphate ($Mg_3(PO_4)_2$) and Newberyite ($MgHPO_4.3H_2O$) were allowed to form in the model and the fit with the observed data was further improved to give the final model (Figure 5.4).

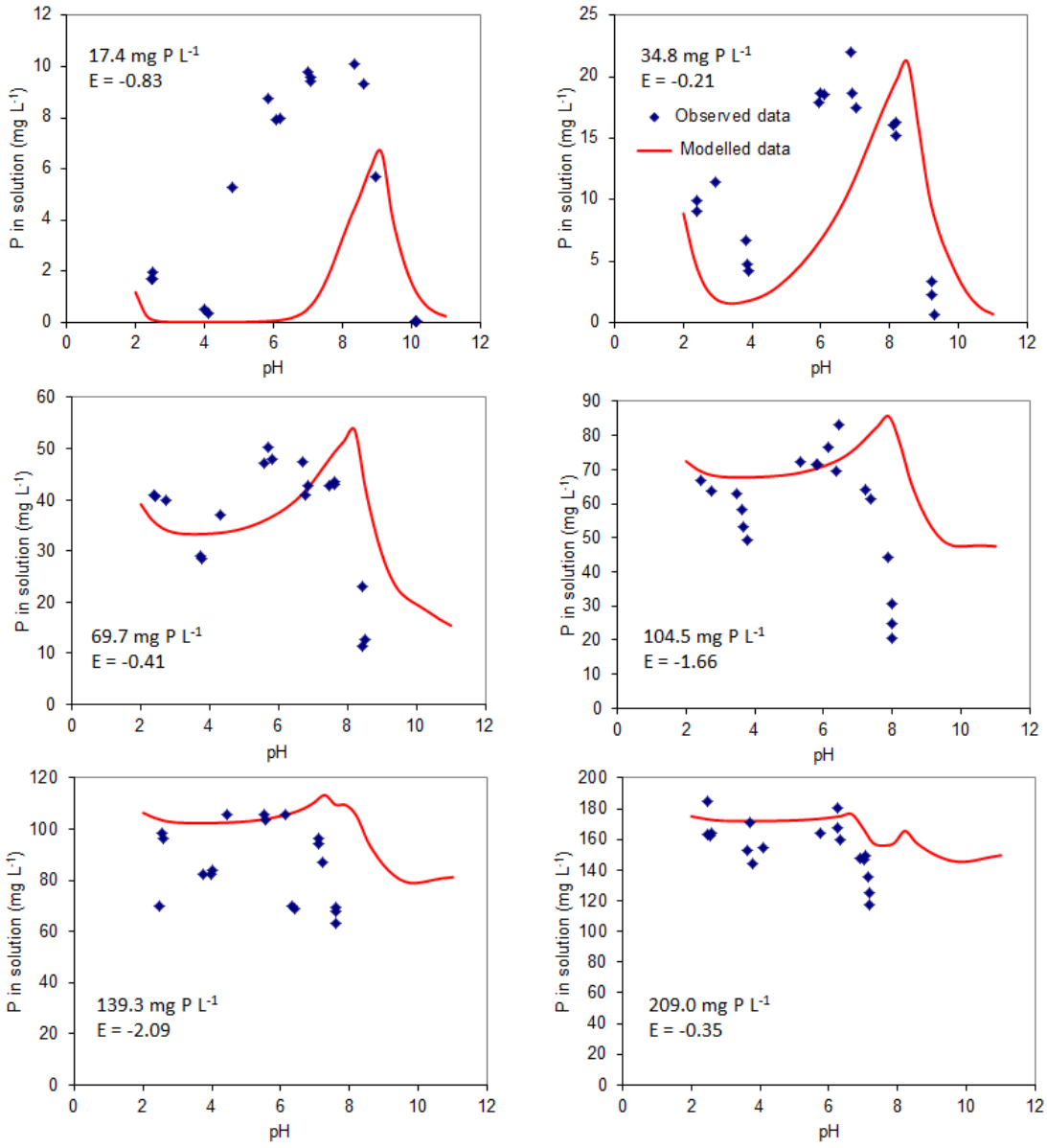

Figure 5.4: Final model fits to observed data for Acomb pellets. HFO-SA = 750 m^2 g^{-1}. P addition of the observed datasets and model efficiency (E) is noted on each graph.

Batch experiments containing Acomb pellets provided the most complex system to model of any of the ochres, with the model having somewhat limited success. The final model had to be constrained by removing Ca- and Mg- P dissolved species to achieve a fit close to that of the observed data. From the fitting of adsorption isotherms to the batch experiments (Chapter 4.2.5.2), P removal by Acomb pellets was found to have a pH dependant relationship. P adsorption capacity was highest at pH 7 (S_{max}: 43.12 mg P g^{-1}) with low values of Langmuir K indicating P adsorption

onto low affinity sites. XRD analysis of the Acomb pellets show calcite to be a major mineral component of the ochre and it is suggested that P adsorption onto calcite surfaces may be a major process in P removal by Acomb pellets, see Chapter 1.3.7.2. It is therefore concluded that in its current state the model is unable to effectively model the processes occurring in the Acomb pellet batch experiments.

5.7.3 Avoca ochre

The modelling of the batch experiments utilising Avoca ochre as an adsorbing material was modelled well with the HFO adsorption model. The addition of Ca minerals brushite and OCP into the system did not improve the fit of the model to the observed dataset either in terms of minimising ΣSSE or increasing the model efficiency. The finalised model for Avoca ochre is therefore left in its initial state, with adsorption onto HFO the only P removal mechanism. The two optimal fits of HFO-SA are 600 and 650 m^2g^{-1}, with the value of 600 m^2g^{-1} selected for the finalised model as this is the surface area of HFO found by other authors (Dzombak and Morel, 1990).

The finalised model fits well to all the observed datasets for Avoca ochre (Figure 5.5). The model efficiency of each fit is above 0, indicating a good fit of the model to the dataset. The lowest model efficiency was found at the highest P addition, but the relatively poor fit of the model may be because the data approximates well to the mean of the dataset. P removal by Avoca ochre is described well by adsorption onto HFO surface sites and thus this is proposed as the dominant P removal mechanism. As with Acomb ochre, the model is predicting too much P in solution at the lower P additions at high pH conditions. For Acomb ochre it was suggested that adsorption onto calcite surfaces may be occurring in the batch experiments which is not included in the model. This is unlikely to be occurring for Avoca ochre, which has a low Ca content of less than 0.06 % by dry weight.

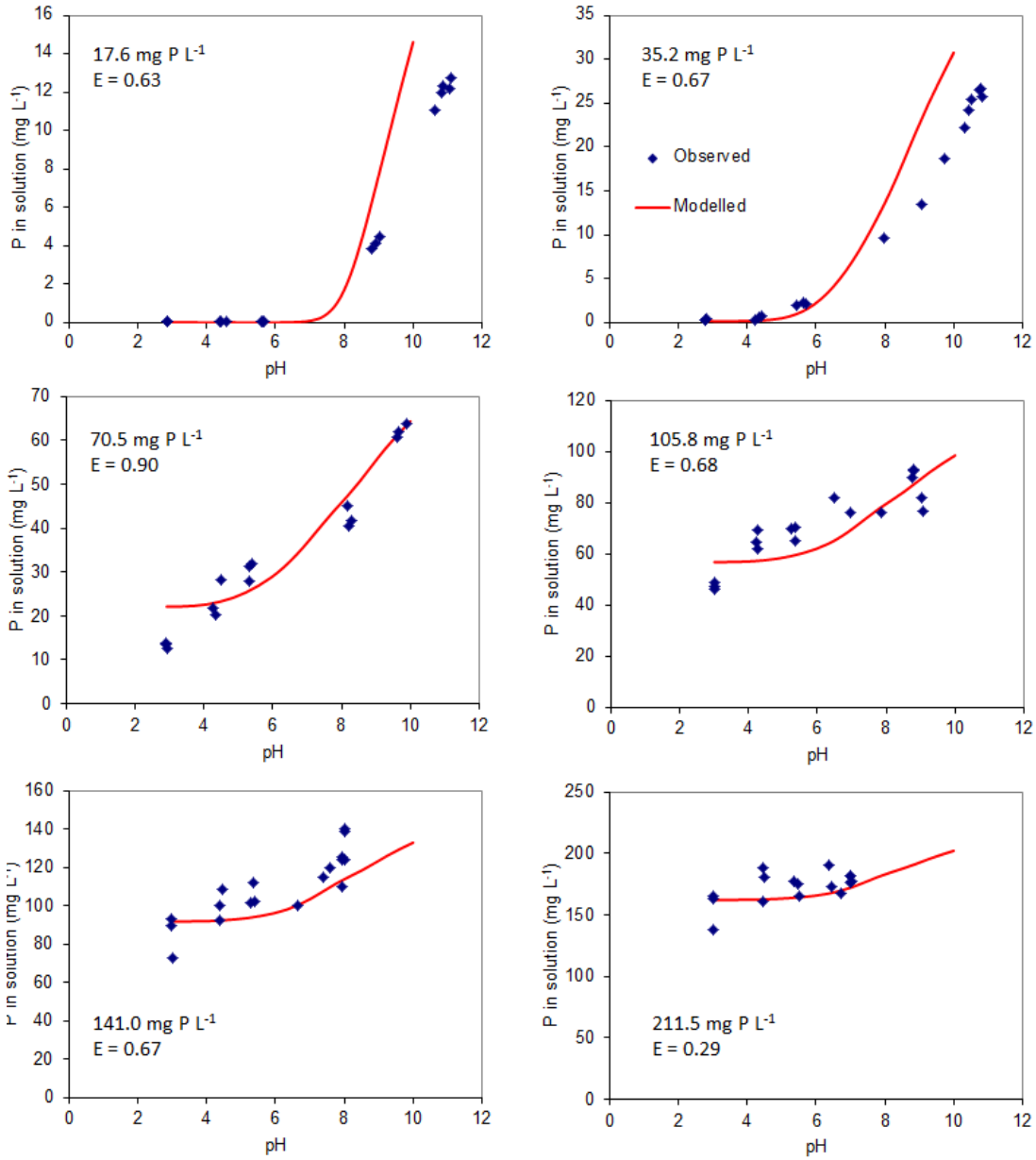

Figure 5.5: Final model fits to observed data for Avoca ochre. HFO-SA = 600 m^2 g^{-1}. P addition of the observed datasets and model efficiency (E) is noted on each graph.

5.7.4 Minto ochre

Minto ochre was relatively well modelled by the initial runs utilising the HFO adsorption model. As with the models for the other ochres under study, Ca minerals were introduced into the model for Minto ochre in an attempt to increase the goodness of fit between modelled output and the observed dataset. The ΣSSE was found to decrease with the incorporation of the Ca minerals, optimally with both Ca

minerals in the model (Table 5.8). Therefore both of these Ca minerals were allowed to form within the final model for Minto ochre.

Table 5.8: The effect of introducing Ca minerals into the model for Minto ochre.

Ca mineral		HFO surface area (m^2 g^{-1})			
		600	650	700	750
None	ΣSSE	187.7	150.8	120.5	95.5
OCP		131.0	103.4	81.7	65.7
Brushite		176.8	141.9	113.4	91.1
Both Ca minerals		129.8	102.4	80.8	65.0

It can be noted in Table 5.8 that ΣSSE decreases with increasing HFO-SA. To investigate whether this trend continued, the HFO-SA in the model was further adjusted upwards to 950 m^2 g^{-1}. The fit of the model to the observed dataset continued to increase with surface area up to 900 m^2 g^{-1} (Table 5.9).

Table 5.9: Adjustment of HFO-SA for the modelling of Minto ochre.

	HFO surface area (m^2 g^{-1})			
	800	850	900	950
ΣSSE	54.5	49.0	48.0	51.04

Within the model the available adsorption sites for P removal by HFO is determined by multiplying HFO content, the site density and the HFO-SA. The increased fit of the model with increasing HFO-SA suggests either that the surface area of HFO is greater than 600 m^2 g^{-1}, or that the inputted value of HFO in the model, determined from ammonium oxalate extraction, has been underestimated. Assuming that the surface area of HFO is 600 m^2 g^{-1} (Dzombak and Morel, 1990) then the HFO oxide content of Minto ochre has been underestimate by 50 % at the optimal fit of the model, HFO-SA equal to 900 m^2 g^{-1}. The final result, with HFO-SA set at 900 m^2 g^{-1} is shown in Figure 5.6.

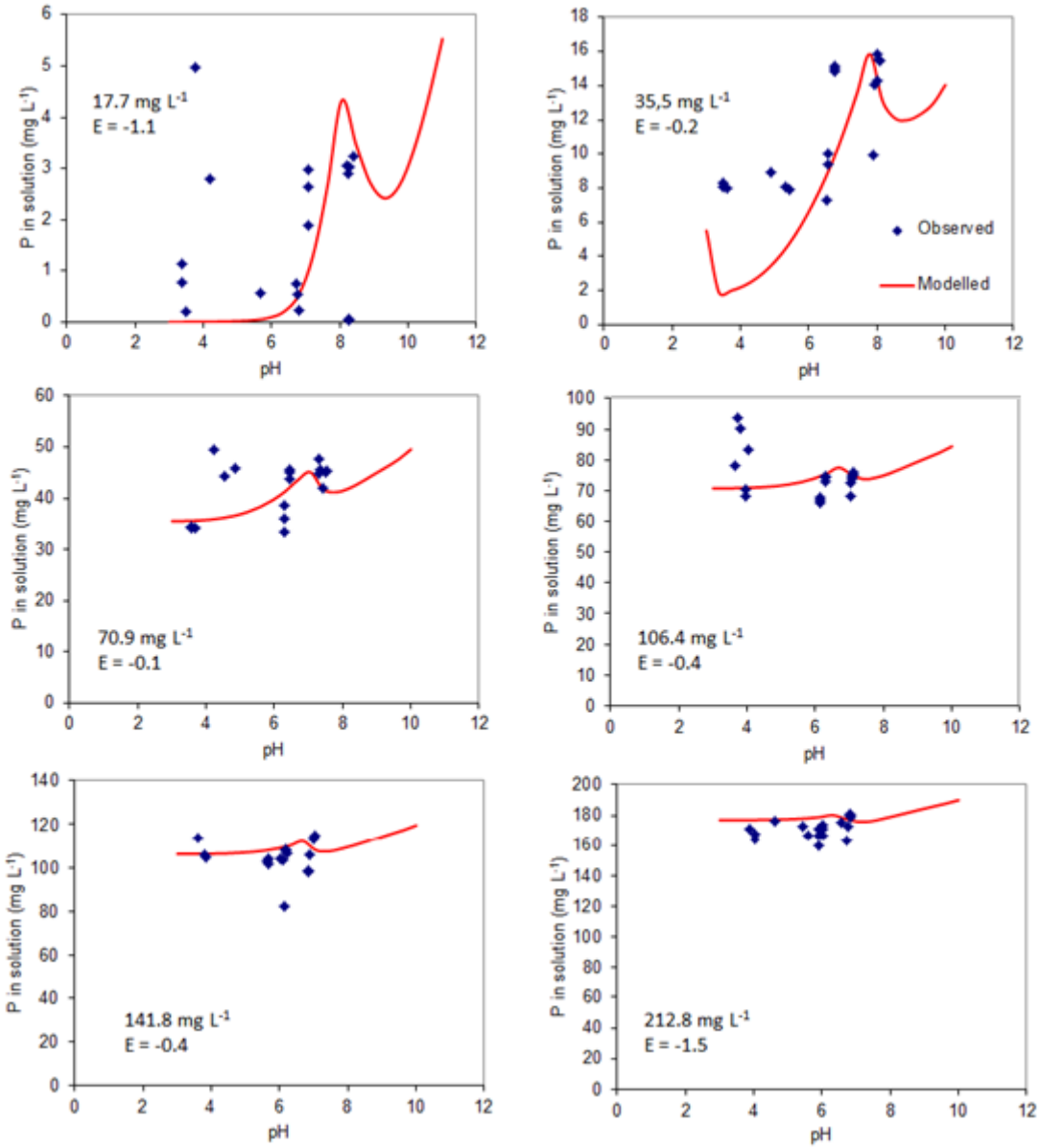

Figure 5.6: Final model fits to observed data for Minto ochre. HFO-SA = 900 m^2 g^{-1}. P addition of the observed datasets and model efficiency (E) is noted on each graph.

Model efficiency (E) is negative for all the fits to observed data in Figure 5.6. Whilst this suggests that the model does not fit the dataset well, for many of the Minto ochre datasets the mean average, which the model efficiency compares the model fit to, is relatively close to the optimal fit. Therefore producing a model which would improve on this and produce an E value >0 is improbable. The model fitting process is also made difficult by the variability in the observed datasets.

Results from the HCl-HNO_3 digest indicate that Minto ochre is largely comprised of Fe (60.9 % by dry weight), with a small amount of Ca (1.27 % by dry weight), (Chapter 3.4). The dominant mineral form of the ochre is goethite. Coupled with the results of the modelling, it is suggested that adsorption onto HFO is the dominant P removal process at neutral and acid pH conditions.

The model was run between pH 6-8, conditions typical of P enriched wastewater streams to investigate the relative importance of P adsorption onto HFO surfaces and Ca mineral formation in the model (Figure 5.7). P is not removed by mineral formation at pH 6 at any of the P concentrations utilised in the batch experiments. For pH 7, small quantities of OCP form for P additions 106.4 mg P L^{-1} and higher. Brushite minerals also form under these conditions, with approximately twice the amount of P removed in this form than for OCP minerals.

At pH 8, whilst the total P removed by ochre is approximately the same as for pH 7, an increasing amount is removed as Ca-P minerals. Brushite and OCP are present in the model runs at 35.5 mg P L^{-1} addition and above with approximately twice the P removal accounted for by brushite formation than for OCP. The P adsorption capacity of Minto ochre has previously been noted as independent of pH (Heal et al., 2003b). Figure 5.7 indicates that this is because as P adsorption onto HFO surfaces declines with increasing pH, Ca-P minerals form to remove approximately the same amount of P.

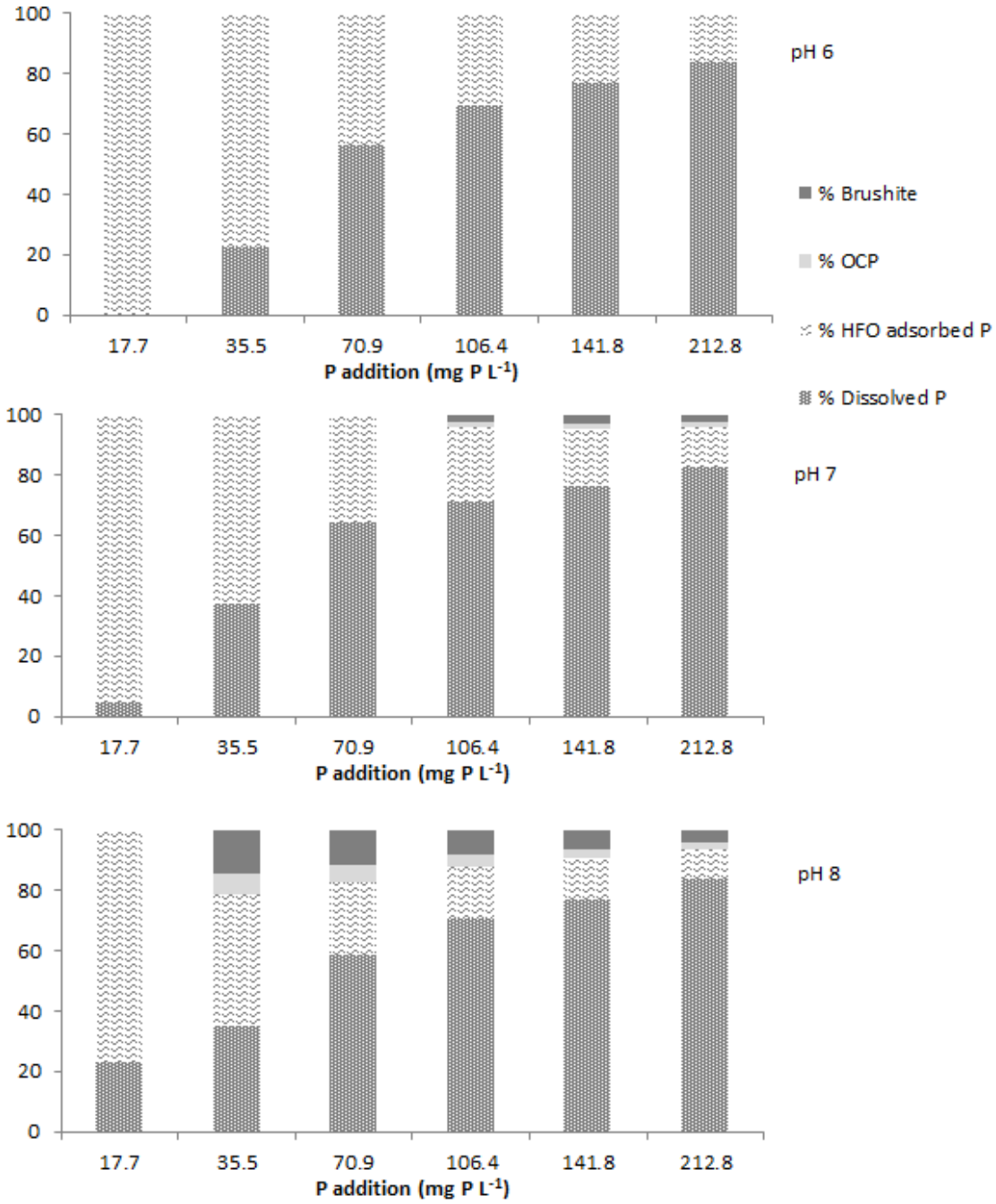

Figure 5.7: Comparison of P removal by adsorption onto HFO and the formation of OCP and brushite minerals for Minto ochre between pH 6 and 8, determined from the ORCHESTRA model.

5.7.5 Polkemmet ochre

For Polkemmet ochre, the majority of ΣSSE calculated for the initial model runs was accounted for by one dataset; P addition 145.0 mg P L^{-1} (Table 5.10). This is due to a

large amount of variation this dataset and it was therefore not included in subsequent model fitting.

Table 5.10: The fit of initial ORCHESTRA model runs to Polkemmet ochre datasets. ΣSSE* is the total SSE not including the 145.3 mg P L^{-1} dataset.

P addition (mg L^{-1})		**HFO surface area (m^2 g^{-1})**			
		600	650	700	750
18.2	SSE	4.9	5.2	6.0	7.2
36.3		3.1	2.6	3.9	7.0
72.7		20.7	16.0	12.5	10.2
109.0		5.4	3.0	1.5	0.9
145.3		98.4	90.1	82.5	75.5
218.0		8.8	6.2	4.1	2.5
	ΣSSE	141.3	123.1	110.5	103.3
	ΣSSE*	42.9	33.0	28.0	27.8

In an attempt to improve model fits, calcium minerals brushite and OCP were incorporated into the model. However this led to a decrease in model efficiency and an increase in the ΣSSE and they were subsequently removed. The fit of the final model set-up can be seen in Figure 5.8, with the HFO-SA set at 750 m^2 g^{-1}. As with Minto ochre, the improved fit with a HFO surface area higher than that suggested in the literature indicates that either the amount of HFO determined from the ammonium oxalate extraction is an underestimate or the surface area of the HFO is higher than 600 m^2 g^{-1}.

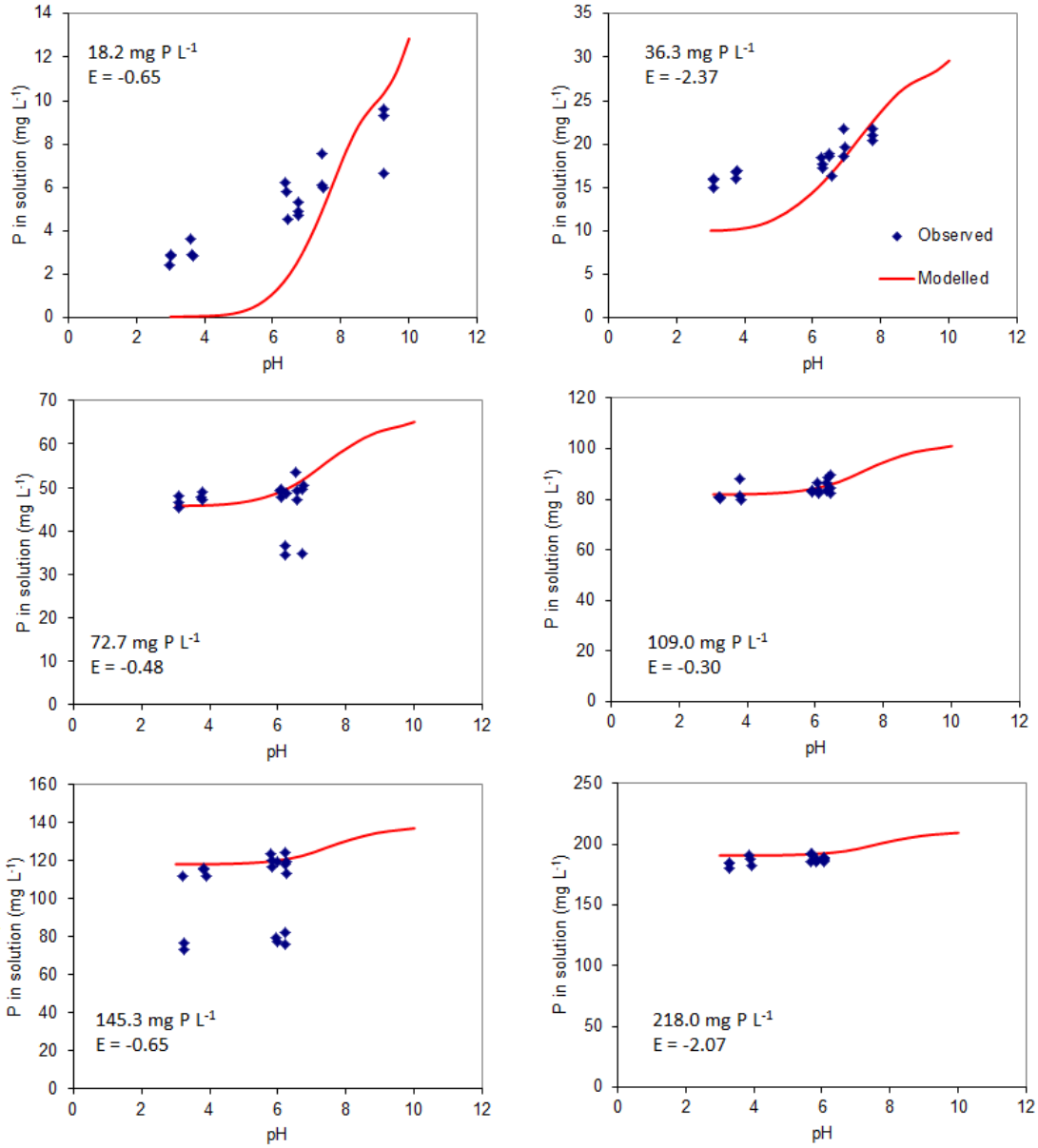

Figure 5.8: Final model fits to observed data for Polkemmet ochre. HFO-SA = 750 m^2 g^{-1}. P addition of the observed datasets and model efficiency (E) is noted on each graph. Whilst the dataset for P addition 145.3 mg P L^{-1} is shown, it was not included during model development.

Despite minimising ΣSSE, the model efficiency of five of the datasets for Polkemmet ochre is <0. For the two lowest P additions, the model is predicting too much P removed from solution at ~pH 7 and below. This indicates that adsorption by HFO is removing too much P in the model and the surface area should be reduced,

however doing this increases the overall ΣSSE. For the three remaining datasets that were modelled, 72.7, 109.0 and 218.0 mg P L^{-1} the model captures the overall trend of the observed data well, but model efficiency is less than 0. This is because the mean of the dataset would actually give a very high fit through the observed data. This reflects the result of previous research on Polkemmet ochre indicating that P removal by the ochre is independent of pH (Heal et al., 2003b).

The range of data derived from the batch experiment for Polkemmet ochre is limited. For pH conditions above pH 7, data is only available for the two lowest P additions, therefore mechanisms of P removal can only be commented on below pH 7. Adsorption onto HFO gives a relatively good fit to the observed datasets, with the exception at the two lowest P additions where the model removes too much P from solution between pH 3-7. This indicates that adsorption onto HFO may be removing too much P in the model. Reducing this leads to a decrease in fit at higher pH values which may be indicative of an adsorption mechanism not being in the model which would remove P under high pH conditions, e.g. adsorption onto calcite.

5.7.6 Silkstone ochre

As with the other ochres, Ca minerals were incorporated into the model for Silkstone ochre in an attempt improve the model fit. The introduction of Ca minerals did not improve the model and were therefore not included in the final design. The finalised model for Silkstone ochre was not altered from that developed in the initial model fits, with HFO-SA set at 450 m^2 g^{-1} (Figure 5.9). The improved fit at a HFO surface area of 450 m^2 g^{-1} rather than that suggested in the literature (600 m^2 g^{-1}; Dzombak and Morel, 1990) may suggest that either the amount of HFO in Silkstone ochre has been overestimated from the ammonium oxalate extraction or that the surface area of the HFO is lower than 600 m^2 g^{-1}.

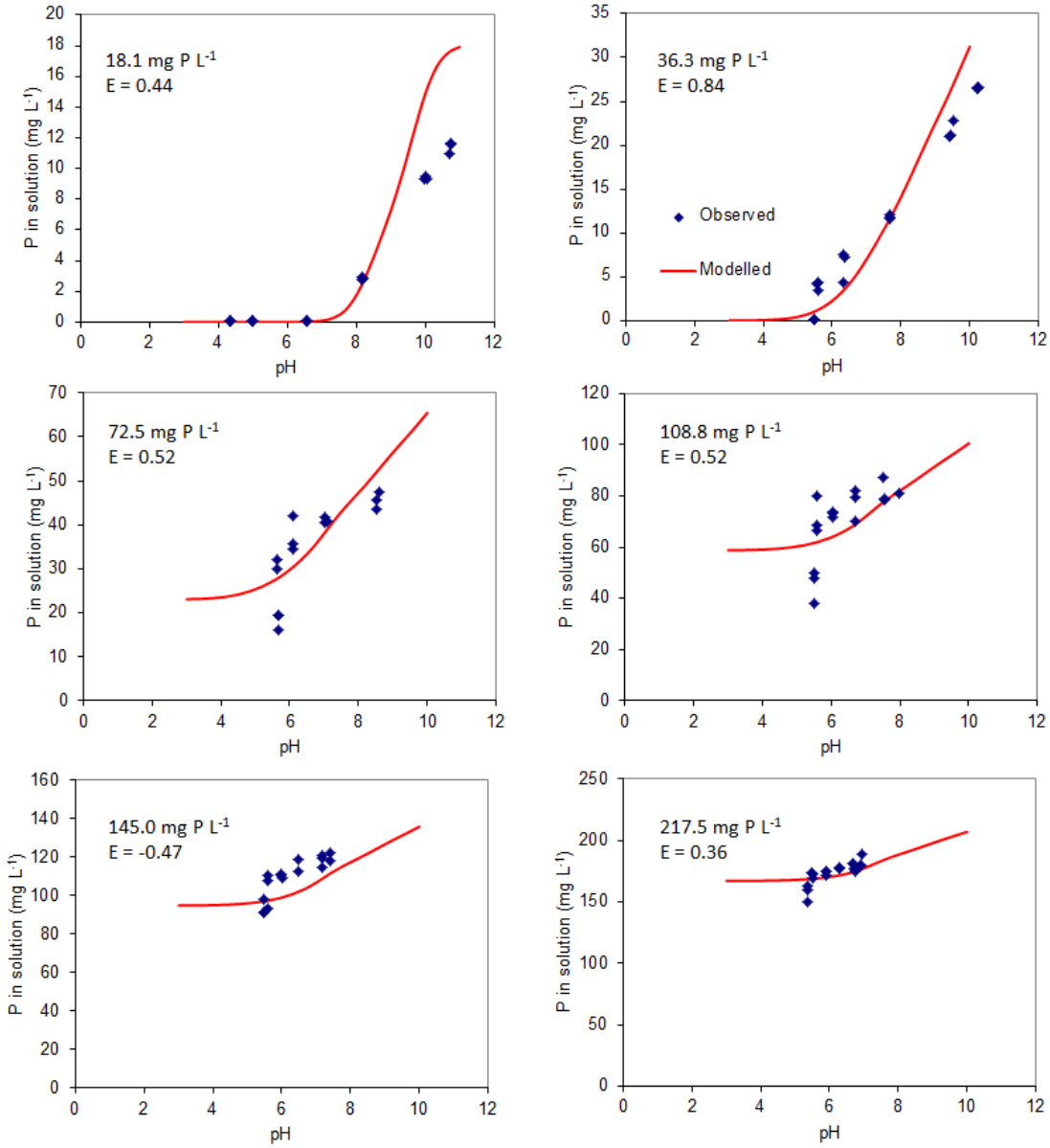

Figure 5.9: Final model fits to observed data for Silkstone ochre. HFO-SA = 450 m^2 g^{-1}. P addition of the observed datasets and model efficiency (E) is noted on each graph.

Model efficiency is greater than zero for all but one of the datasets, 145.0 mg P L^{-1}, indicating a good fit between the modelled data to the observed. The overall high fit of the model suggests adsorption onto the surfaces of HFO is the dominant P removal mechanism for Silkstone ochre.

5.7.7 Ynysarwed ochre

The initial model runs did not fit well to the observed datasets for Ynysarwed ochre (Figure 5.11), with the model predicting more P in solution under high pH conditions than in the observed dataset. To rectify this, Ca minerals were incorporated into the model in an attempt to reduce the ΣSSE (Table 5.11). Whilst the addition of brushite made no difference to the model fit, allowing the formation of OCP in the model greatly increased the fit of the model to the observed data.

Table 5.11: The effect of introducing Ca minerals into the model for Ynysarwed ochre.

Ca mineral		**HFO surface area (m^2 g^{-1})**			
		600	650	700	750
None	ΣSSE	323.1	289.3	267.9	258.1
OCP		60.7	55.8	62.5	80.1
Brushite		323.1	289.3	267.9	258.1
Both Ca minerals		60.7	55.8	62.5	80.1

The model produces a good fit to the observed data at all the tested HFO-SA areas with the optimum model fit when HFO-SA was set at 650 m^2 g^{-1} when OCP was allowed to form (Figure 5.10). Model efficiency is greater than zero for four of the P addition datasets for Ynysarwed ochre suggesting a good fit of the model to the observed data. The model does not describe the observed dataset well for P addition 34.9 mg P L^{-1} at high pH values, predicting too much P in solution in comparison to the observed dataset.

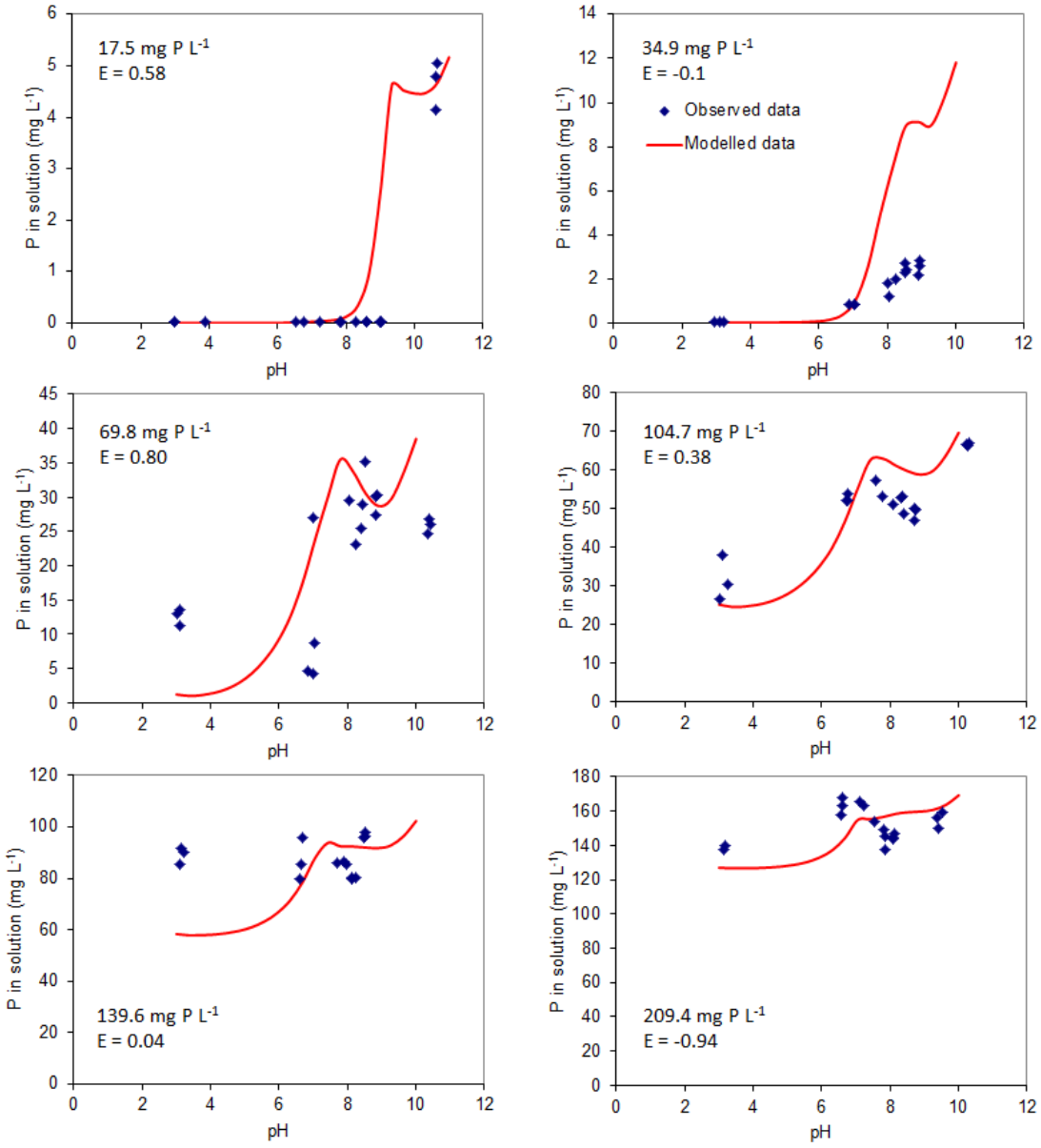

Figure 5.10: Final model fits to observed data for Ynysarwed ochre. HFO-SA = 650 m^2 g^{-1}. P addition of the observed datasets and model efficiency (E) is noted on each graph.

The model fits well to the observed dataset indicating that adsorption onto HFO surfaces and the formation of OCP describe the system well. The model was run between pH 6-8, conditions typical of P enriched wastewater streams to investigate the relative importance of P adsorption onto HFO surfaces and OCP formation (Figure 5.11). OCP was only formed at pH 8 and when P concentrations in the

overlying solution were high. As wastewaters typically have P concentrations < 15 mg L^{-1}, P adsorption onto HFO will be the dominant P removal mechanism for Ynysarwed ochre.

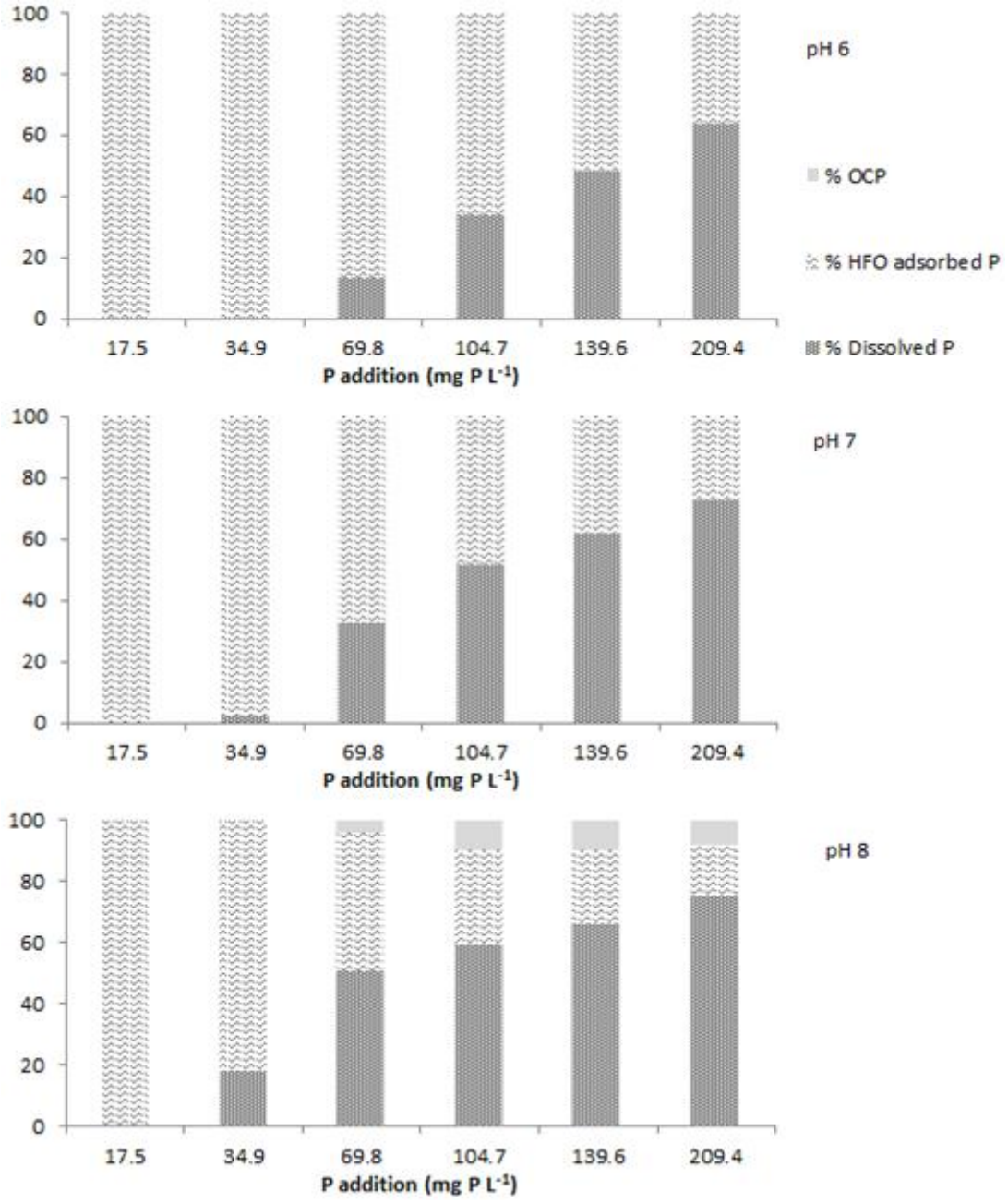

Figure 5.11: Comparison of P removal by adsorption onto HFO and the formation of OCP for Ynysarwed ochre between pH 6 and 8, determined from the ORCHESTRA model.

5.8 Summary Discussion

The use of a chemical model in ORCHESTRA has helped in the development of a more detailed understanding of the mechanisms involved in the removal of P by ochre. Data for four of the ochres (Acomb, Avoca, Polkemmet and Silkstone) was described well by the HFO adsorption model, with HFO surface area altered to optimise fit with the observed dataset. Allowing minerals to form for these ochres did not improve the fit between the modelled and observed datasets. For Acomb ochre, it is suggested that another P removal mechanism may be required to remove P at high pH conditions. This mechanism of removal may be adsorption onto calcite, which is present in the ochre as a minor component.

For Minto and Ynysarwed ochre, the introduction of Ca-P minerals improved the model fit to the observed dataset. Brushite and OCP were allowed to form in the Minto ochre model, with P removal due to mineral formation compensating for decreasing P adsorption onto HFO surfaces as pH increases. This leads to total P removal by Minto ochre being constant, although the relative importance of the removal mechanisms changes with pH. OCP was allowed to form in the model for Ynysarwed ochre leading to a large reduction in ΣSSE. Analysis of the P removal mechanisms between pH 6 and 8 found that OCP formed at pH 8 and for P additions higher than 34.9 mg P L^{-1}.

The modelling of Acomb pellets was largely unsuccessful. Model fits were improved by allowing magnesium phosphate and newberyite minerals to form, but Ca- and Mg- P aqueous species had to be removed to achieve any significant improvement to the model fit. XRD analysis of the pellets show calcite to be a major mineral component of the ochre and it is suggested that P adsorption onto calcite surfaces may be a major removal mechanism which could not be accounted for in this model.

An improvement to the model fitting process could occur by the utilising a statistic which penalises models for using an increased amount of fitting parameters, such as AIC, rather than model efficiency (E). This would prevent the model from becoming over-trained, i.e. if parameters are added to the model which only partially increase fit the fitting statistic may indicate a decrease in the goodness of fit. Further, having trained the model to the data from the batch experiment data it would be beneficial to validate the model by running a further set of batch experiments, with differing experimental conditions, to observe the fit of the trained model to an independent dataset. This would give a better assessment of the model performance than just the test statistics from the model calibration.

Chapter 6
Column experiments

P removal by ochre from solution has been examined in batch experiments over a sweep of pH, for a range of ochres and in the presence of competing ions (Chapter 4). Whilst these laboratory batch experiments indicate the potential of ochre to remove P, in-field filter applications will need to cope with flow-through transport conditions when the kinetics of diffusion and adsorption will play a role.

In a move towards field conditions, column experiments were designed to investigate P removal by two ochres over a range of conditions. Polkemmet ochre and Acomb pellets were selected due to their coarse grained composition making them suitable for use as a filter substrate owing to their relatively high hydraulic conductivity.

A number of variables were tested to examine their effect on P removal by ochre, namely ochre type, flow rate, the presence of competing ions, the effect of a rest period, and for Acomb pellets the effect of altering the pH of the influent. A longer term P removal column experiment was also conducted using a column packed with Polkemmet ochre.

The hydraulic properties of the packed columns were examined by running non-reactive tracers through the columns and modelling the observed dataset in the transport model STANMOD (Studio of Analytical Models). The dispersion coefficients of the packed columns under the two trial flow rates were calculated. This allowed the P removal breakthrough experiments to be parameterised and modelled in STANMOD to determine retardation of P by ochre as well as the partition coefficient, K_d.

6.1. Column experiment methodology

Experiments utilising a column packed with a proposed filter substrate, into which a solution containing the target species is passed through is a commonly used technique to assess P removal (Mann, 1997; Geohring et al., 1999; Johansson, 1999). A variety of Fe-based substrates have been tested for P removal, each with very different column set-ups (Zeng et al., 2004; Streat et al., 2008; Sibrell et al., 2009; Moelents et al., 2011), such as variations in column size, flow rate, influent concentration and whether upward or downward flow conditions are used. There is therefore no set design standard for column experiments, but the experiment should reflect expected field conditions.

An experimental set-up using an upward flow column system, which was originally designed for producing de-ionised water, was adapted to suit the needs of this study. Solutions were allowed to flow into the column set-up from a header tank with flow into the column restricted by use of a pressure regulator. The header tank was kept at a constant head by pumping solution into the tank with an overflow to remove excess solution. The flow rate through the system was adjusted by use of the pressure regulator and such adjustments were required throughout the experiments to ensure the target flow rates were achieved.

6.1.1 Experimental column set-up

An issue often affecting the performance of filter units is the development of preferential flow paths leading to solution being able to bypass a large proportion of the filter substrate. A common attempt to negate this is the use of an upward flow system, which was adopted for this experiment. The column set-up utilised is shown in Figure 6.1. Solution was pumped from the storage tank (a) using a peristaltic pump (b) into a header tank (c) which feeds the column. To control flow, a constant head of solution in the header tank was required. Constant head was maintained by ensuring the flow rate into the header tank from the pump (b) was

higher than that leaving the system (g). An overflow (d) was installed removing any excess solution in the header tank resulting in a constant head.

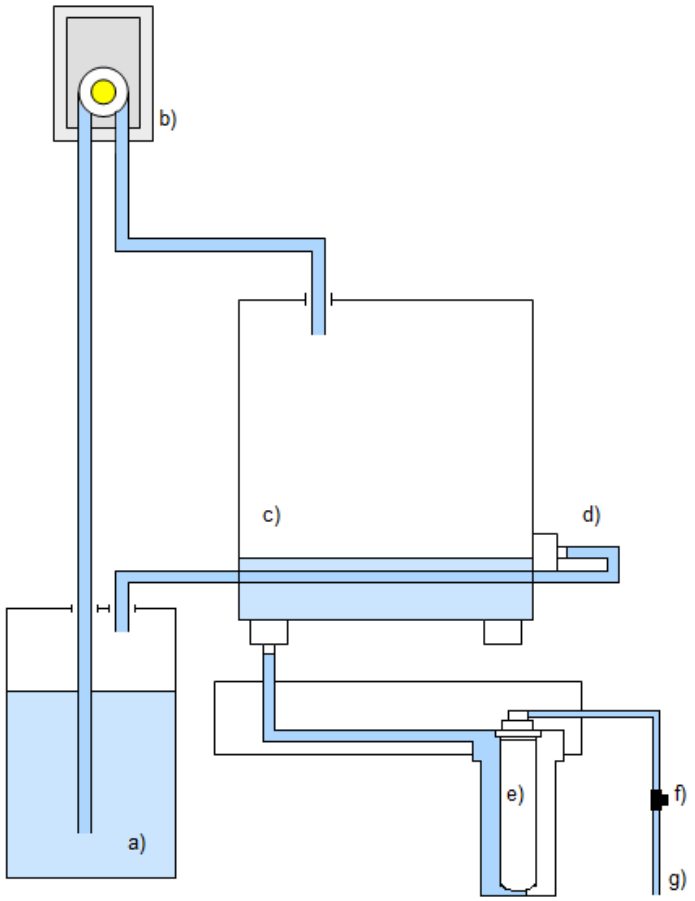

Figure 6.1: Experimental set-up used for the column experiments.

Solution was allowed to flow from the header tank into the column experiment (e) under gravity, flowing upwards through a cylindrical PVC column packed with ochre, with a radius of 3.35 cm, length of 30 cm and a volume of 1055 cm^3. A further control was put on the system so that flow rate could be adjusted; a pressure regulator (f). By adjusting the tap on the pressure regulator the flow rate of the experiment could be altered. A tap on the exit of the header tank which feeds the column set-up allows the experiment to be switched off when required.

Experiments were conducted at two target flow rates; "high flow", representing a short contact time of ten minutes, and "low flow", twenty to thirty minutes contact

time. These flow rates are indicative of those that may be required in the treatment of flow from a septic tank, a potential source of P that could be treated with ochre filters. Flow rate in the experiments drifted from that originally set as conditions in the column changed over time and therefore adjustments were made using the pressure regulator to ensure the targeted flow rate was maintained.

Ochre was packed into the columns by pouring the selected grain size into the column, closing it and then gently shaking the column by hand, allowing more ochre to be packed into the column as the agitation leads to sorting. To determine packing density, the columns were packed on five separate occasions, with the mean packing density displayed in Table 6.1. The maximum possible amount of ochre was packed into the columns as under field conditions it is envisaged that filter units would be tightly packed to give the maximum possible lifespan. It was ensured that this was conducted in a consistent manner for all columns, using the same technique and packing a similar mass of ochre.

Table 6.1: Mean packing density and void space for the ochres under study.

Ochre	Grade (Diameter, mm)	Packing Density (g cm^{-3})	Pore Space (cm^3)
Acomb pellets	5.6-9.5	1.022	490
Polkemmet	2.8-8.0	0.765	661

In order to calculate target flow rates based upon contact times, the available pore space of the columns was calculated. A column was packed with each ochre, closed and then sealed at one end. Measured volumes of water were then poured into the column to calculate the void space (Table 6.1). The column was then opened, emptied and cleaned, with five replicates occurring for each ochre.

6.1.2 Test conditions

P removal by packed columns of ochre was tested over a range of conditions. Firstly two different ochres were used; Polkemmet ochre and Acomb pellets. Both these

ochres have a coarse grain size in comparison with the other ochres under study but have very different P removal properties. The ochres were sieved to remove any fine and very coarse material, with Acomb pellets sieved to 5.6-9.5 mm as this is the target dimension of the pelletisation process. Polkemmet ochre was sieved to a coarse fraction; 2.8-8.0 mm to ensure a high hydraulic conductivity.

From the batch experiments (Chapter 4) it was found that Polkemmet ochre has a consistent P removal capacity across pH 6-8, the conditions expected in the column experiments, of ~11 mg P g^{-1}. The P adsorption capacity of Acomb pellets varies with pH, with the capacity lowest around neutral pHs. However, even at its lowest at pH 6, the P adsorption capacity of Acomb pellets is 34.5 mg P g^{-1}.

Column experiments were run at two target flow conditions; high and low. These flow rates were calculated to give two residence times in the column, ten minutes (high flow rate) and 20-30 minutes (low flow rate). The packed column of Acomb pellets has a pore space of 490 cm^3 (Table 6.1) and therefore the target high flow rate corresponds to 49.0 mL min^{-1} (83.6 cm hr^{-1}) and the low flow rate 16.3-24.5 mL min^{-1} (27.8-41.8 cm hr^{-1}). Polkemmet ochre has a pore space of 661 mL, with associated target flow rates of 66.1 mL min^{-1} (112.8 cm hr^{-1}) and 22.0-33.0 mL min^{-1} (37.5-56.4 cm hr^{-1}). Trials to investigate the effect of "high flow" rates on P removal by the ochres were conducted using a ~10 mg P L^{-1} solution made up using KH_2PO_4 dissolved in de-ionised water (Table 6.2). All other trials were conducted at the lower target flow rate.

The P concentration selected was based upon that typically found in septic tank effluents and highly polluted wastewater streams. Solution was pumped into the header tank from the storage tank, which was emptied and replenished with solution every 12 hours. Samples of the influent were taken each time the solution was replaced in the tank and analysed for total orthophosphate concentration at the James Hutton Institute, Aberdeen, method described in Chapter 4.2.2.

Table 6.2: Column experiment test conditions; SynS denotes synthetic sewage solution (~10.5 mg P L^{-1}), Ac: Acomb pellets, Po: Polkemmet ochre. Each trial is numbered for future reference in brackets. All trials were run for a period of four days unless otherwise stated in the text.

Influent/ Column conditions	**Flow rate**	
	High	**Low**
~10 mg P L^{-1} solution	Ac (T_A), Po (T_1)	Ac (T_B), Po (T_2)
SynS	-	Ac (T_C), Po (T_3)
SynS with rest	-	Ac (T_C*), Po (T_3*)
SynS, pH altered	-	Ac (T_D)
SynS, pH altered, with rest	-	Ac (T_D*)

The effect of competing ions on P removal was investigated for both ochres utilising a synthetic sewage (SynS) solution containing ~10.5 mg P L^{-1} in the form KH_2PO_4. Adapted from the Department of the Environment (1981) guidelines, SynS was made up in de-ionised water and contained 160 mg L^{-1} peptone, 110 mg L^{-1} meat extract, 30 mg L^{-1} urea, 7 mg L^{-1} sodium chloride, 4 mg L^{-1} calcium chloride dehydrate and 2 mg L^{-1} magnesium sulphate heptahydrate.

Following the trials utilising SynS solution, the columns were drained and rested for 48 hours to investigate whether this led to an increase in P removal by the ochre substrate. Sibrell et al. (2009) suggest that resting a packed column of acid mine drainage sludge between P solution applications may increase the P removal capacity of the material. The effect of resting allows P adsorbed on the surface of the ochre to diffuse into the structure of the ochre regenerating highly reactive surface sites (Dzombak and Morel, 1990). When collected from a MWTP, ochre typically has a high water content. Upon drying this water is removed but the highly porous structure remains; it is therefore suggested that the pore structure of the ochre could play a major role in the P adsorption rate and capacity of the ochre (Sibrell et al., 2009). Following the resting period, the columns were reinstalled and SynS solution passed through the column for 48 hours.

The results of the batch experiments indicate that Acomb pellets are most effective at removing P from solution under acidic and basic pH conditions. To investigate whether this is the same in a packed column, a further trial was conducted using a SynS solution with an adjusted pH of ~10 by the addition of 2.05 mL 0.1 M NaOH. Following this, the column was drained and rested for a period of 48 hours. The column was then reinstalled and the pH adjusted SynS solution passed through the column for a further 48 hours.

Column experiments were run continuously but samples were only taken between 9 am and 9 pm. The experiments were initiated at 9 am and systematically sampled from the pipe exiting the column set-up. On the first day of a column experiment samples were taken after 0.5, 1, 1.5, 2, 4, 6, 8 and 12 hours, with samples the following days taken approximately every two hours. Samples were filtered through 0.45 μm cellulose filter paper into polypropane containers and stored at 4°C for no more than seven days prior to analysis for total orthophosphate P. Effluent samples were also analysed for pH using a bench top probe which was calibrated between uses with appropriate pH buffers.

6.2 Chloride tracer experiments

Non-reactive tracer experiments were conducted to garner information on the transport kinetics and hydraulic parameters of the packed columns of ochre at the two target flow rates. Data collected from these experiments was analysed using STANMOD to calculate the transport parameters of the packed columns. The derived dispersion coefficients were then utilised for parameterising transport models for the P removal column experiments.

6.2.1 Transport kinetics

As previously noted, adsorption onto Fe-oxides is a two-step process, with rapid initial adsorption occurring on the particle surface area followed by a much slower approach to equilibrium resulting from intra particle diffusion (Dzombak and

Morel, 1990). Due to this a dual porosity transport model was adopted to fit to the observed data collected from the Cl^- tracer experiments.

Two pilot studies were run whereby de-ionised water was allowed to flow through the experimental set-up with packed columns of either Polkemmet ochre or Acomb pellets. Effluent was collected in a 50 mL receptacle which was continuously analysed for conductivity, used in this study as an analogy for Cl^- concentration, using a conductivity sonde. De-ionised water was passed through the columns until conductivity remained at a constant value for five minutes with background conductivities of ~80 to 120 $\mu S\ cm^{-1}$ found for the columns. Based on this, a Cl^- solution with a much higher conductivity was used for the tracer experiments; 0.1 M NaCl.

6.2.2 Chloride tracer experiment methodology

De-ionised water was passed through the column under study until a constant background concentration of conductivity was recorded (~80-120 $\mu S\ cm^{-1}$). Following this, the tap on the header tank was switched off so that it could be emptied and filled with 0.1 M NaCl solution, as was the solution in the storage tank. The header tank tap was then turned on allowing solution to flow through the column and the conductivity of the effluent was measured continuously. Measurements continued until conductivity reached and maintained a maximum (~11 $mS\ cm^{-1}$) for a period of two minutes. The header tank was then switched off and the experiment paused whilst the Cl^- solution in the header and storage tank was replaced with de-ionised water. The experiment was then resumed and conductivity measurements taken until the baseline conductivity value was achieved.

6.2.3 Determination of column hydraulic parameters

The breakthrough curves calculated from the Cl^- tracer experiments were modelled using a transport model within the STANMOD suite. STANMOD is public domain

modelling package suitable for evaluating solute transport in porous media. Within STANMOD, the CXTFIT model (Version 2.0) was utilised (Toride et al., 1995). This model allows transport parameters to be estimated using a least-squares optimisation method. An inverse modelling approach was utilised, whereby the optimal transport parameter values are calculated iteratively by fitting the transport model, based on the convection-dispersion equation, to the observed dataset.

Using the general user interface (GUI) in STANMOD, the experimental conditions were inputted. Time and concentration were set as dimensionless, therefore the inputted data from the Cl^- tracer experiments needed to be adapted prior to use in the model. Time data was converted using flow rate into pore volumes (Pv) which had passed through the column. Concentration data was converted by dividing effluent concentration by influent concentration (C_{out}/ C_{in}) to give a value between 0 and 1.

Five transport parameters were used to fit the model; the pore water velocity (v), the dispersion coefficient (D), the retardation factor (R), the coefficient of portioning between the equilibrium and non-equilibrium phases (β) and the mass transfer coefficient (ω) for the transfer between the equilibrium and non-equilibrium phases (Toride et al., 1995).

Pore-water velocity (v) was calculated for each experiment (Equation 6.1) and it was therefore a fixed constant in the model.

$$v = \left(\frac{Q/A}{C_{pore}/V}\right) \qquad \text{Equation 6.1}$$

Where; Q is the flow rate through the column ($cm^3\ hr^{-1}$), A is the cross sectional area of the column (cm^2), C_{pore} is the pore space in the column (cm^3) and V is the volume of the column (cm^3). The retardation factor is a coefficient which accounts for the

removal of the solute by the column by chemical processes. As no removal of Cl^- is expected by the packed column, R was set at 1.

D, β and ω were all calculated iteratively by fitting the transport equations in the CXTFIT code to the observed dataset and minimising the sum of squares.

6.2.4 Chloride tracer results

The raw datasets generated from the Cl^- tracer experiments needed to be adjusted for use in STANMOD. Firstly any dead Pv need to be removed from the dataset (Figure 6.2); the amount of de-ionised water remaining in the column set-up from achieving a constant background conductivity reading. This was calculated as the volume of the tubing connecting the header tank to the column (75 cm^3) and the available volume in the column casing (250 cm^3), a total of 325 cm^3. Once this volume of solution had been collected from the experiment it was assumed that Cl^- solution had begun flowing through the column.

A pulse of 0.1 M NaCl was passed through the column until a constant effluent conductivity was achieved for a period of two minutes. Following this, the experiment was switched off with the solution drained from the header tank and storage reservoir and replaced with de-ionised water. The volume of Cl^- solution that is passed through the column experiment can therefore be calculated as the volume remaining in the column casing (250 mL), added to the volume remaining in the column (one PV) and the volume passed through the column until a constant conductivity reading was achieved.

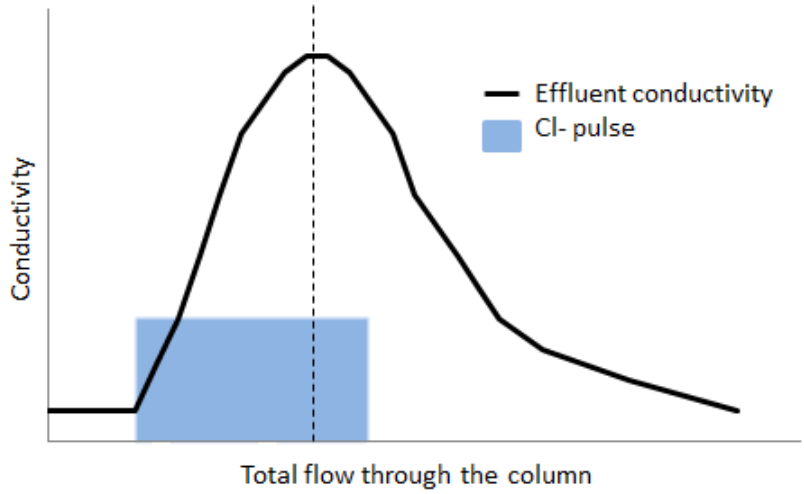

Figure 6.2: Theoretical Cl^- breakthrough curve for column experiments: Dashed line indicates conductivity has reached a constant value. Dead Pv can be seen at the start of the graph before the Cl^- pulse.

Conductivity was used as a surrogate for Cl^- concentration in the column effluent. Conductivity can be measured in real time and sampling for Cl^- would have resulted in a very large number of samples resulting in a high analysis cost. Effluent was collected in a 40 mL vial with conductivity measured using a conductivity probe. Conductivity was linearly converted to Cl^- concentration using Equation 6.2.

$$E_c = I_c(E_\kappa - \frac{B_\kappa}{I_\kappa}) \qquad \text{Equation 6.2}$$

Where; E_C is the Effluent concentration, I_C the influent concentration, E_κ the effluent conductivity, B_κ the background conductivity and I_κ the influent conductivity.

6.2.4.1 Polkemmet ochre

Cl^- tracer experiments were conducted for packed columns of Polkemmet ochre at the two target flow rates, high (66.1 mL min^{-1}) and low (22-33 mL min^{-1}). Summary data from these experiments is shown in Table 6.3.

Table 6.3: Summary statistics from the Cl^- tracer experiments for columns packed with Polkemmet ochre. R^2 is the coefficient of determination for the fitting of the model to the observed dataset. For the modelled parameters; v and R were fixed variables, with D, β and ω solved iteratively by the model.

Flow statistic	Flow rate	
	High	Low
Average flow rate (L hr^{-1})	3.5	1.7
Experiment duration (Pv)	15.6	14.6
Max. Cl^- effluent conc. (g L^{-1})	3.5	3.5
Pv to max. Cl^- conc.	6.29	3.8
C_{out}/ C_{in} =0.5 (Pv)	1.47	0.96
Cl^- recovered (%)	86	87
R^2	0.89	0.90
v	159.6	78.14
D	190.0	64.9
R	1	1
β	0.0250	0.0001
ω	0.02	6.71

The CXTFIT model in the STANMOD suite was fitted to the observed dataset for the Cl^- breakthrough curve recorded under high flow conditions (Figure 6.3). The main discrepancy between the observed dataset and the modelled result is in the shape of the rising limb; the modelled result having a higher gradient than the observed dataset. The gradient of the modelled falling limb fits well to that of the observed dataset. The fitted transport parameters for this flow rate are presented in Table 6.3.

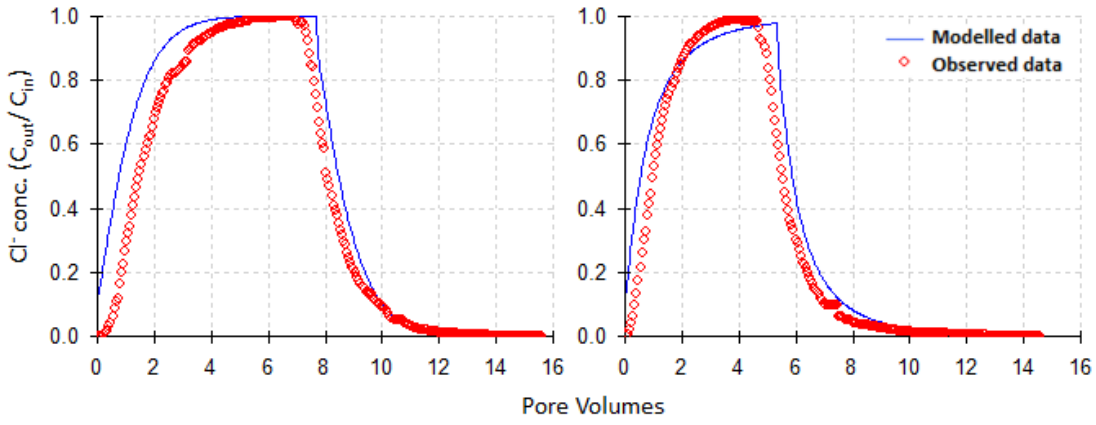

Figure 6.3: Non-reactive tracer breakthrough curve for a column packed with Polkemmet ochre under high flow conditions (L) and low flow conditions (R).

The Cl^- breakthrough experiment was also conducted for a packed column of Polkemmet ochre under low flow conditions, with this data modelled to derive transport parameters (Table 6.3, Figure 6.3). The Cl^- concentration in the observed dataset reaches a peak concentration at around 4 Pv, whilst the model reaches a lower peak concentration at around 5.5 Pv. The rising limbs of the two curves also have a different shape, with the observed dataset having a higher gradient. In contrast, the falling limbs of the two curves are very similar with the difference that the falling limb of the observed data is initiated after less Pv.

6.2.4.2 Acomb pellets

As with the columns packed with Polkemmet ochre, Cl^- tracers at both the flow rates utilised in the Acomb pellet P removal studies were conducted. The CXTFIT model was then fitted to the observed dataset. Summary data and optimised model parameters from these experiments are shown in Table 6.4.

Table 6.4: Summary statistics from the Cl^- tracer experiments for columns packed with Acomb pellets. R^2 is the coefficient of determination for the fitting of STANMOD to the observed dataset. For the modelled parameters; v and R were fixed variables, with D, β and ω solved iteratively by the model.

Flow statistic	Flow rate	
	High	Low
Average flow rate (L hr^{-1})	3.3	1.4
Experiment duration (Pv)	28.7	18.2
Max. Cl- effluent conc. (g L^{-1})	3.3	3.4
Pv to max. Cl- conc.	6.6	3.1
C_{out}/ C_{in} =0.5 (Pv)	0.72	0.89
Cl^- recovered (%)	88	95
R^2	0.95	0.95
v	202.7	83.8
D	188.0	37.0
R	1	1
B	0.0001	0.0001
Ω	3.43	9.08

The observed dataset and associated model fit for Acomb pellets under high flow conditions is presented in Figure 6.4.

Under high flow conditions, the initial gradient of the rising limb and the shape of the falling limb fit the observed dataset well (Figure 6.4). The model does not fit the observed dataset well at high Cl^- concentrations. The model fit predicts a higher maximum Cl^- concentration and a longer rising limb than was observed in the experimental dataset.

The model fit under low flow conditions is an improvement to that seen for high flow conditions (Figure 6.4). The rising and falling limbs have a similar gradient and the model and observed dataset reach the same maximum Cl^- concentration. The timing of the maximum Cl^- concentration is later for the model fit, ~5 Pvs, than for than the observed dataset, ~3 Pvs.

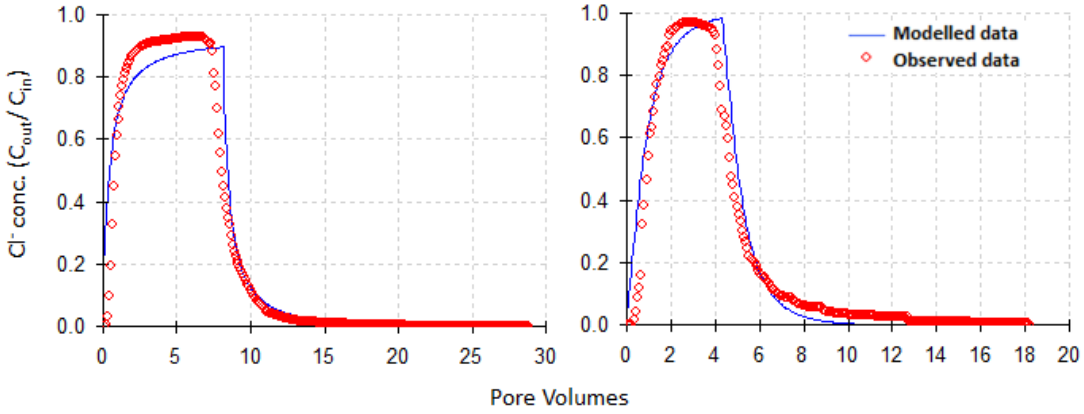

Figure 6.4: Non-reactive tracer breakthrough curve for a column packed with Acomb pellets under high flow conditions (L) and low flow conditions (R).

Overall, the modelled results for Polkemmet ochre and Acomb pellets fitted the observed Cl^- breakthrough curves relatively well and the transport parameters will be used for the modelling of the P removal column experiments. Some of the discrepancy between the observed dataset and the model may be due to the unusual design of the column experiment. The set-up has a large volume of dead pore space in the connecting pipework between the column and header tank and in the casing which surrounds the column. Whilst this dead volume has been removed from the observed dataset, it may be having an effect on the flow of the Cl^- pulse before it reaches the column. Whilst this dead volume is not a concern for long term P removal studies, conducted in timescales of days to weeks, it may have an effect on high resolution Cl^- tracer experiments which are conducted over a few hours.

An assessment of the column set-up was conducted by calculating the pvs required to achieve 50 % Cl^- breakthrough. Theoretically, the breakthrough of a conservative tracer through a system after 1 Pv should be equal to 50 %, e.g. $C_{out}/C_{in} = 0.5$ (Hoehn and Roberts, 1982). Therefore, breakthrough quicker than this (i.e. less than 1 Pv) is faster than would be expected suggesting preferential flow-paths forming or there is sources of tracer in the column substrate. Alternatively, values slower indicate the possibility of sinks or delays due to sorption. Of the tracer experiments conducted,

C_{out}/C_{in} =0.5 occurred at greater than 1 Pv for Polkemmet ochre under high flow conditions, at 0.96 Pvs for Polkemmet under low flow conditions, and below 1 for both Acomb pellet trials (Table 6.3, 6.4).

Pv values lower than 1 may suggest that the pore volume of the column is less than was calculated empirically (Table 6.1). However, the methodology utilised to determine Pv, filling the column with measured volumes of solution, indicates this is not so, i.e. it is not possible to fill a column with more solution than the available pore space. Therefore the tracer must be moving through the column faster than expected due to some other factor or experimental design flaw, such as a high rate of vertical diffusion, preferential flow paths becoming established, sources of conductivity being released from the column substrate, or due to the variability of the flow rate utilised.

The breakthrough of Cl^- through Polkemmet ochre at high flow conditions was slower than expected (C_{out}/ C_{in} = 0.5 at 1.47 Pv). This suggests that the pore space in the column may have been underestimated. This result is inconclusive however as under the low flow conditions 50 % breakthrough occurred at ~1 Pv. The result may be due to Cl^- being retarded through the column, or due to the variable flow rate of the experiment. Utilising this data, the pore volume of the column could be recalculated, i.e. flow passed through the column when C_{out}/ C_{in} =0.5. Due to the inconclusive nature of the results, Pv was kept as calculated empirically for each ochre, Table 6.1.

6.3 P removal column experiments

P removal from solution by columns packed with ochre was tested over a range of conditions, by altering the flow rate of the experiment, changing the solution composition, and by incorporating a rest period (Table 6.2). Effluent samples were standardised to C_{out}/ C_{in} which is calculated by dividing the P concentration of the effluent by that of the influent.

6.3.1 Polkemmet ochre

P removal by a packed column of Polkemmet ochre was tested under a variety of conditions. Summary statistics from these trials indicate the relative effectiveness of Polkemmet ochre at removing P from solution (Table 6.5). P removal efficiency (%) is a proportional figure of the amount of P which was removed from solution by the packed columns. T_1, which was operated at a relatively high flow rate allowing for a target residence time of ten minutes, had the lowest P removal efficiency, 33%. The highest effluent concentration, C_{out}/ C_{in}, was also noted in T_1; 0.73. The highest P removal efficiency was found in T_2. This trial targeted a relatively low flow rate with a residence time of between 20 and 30 minutes with no competing ions in solution. T_2 had a P removal efficiency of 70% with C_{out}/ C_{in} reaching a maximum of 0.51.

Table 6.5: Summary results for column experiments investigating P removal by Polkemmet ochre: C_{out}/ C_{in} maximum is typically at the end of the experiment.

	Column Experiment				
	T_1	**T_2**	**T_3**	**T_3***	**T_3+T_3***
Ochre in column (g)	894.4	894.4	897.9	897.9	897.9
Total through-flow (Pv)	424	227	249	118	367
Av. flow rate (L hr^{-1})	3.8	1.6	1.7	1.6	1.6
Max. flow rate (L hr^{-1})	4.6	1.9	1.9	1.7	1.9
Min. flow rate (L hr^{-1})	3.2	1.3	1.0	1.3	1.0
C_{out}/ C_{in} max.	0.73	0.51	0.53	0.43	0.53
Total P dose (mg)	3293	1749	1883	893	2776
Total P removed (mg)	1080	1226	1273	594	1867
P removal efficiency (%)	33	70	68	67	67
mg P g^{-1} ochre	1.21	1.36	1.42	0.66	2.08

P removal by a packed column of Polkemmet ochre with a target residence time of ten minutes was examined in T_1 (Figure 6.5). The flow rate drifted throughout the experiment and was corrected using the pressure regulator to ensure it was close to

the targeted flow rate. Flow varied between 3.2 and 4.6 L hr^{-1} over the experiment, at an average of 3.8 L hr^{-1}.

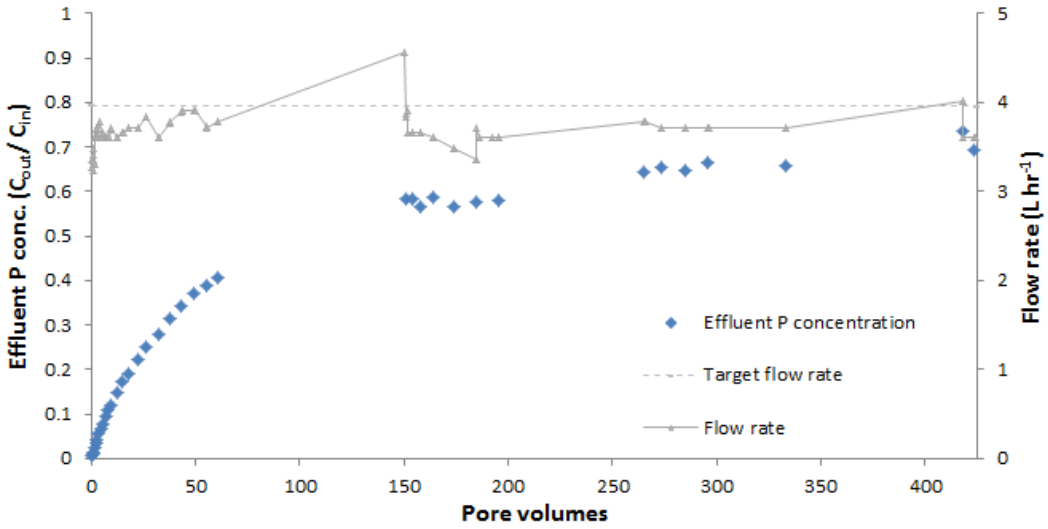

Figure 6.5: Column effluent P concentration and flow rate of solution through the column for T_1. Target flow rate indicated as a dashed line; 3.97 L hr^{-1}. P concentration 11.75 ± 0.34 (1 s.d.) mg L^{-1} from five influent samples.

The breakthrough of P in T_1 is rapid, with C_{out}/ C_{in} ~0.35 after 50 Pv and ~0.7 by the end of the experiment. The experiment was repeated with another packed column of Polkemmet ochre with a higher target residence time (20-30 minutes), T_2. The pressure regulator was used to keep the flow rate through the column between 1.32-1.98 L hr^{-1} to ensure the target residence time was achieved. P breakthrough was much slower in T_2, with C_{out}/ C_{in} ~0.2 at 50 Pv, reaching 0.51 at the end of the experiment (Figure 6.6).

Effluent P concentration increases steadily throughout the experiment, but a relationship between P concentration and flow rate can be seen during particular sampling events. For example during the sample event between ~50-75 Pv; a high P concentration is recorded in the effluent initially which correlates with the highest flow rate, following a reduction in flow rate the P effluent concentration decreases. This relationship highlights the importance of residence time, with adsorption sites removing P from solution if sufficient contact time is given.

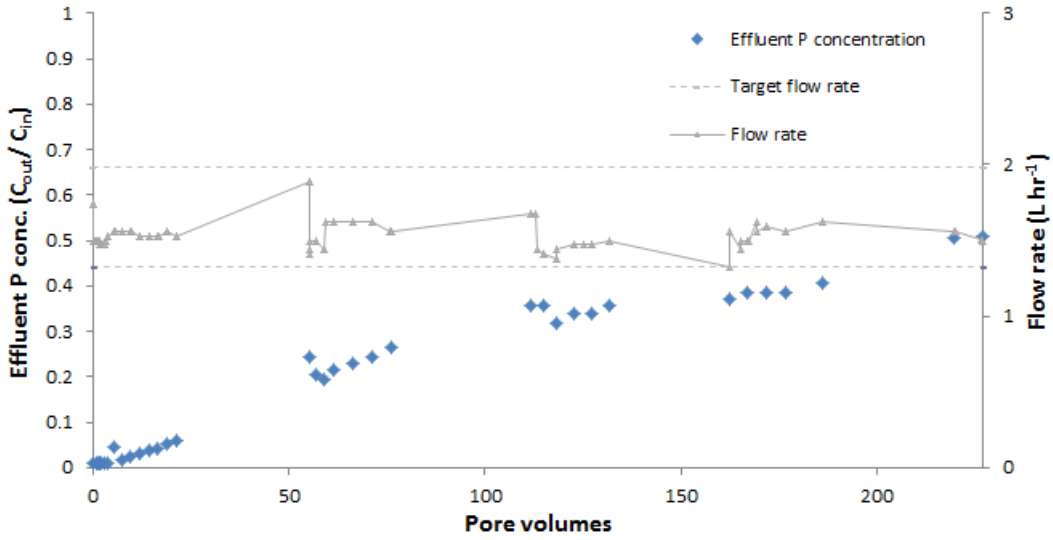

Figure 6.6: Column effluent P concentration and flow rate of solution through the column for T_2. Target flow rate indicated as dashed lines; 1.32- 1.98 L hr^{-1}. P concentration 11.66 ± 0.66 (1 s.d.) mg L^{-1} from six influent samples.

Following T_2, another column was packed with Polkemmet ochre to investigate P removal in the presence of competing ions; T_3. For comparative reasons, the designed residence time was kept at 20- 30 minutes. The breakthrough curve for T_3 is similar to that produced for T_2, with effluent P concentration increasing gradually with Pvs (Figure 6.7). As with T_2, Cout/ Cin is ~ 0.2 at 50 Pv and does not exceed 0.6 during the experiment. The average flow rate in T_3 was slightly higher than T_2, 1.7 compared to 1.6 L hr^{-1}, and this may contribute to the decreased P removal efficiency of the packed column, 68%.

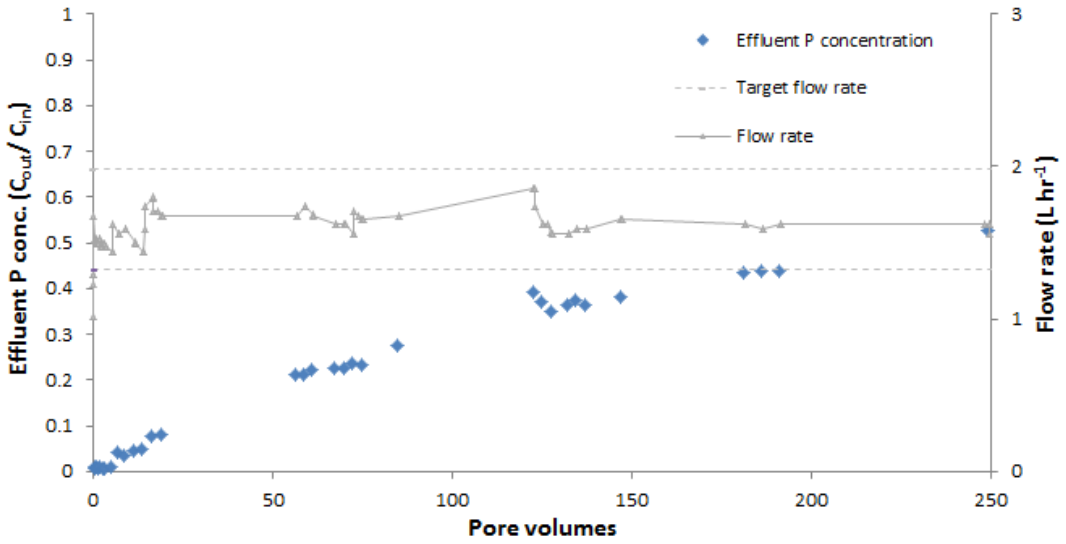

Figure 6.7: Column effluent P concentration and flow rate of solution through the column for T_3. Target flow rate indicated as dashed lines; 1.32- 1.98 L hr^{-1}. P concentration 11.43 ± 0.32 (1 s.d.) mg L^{-1} from six influent samples.

Following the completion of T_3, the column of ochre was removed from the experimental set-up, drained of solution and rested for 48 hours. Following this the column was reinstalled and SynS solution passed through the column for a further 48 hours to investigate the effect of resting the packed column on subsequent P removal.

The flow rate and P effluent concentration for this subsequent trial, T_3*, can be seen in Figure 6.8. Flow rate was fairly stable throughout the experiment, at an average of 1.6 L hr^{-1} and varying between 1.3-1.7 L hr^{-1}. Resting the column of ochre increased the P removal rate. At the termination of T_3, C_{out}/ C_{in} was 0.53, a figure that is not reached in the subsequent 118 Pv in T_3*.

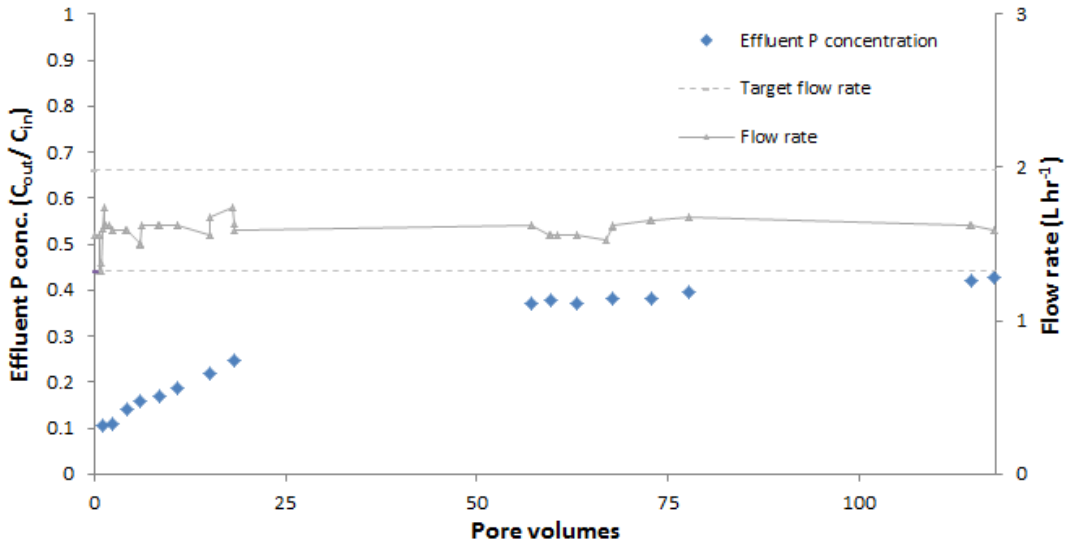

Figure 6.8: Column effluent P concentration and flow rate of solution through the column for T_3*. Target flow rate indicated as dashed lines; 1.32- 1.98 L hr^{-1}. P concentration 11.49 ± 0.18 (1 s.d.) mg L^{-1} from four influent samples.

The effect of resting the column can be better seen in Figure 6.9. By resting the column it is possible to run an increased number of pore volumes of P enriched solution through the column at a better P removal efficiency.

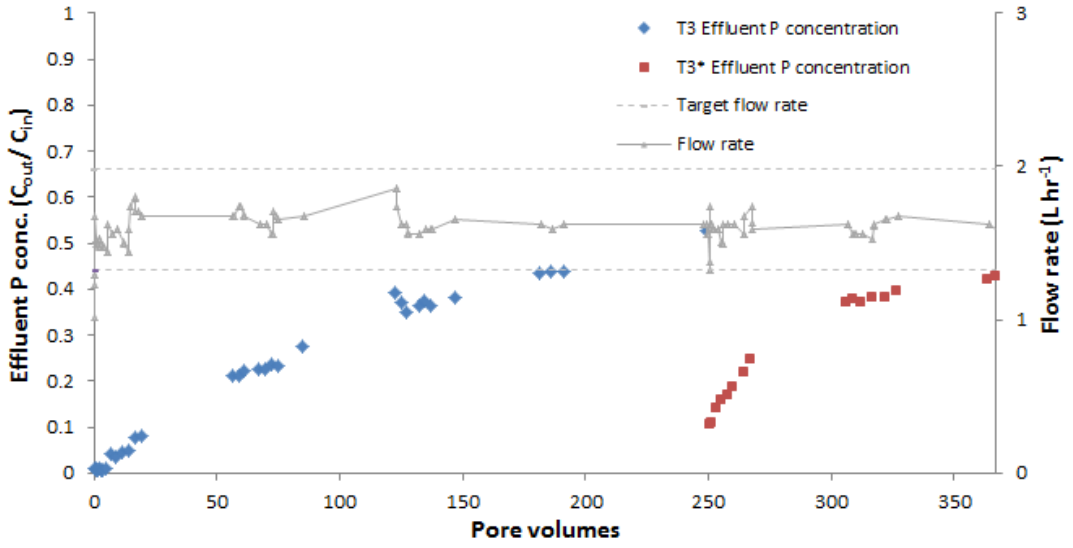

Figure 6.9: Column effluent P concentration and flow rate of solution through the column for T_3 and then T_3*. Target flow rate indicated as dashed lines; 1.32- 1.98 L hr^{-1}. P concentration 11.46 ± 0.26 (1 s.d.) mg L^{-1} from ten influent samples.

The breakthrough curves for T_2 and T_3, which were operated at the same flow rate but with T_3 having competing ions in solution have a very similar shape (Figure 6.10). The breakthrough curve of T_1 is steeper than the other trials reflecting the effect of the higher flow rate utilised in this trial. P concentration in the effluent of trial T_3* breaks through quickly, with C_{out}/C_{in} above 0.1 is less than 1 Pv.

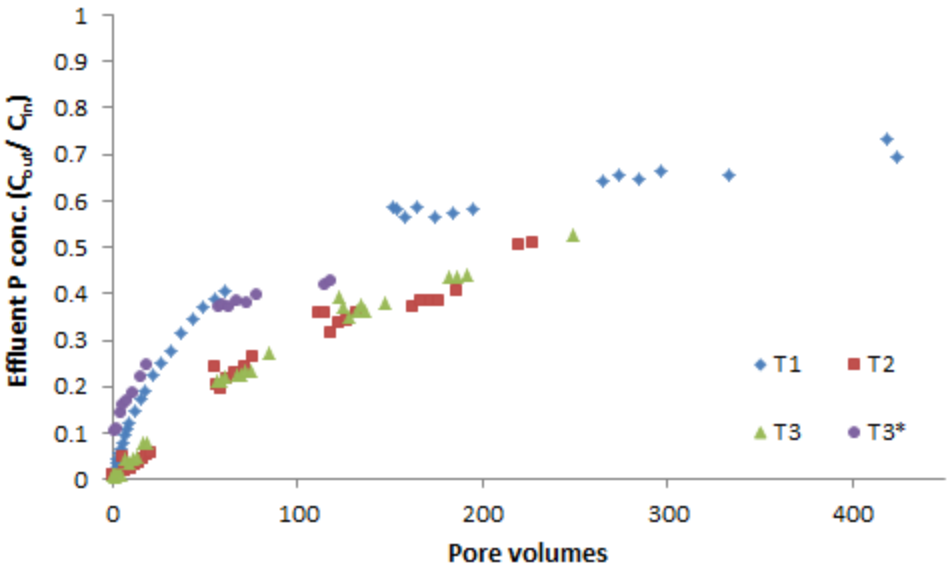

Figure 6.10: P breakthrough curves for column experiments utilising Polkemmet ochre as a filter substrate.

6.3.2 Acomb pellets

P removal by columns packed with Acomb pellets was investigated over a range of conditions as detailed in Chapter 6.1.2. Summary statistics from these trials indicate the relative effectiveness of Acomb pellets at removing P from solution (Table 6.6). P removal efficiency gives an overall indication of the proportion of P removed from solution by the ochre over the course of the various trials. The highest P removal efficiency occurred in T_D and T_D*, where the influent was pH adjusted to ~ pH 10, with 38% of the P passed through the column removed by the Acomb pellets. The lowest P removal efficiency occurred in trial T_C*, 23 %, which tested P removal by a column of rested Acomb pellets at removing P from a SynS solution. The highest effluent P concentration was noted in trial T_A, with a C_{out}/ C_{in} value of 0.86.

Table 6.6: Summary results for column experiments investigating P removal by Acomb pellets: C_{out}/ C_{in} maximum is typically at the end of the experiment.

	Column Experiment							
	T_A	T_B	T_C	T_C*	T_C+T_C*	T_D	T_D*	T_D+T_D*
Ochre in column (g)	993	974	995	995	995	1006	1006	1006
Total throughflow (Pv)	311	271	273	134	407	267	125	392
Av. flow rate (L hr^{-1})	3.1	1.3	1.4	1.4	1.4	1.4	1.3	1.3
Max. flow rate (L hr^{-1})	3.6	1.7	2.4	1.6	2.4	1.9	2.0	2.0
Min. flow rate (L hr^{-1})	1.6	0.8	1.0	1.2	1.0	0.9	0.8	0.8
C_{out}/ C_{in} max.	0.86	0.80	0.84	0.83	0.84	0.73	0.75	0.75
Total P dose (mg)	1665	1490	1456	731	2187	1470	692	2162
Total P removed (mg)	445	458	362	167	529	555	266	821
P removal efficiency (%)	27	31	25	23	24	38	38	38
mg P g^{-1} ochre	0.45	0.47	0.36	0.17	0.53	0.55	0.26	0.82

P removal by a packed column of Acomb pellets with a target residence time of ten minutes was examined in T_A (Figure 6.11). Flow rate drifted from the target of 2.94 L hr^{-1} throughout the experiment, and was corrected using the pressure regulator.

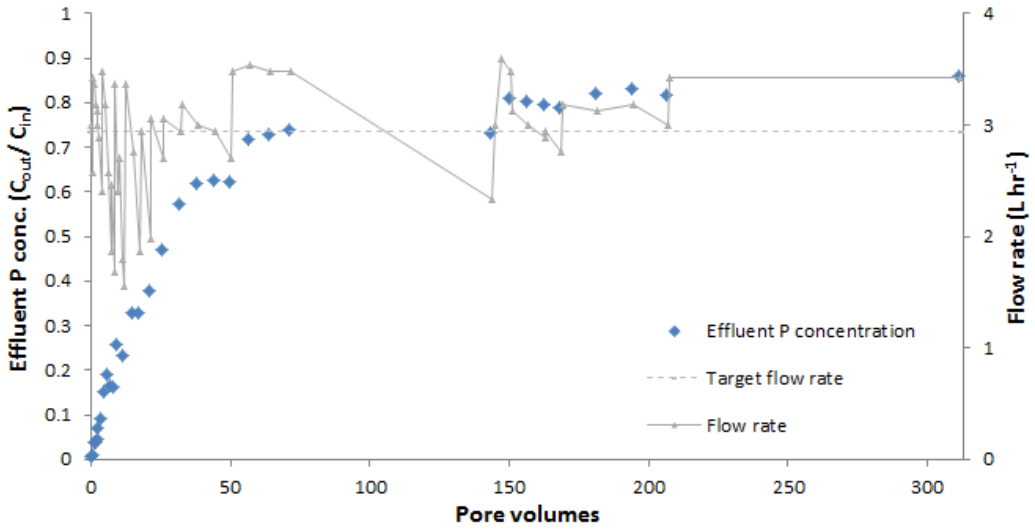

Figure 6.11: Column effluent P concentration and flow rate of solution through the column for T_A. Target flow rate indicated as the dashed line; 2.94 L hr^{-1}. P concentration 10.92 ± 0.12 (1 s.d.) mg L^{-1} from five influent samples.

The breakthrough of P is rapid in T_A, with C_{out}/ C_{in} ~0.65 after 50 Pv, with 86 % of the P in the influent breaking through the column by the end of the trial. The experiment was repeated using another packed column of Acomb pellets with a longer residence time of 20-30 minutes, T_B. The breakthrough of P for T_B is similar to that seen in T_A, with C_{out}/ C_{in} ~0.60 after 50 Pv (Figure 6.12). The P removal efficiency of the trial, 31%, is only slightly higher than the 27% removal rate in T_A which continued for a further 40 Pv.

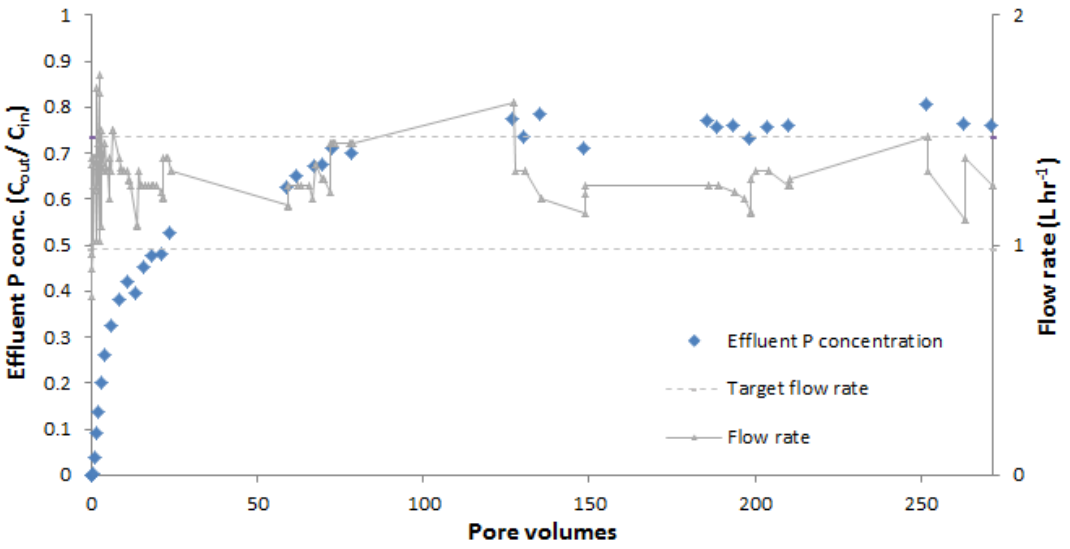

Figure 6.12: Column effluent P concentration and flow rate of solution through the column for T_B. Target flow rate indicated as dashed lines; 0.98-1.47 L hr^{-1}. P concentration 11.22 ± 0.35 (1 s.d.) mg L^{-1} from five influent samples.

Trial T_C investigated the effect of competing ions on the removal of P by Acomb pellets (Figure 6.13). For comparative reasons the target flow rate for this trial was the same as T_B, with the average flow rate recorded for T_C slightly higher than that in T_B, 1.4 compared to 1.3 L hr^{-1}. P breakthrough for trial T_C was rapid with C_{out}/ C_{in} ~0.4 after 1 Pv, reaching ~0.7 by 50 Pv and 0.84 at the end of the experiment.

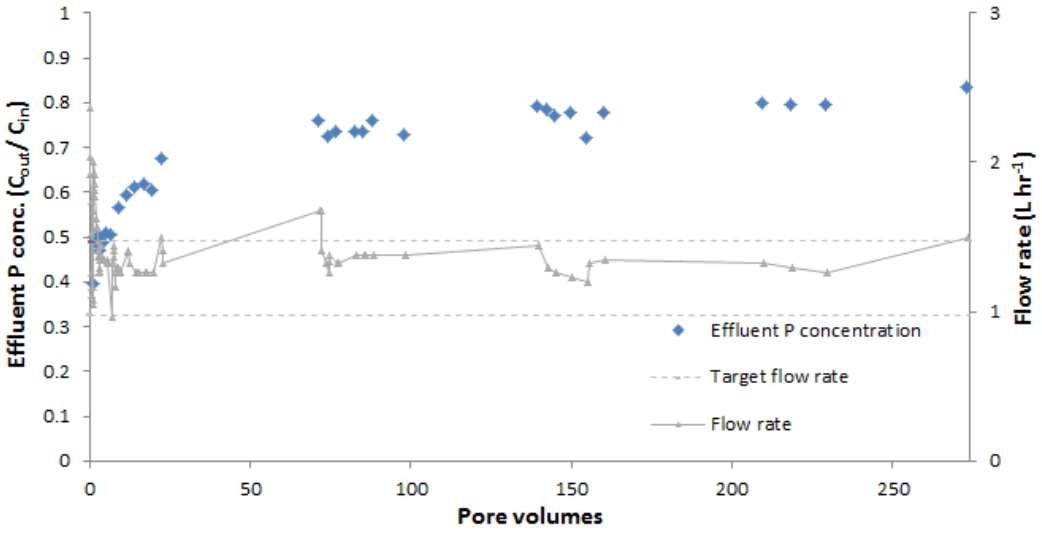

Figure 6.13: Column effluent P concentration and flow rate of solution through the column for TC. Target flow rate indicated as dashed lines; 0.98-1.47 L hr^{-1}. P concentration 10.88 ± 0.22 (1 s.d.) mg L^{-1} from five influent samples.

The trials examining the effect of competing ions on the removal of P by Polkemmet ochre suggest that competing ions had little effect on the breakthrough of P. When using Acomb pellets as a filter substrate, however, the breakthrough curve is much higher in the presence of competing ions, TC, meaning that less P is being removed by the column of Acomb pellets in the presence of competing ions. Whilst this may be as a direct effect of the competing ions, it may also be due to the pH of the influent. The effluent pH in TB is much higher than for TC as a result of the influent composition, resulting in conditions more suitable for P removal by Acomb pellets (Figure 6.14).

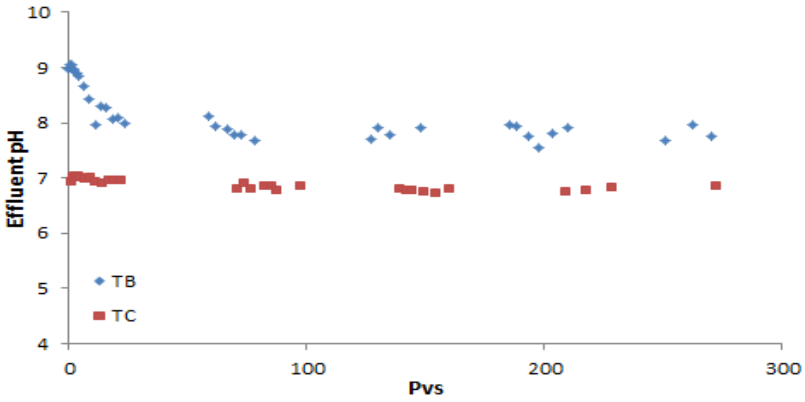

Figure 6.14: Effluent pH for column experiment TB and TC.

Following the completion of trial T_C, the column was removed from the experimental set-up, drained and allowed to rest for a period of 48 hours. The column was then reinstalled, with P enriched SynS solution passed through the column for a further 48 hours, T_C*. The P breakthrough for Tc* was rapid, with C_{out}/C_{in} ~0.4 after 1 Pv (Figure 6.15). The effect of the rest period was to lower the P concentration of the effluent, but this effect was short in duration, with C_{out}/C_{in} ~0.8 after 20 Pv. The effect of resting the column on P removal can be better seen in Figure 6.15.

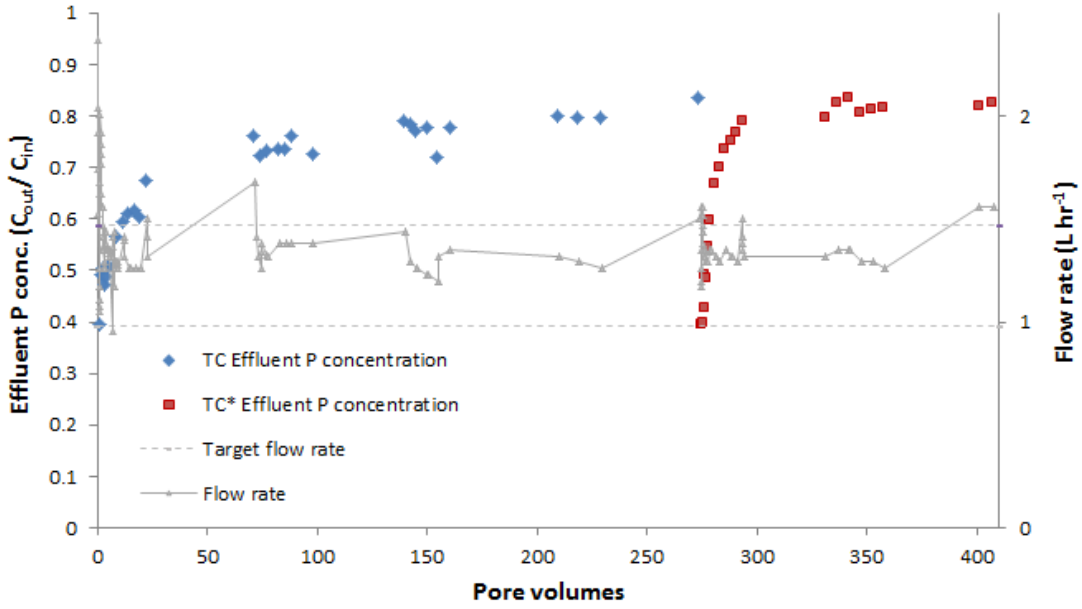

Figure 6.15: Column effluent P concentration and flow rate of solution through the column for T_C and T_C*. Target flow rate indicated as dashed lines; 0.98-1.47 L hr^{-1}. P concentration 10.99 ± 0.23 (1 s.d.) mg L^{-1} from nine influent samples.

Due to the low levels of P removal in the trial using a SynS influent, the experiment was repeated, using a SynS influent solution with pH adjusted to ~pH 10 (Figure 6.16), a condition where Acomb pellets have a high P adsorption capacity (Chapter 4.3.3). As a result of this pH adjustment in trial T_D the initial breakthrough of P is much lower than in T_C, where C_{out}/C_{in} was ~0.4 after 1 Pv. P removal over the course of the experiment was higher than in trial T_C, with T_D having the largest P removal efficiency of any of the trials utilising Acomb pellets as a column substrate, 38%. At

the end of the experiment C_{out}/C_{in} had reached 0.7, the lowest maximum effluent P concentration found in any trial using Acomb pellets.

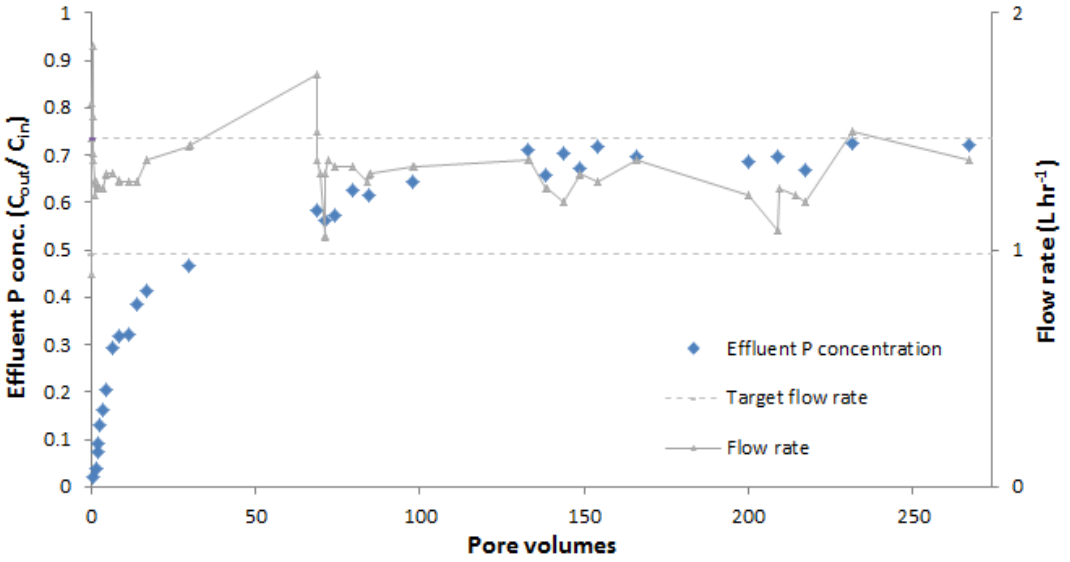

Figure 6.16: Column effluent P concentration and flow rate of solution through the column for T_D. Target flow rate indicated as dashed lines; 0.98-1.47 L hr^{-1}. P concentration 11.24 ± 0.19 (1 s.d.) mg L^{-1} from five influent samples.

Following the completion of this experiment, the column was drained and rested for a period of 48 hours. Following this pH adjusted SynS solution was passed through the column for a further period of 48 hours to investigate the effect of a rest period on P removal by the column (Figure 6.17). Following the rest period, the P concentration in the effluent is greatly reduced, reaching the concentration recorded at the end of T_D after ~100 Pv. By resting, P removal by the column of Acomb pellets was prolonged at a high efficiency; 38%.

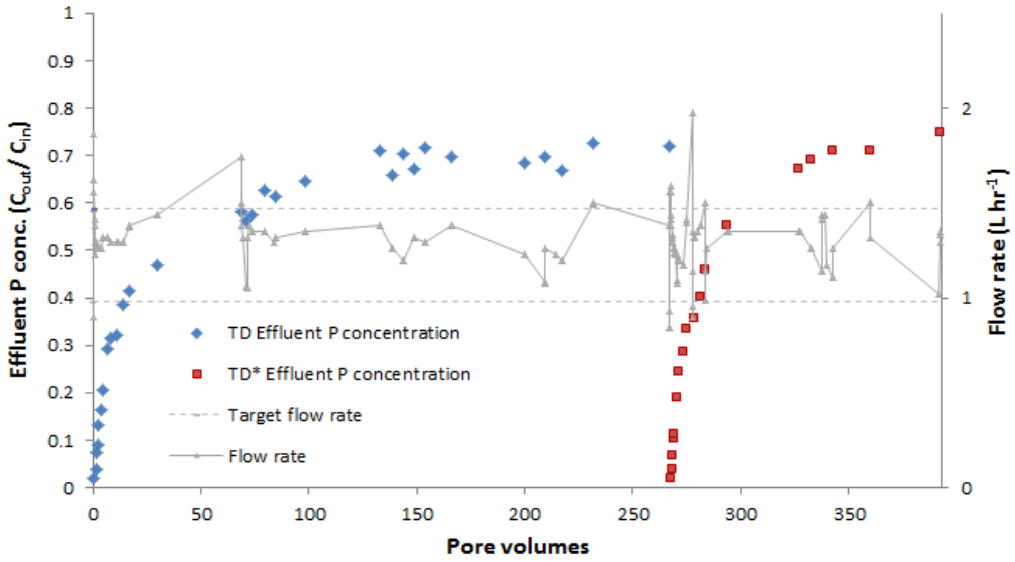

Figure 6.17: Column effluent P concentration and flow rate of solution through the column for T_D and T_D*. Target flow rate indicated as dashed lines; 0.98-1.47 L hr^{-1}. P concentration 11.26 ± 0.18 (1 s.d.) mg L^{-1} from nine influent samples.

The breakthrough curves of the packed columns using Acomb pellets are plotted on Figure 6.18. The breakthrough curve for trial T_D is below that for any of the other trials utilising Acomb pellets, with the highest breakthrough curve for T_C*, although this trial was run for less than 150 Pv. Trials Tc and T_C* have the highest initial breakthrough P concentration, with C_{out}/ C_{in} values of ~0.4 after less than 1 Pv.

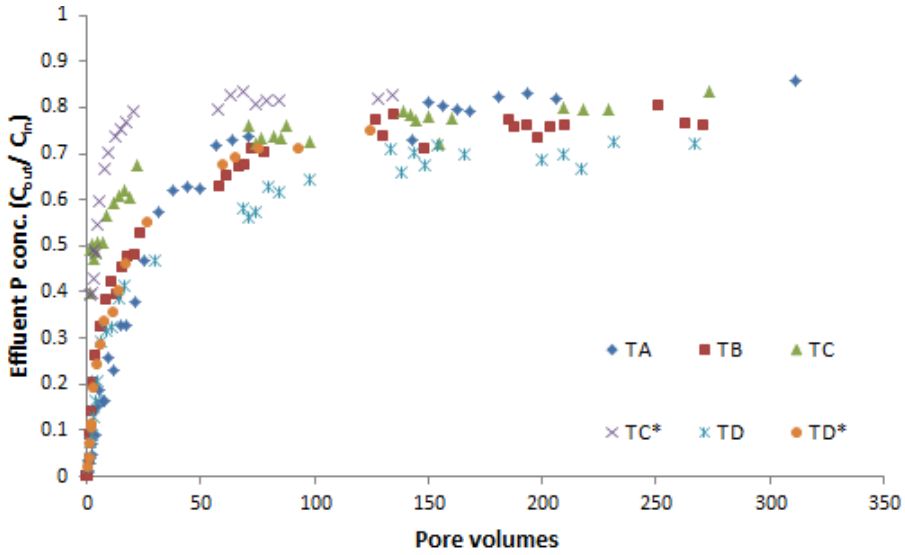

Figure 6.18: P breakthrough curves for column experiments utilising Acomb pellets as a filter substrate.

6.4 Modelling the P breakthrough curves in STANMOD

Whilst P removal breakthrough curves can be compared visually to determine the optimal filter set-up, determining the partition coefficient, K_d, gives a useful metric to compare the movement of an adsorbing species through a substrate. K_d will be calculated by inverse modelling the observed data sets for the P removal trials in STANMOD, utilising the values of the dispersion coefficient (D) calculated from the Cl^- tracer breakthrough experiments.

For each column experiment the pore water velocity coefficient, v, was calculated and inputted into the model with D. The model parameters β, ω and R were the solved iteratively to optimise the fit between the model and the observed dataset. The retardation factor, R, is the relationship between the velocity of water through a controlled volume and the velocity of a contaminant through the same volume (Equation 6.3). It therefore indicates the sorption of contaminant from solution and can also be calculated using Equation 6.4.

$$R = V_p/V_c \qquad \text{Equation 6.3}$$

Where V_p is velocity of water through a control volume and V_c is the velocity of a contaminant through a control volume (USEPA, 1999).

$$R = 1 + \frac{\rho_b K_d}{\theta} \qquad \text{Equation 6.4}$$

Where p_b is the packing density (g cm^{-3}) and θ is the water content of the column at saturation (cm^3 cm^{-3}) and K_d is the partition coefficient (cm^3 g^{-1}).

The retardation factor is calculated in STANMOD, allowing Equation 6.4 to be rewritten to determine the partition coefficient, K_d. K_d is a common metric utilised to infer the sorption of a contaminant to a soil (USEPA, 1999), expressing the relationship between the concentration of a species adsorbed and that remaining in solution (Martinez et al., 2006).

6.4.1 Polkemmet ochre

Results of modelling the datasets for Polkemmet ochre are presented in Table 6.7, with an example of the model fit given in Figure 6.19. The value of K_d was much higher under low flow conditions, T_2, than for high flow conditions, T_1. This indicates that P removal by the packed column was more effective with a higher contact time. In the presence of competing ions, T_3, K_d was lower than in T_2: 250.9 compared to 293.2 $cm^3\ g^{-1}$. The column was therefore less effective at removing P in the presence of competing ions. Following T_3, the column of ochre was rested for 48 hours before SynS solution was passed through the column for a further 48 hours (T_3*). The K_d value for T_3* is the lowest for any of the trials, 158.0 $cm^3\ g^{-1}$. This relatively low value of K_d is due to the rapid breakthrough of P in the observed dataset. This rapid breakthrough of P may be due to the fact that many of the ochre surface sites, originally available for P adsorption, are saturated as a result of T_3.

Table 6.7: Summary results from the fitting of STANMOD to P removal column experiments for Polkemmet ochre. For the modelled parameters v and D are fixed parameters, with R, β and ω solved iteratively in the model. R^2 is the coefficient of determination for the fitting of STANMOD to the observed dataset.

Flow statistic	**Column experiment**			
	T_1	T_2	T_3	T_3*
v	172.5	72.6	77.2	72.6
D	190.0	64.9	64.9	64.9
R	284.4	479.4	410.4	258.8
β	0.001	0.272	0.189	0.0247
ω	8.59	3.79	5.53	4.68
K_d	173.7	293.2	250.9	158.0
R^2	0.94	0.99	0.99	0.94

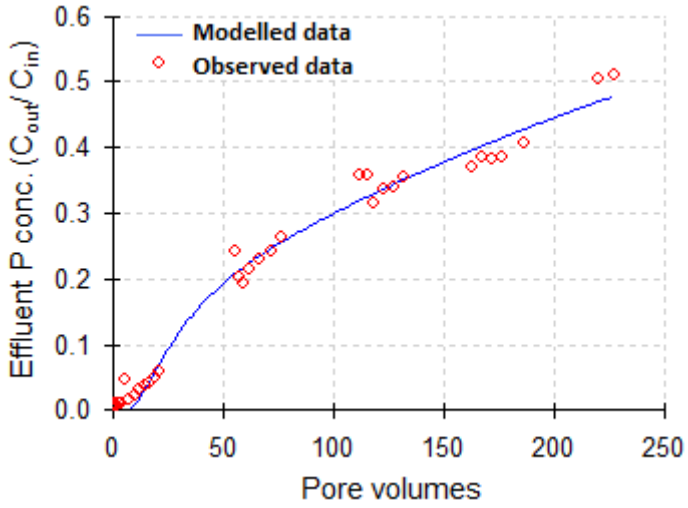

Figure 6.19: STANMOD model fit to the observed dataset for P removal by a packed column of Polkemmet ochre under low flow conditions, T_2.

6.4.2 Acomb pellets

Results of modelling the datasets for P removal in the Acomb pellet column experiments is presented in Table 6.8 with an example of the model fit presented in Figure 6.20. Values of K_d were much lower for all trials involving Acomb pellets than for Polkemmet ochre. The lowest K_d values occurred under high flow conditions (T_A) and for trials conducted after a rest period (T_C* and T_D*). As discussed for trial T_3*, the substrate in trials T_C* and T_D* had already been used to remove P from solution, and as such P breakthrough was rapid resulting in low K_d values.

Decreasing flow rate increased P removal by Acomb pellets, with the K_d value for T_B (low flow conditions), 55.1 cm^3 g^{-1} compared to 29.3 cm^3 g^{-1} in T_A (High flow conditions). The presence of competing ions in trial T_C led to a lower value of K_d than in trial T_B, however it is not clear whether this decrease in P removal is due to the competing ions or the different pH conditions of the influents. The highest K_d value of the trials conducted (71.5 cm^3 g^{-1}), indicating the best conditions for P removal by Acomb pellets, was calculated for trial T_D, where the influent pH was altered to ~pH 10.

Table 6.8: Summary results from the fitting of STANMOD to P removal column experiments for Acomb pellets. For the modelled parameters v and D are fixed parameters, with R, β and ω solved iteratively in the model. R^2 is the coefficient of determination for the fitting of STANMOD to the observed dataset.

Flow statistic	Column experiment					
	T_A	T_B	T_C	T_C*	T_D	T_D*
v	189.8	79.59	85.71	85.71	85.71	79.59
D	188.0	37.0	37.0	37.0	37.0	37.0
R	65.5	122.3	96.0	59.0	158.3	68.2
β	0.0004	0.0679	0.0175	0.0640	0.0610	0.1200
ω	11.46	0.95	0.73	0.36	1.15	1.44
K_d	29.3	55.1	43.2	26.3	71.5	30.5
R^2	0.95	0.97	0.89	0.94	0.97	0.94

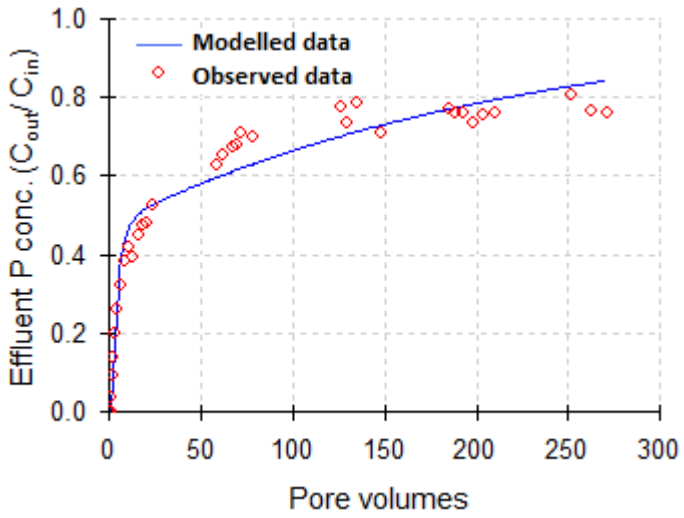

Figure 6.20: STANMOD model fit to the observed dataset for P removal by a packed column of Acomb pellets under low flow conditions, T_2.

6.5 Long term P removal column experiment

Drawing on the information gathered in Chapter 5.3 and 5.4, a column experiment was designed to investigate the effectiveness of a packed column of ochre over a longer time span. A column was packed with Polkemmet ochre and installed into the column set-up. A ~10 mg P L^{-1} solution was then passed through the column for a period of 48 hours with samples from the influent and effluent taken periodically. The column was then switched off for a period of 48 hours for a rest period, with the

header tank and reservoir emptied. After this rest period, the experiment was run for a further 48 hours following which the rest period was repeated. This cycle of operation and rest occurred nine times, with over 1000 Pvs of solution passed through the column over the course of the 34 day experiment. Samples were filtered through 0.45 μm cellulose filter paper, stored in polypropane containers at 4°C for no longer than one week, and were examined for total orthophosphate content at the James Hutton Institute, method described in Chapter 4.2.2.

6.5.1 Results

Periodic resting of the packed column led to sustained high P removal rates. P removal efficiency of the first four P applications was above 80 % (Table 6.10, Figure 6.21), meaning that for over 400 Pv, >80 % of P in solution was removed by the ochre substrate. Whilst it declined over the course of the experiment, P removal efficiency was still >70 % after over 1000 Pv of solution had passed through the column. Over the course of the experiment, the ochre substrate removed 6.87 g of P, equating to 7.68 mg P g^{-1} ochre.

Table 6.9: Summary results for the long term Polkemmet ochre column experiment. C_{out}/ C_{in} maximum is typically at the end of the experiment. 894.88 g ochre was packed in the column.

	P application								
	1	**2**	**3**	**4**	**5**	**6**	**7**	**8**	**9**
Total throughflow (Pv)	113.1	113.2	108.2	112.8	114.0	114.8	114.9	111.3	113.2
Av. flow rate (L hr^{-1})	1.56	1.56	1.49	1.55	1.57	1.58	1.58	1.53	1.56
Max. flow rate (L hr^{-1})	1.77	1.68	1.77	1.74	1.74	1.80	1.98	1.74	1.62
Min. flow rate (L hr^{-1})	1.26	1.41	1.20	1.38	1.44	1.44	1.44	1.38	1.26
C_{out}/ C_{in} max.	0.11	0.19	0.15	0.21	0.27	0.26	0.28	0.32	0.36
Total P dose (mg)	945.4	946.5	904.8	943.5	952.9	959.7	961.0	930.7	946.4
Total P removed (mg)	858.8	812.5	795.7	781.9	753.8	764.77	744.9	686.9	671.7
P removal efficiency (%)	90.8	85.8	87.9	82.9	79.1	76.6	77.5	73.8	71.0

A linear trend line was fitted to the observed dataset (Figure 6.21) to describe the relationship between P removed by the column and Pv that had passed through the column. Based upon this linear assumption of the relationship, the P removed can be projected for higher Pvs (Table 6.10). At 2000 Pv, the packed column is still removing more that 50 % of the P in the influent. The column becomes saturated with P at 4663.5 Pv, with $C_{out}/C_{in} = 1$.

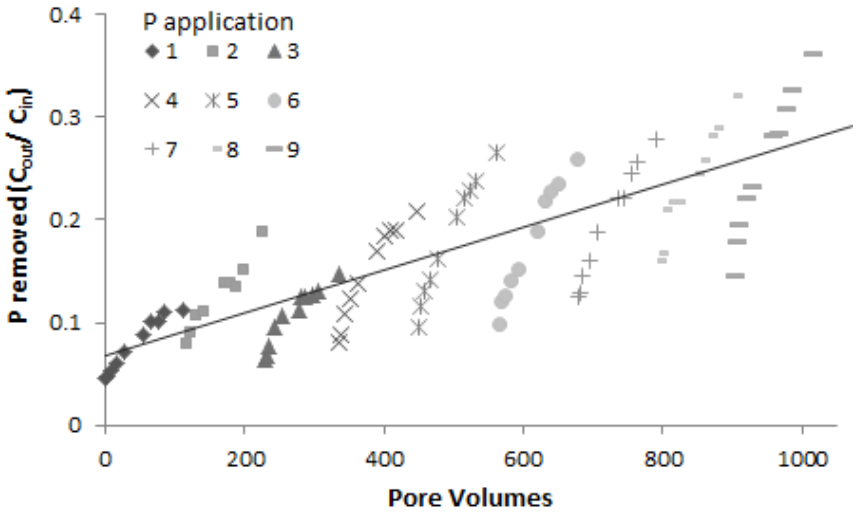

Figure 6.21: P removal over the course of the long-term Polkemmet ochre column experiment. Following the final sample for each P application the column was rested for 48 hours prior to the following P application. Linear trend line fitted to the dataset; $y=0.0002x + 0.0673$, $R^2 = 0.66$.

Table 6.10: Projected P removal rates by the long term Polkemmet ochre packed column assuming a linear relationship between P removed and pore volumes, with continued alternate two day periods of operation and resting.

P removed	**Pore volumes**				
	500	1000	2000	3000	4000
C_{out}/ C_{in}	0.17	0.27	0.47	0.67	0.87

Introducing regular resting periods has greatly increased the longevity of Polkemmet ochre for removing P from solution. This should therefore be incorporated into filter designs using ochre, with the suggestion that ochre filters

should be run in parallel. This would allow one filter to rest and regenerate surface sites for adsorption whilst the other filter treats P enriched water.

6.5 Summary discussion

A number of key conclusions can be drawn as a result of the column experiments investigating P removal. Firstly, flow rate and thus contact time plays a major role in the removal of P from solution by Polkemmet ochre. Under the lower contact time, P removal efficiency was 33%, with this more than doubled to 70% as an effect of increasing contact time to between 20-30 minutes. Increasing contact time was not as effective for Acomb pellets, with P removal efficiency increased from 27% for trial T_A to 31% for trial T_B.

The effect of competing ions was investigated by passing SynS solution through columns packed with ochre in trials T_3 and T_C. For Polkemmet ochre (T_3) the presence of competing ions did not appear to have any significant effect on the removal of P, with the breakthrough curve having a similar shape and gradient to that from T_2. For Acomb pellets, P removal was far lower in T_C which may reflect the pH of the influent rather than any competing ions in solution.

In SynS the only ions expected to be competing for adsorption sites are sulphate and organic forms of P. In experimental systems containing much higher sulphate concentrations than this experiment, the influence of the competing species on P adsorption is small, due to the much higher affinity of P for the reactive surface sites (Geelhoed et al., 1997). Therefore, in the column experiments where sulphate is only present at a low concentration (0.26 mg S L^{-1}) it is unlikely to have much of a competitive effect.

The presence of organic forms of P may have a competitive effect with P added as KH_2PO_4. However, KH_2PO_4 was selected for use due to its inorganic form; with PO_4^{3-} becoming isolated for adsorption onto reactive surfaces and it is therefore

unlikely that organic forms of P would outcompete it. Whilst the presence of organic P may have a minor effect on the sorption of inorganic P, it would instead become adsorbed, resulting in no overall effect on the total P removed from solution.

Altering the pH of the SynS influent to a column packed with Acomb pellets was investigated in T_D. In comparison with T_C, P removal was much higher in T_D, with initial P breakthrough also lower. Of all the trials using Acomb pellets, P removal efficiency was highest for trial T_D, indicating that the pH conditions of the influent are important for treatment systems using Acomb pellets. This is most likely due to the sorption mechanisms occurring under higher pH conditions, with P adsorbing onto surfaces of calcite, see Chapter 1.3.7.2.

The introduction of a rest period of 48 hours before a second application of P enriched solution in T_3*, T_C* and T_D* increased the P removal efficiency of the columns. This was particularly apparent in trials T_3* and T_D*, where effluent P concentration was reduced to levels measured at the start of T_3 and T_D. Effluent concentrations in T_D* returned to those recorded at the termination of T_D after approximately 100 Pvs, with the effluent P concentrations in T_3* not returning to the high recorded in T_3 for the 118 Pv experiment duration.

Finally the effect of ochre type should be noted, with Polkemmet ochre performing better than Acomb pellets in all comparable trials especially in the trial utilising SynS influent; T_3-T_3*, T_C-T_C*. In these trials, Polkemmet ochre removed more than double the amount of P from solution than Acomb pellets.

Drawing on the results of the column experiments, a longer term study was conducted using Polkemmet ochre at the low flow rate, with no competing ions and periodic resting of the column substrate. The P removal efficiency of the packed column was greatly increased and it is concluded that resting the ochre allows

surface sites to regenerate, as adsorbed particles diffuse into the ochre matrix as suggested by Dzombak and Morel (1990) and Sibrell et al. (2009). Periodic resting of ochre substrate is therefore paramount to maximise the lifespan of filter systems.

Whilst this study investigates the effect of ochre type, flow rate, the presence of competing ions, the effect of a rest period and, for Acomb pellets the effect of altering the pH of the influent on P removal, there are a number of other variables which could be examined. Firstly, P removal by other ochre types and grain sizes could be investigated. The pH of the influent could be adjusted across a much wider range to investigate the effect of this on P removal. The influent composition could be further altered, using natural waters or real sewage with P in different forms to that utilised in this study. The P concentration of the influent could also be altered to investigate the breakthrough of P at a range of concentrations.

Chapter 7
Discussion

In this Chapter, the major findings of this study are discussed and put into context alongside previous research, highlighting how this research has furthered our understanding of P sorption by ochre. The methods utilised are critiqued with associated recommended improvements suggested for future research. In light of the findings of this study, practical deployments of ochre in the field are then discussed considering ochre for use as a filter substrate, as an additive to manures, to remove P in a CSTR, and as a substrate for use in a PRB.

7.1 Major research findings

The major research findings of this thesis are a product of the objectives set out in Chapter 1.5. These findings are discussed in the following sections, put into context alongside previous research and the implications of these results highlighted. Methodologies are critiqued where appropriate and suggestions for future research highlighted.

Few comparative studies of ochres for the removal of P from wastewaters have occurred, with the notable exception of Heal et al. (2003b) and Sibrell et al. (2009) where a comparison of two and six ochres occurred respectively. Examining seven ochres in this study has allowed for informative contrasts to be noted regarding the composition, and dominant P removal mechanisms, of the ochres. This has then informed assessment of which of the ochres are suitable for further investigation in this study, and could inform future research.

Silkstone and Ynysarwed ochres examined in this study had not previously been analysed as potential P adsorbents and this research thus yields new knowledge about them. Whilst the other ochres have been the subject of prior research, their detailed characterisation in this study supports the prediction by Brown et al. (2002)

that ochre composition varies with time as factors affecting its formation and composition change. Chapters 4 and 5 illustrate how components of ochre composition can influence P removal capacity, further supporting the need for detailed, up-to-date characterisation.

7.1.1 Ochre composition

Seven ochres were selected from across the UK and Ireland based on a variety of factors, including previous body of research, conditions under which the ochre was formed (passive and active treatment works), the presence of PTEs, and ochre particle size. The ochres were analysed for a range of chemical properties including pH, composition determined by acid digest, ammonium oxalate extractable Fe, and mineralogical analysis in order to characterise the ochres and inform further research and analysis.

A range of parameters with noted significance for the sorption of P were determined for the ochres (Table 7.1). The four elements most commonly associated with the removal of P in wastewater technology are Al, Ca, Fe and Mg. Elemental concentrations of these elements were determined by acid digest for the seven ochres. Each ochre contained between 42.1 and 68.4 % of these elements in their composition. Ammonium oxalate extraction was utilised in this study to determine what proportion of Fe content present in the ochres was in the form of amorphous minerals (Table 7.1). This is an important variable for analysis as amorphous minerals have a much higher surface area than crystalline minerals, and thus provide a larger surface area for adsorption. B.E.T surface area of the ochres was also determined (Table 7.1).

Table 7.1: Selected indicators of the chemical composition and B.E.T surface area of the seven ochres under study. Fe-ox is the ammonium extractable Fe, B.E.T is the B.E.T surface area. All results except B.E.T (m^2g^{-1}) presented as % content by dry weight.

Ochre type	**Elemental concentration (%)**					
	Al	Ca	Fe	Mg	Fe-ox	B.E.T
Acomb	0.33	2.91	56.9	0.24	14.8	184
Acomb pellets	3.63	10.80	31.5	2.82	10.1	104
Avoca	0.72	0.06	50.3	0.36	18.6	56
Minto	0.17	1.27	60.9	0.55	9.0	113
Polkemmet	3.40	0.96	44.6	0.46	8.2	98
Silkstone	0.47	0.44	41.0	0.17	23.9	243
Ynysarwed	0.63	1.56	31.8	34.4	23.7	220

Ochres containing a high composition of the four elements related to P removal, a high proportion of the Fe in the form of amorphous minerals, and an associated high surface area should provide a high P adsorption capacity. Detailed characterisation of the ochres, and consideration of the roles the various components play in P removal, is crucial to understanding P removal capacities however. Materials containing high proportions of both Al and Fe have also been noted to have high adsorption capacities for example (Ainsworth et al., 1985). Therefore, whilst Minto ochre has the highest proportion of Fe in its composition, it has a low Al content, only 8.2 % of the Fe in its composition is in the form of amorphous minerals, and the material has a middling B.E.T. surface area in comparison to the other ochres. The P adsorption capacity of Minto ochre may not be as high as other ochres under study with lower Fe content.

Of the ochres under study, it is proposed that Silkstone ochre may be the optimal adsorbent of P. This ochre has a relatively high elemental Fe content, of which a large proportion is in an amorphous state, reflecting the high B.E.T surface area.

This ochre is characterised by relatively low concentrations of the Al, Ca and Mg, however, and therefore the P removal mechanisms of the ochre may be largely restricted to P adsorption onto Fe surface sites. This may limit the range of conditions under which Silkstone ochre can be applied to sorb P.

The mineralogy of an ochre will influence its P removal capacity and the dominant mechanisms of P sorption occurring. Previous studies have indicated that ochre contains a variety of Fe hydroxides, such as goethite, ferrihydrite and jarosite (Heal et al., 2003b; Fenton et al., 2009) The mineralogy of the ochres in this study was determined by XRD analysis, Chapter 3.6. All of the ochres were found to contain goethite, with three of the ochres containing calcite (Table 7.2). Adsorption onto these mineral surfaces is suggested in this research as the major P removal mechanisms occurring in systems containing ochre, with adsorption to goethite dominant under low pH conditions and onto calcite surfaces under neutral to high pH. The amount of these minerals in the ochre composition will therefore strongly influence the P adsorption capacity of the ochres at varying pH conditions.

Table 7.2: Ochre mineral content as determined by XRD, Chapter 3.6.

	Mineral content (%)	
Ochre Type	Goethite	Calcite
Acomb ochre	54	14
Acomb pellets	35	52
Avoca	20	-
Minto	100	-
Polkemmet	35	-
Silkstone	16	-
Ynysarwed	16	11

Minto ochre was found to be comprised as approximately 100 % goethite. This agrees with the result of the acid digest, with Minto ochre 60.9 % elemental Fe,

which corresponds to approximately 100 % FeO.OH. High concentrations of goethite were also detected in Acomb ochre, Acomb pellets, and Polkemmet ochre, suggesting these ochres will have a particularly high P adsorption capacity under acidic conditions.

Calcite was identified in three of the ochres, Acomb pellets, Acomb ochre, and Ynysarwed ochre (Table 7.2). Calcite has not been detected in previous research and as such has not been suggested as a P removal mechanism by ochre. High Ca content has been acknowledged previously in ochre, e.g. Minto and Brandy Camp ochre (Heal et al., 2003; Sibrell et al., 2009) and as such, Ca has been recognised as a potentially sorbing component of some ochres, but the mechanism had not been proposed. In this research it is suggested that adsorption onto surfaces of calcite is one of the dominant P removal mechanisms for Acomb ochre, Acomb pellets, and Polkemmet ochre, with the process occurring under high pH conditions (pH>7). This research has therefore advanced our knowledge of P sorption by ochre, suggesting a second major P removal mechanism for some ochres.

7.1.2 Batch experiment results

The importance of fitting adsorption isotherms to batch experiment data over a range of pH conditions can be seen in Table 7.3. The P adsorption capacity of four ochres was found to have a negative relationship with pH. This is due to pH dependant nature of the P removal mechanisms occurring in the ochres. Therefore the P adsorption capacity of a material is only relevant at the pH conditions it was measured. There is therefore a need for a method to enable the calculation of adsorption capacities and associated parameters at discrete pH values.

Table 7.3: P adsorption capacity (S_{max} (mg g^{-1}) displayed above K_f) derived from the fitting of Langmuir and Freundlich isotherms to the P adsorption batch experiment data. Underlined P adsorption capacities indicate the isotherm which provided the optimal fit to the dataset i.e. the lowest value of AIC (this couldn't be determined for Ynysarwed ochre between pH 4 and 8). - indicates data was not available to plot adsorption isotherms at this pH.

		pH						
Ochre		3	4	5	6	7	8	9
Acomb	S_{max}, K_f	-	15.5 12.2	14.9 11.9	14.3 11.0	13.0 8.4	12.8 6.6	12.8 4.86
Acomb pellets		19.0 6.6	19.0 3.3	24.4 1.8	34.5 1.3	43.1 1.64	-	-
Avoca		29.8 15.7	24.6 20.8	20.5 16.8	17.2 15.4	14.8 9.7	-	-
Minto		-	12.7 4.8	14.4 4.3	14.2 4.2	11.8 4.5	-	-
Polkemmet		-	11.0 4.2	10.6 4.2	11.1 3.5	-	-	-
Silkstone		-	-	-	17.2 13.9	13.0 8.4	-	-
Ynysarwed		-	25.8 22.6	24.0 20.6	22.6 17.4	21.7 12.9	21.8 7.6	16.4 8.0

The adsorption capacities of Minto and Polkemmet ochres determined in this study are lower than previously reported (21.5 and 17.8 mg P g^{-1} respectively; Heal et al., 2003b) and this may be due to a variety of reasons. The Minto ochre utilised in this study contained lower concentrations of Fe (608 compared to 675 g kg^{-1}) and Ca (12.7 compared to 118 g kg^{-1}), both of which have a high affinity for P. The mineralogy noted in this study also differs from Heal et al., (2003) where goethite and ferrihydrite minerals were present compared to only goethite in this study. Ferrihydrite, associated with young sediments, is an amorphous mineral and thus

provides a higher surface area for adsorption to occur than more crystalline minerals such as goethite. As with Minto ochre, the composition of Polkemmet ochre contains lower concentrations of Fe (447 compared to 650 g kg^{-1}) and Ca (9.63 compared to 70 g kg^{-1}) in this study which may be contributing to the lower adsorption capacity. Ferrihydrite was also present in the sample utilised by Heal et al. (2003b), whereas only goethite is present in this study, which may be providing a lower surface area for adsorption. The cause of these differences in the composition of the ochres is most likely temporal variability at the MWTPs (Brown et al., 2002) and the transformation of younger Fe hydroxide minerals into goethite between the sampling time and the experiments being conducted.

Another possible reason for the lower P adsorption capacity calculated in this research is methodological differences with the previous study. Batch experiments with overlying P concentrations of up to 1000 mg P L^{-1} were conducted by Bozika (2001) cited in Heal et al. (2003b). Higher P concentrations give lower experimental pH conditions, which in turn influence the sorption reactions occurring (Cucarella and Renman, 2009). It is suggested that the high P concentrations in the previous research led to lower experimental pH conditions resulting in an increased amount of adsorption and thus an overestimation of the adsorption capacity of the ochres. High P concentrations can also lead to equilibrium conditions which do not reflect those which occur at lower P concentrations (Cucarella and Renman, 2009), with materials having different behaviours at high and low P concentrations. This may be reflected in the lower P adsorption capacity determined in this study.

The P adsorption capacity of Avoca ochre was found to be pH dependant, with S_{max} 29.76 mg P g^{-1} at pH 3, declining to 14.79 mg P g^{-1} at pH 7. This result is similar to that previously derived of 16-21 mg P g^{-1} (Fenton et al., 2009). The high Langmuir K values calculated for Avoca ochre, ignoring the spurious result at pH 4, which decline with increasing pH indicate the dominance of adsorption reactions, most likely onto Fe-surfaces as the ochre contains 502.98 g Fe kg^{-1}. The ochre has a low Ca

content, thus P removal mechanisms associated with Ca under high pH conditions, such as adsorption onto calcite, are not occurring and the ochre therefore has a lower P adsorption capacity at higher pH.

The P adsorption capacity of Acomb ochre is also pH dependent, but, in contrast to Avoca ochre, S_{max} declines at a much slower rate, from 15.51 mg P g^{-1} at pH 4 to 12.77 mg P g^{-1} at pH 9. As with Avoca ochre, high values of Langmuir K under low pH conditions indicate adsorption occurring, most likely onto Fe- surfaces. Under basic pH conditions the relatively high P adsorption capacity may indicate sorption mechanisms associated with Ca occurring, most likely adsorption onto surfaces of calcite, with the ochre composition 14 % calcite (Chapter 3.6). The lower Langmuir K values at higher pH conditions indicate a lower affinity between the adsorbate and adsorbent which would be expected with an increasing dominance of adsorption onto calcite surfaces.

The pelletisation of Acomb involves incorporating Ca, Al and Mg additives, this is reflected in the higher concentrations of these elements in the pellets compared to other ochres (Table 7.1). These elements all have a high affinity for P resulting in the increased P adsorption capacity of Acomb pellets in comparison to Acomb ochre. The increasing values of S_{max} with pH may be due to the high calcite content of the ochre, 52 % (Chapter 3.6), with adsorption onto these surfaces occurring > pH 7.

Whilst the high P adsorption capacity of the material under neutral pH conditions make it seem attractive for use in wastewater streams, it is suggested that the dominant P removal mechanism is adsorption onto calcite surfaces. Calcite has a lower affinity for P than Fe hydroxides, with a slower associated reaction time (< 3 hours, Sø et al., 2011). Therefore the utilisation of Acomb pellets under these conditions as a filter substrate would require a higher contact time to ensure that the adsorption reactions occurred.

Ynysarwed ochre has a high P adsorption capacity of 25 mg P g^{-1} at pH 4 and whilst this declines with increasing pH it is still >20 mg P g^{-1} at pH 8. This may be due to the high amounts of Fe and Mg present in the ochre (318.81 and 343.57 g kg^{-1} respectively), a combination of elements noted to produce materials with a large adsorption capacity (Ainsworth et al., 1985). The ochre also has a high B.E.T. surface area providing a large area for adsorption to occur.

Whilst isotherms could only be calculated at pH 6-7 for Silkstone ochre (Table 7.3), data was also derived at pH 5.5 and 6.5 to which the Langmuir isotherm was fitted, giving S_{max} values of 21.95 and 13.96 mg P g^{-1} respectively. It is therefore suggested that the P adsorption capacity of Silkstone ochre is pH dependant, declining with increasing pH, as with Acomb and Avoca ochre. Silkstone ochre has a low Ca content, 4.42 g kg^{-1}, and therefore P removal mechanisms under high pH conditions, such as adsorption onto calcite surfaces, are limited.

The novel methodology utilised in this research has enabled the calculation of P adsorption capacities and associated parameters for the ochres at a range of discrete pH conditions. The effect of pH on P adsorption by ochre had not been accounted for in previous research. In its present state, however, the method has a number of limitations.

The plotting of adsorption isotherms to the batch experiments required the fitting of trend lines to the raw dataset to derive data points at discrete pH values. Whilst this approach has allowed the derivation of P adsorption characteristics at discrete pH values, there are a number of issues concerning this approach. Firstly, the fit of the trend lines to the datasets was not always good, with R^2 low for many of the datasets. The trend lines did however tend to capture the overall shape of the datasets. The reason for low values of R^2 for many of the trend lines was due to a high amount of variance in the datasets. By using trend lines, much of this variance is discounted and thus uncertainty in the results increases. There are a number of

reasons for the variance in the datasets, such as the data was only collected in triplicate, the experiments covered a wide range of pH conditions, and it may be that the sample of ochre used in the experiments was not large enough to be representative.

Therefore, it is acknowledged that there is uncertainty associated with the results of the batch experiments where adsorption isotherms where plotted to interpolated data. A variety of approaches could be employed to reduce the variance of the datasets in future experimental work. A larger amount of experiments could be conducted, or the same amount over a smaller range of pH conditions. Further, the experiments could be scaled up, therefore utilising a larger sample of ochre which may be more representative and thus reduce variability in the results.

Another improvement to the method would be to decrease the drift in pH that occurs between pH equilibrium and at the end of the experiment. As discussed in Chapter 4.2.3 the reason for this drift in pH is mainly due the speciation and deprotonation of orthophosphate, and the release of H^+ ions associated with ligand and bidentate adsorption reactions. The effect of this drift in pH could be reduced by the addition of P solutions adjusted to the pH that of the receiving experiment. However, a drift in pH conditions will still ensue due to the adsorption reactions occurring in the experiments following the P addition. This could be resolved by maintaining the pH conditions of the experiments by the further addition of acid and base (Streat et al., 2008). Following this approach would also mean that batch experiment raw data was at discrete pH conditions and could be utilised, without transformation, for the fitting of adsorption isotherms at fixed pH values.

7.1.3 Surface complexation modelling

Batch experiment data investigating P adsorption by ochre is commonly fitted with adsorption isotherms to determine the adsorption characteristics of the material (Fenton et al., 2009; Heal et al., 2003b; Sibrell et al., 2009; Wei et al., 2008) and has

subsequently been conducted in this study. Whilst fitting adsorption isotherms gave some indication of the mechanisms involved in P removal, chemical equilibrium and speciation models can be utilised to better understand the sorption mechanisms occurring in systems containing ochre. Such modelling of systems containing ochre had not been conducted in any of the studies named above.

All seven ochres were modelled within ORCHESTRA, using data from the acid digest and ammonium oxalate extraction to characterise the chemical composition of the ochres. The conditions of the P adsorption batch experiments were then input into the model, and P removal mechanisms incorporated in order to improve the fit between modelled and observed equilibrium P concentrations. The dominant P removal mechanisms for each ochre were determined from this.

Adsorption onto HFO surface sites was found to be the dominant P removal mechanism for all six ochres which were modelled successfully. For four of the ochres (Acomb, Avoca, Polkemmet and Silkstone), allowing the formation of various minerals in the model led to no improvement in model fit. Therefore, in the models describing P removal by these ochres the only P sorption mechanism occurring is adsorption onto HFO. For Acomb ochre it is noted that an improved fit could be obtained if a P removal mechanism was present at pH > 7. Due to Acomb ochre containing 14 % calcite (Chapter 3.6), adsorption onto to these surfaces is suggested as a potential removal mechanism to achieve this.

For Minto and Ynysarwed ochres, the model fits to the observed datasets were improved by the inclusion of Ca-P minerals in the model. Analysis of the conditions when these minerals form in the model reveal they are formed above pH 7, and when P concentrations in the overlying solutions are higher than expected in targeted wastewater streams, e.g. > 100 mg P L^{-1}. It is therefore unlikely that the precipitation of these minerals will be a major P removal mechanism at the

suggested environmental applications. Adsorption onto surfaces of HFO will be the dominant P removal mechanism.

Formation of Ca-P minerals in batch experiments containing these two ochres indicate that the P adsorption capacity of the ochres will be overestimated from the fitting of the adsorption isotherms in comparison to what would be expected under field conditions, where Ca-P minerals would not be expected to form e.g. < 100 mg P L^{-1}. As discussed in Chapter 7.1.2, the P adsorption capacity of Minto ochre has previously been determined as higher than calculated in this research. It is suggested that this is due to the formation of Ca-P minerals in the previous study where the ochre had a far higher Ca content, and P concentrations in the batch experiments of up to 1000 mg P L^{-1} were utilised (Heal et al., 2003b).

The modelling of Acomb pellets was less successful than for the other ochres under study (Chapter 5.7.2). Adsorption onto HFO surfaces did not describe the batch experiment data well. The high calcite content of the ochre was highlighted in the interpretation of fitting the adsorption isotherms to the experimental data and indicated as a potential P removal mechanism at neutral to high pH values. Thus, as the ORCHESTRA model was not set up to model this P removal mechanism, the optimal fit to the dataset was poor.

Modelling P sorption by ochre has not been done before, with previous research concentrating on the fitting of adsorption isotherms to batch experiment data to indicate the dominant P removal processes. Whilst it wasn't possible to produce a good fit between the model and all the datasets, the results show that adsorption on HFO surfaces is the dominant P removal mechanism for many of the ochres under neutral to low pH conditions. The fitting process also highlighted conditions under which the model was not performing well, i.e. for some of the ochres at high pH conditions, suggesting the absence of P removal mechanisms, such as adsorption onto calcite. Therefore further development of a SCM to represent P sorption by

ochre should prioritise the incorporation of adsorption onto calcite surfaces (see Sø et al., 2011).

Another limitation of this study is that there was no independent data to validate the model with following calibration. Such validation would give a better assessment of model performance than just the test statistics from the calibration process.

The HFO-SA in the models was typically set above the theoretical value from the literature, (600 m^2 g^{-1}; Dzombak and Morel, 1990), in order to achieve the optimal fit to the calibration datasets. It is suggested that this is due to the total amount of HFO in the model being underestimated, with the increased surface area compensating for this. The amount of HFO in each model was determined based on the ammonium oxalate extractable Fe, with the view that this would give the best estimate of the Fe content of the ochres in amorphous mineral forms. However, the amorphous Fe mineral content was only a fraction of elemental Fe present in the ochres, and any crystalline Fe structures, whilst capable of removing P, are not represented in the HFO content. Whilst crystalline structures have a lower surface area for adsorption, their exclusion from the modelling process has led to an overestimation of the HFO-SA.

The lower the fraction of ammonium oxalate extracted Fe determined, and thus inputted into the model as HFO, the greater the HFO-SA had to be set at to achieve model optimisation. This overestimation of HFO-SA is therefore accounting for the available surface area for adsorption on more crystalline Fe minerals (Figure 7.1).

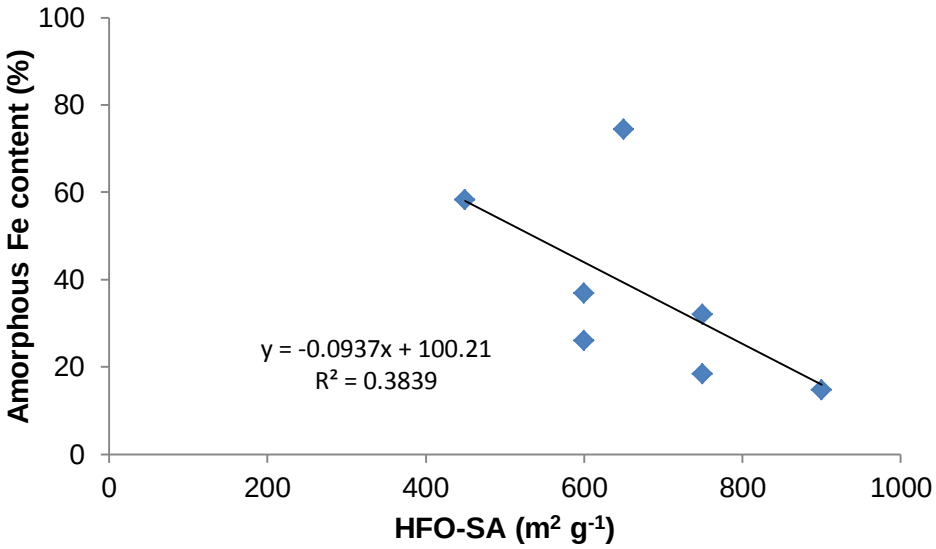

Figure 7.1: Model calibrated HFO-SA compared against ochre Fe content determined by ammonium oxalate extraction.

Therefore, whilst HFO-SA is not giving a representative surface area for the amorphous Fe minerals, it is instead acting as a parameter in the model, so that the total surface sites available for adsorption on all the Fe surfaces in the model can be approximated.

7.1.4 Column experiments

Column experiments were completed to investigate P removal by ochre under flow-through transport conditions in order to better understand the role of the kinetics of diffusion and adsorption that would be present under potential field conditions. Two granular ochres, Polkemmet ochre and Acomb pellets, were selected for study due to their high hydraulic conductivity, with P removal investigated over a range of conditions which may be encountered in the field. Few studies of P removal by packed columns of ochre have been conducted. A notable exception utilising Friendship Hill ochre was conducted by Sibrell et al., (2009, see Chapter 2.5.1). The P concentration in the experiment was 0.13 mg P L^{-1}, which is far lower than that of suitable wastewater streams identified in this study, ~1-15 mg P L^{-1}.

Polkemmet ochre was found to be more effective at removing P than Acomb pellets in all the various trials. It is suggested that this is due to the different P removal mechanisms occurring in the column experiments, with P adsorption onto surfaces of goethite dominant for columns of Polkemmet ochre, and adsorption onto calcite suggested as the dominant P removal mechanism for Acomb pellets under neutral pH conditions. The kinetics of adsorption onto surfaces of ochre containing high amounts of goethite, including Polkemmet, has been noted to be rapid in batch experiments, with P concentrations decreasing from 5 mg P L^{-1} to < 0.01 mg P L^{-1} within eight minutes of contact time (Heal et al., 2003b). In contrast to this, P adsorption onto calcite is a slower process, see Chapter 1.3.7.2, and it may therefore be that the contact time in the column experiments, 10-30 minutes, is not sufficient for much of the calcite adsorption reactions to occur. The kinetics of adsorption are pH dependant, and as such the P removal efficiency of Acomb pellets was improved by altering the pH of the influent to ~pH 10 where adsorption reactions onto calcite occur at a faster rate (Karageorgiou et al., 2007). The production of Acomb pellets has therefore produced a filter substrate with low kinetics of P removal over the pH conditions of expected operation, pH 6-8. This highlights the importance of adsorption kinetics, as relatively low contact times will be required in filter units in order to treat the majority of wastewater streams.

The long term P removal column experiment drew on the findings of the individual column experiments to select the conditions under which a packed column would be most effective at removing P over an extended time period. The column was therefore packed with Polkemmet ochre, run at the lower of the two selected flow rates, with no competing ions and periodic resting of the column.

The column set-up was highly effective at removing P to low concentrations. After over 1000 Pvs, C_{out}/ C_{in} had not exceeded 0.36. This is considerably lower than for any of the other Polkemmet ochre column experiments which were conducted over fewer Pvs. The total P removed by the long term experiment was 7.68 mg P g^{-1}

ochre. This is approaching the P adsorption maximum of Polkemmet ochre derived from the P adsorption batch experiments, ~10-11 mg P g^{-1} (Chapter 4.2.5.6). The results of the column experiment thus suggest that the P adsorption capacity of Polkemmet ochre is higher than that calculated in the batch experiments, with the ochre predicted to remove P from the influent for several thousand more Pvs (C_{out}/C_{in} = 1 after 4663.5 Pvs; derived in Chapter 6.5.1). An empirical estimate of the P adsorption capacity was also calculated from the results of the ammonium oxalate extractable Fe, 22.7 mg P g^{-1} (Chapter 3.5.2), and by a previous author as 21.5 mg g^{-1} (Bozika, 2001). It is therefore concluded that the P adsorption capacity for Polkemmet ochre may be higher than that determined in the P adsorption batch experiment.

The experimental set-up utilised in the long term column trial achieved a very high P removal efficiency thus supporting the selection of the conditions to achieve an optimal experimental design. Especially noteworthy is the use of a regular resting period. This supports the findings of Dzombak and Morel (1990) and Sibrell et al. (2009) who suggest that P adsorption onto the surface of Fe-oxides is followed by the migration of the adsorbed species into the matrix of the ochre. By resting the column, surface sites are regenerated as adsorbed P diffuses into the ochre matrix. It is therefore proposed that ochre filters should be used in parallel to allow one filter to rest and regenerate surface sites whilst the other adsorbs P.

These findings thus shed new light on P removal by granular ochre under flow-through transport conditions. The creation of pelleted ochre with high calcite content has produced a filter material that requires a high contact time in order to remove P under flow-through transport conditions and thus has limited applicability in treating wastewater streams. The results of the Polkemmet column experiment, wherein ideal conditions were created based on experiments across the thesis, highlight the utility of the findings in this study and the extent to which this work could be used to optimise P removal by this ochre. Whilst these conditions are

acknowledged to be laboratory based, they highlight how an improved process-based understanding of P removal can be utilised to inform filter design, which in this instance enables total P removed to approach the theoretical P adsorption maximum. The findings thus have real in-field application.

There remains scope to greatly expand the experimental conditions of the column experiments in future research, investigating the effect of flow rate, ochre type, P concentrations, pH conditions, running columns to exhaustion, and testing P removal from target wastewater streams to outline a few. Conducting such experiments would assist in further optimising filter design prior to implementation in the field.

7.1.5 Other research findings

A number of other factors were investigated in the course of this research, most notably the effect of competing ions on the removal of P in both batch and column experiments, and the release of PTEs during batch experiments.

The effect of competing ions on P sorption by ochre was investigated in batch experiments for three ochres: Acomb, Acomb pellets and Polkemmet. Given the potential end use of ochre for the treatment of P-rich sewage effluent, either from a WWTP or a septic tank, SynS was utilised as a source of competing ions. The presence of competing ions in the batch experiments did not significantly reduce the P removal capacity of the three ochres and in some cases led to a statistically significant increase in the P adsorption capacity of the ochre. Column experiments were also conducted investigating P removal from a SynS solution. For Polkemmet ochre the presence of competing ions did not have any significant effect on P removal, and any effect noted for the trial using Acomb pellets is attributed to the difference in pH conditions rather than the presence of competing species.

Overall, little evidence was found to suggest that the P adsorption capacity or efficiency of ochres to remove P was reduced in the presence of competing ions. It should be noted however, that the only competing ions in SynS are weakly adsorbing sulphate and organic forms of P. Due to the high affinity of inorganic P to the surface sites in the batch experiments the presence of these ions should not be expected to have a large impact on P sorption in the experiments. A much more expansive approach is required to investigate the effects of competing ions and it is suggested this could be achieved by conducting batch experiments utilising wastewater streams which are the potential targets for treatment prior to the implementation of field trials.

The release of PTEs from ochre is a concern regarding their use in environmental applications, such as in-stream filter units. The primary aim of this thesis, however, was to develop an understanding of the P removal processes occurring for the varying ochres and to determine the optimum conditions for using a filter of ochre substrate to remove P from wastewaters. Owing to this priority, no stand-alone experiments were conducted specifically to investigate the release of PTEs from ochres. It was instead investigated by further analysis of some experiments originally aimed at examining P removal by the ochres. Alongside this, the release of the major elements that comprise ochre was also investigated (see Chapter 4.4).

Of the major elemental components of ochre (Al, Ca, Fe and Mg) under the pH conditions of wastewater streams, pH 6-8, Ca and Mg were detected in solution at varying concentrations for all the ochres under study, with Al and Mg not detected in solution at these pH conditions. For six of the ochres, Ca was the analyte measured at the highest concentration between pH 6 and 8, with the exception Ynysarwed ochre, where it was Mg (Chapter 4.4).

The release of PTEs (Al, As, Cu, Mn, Ni, Pb and Zn) and the major elemental components of ochre was also investigated in a sample of the P adsorption batch

experiments containing Polkemmet ochre and Acomb pellets. Of the PTEs under study, very few were found in concentrations above the various detection limits between pH 6-8. Mg most notably was detected in solution in the experiments conducted with Acomb pellets up to concentrations ~10 mg L^{-1} at pH 6. With the exception of Zn, released from Polkemmet ochre (~0.05 mg L^{-1}), no other PTEs were detected in solution between pH 6-8.

Overall, PTE release from the ochres was low, indicating that any PTEs within the ochre composition are strongly bound to the ochre and should not go into solution from use of the ochres at the anticipated pH conditions in wastewaters (pH 6-8).

7.2 Practical deployment of ochre

In the following section, the deployment of ochre in a variety of scenarios is discussed drawing on the knowledge garnered from the literature review and the results of this research. The focus of this thesis has been to determine a process based understanding of P sorption by ochre to inform the development of filter units to treat P enriched waters, and thus the implications of this research is initially discussed.

Alternative end-uses for the utilisation of ochre are then suggested which would make use of the materials high P sorption capacity, namely the creation of fertiliser with a low SRP content, and the potential for using ochre in CSTRs and PRBs.

7.2.1 Filter units

Following the completion of batch experiments in previous research, ochre has been deployed in the field, most notably by Dobbie et al., (2009). The performance of such filter units has typically under achieved the potential of ochre that was shown under laboratory conditions. The results of this thesis can be utilised to garner a better understanding of how such filter systems can be optimised to achieve optimal performance.

Most ochres dry to a fine-grained powder and therefore not suitable for use as a filter substrate due to their low hydraulic conductivities. An attempt to address this has been to pelletise ochres using Ca rich additives as a binding agent to produce near spherical pellets, see Chapter 2.4. This produces a substrate with a high hydraulic conductivity and a P adsorption capacity determined under laboratory conditions equivalent to ochre in its natural form (Aumônier et al., permission copy). In this research, Acomb pellets were found to have the highest P adsorption capacity of the ochres under study, with this capacity highest under neutral to basic pH conditions. The pelleted ochre contains a high calcite content, 52 %, and it is suggested that adsorption onto calcite is the dominant P removal mechanism occurring at neutral to high pH conditions. P adsorption onto calcite surfaces has slower reaction kinetics than P adsorption onto goethite, and thus by creating a filter substrate rich in calcite this increases the necessary contact time required for P removal. The pH of wastewater streams is typically between pH 6-8 and thus in applications of Acomb pellets to treat such waters, adsorption onto calcite surfaces will be the dominant P removal mechanism. It is suggested that the effect of this can be seen in the research conducted by Dobbie et al., (2009), where a filter of pelleted ochre was utilised to treat wastewater. In phase 3 and 4 of this experiment the filter unit contained pelleted ochre, with a contact time of approximately 26 and 120 minutes in each phase respectively. TP removal was far greater in phase 4 of the experiment, up to 95 % removal, than in phase 3, < 20 %. This agrees with the finding of this study, that adsorption onto calcite is the dominant P removal mechanism for the pelleted ochres, with the reactions slow (< 3 hours, Sø et al., 2011) in comparison to adsorption to goethite. Therefore filter units containing Acomb pellets would require a contact time of 2-3 hours to allow for the adsorption onto calcite surfaces to occur.

The lifespan of filter units is often estimated by using the P adsorption capacity of ochres determined from the fitting of adsorption isotherms to batch experiment data (Dobbie et al., 2009). In this thesis, the P adsorption capacity of the ochres was

determined at discrete pH values and was found to be relatively low under neutral pH conditions. Further, the P adsorption capacity of ochre in this study was found to be lower than in comparable studies, i.e. Minto and Polkemmet ochre (Heal et al., 2003b). It is therefore suggested that the lifespan of filter units utilising an ochre substrate will be lower than previously determined, with this capacity dependent upon the ochre type and the pH of the overlying solution. The P adsorption capacity of the ochres in this study is still relatively high in comparison to other materials proposed as adsorbents to treat P enriched waters. For example, at pH 6, the ochres were found to have a P adsorption capacity of 11.1-34.5 mg P g^{-1}. This compares well to a review paper by Cucarella and Renman (2009) where only four out of 42 proposed P adsorbents have a P adsorption capacity greater than 11.1 mg P g^{-1}.

As discussed for the column experiments, future research should be conducted to investigate P removal by ochre at a range of P concentrations. This should concentrate at examining P removal by a packed column of ochre at lower overlying P concentrations, such as < 1 mg P L^{-1}. Batch experiments have been conducted investigating P adsorption by a Fe hydroxide rich waste product at varying overlying P concentrations (Mezenner and Bensmaili, 2009). Whilst the total P removed increases with overlying P concentration, this occurs at a lower P removal efficiency, with it also taking longer for the system to achieve equilibrium. It is suggested that this is due to an increased dominance of P adsorption on to highly reactive surface sites at lower P concentrations (Parfitt, 1989). Therefore packed filters of ochre may require less contact time for adsorption at lower P concentrations and would achieve a higher P removal efficiency. Further research is required to confirm this and should be conducted as laboratory column experiments.

The utilisation of a resting period in the column experiments greatly improved the P removal efficiency of the packed columns, particularly in those containing Polkemmet ochre, supporting the findings of Dzombak and Morel (1990) and Sibrell

et al. (2009). It is therefore suggested that filter units containing ochre should be run in parallel, with flow regularly switched between the units to allow the ochre to rest. This will ensure a far higher P removal efficiency than the implementation of a single filter unit.

As discussed in Chapter 1, P is a finite resource and P recovery will be of increasing importance over the decades to come. Prior to any larger scale installation of ochre filters, elution tests should be conducted on exhausted columns, potentially with a 0.1 M NaOH solution (Sibrell et al., 2009), to investigate whether P can be stripped from the columns. This P rich solution may then be used for the formation of struvite for use in the fertiliser industry. Further research should also examine whether the columns are suitable for re-use as a P adsorbent following elution, potentially producing a cycle of P capture and recovery.

The next step in the development of ochre as a filter system to treat P enriched surface waters is the application of ochre at a field scale. It is suggested that Polkemmet ochre is utilised for this purpose where the flow rate is constant and not episodic. Ochre filters should be run in parallel with a designed contact time of at least thirty minutes to ensure a high P removal efficiency. If the filter unit is being used to treat septic tank effluent, the tank should be examined to ensure it is working effectively to reduce the risk of bio-fouling the filter unit. Polkemmet ochre is preferred to others in the study as it has a granular form, and thus a high hydraulic conductivity. Its potential for P removal in optimised conditions has been tested in a series of column experiments to inform this filter design and tailored deployment, and improved understandings of its mechanisms of P removal would aid in the effective evaluation and modification of field trials.

7.2.2 Slow release fertiliser

Due to the rapid kinetics of adsorption and high P adsorption capacity of ochre it is suggested that research should also be conducted utilising ochre as an additive to P-rich manures and sewage sludges to the effect of binding the highly soluble P content. This would have the advantage of producing a slow release fertiliser whilst also preventing incidental losses from agricultural land.

Of the ochres selected in this study, only Polkemmet dries to a coarse particle size and is thus suitable for use in filter units. The pelletisation of ochre changes not only the P adsorption characteristics of the material, as has been seen for Acomb in this study, but requires both expertise and capital to produce. It would therefore be beneficial to develop an end-use for fine-grained ochre where these resources are not available. Ochre saturated with P under laboratory conditions has been shown to be an effective slow release fertiliser in both pot and field trials (Dobbie et al., 2005). The application of P-saturated ochre to land in the place of conventional P fertilisers has no negative impacts on crop yield or soil quality (see Chapter 2.6.1).

Previous research investigating the addition of materials with a high Fe- or Al-content to manures has shown the ability of such materials to reduce the available P content. Dao et al. (2001) examined the immobilisation of SRP in poultry manure by the addition of the two waste products, one with a high Al content, a water treatment residual, and the other having a high Fe content, a by-product of the titanium oxide production process. The addition of either material reduced the SRP content of the manures, with the Fe rich material the more efficient of the two. Compositing the manure/ waste product mixture had no significant effect on the immobilization of P and allowed the stabilization of nitrogen to occur. Dao et al. (2001) therefore suggest that Al, or preferably Fe mineral by-products can be added to composted manures as a land management technique to reduce incidental pollution incidents. Similar research has also been conducted on other P-rich manures, such as the addition of ferric chloride and aluminium sulphate to swine

manure (Ndegwa et al., 2001) and the addition of Al and Fe rich residues to poultry litter (Codling et al., 2000). This research also indicated that the addition of waste products with a high Fe or Al content to manures can reduce the SRP content of the manure, thus reducing the chances of incidental pollution.

It is therefore suggested that fine-grained ochre could be utilised in the same manner, to produce P-rich and slow release fertilisers by the addition of ochre to manure and sewage sludge. Small scale laboratory based experiments will be required to determine the ochre dose rate for addition to different manures. This will differ with the P concentration of the manure and also the ochre utilised. Following this, pot experiments should be conducted ensuring that the use of the ochre-manure mixtures have no adverse effect on crop yield and to assess the release of P over a growing season. Following this field trials and then full scale application of the ochre-manure mixture could occur. Any Fe rich ochres would be suitable for this end use as long as they have low concentrations of PTEs. For these reasons, Acomb, Minto and Polkemmet ochre are suggested as excellent candidates for future research.

7.2.3 Continuously stirred tank reactor

Of the ochres which were studied, Silkstone ochre in particular was an excellent candidate for removing P from wastewaters, with high values of S_{max} and Langmuir K derived from the P adsorption batch experiments. However the fine-grained nature of the ochre means that in its present form it would only be suitable for use in dosing treatments. It may therefore be applicable in WWTPs where technology may be present for the dosing and recovery of fine grained materials.

One form of utilising ochre in a WWTP would be in a CSTR, scaling up from research conducted by Wei et al., (2008), whereby two streams are mixed in a CSTR, one containing wastewater and the other a suspension of ochre. Preliminary research would be required to determine the optimum ochre dosage rate and

contact time, with this varying with the influent P concentration, the ochre utilised, and the target effluent P concentration.

This would have the effect of producing an effluent with a low P concentration but also a P enriched ochre sludge. This sludge could then be amended with composting materials to produce a fertiliser for application to land. The ochre dose rate could be altered to treat fluctuations in the influent P concentration ensuring discharge consents could be met. It is suggested that the WWTP should be near to the MWTP to keep transportation costs down.

7.2.4 Permeable reactive barrier

The treatment of groundwater using ochre in a PRB was initially discounted (Chapter 1) due to the potential of reducing conditions causing P, that was adsorbed to Fe complexes, to be released as Fe becomes soluble. Mixtures of Fe oxides and alkaline materials (limestone and silica sand) have proved successful, however, at removing P in long term column experiments and field applications (Baker et al., 1997). It is therefore suggested that ochre could be used in an alkaline mixture for use a PRB substrate. More research would be required to verify this, however. This study contributes to this work by elucidating the composition and properties of Acomb pellets, wherein the pelletisation process has produced an ochre with a high pH (9.68 or 11.20 when crushed, Chapter 3.2), containing goethite and calcite minerals. This pelletisation process inadvertently produced an alkaline ochre potentially suitable as a PRB substrate; further investigation into this potential end use is therefore recommended.

Chapter 8

Conclusions

The primary aim of this thesis has been to develop a more detailed and mechanistic understanding of the processes involved in the removal of P by ochre. In agreement with previous research, adsorption onto the surfaces of Fe hydroxides, in particular onto goethite, is proposed as the dominant P removal mechanism for all the ochres under low pH conditions. Three of the ochres, Acomb, Acomb pellets, and Ynysarwed ochre, were found to have relatively high calcite contents with associated higher P adsorption capacities than the other ochres at high pH conditions. It is therefore suggested that for these ochres, adsorption onto calcite is removing P at high pH conditions. These mechanisms of P removal were determined from the interpretation of the fitting of adsorption isotherms to the batch experiment data and the modelling these experiments in a SCM.

This comparative study characterised seven ochres from across the UK and Ireland in terms of their chemical composition and P adsorption properties. Elemental analysis, ammonium oxalate extractable Fe and B.E.T surface area were all utilised to indicate the potential of the ochres to adsorb P. This information was especially valuable for interpreting the results of batch and column experiments (Chapters 4 and 6), parameterising a SCM in ORCHESTRA to determine the P removal mechanisms occurring (Chapter 5), and informing filter design and recommendations of individual ochres for future use and research (Chapter 7).

The P adsorption capacity of the ochres, determined from batch experiments utilising a novel methodology, was shown to vary with pH. This highlights the importance of calculating adsorption characteristics at the pH conditions under which an adsorbing substrate will be utilised in potential field applications. A negative relationship between increasing pH and P adsorption capacity was found

for Acomb, Avoca, Silkstone and Ynysarwed ochre, with adsorption onto goethite suggested as the dominant P removal mechanism. The P adsorption capacity of Minto and Polkemmet ochre was found to be relatively constant across the pH range under study in agreement with previous research (Heal et al., 2003b), with adsorption onto surfaces of goethite again suggested as the dominant P removal mechanism. Acomb pellets were found to have the highest P adsorption capacity of any of the ochres under study, with this capacity greatest under acidic and high pH conditions. It is suggested that this is due to adsorption to goethite at low pH conditions and onto calcite at high pH conditions. All the ochres have high P adsorption capacities at the conditions expected of wastewater streams (~pH 7), ranging between 11.8 and 43.1 mg P g^{-1}. This is greater than many other materials investigated as P adsorbents (Cucarella and Renman, 2009).

A detailed set of column experiments were conducted investigating various conditions expected to affect filter performance. Polkemmet ochre was found to have a higher P removal efficiency than Acomb pellets, with P removal highest when flow rate through the system was low and the filter unit was periodically rested to regenerate surface sites. Acomb pellets have a high calcite content, 52 %, and as such it is suggested that adsorption onto surfaces of calcite is the dominant P removal mechanism for the pelleted ochre at neutral to high pH conditions. P adsorption onto calcite has slower reaction kinetics than onto surfaces of goethite. Therefore the pelletisation of the ochre has produced a filter substrate that requires a higher contact time for adsorption reactions to occur.

Recommended conditions for field trial filter application have been suggested based upon the results of the column experiments (Chapter 7.2). Filters of Polkemmet ochre operating in parallel are suggested most strongly to treat septic tank effluent or part of the wastewater stream from a WWTP, with the two filters acting alternately to allow for filter substrate to rest and regenerate surface sites. Alternative end-uses for ochre are also proposed that would capitalise on the ochres

high affinity for P, such as use in a CSTR and as an additive to P rich fertilisers. Acomb pellets are also proposed for use as a PRB substrate due to their composition of Fe oxides and alkaline materials.

Overall, the improved process-based understanding of P removal by the seven ochres under study has contributed new knowledge with regards to the efficiency with which, and mechanisms by which, they remove P across a range of different chemical and physical conditions. This study then offers recommendations for the optimal conditions necessary for the effective use of various ochres in the treatment of aquatic P pollution, delimits the necessary foci of potential field trials, and, in combining literature, experimental and modelling analysis, offers a useful platform for further work on the use of ochre to treat P enriched wastewater streams.

References

Ainsworth, C.C., Sumner, M.E. and Hurst, V.J. (1985) Effect of aluminium substitution in goethite on phosphorus adsorption: adsorption and isotopic exchange. *Soil Sci. Soc. Am. J.*, **49**, 1142-1149.

Ali, M.A. and Dzombak, D.A. (1996) Effects of simple organic acids on sorption of Cu^{2+} and Ca^{2+} on goethite. *Geochim. Cosmochim. Ac.*, **60**, 291-304.

Aumônier, J., Glendinning, S. & Bowden, L.I. (Unpublished) Stabilization of phosphorus in an ochre cement matrix. Permission copy.

Ayoub, G.M., Koopman, B. and Pandya, N. (2001) Iron and aluminium hydroxyl (oxide) coated filter media for low-concentration phosphorus removal. *Water Environ. Res.*, **73**, 478-485.

Bagot, W.D.G. (2002) *Granulation of ochre obtained from Mine Water Treatment Plants for use in the Abatement of Phosphorus Pollution from Sewerage and Agricultural Runoff*. MSc Thesis, Univ. of Newcastle-upon-Tyne, UK.

Baker, M.J., Blowes, D.W. and Ptacek, C.J. (1997) Phosphorus adsorption and precipitation in a permeable reactive wall: applications for wastewater disposal systems. *Land Cont. and Recl.*, **5**, 189-193.

Baker, M.J., Blowes, D.W. and Ptacek, C.J. (1998) Laboratory development of permeable reactive mixtures for the removal of phosphorus from onsite wastewater disposal systems. *Env. Sci. Technol.*, **32**, 2308-2316.

Baldock, D. and Bennett, G. *Agriculture and the polluter pays principle; a study of six EC countries*. Institute for European Environmental Policy, London, UK.

Banks, D., Younger, P.L., Arnesen, R.T., Iversen, E.R. and Banks, S.B. (1997) Mine-water chemistry: the good, the bad and the ugly. *Environ. Geol.*, **32**, 3, 157-176.

Banks, S. (2003) The Coal Authority Minewater Treatment Programme: an update on the performance of operational schemes. *Land Cont. and Recl.*, **11** (2), 161-164.

Bastin, O., Janssens, F., Dufey, J. and Peeters, A. (1999) Phosphorus removal by a synthetic iron oxide-gypsum compound. *Ecol. Eng.*, **12**, 339-351.

Bigham, J. M., Schwertmann, U., Trania, S.J., Winland, R.L. and Wolf, M. (1996) Schwertmannite and the chemical modelling of iron in acid sulphate waters. *Geochim. Cosmochim. Ac.*, **60**, 2111-2121.

Biswas, B.K., Inoue, K., Ghimire, K.N., Ohta, S., Harada, H., Ohto, K. and Kawakita, H. (2007) The adsorption of phosphate from an aquatic environment using metal-loaded orange waste. *J. Colloid Interf. Sci.*, **312**, 214-223.

Blowes, D.W. and Ptacek, C.J. (1994) *System for treating contaminated groundwater (Redox Curtain)*. US Patent number US5362394.

Boaventura, R., Pedro, A.M., Coimbra, J. and Lencastre, E. (1996) Trout farm effluents: Characterization and impact on the receiving streams. *Environ. Pollut.*, **95**, 379-387.

Bolster, C.H. (2010) ***Microsoft Excel Spreadsheets for Fitting Sorption Data*. Available online from** www.ars.usda.gov/pandp/docs.htm?docid=14971. Accessed on 01/04/2011.

Bolster, C.H. and Hornberger, G.M. (2007) On the use of linearized Langmuir equations. *Soil Sci. Soc. Am. J.*, **71**, 1796-1806.

Boujelben, N., Bouzid, Z., Elounear, M., Feki, M., Jamoussi, F. and Montiel, A. (2008) Phosphorus removal from aqueous solution using iron coated natural and engineered sorbents. *J. Hazard. Mater.*, **151**, 103-110.

Bouma, J. (1979) Subsurface applications of sewage effluent. In: Beatty, M.T., Petersen, G.W. and Swindale, L.D. *Planning the Uses and Management of Land (Agronomy)*. American Society of Agronomy, Madison, USA.

Bozika, E. (2001) *Phosphorus Removal from Wastewater Using Sludge from Mine Drainage Treatment Settlement Ponds*. MSc thesis, Univ. of Edinburgh, UK.

Brady, K.S., Bigham, J.M., Jaynes, W.F. and Logan, T.J. (1986) Influence of sulphate on Fe-oxide formation: comparisons with a stream receiving acid mine drainage. *Clay. Clay Miner.*, **34**, 266-274.

Braskerud, B.C. (2002) Factors affecting phosphorus retention in small constructed wetlands treating agricultural non-point source pollution. *Ecol. Eng.*, **1**, 41-61.

Brinker, A. and Rosch, R. (2005) Factors determining the size of suspended solids in a flow-through fish farm. *Aquacult. Eng.*, **33**, 1-19.

British Standard (1987) *Pyknometers Part 2: Methods for Calibration and use of Pyknometers.* BSI 733-2, UK.

British Standard (2005) *Soil Quality- Determination of pH*. BS ISO 10390. UK.

Brown, M., Barley, B. and Wood, H. (2002) *Minewater Treatment: Technology, Application and Policy.* IWA Publishing, London, UK.

Brunauer, S., Emmnett, P.H. and Teller, E. (1938) Adsorption of gases in multimolecular layers. *J. Am. Chem. Soc.*, **60**, 309-319.

Buckingham, D. and Jasinski, S.M. (2006) *Phosphate rock statistics, historical statistics for mineral and material commodities in the United States, Data series 140*. US Geological Society, USA.

Bush, A.M. (2001) *An investigation into the use of iron ore sludge to remove phosphorus in the river Leet, in an attempt to mitigate eutrophic conditions*. MSc thesis, Univ. of Edinburgh, UK.

Canter, L.W. and Knox, R.C. (1985) *Septic tank system effects on groundwater quality*. Lewis Publishers, Boca Raton, USA.

Carlsson, H., Aspegren, H., Lee, N. and Hilmer, A. (1996) Calcium phosphate precipitation in biological phosphorus removal systems. *Water Res.* **31**, 1047-1055.

Carr, S. (2007) *An investigation into the removal of Phosphorus with the use of ochre: Installation on a pilot scale at Nafferton Farm, Northumberland*. MSc Thesis, Univ. of Newcastle.

Carty, A., Scholz, M., Heal, K., Gouriveau, F. and Mustafa, A. (2008) The universal design, operation and maintenance guidelines for farm constructed wetlands (CFW) in temperate climates. *Bioresource Technol.*, **99**, 6780-6792.

Chadwick, D.R. and Chen, S. (2002) Manure. In: Haygarth, P.M. and Jarvis, S.C. (Eds) *Agriculture, Hydrology and Water Quality.* CABI Publishing, Wallingford, UK. 57-82.

Clark, E.R., Harman, J.P. and Forster, J.R.M. (1985) Production of metabolic and waste products by intensively farmed rainbow-trout, Salmo gairdneri Richardson. *J. Fish Biol.*, **27**, 381-393.

Clarke, E. (2004) *Phosphorus Stripping Pilot Study at Nafferton Farm*. MSc Thesis, Newcastle University, UK.

Codling, E.E., Chaney, R.L. and Mulchi, C.L. (2000) Use of Aluminium and Iron Rich residues to Immobilize Phosphorus in Poultry Litter and Litter amended Soils. *J. Environ. Qual.*, **29**, 1924-1931.

Commission of the European Communities (2007) Towards sustainable water management in the European Union – first stage in the implementation of the Water Framework Directive. *ECCOM*, **128**, 1-13.

Commission Regulation (EC) No. 466/ 2001 of 8 March 2001 setting maximum levels for certain contaminants in foodstuffs. *Off. J. Eur. Communities,* **L77**, 1-13.

Cooney, D.O. (1999) *Adsorption Design for Wastewater Treatment.* Lewis Publishers, Boca Raton, USA.

Cordell, D., Drangert, J-O. and White, S. (2009) The story of phosphorus: Global food security and food for thought. *Global Env. Chang.*, **19**, 292-305.

Cornell, R.M. and Schwertmann, U. (2003) *The Iron Oxides: Structure, Properties, Reactions, Occurrences and Uses*. Wiley-VCH GmbH & Co. KGaA, Weinheim, Germany.

Cucarella, V. and Renman, G. (2009) Phosphorus sorption capacity of filter materials used for on-site wastewater treatment determined in batch experiments- A comparative study. . *J. Environ. Qual.*, **38**, 381-392.

Cundy, A.B., Hopkinson, L. and Whitby, R.L.D. (2008) Use of iron-based technologies in contaminated land and groundwater remediation: A review. *Sci. Total Environ.*, **400**, 42-51.

D'Arcy, B.J. and Frost, A. (2001) The role of best management practices in alleviating water quality problems associated with diffuse pollution. *Sci. Total Environ.*, **265**, 359-367.

D'Arcy, B.J., Ellis, J.B., Ferrier, R.C. and Jenkins, A. (2000) *The Environmental and Economic Impacts of Diffuse Pollution in the UK*. Terence Dalton Publishers – CIWEM, Lavenham, UK.

Dakora, F.D. and Phillips., D.A. (2002) Root exudates as mediators of mineral acquisition in low-nutrient environments. *Plant Soil*, **245**, 35-47.

Daniel, T.C., Sharpley, A.N. and Lemunyon, J.L. (1998) Agricultural phosphorus and eutrophication: A symposium overview. *J. Environ. Qual*., **27**, 251-257.

Dao, T.H., Sikora, L.J., Hamasaki, A. and Chaney, R.L. (2001) Manure phosphorus extractability as affected by aluminium- and iron by-products and aerobic compositing. *J. Environ. Qual*., **30**, 1693-1698.

Davis, J.A. and Leckie, J.O. (1978) Surface ionization and complexation at the oxide/ water interface. II Surface properties of amorphous iron oxyhydroxide and adsorption of metal ions. *J. Colloid Interf. Sci.*, **67**, 90-107.

Davis, J.A., and Kent, D.B. (1990) Surface Complexation Modeling in Aqueous Geochemistry. In: Hochella, M.F. and White, A.F. *Reviews in Mineralogy, Volume 23: Mineral-Water Interface Geochemistry.* Mineralogical Society of America, Washington, D.C, USA.

Department for Environment, Food and Rural Affairs. (2004) *Diffuse Pollution of Water*. DEFRA publication, UK.

Department of the Environment (1981) *Methods for the examination of waters and associated materials*. Department of the Environment, UK.

Department of the Environment (1995) *Landfill Design, Construction and Operational Practice.* Waste Management Paper 26B, Department of the Environment, UK.

Deppe, T., and Benndorf, J. (2002) Phosphorus reduction in a shallow hypereutrophic reservoir by in-lake dosage of ferrous iron. *Water Res.*, **36**, 4525-4534.

Dijkstra, J.J., Meeussen, J.C.L. & Comans, R.N.J. (2009) Evaluation of a Generic Multisurface Sorption Model for inorganic soil contaminants. *Env. Sci. Technol.*, **43,** 6196-6201.

Dimoliatis, D. (2002) *Potential use of ochre in-stream filters to reduce phosphorus concentrations in the Leet Water, Berwickshire*. MSc thesis, Univ. of Edinburgh, UK.

Dixit, S. and Hering, J.G. (2003) Comparison of Arsenic (V) and Arsenic (III) sorption onto iron oxide minerals: Implications for arsenic mobility. *Environ. Sci. Technol.* **37**, 4182-4189.

Dobbie, K.E., Heal, K.V. and Smith, K.A. (2005) Assessing the performance as a fertiliser and the environmental acceptability of phosphorus-saturated ochre. *Soil Use Manage.*, **21**, 231-239.

Dobbie, K.E., Heal, K.V., Aumônier, J., Smith, K.A., Johnston, A., and Younger, P.L. (2009) Evaluation of iron ochre from mine drainage treatment for removal of phosphorus from wastewater. *Chemosphere*, **75**, 795-800.

Doi, M., Warren, G., and Hodson, M.E. (2005) A preliminary investigation into the use of ochre as a remedial amendment in arsenic-contaminant soils. *Appl. Geochem.*, **20**, 12, 2207-2216.

Douglas, G.B., Adeney, J.A., and Robb, M.S. (1999) A novel technique for reducing bioavailable phosphorus in water and sediments. In: *International Association Water Quality Conference on Diffuse Pollution*, pp. 517–523.

Douglas, G.B., Robb, M.S., Coad, D.N. and Ford, P.W. (2004) In: Valsami-Jones, E. (ed) *Phosphorus in Environmental Technology: Principles and Applications*, IWA Publishing, London, UK. pp.291-311.

Drits, V.A. and Bookin, A.S. (2001) Crystal Structure and X-ray Identification of Layered Double Hydroxides. In: Rives, V. (ed) *Layered Double Hydroxides: Present and Future*. Nova Science Publishers, New York, USA.

Drizo, A., Frost, C., Grace, J. and Smith, K. (1999) Physico-chemical screening of phosphate-removing substrates for use in constructed wetland systems. *Water Res.*, **33**, 3595-3602.

Dudeney, A.W.L. (2003) *Report to the Coal Authority: Research on Sludge Utilisation, March-September.* London, UK.

Dudeney, A.W.L., Tarasova, I.I., and Tyrologou, P. (2004) Co-utilisation of mineral and biological wastes in mine site restoration. *Miner. Eng.*, **17**, 131-139.

Dudley, B. and May, L. (2007) Estimating the phosphorus load to waterbodies from septic tanks. *NERC open research archive*, available online from http://nora.nerc.ac.uk/2531. Accessed 11/12/2010.

Dunne, E.J., Culleton, N., O'Donovan, G., Harrington, R. and Olsen, A.E. (2005) An integrated constructed wetland to treat contaminants and nutrients from dairy farmyard and dirty water. *Ecol. Eng.*, **24**, 221-234.

Dzombak, D.A. and Morel, F.M.M. (1990) *Surface Complexation Modelling-Hydrous Ferric Oxides.* John Wiley & Sons, New York, USA.

Dzombak, D.A. and Morel, F.M.M. (1990) *Surface complexation modelling: Hydrous Ferric Oxide*. Wiley, New York, USA.

Edwards, A.C. and Withers, P.J.A. (2008) Transport and delivery of suspended solids, nitrogen and phosphorus from various sources to freshwaters in the UK. *J. Hydrol.*, **350**, 144-153.

Edwards, A.C., Kay, D., McDonald, A.T., Francis, C., Watkins, J., Wilkinson, J.R. and Wyer, M.D. (2008) Farmyards, an overlooked source for highly contaminated runoff. *J. Environ. Manage.*, **87**, 551-559.

European Economic Community (1975) Council Directive (75/440/EEC) of 16 June 1975, concerning the quality required of surface water intended for the abstraction of drinking water in the member states. *Off. J. Eur. Communities*, **L. 194**.

European Economic Community (1976) Council Directive (76/464/EEC) of 4 May 1976 on pollution caused by certain dangerous substances discharged into the aquatic environment of the community. *Off. J. Eur. Communities*, **L. 129**.

Emsley, J. and Hall, D. (1976) *The Chemistry of Phosphorus.* Harper and Row Publishers, London, UK.

Enfield, C.G. (1975) Fate of water phosphorus in soil. *J. Irr. Drain. Div-ASCE,* **101**, 145-155.

Environment Agency. (2007) *The Unseen Threat to Water Quality*. Environment Agency, Bristol, UK.

Environment Agency (2008) *Abandoned mines and the water environment*. Science Project SC030136-41. Environment Agency, Bristol, UK.

European Commission. (1991) Directive 91/271/EEC of 21 May 1991 concerning urban waste-water treatment. *Off. J. Eur. Communities,* **L135**, 40-52.

European Commission. (2000) Directive 2000/60/EC of the European parliament and of the council of 23 October 2000 establishing a framework for community action in the field of water policy. *Off. J. Eur. Communities,* **L327**, 1-73.

European Fertilizer Manufacturers Association. (2000) *Phosphorus: Essential element for food production.* European Fertilizer Manufacturers Association, Brussels, Belgium.

EUWFD (2010) *Sources of pollution: Diffuse pollution*. Available online from www.euwfd.com/html/sources_of_pollution_-_diffuse_pollution.html. Accessed on 01/02/2011.

Farmer, V.C., Russell, J.D. and Smith, B.F.L. (1983) Extraction of inorganic forms of translocated Al, Fe and Si from a podzol Bs horizon. *J. Soil Sci.*, **34**, 571-576.

Fenton, O., Healy, M.G. and Rodgers, M. (2009) Use of ochre from an abandoned metal mine in the south east of Ireland for phosphorus sequestration from dairy dirty water. *J. Environ. Qual*. **38**, 1-6.

Fontes, M.P.F. and Weed, S.B. (1996) Phosphate adsorption by clays from Brazilian oxisols: relationships with specific surface area and mineralogy. *Geoderma*, **72**, 37-51.

Freeman, J.S. and Rowell, D.L. (1981) The adsorption and precipitation of phosphate onto calcite. *J. Soil Sci.* **32**, 75-84.

Frossard, E., Brossard, M., Hedley, M.J. and Metherell, A. (1995) Reactions controlling the cycling of P in soils. In SCOPE 54 – Phosphorus in the Global Environment – Transfers, Cycles and Management (Ed. Tiessen, H.), Wiley, J. and Sons Ltd., Chichester, pp. 107-137.

Frost, A. (1996) Loch Leven and diffuse pollution. In: Petchey, A.M., D'Arcy, B.J. and Frost, C.A. (Ed.s) *Diffuse pollution and agriculture.* Scottish Agricultural College, Aberdeen, UK. pp. 174-182.

Gallagher, V. and O'Connor, P. (1999) The Avoca mine site, *P. Roy. Irish Acad. B*, **99B**, 43-57.

Geelhoed, J.S., Hiemstra, T. and Van Riemsdijk, W.H. (1997) Phosphate and sulphate adsorption on goethite: Single anion and competitive adsorption. *Geochim. Cosmochim. Ac.* **61**, 2389-2396.

Geroni, J.N., Sapsford, D.J. and Watson, I. (2010) The Potential for semi-passive mine water Treatment by CO_2 stripping at Ynysarwed, S. Wales. In: Wolkersdorfer, C. and Freund, A. (Ed.s) 'Mine Water and Innovative Thinking', *Proceedings of the International Mine Water Association Symposium 2010 Sydney. CBU Press, Nova Scotia, Canada.*

Goehring, L.C., Steenhuis, T.S., Brooks, A.S., Rosenwald, M.N., Chen, J. and Putman, V.J. (1999) Cost-effective phosphorus removal from secondary wastewater effluent through mineral adsorption. *Final Report Prepared for the Town of Willisboro,* Essex County, New York, USA.

Goldberg, S. (1995) Adsorption Models Incorporated into Chemical Equilibrium Models. In: Loeppert, R.H., Schwab, A.P. and Goldberg, S. *Chemical Equilibrium and Reaction Models*. SSSA Special Publication No. 42, Wisconsin, USA.

Gouriveau, F. (2009) *Constructed Farm Wetlands (CFWs) designed for remediation of farmyard runoff: an evaluation of their water treatment efficiency, ecological value, costs and benefits.* PhD Thesis, Univ. of Edinburgh, UK.

Grant, N. and Moodie, M. (1997) *Septic Tanks: An overview* [2nd Ed.]. CAT publications, Cardiff, Wales.

Grüneberg, B. and Kern, J. (2001) Phosphorus retention capacity of iron-ore and blast furnace slag in sub-surface flow constructed wetlands. *Water Sci. Technol.*, **44**(11-12), 69-75.

Guzzon, A., Bohn, A., Diociaiuti, M. and Albertano, P. (2008) Cultured phototrophic biofilms for phosphorus removal in wastewater treatment. *Water Res.*, **42**, 4357-4367.

Haghseresht, F. (2006) A revolution in phosphorus removal. *Phoslock technical report, October 2006, Report No. PS-06.*

Hancock, S. (2004) *Ochre Arisings and Composition in the UK*. MSc Thesis, Imperial College London.

Hancock, S. (2005) Quantifying Ochre Arisings: Output from the UK Coal Authority's Mine Water Treatment Sites. In: Loredo, J. and Pendás, F. (Ed.s) *Mine Water 2005 – Mine Closure*, 395-402.

Haworth, A. (1990) A review of the modelling of sorption from aqueous solution. *J. Colloid Interf. Sci.*, **32**, 43-78.

Haygarth, P.M. and Jarvis, S.C. (1999) Transfer of phosphorus from agricultural soils. *Adv. Agron.*, **66**, 195-249.

Heal, K. V., Younger, P.L., Smith, K.A., Glendinning, S., Quinn, P., and Dobbie, K.E. (2003a) Novel use of ochre from mine water treatment plants to reduce point and diffuse phosphorus pollution. *Land Contam. Recl.,* **11**, 145-152.

Heal, K.V., Smith, K.A., Younger, P.L., McHaffie, H. and Batty, L.C. (2003b) Removing phosphorus from sewage effluent and agricultural runoff using recovered ochre. In: Valsami-Jones, E. (Ed.) *Phosphorus in Environmental Technology: Principles and Applications*, IWA Publishing, London. pp.320-334.

Hedin, R.S. (2003) Recovery of marketable iron oxide from mine drainage. *Land Contam. Recl.,* **11**, 2, 93-97.

Hilton, J. (2003) Reducing diffuse pollution to rivers: a dictionary of best management practices. *Conserving Natura 2000 Rivers Conservation Technique Series No. 10.* English Nature, Peterborough, UK.

Hively, W.D., Bryant, R.B. and Fahey, T.J. (2005) Phosphorus concentrations in overland flow from diverse locations on a New York dairy farm. *J. Environ. Qual*. **34**, 1224-1233.

Hoehn, E. and Roberts, P.V. (1982) Advection-Dispersion interpretation of tracer observations in an aquifer. *Ground water*. **20**, 457-465.

Holford, I.C.R., Wedderburn, R.W.M. and Mattingly, G.E.G. (1974) A Langmuir two-surface equation as a model for phosphate adsorption by soils. *J. Soil. Sci.* **25**, 242-255.

Holman, I.P., Howden, N.J.K., Bellamy, P., Willby, N., Wheland, M.J. and Rivas-Casado, M. (2010) An assessment of the risk to surface water ecosystems of groundwater-P in the UK and Ireland. *Sci. Total Environ.*, **408**, 1847-1857.

Huang, C.P. and Stumm, W. (1973) Specific adsorption of cations on hydrous γ-Al_2O_3. *J. Colloid Interf. Sci.*, **43**, 409-420.

Huang, S.H. and Chiswell, B. (2000) Phosphate removal from wastewater using spent alum sludge. *Water Sci. Technol*., **42**, 295-300.

Hubbert, M.K. (1949) Energy from fossil fuels. *Science.* **109**, 103.

Hylander, L.D. and Simán, G. (2001) Plant availability of phosphorus sorbed to potential wastewater treatment materials. *Biol. Fert. Soils,* **34**, 42-48.

International Fertilizer Industry Association (2006) *Sustainable development and the fertilizer industry.* Available online from www.fertilizer.org/ifa/Home-Page/ SUSTAINABILITY/Sustainable-development. Accessed on 16/02/2011.

Interstate Technology Regulatory Council (2005) *Permeable reactive barriers: Lessons learned/ New directions.* ITRC, Washington DC, USA.

Jandl, R., Kopeszki, H., Bruckner, A., and Hager, H. (2003) Forest soil chemistry and mesofauna 20 years after an amelioration fertilization. *Restor. Ecol.*, **11**, 239-246.

Jarvie, H.P., Haygarth, P.M., Neal, C., Butler, P., Smith, B., Naden, P.S., Joynes, A., Neal, M., Wickham, H., Armstrong, L., Harman, S. and Palmer-Felgate, E.J.

(2008) Stream water chemistry and quality along an upland-lowland rural land-use continuum, south west England. *J. Hydrol.*, **350**, 215-231.

Jasinski, S.M. (2007) *Phosphate rock, mineral commodity summaries*. U.S. Geological Survey, United States Government Printing Office, Washington D.C, USA.

Jasinski, S.M. (2008) *Phosphate rock, mineral commodity summaries*. U.S. Geological Survey, United States Government Printing Office, Washington D.C, USA.

Jeong, Y., Maohong, F., Van Leeuwen, J. and Belczyk, J.F. (2007) Effect of competing solutes on arsenic (V) adsorption using iron and aluminium oxides. *J. Environ Sci. (China)*, **19**, 910-919.

Johansson, L. (1999) Blast furnace slag as phosphorus sorbents-column studies. *Sci. Total Environ.*, **229**, 89-97.

Johansson, L. (1999) Industrial by-products and natural substrata as phosphorus sorbents. *Environ. Technol.*, **20**, 309-316.

Johansson-Westhom, L. (2006) Substrates for phosphorus removal – potential benefits for on-site wastewater treatment?. *Water Res*., 40, 23-36.

Junkins, R., Deeney, K. and Eckhoff, T. (1983) *The Activated Sludge Process: Fundamentals of Operation.* Ann Arbor Science Publishers, Michigan, USA.

Kallis, G. and Butler, D. (2001) The EU water framework directive: measures and implications. *Water Policy*, **3**, 125-142.

Kang, S-K., Choo, K-H., and Lim, K-H. (2003) Use of iron oxide particles as adsorbents to enhance phosphorus removal from secondary wastewater effluent. *Separ. Sci. Technol.*, **38** (15), 3853-3874.

Karageorgiou, K., Paschalis, M. and Anastassakis, G.N. (2007) Removal of phosphate from solution by adsorption onto calcite used as a natural adsorbent. J. Hazard. Mater. **A139**, 447-452.

Kim, L-H., Choi, E. and Stenstrom, M.K. (2003) Sediment characteristics, phosphorus types and phosphorus release rates between river and lake sediments. *Chemosphere*, **50**, 53-61.

Kleinmann, R.L.P. (2006) Acid Mine Water Treatment using Engineered Wetlands. In: Kleinmann, R.L.P. and Booth, C. (Ed.s) 'Mine Water and the Environment', *Proceedings of the International Mine Water Association Sympsosium 2006. St. Louis, USA, USA.*

Kotak, B.G., Kenefick, S.L., Fritz, D.L., Rousseaux, C.G., Prepas, E.E. and Hrudley, S.S. (1993) Occurrence and toxicological evaluation of cyanobacterial toxins in Alberta Lakes and farm dugouts. *Water Res.*, **27**, 495-506.

Kunimatsu, T., Sudo, M. and Kawachi, T. (1999) Loading rates of nutrients discharging from a golf course and a neighbouring forested basin. *Water Sci. Technol*., 39 (12), 99-107.

Lake, B.A., Collidge, K.M., Norton, S.A. and Amirbahman, A. (2007) Factors contributing to the internal loading of phosphorus from anoxic sediments in six Maine, USA, lakes. *Sci. Total Environ.*, **373**, 534-541.

Lamont-Black, J., Younger, P.L., and Batty, L. (2001) *Factual report of test results for use in designing phosphate removal by passive wetlands.* Department of Civil Engineering, Univ. of Newcastle, Newcastle, UK.

Langmuir, I. (1918) The adsorption of gases on plane surfaces of glass, mica and platinum. *J. Am. Chem. Soc.*, **40**, 1361-1403.

Li, Y., Liu, C., Luan, Z., Peng, X., Zhu, C., Chen, Z., Zhang, Z., Fan, J. and Jia, Z. (2006) Phosphate removal from aqueous solutions using raw and activated red mud and fly ash. *J. Hazard. Mater.*, **137**, 374-383.

Lijklema, L., Koelmans, A.A. and Portielje, R. (1993) Water quality impacts of sediment pollution and the role of early diagenesis. *Water Sci. Technol.*, **28 (8-9)**, 1-12.

Line, D.E., White, N.M., Osmond, D.L., Jennings, G.D. and Mojonnier, C.B. (2002) Pollutant export from various land uses in the Upper Neuse River Basin. *Water Environ Res.*, **74**, 100-108.

Lumsdon, D.G. (1995) Predicting Speciation and Computer Simulation. In: Ure, A.M. and Davidson, *C.*M. *Chemical Speciation in the Environment.* Blackie Academic and Professional, London, UK.

Lumsdon, D.G. (2004) Partitioning of organic carbon, aluminum and cadmium between solid and solution in soils: application of a mineral-humic particle additivity model. *Eur. J. Soil Sci.*, **55**, 271–285.

MacNaeidhe, F.S. (2001) Effect of application of basic slag and superphosphate on herbage yield and on soil and herbage concentrations of phosphorus in organic grassland. *Biol. Agric. Hortic.*, **19**, 231-245.

MAFF (1998) *The soil code – code of good Agricultural practice for the protection of soil.* MAFF Publications, UK.

Mann, R. (1997) Phosphorus adsorption and desorption characteristics of constructed wetland gravels and steelworks by-products. *Aust. J. Soil. Res.*, **35**, 375-384.

Mann, R.A. and Bavor, H.J. (1993) Phosphorus removal in constructed wetlands using gravel and industrial waste substrata. *Water Sci. Technol.*, **27(1)**, 107-113.

Markis, K.C., El-Shall, H., Harris, W.G., O'Connor, G.A. and Obreza, T.A. (2004) Intraparticle phosphorus diffusion in a drinking water treatment residual at room temperature. *J. Colloid Interf. Sci.*, **277**, 417-423.

Martinez, D., Mascioli, S. and Bocanegra, E. (2006) Determination of Zn partition coefficient and simulation of reactive transport from landfills in Mar Del Plata, Argentina. *Environ. Geol.*, 51, 463-469.

May, L. and Gunn, I.D.M. (2000) *An assessment of the possible impact of gulls from a proposed landfill site on the nutrient load to Loch Ussie, Easter Ross, Scotland*. Report to S.I.T.A Northeast by the Institute of Freshwater Ecology, IFE Report No. ED/C01468/1. Edinburgh, UK.

Mayer, D.G. and Butler, D.G. (1993) Statistical validation. *Ecol. Model.*, **68**, 21-32.

McHaffie, H., Heal, K.V. and Smith, K.A. (2000) *Using Sludge from Mine Drainage Treatment Settlement Ponds for Phosphorus Removal from Wastewaters: Report to Coal Authority.* Institute of Ecology and Resource Management, Univ. of Edinburgh, UK.

McKay, M.C. (1996) *Use of Adsorbents for the Removal of Pollutants from Wastewaters.* CRC Press, Boca Raton, USA.

McKeague, J.A. and Day, J.H. (1966) Dithionite- and oxalate-extractable Fe and Al as aids in differentiating various classes of soils. *Can. J. Soil Sci.*, **46**, 13-22.

Meeussen, J.C.L (2011) *ORCHESTRA: Introduction*. Available online from www.meeussen.nl/orchestra/. Accessed on 10/01/2011.

Meeussen, J.C.L. (2003) ORCHESTRA: An object-orientated framework for implementing chemical equilibrium models. *Env. Sci. Technol.*, **6**, 1175-1182.

Mezenner, N.Y. and Bensmaili, A. (2009) Kinetics and thermodynamic study of phosphate adsorption on iron hydroxide-eggshell waste. *Chem. Eng. J.* **147**, 87-96.

Micromeritics (2001) *Gas sorption analysis.* Available online from www.micromeritics.com/Repository/Files/Gas_Sorption.pdf. Accessed on 10/1/2011.

Miller, M.L., Bhadha, J.H., O'Connor, G.A., Jawitz, J.W. and Mitchell, J. (2011) Aluminium water treatment residuals as permeable reactive barrier sorbents to reduce phosphoru losses. *Chemosphere*, **83**, 978-83.

Moelants, N., Smets, I.Y. and Van Impe, J.F. (2011) The potential of an iron rich substrate for phosphorus removal in decentralized wastewater treatment systems. *Sep. Purif. Technol.*, **77**, 40-45.

Morse, G.K., Brett, S.W., Guy, J.A. and Lester, J.N. (1998) Review: Phosphorus removal and recovery technologies. *Sci. Total Environ.*, **212**, 69-81.

Moss, B. (1988) A land awash with nutrients - the problem of eutrophication. *Chem. Ind-London*, **11**, 407-411.

Moss, B. (2008) The Water Framework Directive: Total environment or political compromise? *Sci. Total Environ.*, **400**, 32-41.

Münch, E.V. and Barr, K. (2000) Controlled struvite crystallisation for removing phosphorus from anaerobic digester sidestreams. *Water Res.*, **35**,(1), 151-159.

Murphy, J. and Riley, J.P. (1962) A modified single solution method for the determination of phosphate in natural waters. *Anal. Chim. Acta*, 27, 31-36.

Nash, J. E. and Sutcliffe, J. V. (1970) River flow forecasting through conceptual models part I -- A discussion of principles. *J. Hydrol*., **10**, 282-290.

Ndegwa, P.M., Zhu, J. and Luo, A. (2001) Effects of solid levels and chemical additives on removal of solids and phosphorus in swine manure. *J. Environ. Eng.,* **127**, 1111-1115.

Nichols, P. (2006) *Undergraduate Dissertation*. Univ. of Newcastle, UK.

Noyes, R. (1991) *Handbook of Pollution Control Processes.* Noyes Publications, New Jersey, USA.

Nriagu, J.O. and Moore, P.B. (1984) *Phosphate Minerals.* Springer-Verlag, Berlin, Germany.

O'Neill, P. (1998) *Environmental Chemistry* [3rd Ed.]. Blackie Academic and Professional, London, UK.

Ohlinger, K.N., Young, T.M. and Schroeder, E.D. (1998) Predicting struvite formation in digestion. *Water Res.*, **32** (12), 3607-3614.

Oliveira, M., Machado, A.V. and Nogueira, R. (2010) Development of permeable reactive barrier for phosphorus removal. *Mater. Sci. Forum,* **636-637**, 1365-1370.

Oliveira, M., Ribeiro, D., Nobrega, J.M., Machado, A.V., Brito, A.G. and Nogueira, R. (2011) Removal of phosphorus from water using active barriers: Al2O3 immobilized onto polyolefins. *Environ. Technol*., **32**, 989-995.

Palmstrom, N.S., Carlson, R.E. and Cooke, G.D. (1988) Potential links between eutrophication and formation of carcinogens in drinking water. *Lake Reserv. Manage*., **4**, 1-15

Parfitt, R.L. (1989) Phosphate reactions with natural allophone, ferrihydrite and goethite. *J. Soil Sci.,* **40**, 359-369.

Parfitt, R.L. and Childs, C.W. (1988) Estimation of forms of Fe and Al: A review and analysis of contrasting soils by dissolution and Moessbauer spectroscopy. *Aust. J. Soil. Res.,* **26**, 121-144.

Peavy, H.S. (1978) *Groundwater Pollution from Septic Drainfields.* Montana State University, Montana, USA.

Petticrew, E.L. and Arocena, J.M. (2001) Evaluation of iron-phosphate as a source of internal lake phosphorus loadings. *Sci. Total Environ.*, **266**, 87-93.

Phoslock Newsletter (2007) *Lake restoration and reservoir management*. Phoslock Water Solution Ltd, Sydney, Australia.

Pionke, H.B., Gburek, W.J., Sharpley, A.N. and Zollweg, J.A. (1997) Hydrological and chemical controls on phosphorus loss from catchments. In: Tunney, H. (Ed.) *Phosphorus Loss from Soil to Water.* Centre for Agriculture and Biosciences International, England. pp. 225-242.

Poe, A.C., Pichler, M.F., Thompson, S.P. and Paerl, H.W. (2003) Denitrification in a constructed wetland receiving agricultural runoff. *Wetlands,* **23**, 817-826.

Pretty, J.N., Mason, C.F., Nedwell, D.B., Hine, R.E., Leaf, S. and Dils, R. (2003) Environmental costs of freshwater eutrophication in England and Wales. *Env. Sci. Technol.*, **37**, 201-208.

Pulford, I.D. (1986) Mechanisms controlling zinc solubility in soils. *J. Soil Sci.*, **37**, 427-438.

Redfield, A.C. (1934) On the proportions of organic derivations in seawater and their relation to the composition of plankton. In Daniel, R.J. *James Johnstone Memorial Volume.* University Press of Liverpool, UK.

Rice, R.W., Izuno, F.T. and Garcia, R.M. (2002) Phosphorus load reductions under best management practices for sugarcane cropping systems in the Everglades Agricultural Area. *Agr. Water Manage.*, **56**, 17-39.

Ritcey, G.M. (1989) *Tailings Management: Problems and Solutions in the Mining Industry.* Elsevier, Amsterdam, Netherlands.

Roseth, R. (2000) Shell sand: a new filter medium for constructed wetlands and waste-water treatment. *J. Environ. Sci. Heal. A*, **35**, 1335-1355.

Sakadevan, K. and Bavor, H. (1998) Phosphate adsorption characteristics of soils, slags and zeolites to be used as substrates in constructed wetland systems. *Water Res.*, **32**, 393-399.

Scheffer, M., Westley, F. and Brock, W. (2003) Slow response of societies to new problems: causes and costs. *Ecosystems*, **6**, 493-502.

Scottish Environment Protection Agency. (2002) *Water Framework Directive – Your questions answered*. SEPA publications, Stirling, UK.

Scottish Environment Protection Agency. (2005) *Diffuse Pollution Initiative Home page*. Available online from www.sepa.org.uk/dpi/index. Accessed on 07/01/2009.

Scottish Environment Protection Agency. (2008) *Septic tanks: Important changes to the control of small private sewage discharges*. Available online from www.sepa.org.uk/water/ water_publications.aspx. Accessed on 12/03/2010.

Scottish Natural Heritage (2010) *Freshwater Aquaculture*. Available online from www.snh.gov.uk/land-and-sea/managing-freshwater/freshwater-aquaculture/. Accessed on 11/12/2010.

Sharpley, A.N., Chapra, S.C., Wedepohl, R., Sims, J.T., Daniel, T.C. and Reddy, K.R. (1994) Managing agricultural phosphorus for protection of surface waters: Issues and options. *J. Environ. Qual.*, **23**, 437-451.

Sharpley, A.N., Smith, S.J., Jones, O.R., Berg, W.A. and Coleman, G.A. (1992) The transport of bioavailable phosphorus in agricultural runoff. *J. Environ. Qual.*, **21**, 30-35.

Sibrell, P.L., Montgomery, G.A., Ritenour, K.L. and Tucker, T.W. (2009) Removal of phosphorus from agricultural wastewaters using adsorption media prepared from acid mine drainage sludge. *Water Res.*, **43**, 2240-2250.

Singer, P.C. and Stumm, W. (1970) Acid mine drainage: the rate determining step. *Science*, **167**, 1121-1123.

Singh, B., Wilson, M.J., McHardy, W.J., Fraser, A.R., and Merrington, G. (1999) Mineralogy and chemistry of ochre sediments from an acid mine drainage near a disused mine in Cornwall, UK. *Clay Miner.*, **34**, 301-317.

Smyth, D.J.A., Blowes, D.W., Ptacek, C.J., Baker, M.J., Ford, G., Foss, S. and Bernstene, E. (2002) Removal of phosphate and waterborne pathogens from wastewater effluent using permeable reactive materials. In: Stolle, D., Piggott, A.R. and Crowder, J.J. (Ed.s), *Ground and Water: Theory to practice – Proceedings of the 55th Canadian Geotechnical and 3rd joint IAH-CNC and CGS Groundwater Speciality Conferences,* Southern Ontario Section of the Canadian Geotechnical Society, Ontario, Canada, pp. 1123-1128.

SNIFFER (2006) *Diffuse Pollution Screening Tool Stage III. Final Report.* Research with ADAS Consulting, Macaulay Institute for Soil Research, HR Wallingford (Firm) and Scotland and Northern Ireland Forum for Environmental Research. Project WFD77, SNIFFER, Edinburgh, UK.

Sø, H.U., Postma, D., Jakobsen, R. and Larsen, F. (2011) Sorption of phosphate onto calcite; results from batch experiments and surface complexation modelling. *Geochem. Cosmochim. Ac*., **75**, 2911-2923.

Sobek, A.A., Rastogi, V. and Benedetti, D.A. (1990) Prevention of water pollution problems in mining: The bactericide technology. *Mine Water Env.,* **9**, 133-148.

Søvik, A.K. and Kløve, B. (2005) Phosphorus retention processes in shell sand filter systems treating municipal wastewater. *Ecol. Eng.* **25**, 168-182.

Sparks, D.L. (2003) *Environmental Soil Chemistry.* Elsevier Science, Boston, USA.

Sposito, G. (1984) *The Surface Chemistry of Soils*. Oxford University Press, Oxford, UK.

Stratful. I., Scrimshaw, M.D. and Lester, J.N. (2001) Conditions influencing the precipitation of magnesium ammonium phosphate. *Water Res.*, **35**, 4191-4199

Streat, M., Hellgardt, K. and Newton, N.L.R. (2008) Hydrous ferric oxide as an adsorbent in water treatment. 3: Batch and mini-column adsorption of arsenic, phosphorus, fluorine and cadminium ions. *Process Saf. Environ*., **86**, 21-30.

Stumm, W. and Morgan, J.J. (1996) *Aquatic Chemistry: chemical equilibria and rates in natural waters* [3rd Ed.]. Wiley Interscience, New York, USA.

Stumm, W., Huang, C.P. and Jenkins, S.R. (1970) Specific chemical interaction affecting the stability of dispersed systems. *Croat. Chem. Acta.*, **42**, 223-245.

Suziki, T., Inomata, S. and Sawada, K. (1986) Adsorption of phosphate on calcite. J. Chem. Soc. Faraday T. **82**, 1733-1743.

Swan River Trust. (2001) Phosphorus in the Canning-1999-2000 Phoslock™ trials. *River Science*, **17**,1-8.

Talbot, L. (2006) *An Investigation into the Phosphorus Removal Capacity of Removed Ochre: Installation of an in-stream filter unit at Nafferton Farm, Northumbria*. MSc Dissertation, Newcastle University, UK.

Tanada, S., Kabayama, M., Kawasaki, N., Sakiyama, T., Nakamura, T., Araki, M. and Tamura, T. (2003) Removal of phosphate by aluminium oxide hydroxide. *J. Colloid Interf. Sci.*, **257**, 135-140.

Tello, A., Corner, R.A. and Telfer, T.C. (2010) How do land-based salmonid farms affect stream ecology? *Environ. Pollut.*, **158**, 1147-1158.

Toride, N., Leij, F.J. and van Genuchten, M. T. (1995) The CXTFIT code for estimating transport parameters from laboratory or field tracer experiments. Version 2.0. *Research Report No. 137.* U.S. Salinity Laboratory, CA, USA.

Torrent, J., Schwertmann, U. and Barrón, V. (1992) Fast and slow phosphate sorption by goethite-rich natural materials. *Clay Clay Miner.* **40**, 14-21.

Tunesi, S., Poggi, V. and Gessa, C. (1998) Phosphate adsorption and precipitation in calcareous soils: the role of calcium ions in solution and carbonate minerals. *Nut. Cyc. Agroeco.*, **53**, 219-227

Ueno, Y. and Fujii, M. (2001) Three years experience of operating and selling recovered struvite from full-scale plant. *Environ. Technol.*, **22**, 1373-1381.

UK Technical Advisory Group on the Water Framework Directive (2007) *A UKTAG Report on the remaining proposed Surface Water Environmental Standards and Conditions* [public consultation document]. Available online from www.wfduk.org. Accessed on 20/04/2009.

United States Environmental Protection Agency (1995) *A Guide to the Biosolids Risk Assessments for the EPA Part 503 Rule.* USEPA Publications, EPA/832/B-93/005, USA.

United States Environmental Protection Agency (1998) *Permeable reactive barrier technologies for contaminant remediation*. USEPA Publications, EPA/600/R-98/125, USA.

United States Environmental Protection Agency (2002) *Onsite Wastewater Treatment Systems Technology Factsheet 8: Enhanced Nutrient Removal- Phosphorus*. USEPA Publications, EPA/600/R-00/008, USA.

Unob, F., Wongsin, B., Phaeon, N., Puanngaum, M. and Shiowatana, J. (2007) Reuse of waste silica as adsorbent for metal removal by iron oxide modification. *J. Hazard. Mater.*, **142**, 455-462.

USEPA (1999) *Understanding Variation in Partition Coefficient, Kd, Values*. Available online from www.epa.gov/radiation/cleanup. Accessed on 03/02/2011.

Valsami-Jones, E. (2004) The geochemistry and mineralogy of phosphorus. In: Valsami-Jones, E. (ed) *Phosphorus in Environmental Technology: Principles and Applications*, IWA Publishing, London, UK. pp.20-50.

Varjo, E., Liikanen, A., Salonen, V-P. and Martikainen, P.J. (2002) A new gypsum-based technique to reduce methane and phosphorus release from sediments of eutrophied lakes: (Gypsum treatment to reduce internal loading) *Water Res.,* **37**, 1-10.

Vesilind, P.A. (2003) *Wastewater Treatment Plant Design.* IWA Publishing, London, UK.

Viraraghavan, T., and Warnock, R.G. (1976) Efficiency of a Septic Tile system. *J. Water Pollut. Con. F.,* **48**, 934-944.

Wei, X., Viadero Jr, R.C. and Bhojappa, S. (2008) Phosphorus removal by acid mine drainage sludge from secondary effluents of municipal wastewater treatment plants. *Water Res.*, **42**, 3275-3284.

Whelan, B.R. and Titamnis, Z.V. (1982) Daily chemical variability of domestic septic tank effluent. *Water, Air, Soil Poll.*, **17**, 131-139.

White, P.J. and Hammond, J.P. (2009) The sources of phosphorus in the waters of Great Britain. *J. Environ Qual.,* **38**, 13-26.

Winter, J.G. and Dillon, P.J. (2006) Export of nutrients from golf courses on the Precambrian Shield. *Environ. Pollut.,* **141**, 550-554.

Withers, P.J.A., Edwards. A.C. and Foy, R.H. (2001) Phosphorus cycling in UK agriculture and implications for phosphorus loss from soil. *Soil Use Manage.,* **17**, 139-149.

Withers, P.J.A., Ulén, B., Stamm, C. and Bechmann, M. (2003) Incidental phosphorus losses – are they significant and can they be predicted? *J. Plant. Nutr. Soil Sci.,* **166**, 459-468.

World Health Organisation (2011) *Guidelines for drinking-water quality: fourth edition*. Available online from www.who.int, Accessed on 01/08/2011.

Xu, D.J., Xu, J., Wu, J. and Muhammad, A. (2006) Studies on the phosphorus sorption capacity of substrates used in constructed wetland systems. *Chemosphere*, **63**, 344-352.

Younger, P. (1997) The longevity of minewater pollution: a basis for decision making. *Sci. Total Environ.*, **194-195**, 457-466.

Zeng, L., Li, X. and Lin, J. (2004) Adsorptive removal of phosphate from aqueous solutions using iron oxide tailings. *Water Res.,* **38**, 1318-1326.

Zhong, B., Stanforth, R., Wu, S. and Paul Chen, J. (2006) Proton interaction in phosphate adsorption onto goethite. *J. Colloid Interf. Sci.* **308**, 40-48.